ISBN 978-1-927797-43-3
ISSN 1198-273X

PICES SCIENTIFIC REPORT
No. 60, 2020

Report of Working Group 30 on Assessment of Marine Environmental Quality of Radiation around the North Pacific

NORTH PACIFIC MARINE SCIENCE ORGANIZATION

PICES

PICES Scientific Report No. 60
2020

Report of Working Group 30
on
Assessment of Marine Environmental Quality of Radiation around the North Pacific

edited by
Wen Yu, Yusheng Zhang, John N. Smith and Kathryn A. Higley

December 2020

North Pacific Marine Science Organization (PICES)
P.O. Box 6000, Sidney, BC, V8L 4B2, Canada
www.pices.int

PICES Scientific Reports

Published since 1993, the PICES Scientific Report series includes final reports of PICES expert groups, proceedings of PICES workshops, data reports and reports of planning activities. Formal peer reviews of the scientific content of these publications are not generally conducted.

PICES Scientific Reports can be found at: https://meetings.pices.int/publications/scientific-reports.

This report was developed under the guidance of the PICES Science Board and its Marine Environmental Quality Committee. The views expressed in this report are those of participating scientists under their responsibilities.

Front cover:
Fukushima Dai-ichi Nuclear Power Plant (Photo credit: source unknown)

This document should be cited as follows:

Yu, W., Zhang, Y.S., Smith, J.N. and Higley, K.A. (Eds.) 2020. Report of Working Group 30 on Assessment of Marine Environmental Quality of Radiation around the North Pacific. PICES Sci. Rep. No. 60, 179 pp.

Table of Contents

Acknowledgements

The editors would like to thank the members of WG 30 for their contributions to the country reports, and Dr. John N. Smith (WG member from Canada) for his contribution to the *Executive Summary, Section 1, Section 4 and Section 10* of this report, Dr. Wen Yu, Dr. Wu Men, Prof. Yusheng Zhang (WG members from the People's Republic of China) and Dr. Jianhua He (Third Institute of Oceanography, MNR, China) for their contribution to *Section 1*, *Section 3*, *Section 6* and *Section 7*, Dr. Takami Morita and Dr. Tomowo Watanabe (WG members from Japan) for their contribution to *Section 2* and *Section 3*, Dr. In-Seong Han, Dr. Kyung Tae Jung, Dr. Suk Hyun Kim and Dr. Young-Il Kim (WG members from the Republic of Korea) for their contribution to *Section 3* and *Section 5*, and Prof. Kathryn A. Higley (WG member from the United States of America) and Dr. Delvan Neville (State University of Oregon, the USA) for their contribution to *Section 6*. *Section 8, Section 9* and *Section 10* were completed by all the WG members together.

Research work related to this report was supported by the Integrated Fukushima Ocean Radionuclide Monitoring (InFORM) Network, a grant from MEOPAR (Marine Environmental Observation, Prediction and Response Network) of Canada, the Northwestern Pacific Marine Environmental Monitoring Project of the State Oceanic Administration of the People's Republic of China, China–Korea Joint Ocean Research Center nuclear safety project, KIOST major project (PE99501) of the Republic of Korea and FIO project from NSFC (41506035) of the People's Republic of China.

Contributing Researchers and Their Areas of Expertise

Canada

Jay T. Cullen
Chemical oceanography
University of Victoria
jcullen@uvic.ca

Jonathan P. Kellogg
Oceanography
University of Victoria
jkellogg@uvic.ca

Jean-François Mercier
Health physics
Health Canada
jean-francois.mercier@canada.ca

John N. Smith
Isotope oceanography
Bedford Institute of Oceanography
John.Smith@dfo-mpo.gc.ca

Marc Trudel
Biological oceanography
St. Andrews Biological Station
Marc.Trudel@dfo-mpo.gc.ca

Japan

Daisuke Ambe
Environmental radioactivity
Japan Fisheries Research and Education Agency
ambe@affrc.go.jp

Ken Fujimoto
Environmental radioactivity
Japan Fisheries Research and Education Agency
fujiken@affrc.go.jp

Hideki Kaeriyama
Chemical oceanography
Japan Fisheries Research and Education Agency
kaeriyama@affrc.go.jp

Shizuho Miki
Environmental radioactivity
Japan Fisheries Research and Education Agency
mikish@affrc.go.jp

Takami Morita
Environmental radioactivity
Japan Fisheries Research and Education Agency
takam@affrc.go.jp

Yuya Shigenobu
Environmental radioactivity
Japan Fisheries Research and Education Agency
yshig@affrc.go.jp

Tomowo Watanabe
Oceanography
Japan Fisheries Research and Education Agency
wattom@affrc.go.jp

People's Republic of China

Jianhua He
Radioactivity monitoring
Third Institute of Oceanography, Ministry of Natural Resources
hejianhua@tio.org.cn

Hongzhi Li
Radiometry
National Ocean Technology Center
lihongzhi6535@126.com

Wu Men
Radioactivity monitoring
Third Institute of Oceanography, Ministry of Natural Resources
menwu@tio.org.cn

Tao Yu
Radioactivity monitoring
Third Institute of Oceanography, Ministry of Natural Resources
yutao@tio.org.cn

Wen Yu
Radiation protection
Third Institute of Oceanography, Ministry of Natural Resources
yuw@bnu.edu.cn

Zhi Zeng
Radiometry
Tsinghua University
zengzhi@tsinghua.edu.cn

Yusheng Zhang
Marine radioecology and ecotoxicology
Third Institute of Oceanography, Ministry of Natural Resources
zhangyusheng@tio.org.cn

Chang Zhao
Simulation modelling
First Institute of Oceanography, Ministry of Natural Resources
zhaoc@fio.org.cn

Republic of Korea

Gi Hoon Hong
Radiochemistry
Korea Institute of Ocean Science and Technology
ghhong@kiost.ac.kr

Kyung Tae Jung
Circulation, radioactivity transport and fate modeling in ocean
Korea Institute of Ocean Science and Technology
ktjung@kiost.ac.kr

Kyeong Ok Kim
Wave, radioactivity transport and fate modeling in ocean
Korea Institute of Ocean Science and Technology
kokim@kiost.ac.kr

Suk Hyun Kim
Radiochemistry
Korea Institute of Ocean Science and Technology
shkim@kiost.ac.kr

Young Ill Kim
Radiochemistry
Korea Institute of Ocean Science and Technology
yikim@kiost.ac.kr

United States of America

Kathryn A. Higley
Radiation protection
Nuclear Engineering and Radiation Health Physics, Oregon State University
kathryn.higley@oregonstate.edu

Delvan Neville
Radiation protection
Nuclear Engineering and Radiation Health Physics, Oregon State University
dnevill@gmail.com

Abbreviations and Acronyms

Bq	SI unit used to describe the rate of radioactive decay
CF	Concentration Factor
CMW	Central Mode Water
CNA	Chernobyl Nuclear Accident
CR	Concentration Ratio
CT	Computerized Tomography
DCC	Dose Conversion Coefficient
DCF	Dose Conversion Factor
DCMW	Denser Central Mode Water
DICE-CT	Diffusible-Iodine Contrast-Enhanced CT
ERRJ	Environmental Radioactivity and Radiation in Japan
FDNPP	Fukushima Dai-ichi Nuclear Power Plant
IAEA	International Atomic Energy Agency
ICRP	International Commission on Radiological Protection
InFORM	Integrated Fukushima Ocean Radionuclide Monitoring Network
INES	International Nuclear and Radiological Event Scale
KINS	Korea Institute of Nuclear Safety
LCMW	Lighter Central Mode Water
MDA	Minimum Detected Activity
MDC	Minimal Detected Concentration
MDL	Minimum Detection Limit
MRI	Magnetic Resonance Imaging
ND	Not Detected (below minimum detectable activity)
NPIW	North Pacific Intermediate Water
NPP	Nuclear Power Plant
STMW	Subtropical Mode Water
TEPCO	Tokyo Electric Power Corporation
UNSCEAR	United Nations Scientific Committee on the Effects of Atomic Radiation

Executive Summary

In August, 2013 the North Pacific Marine Science Organization (PICES) approved the formation of an interdisciplinary Working Group on *Assessment of Marine Environmental Quality of Radiation around the North Pacific* (WG 30). This Working Group was proposed by China during the PICES 2012 Annual Meeting in Japan and was designed to engage the PICES scientific community in an effort to discuss and assess our current understanding of the impact of the 2011 Fukushima Dai-ichi Nuclear Power Plant (FDNPP) accident on the marine environment of the North Pacific Ocean. This was an unusual mandate for a PICES working group because it addressed a very specific event whose impacts and consequences were unfolding in real time as WG 30 undertook its deliberations. As a result, the annual meetings of WG 30 became a forum for the timely exchange of new information among the PICES member countries and among some of the research teams most active in documenting and evaluating environmental changes associated with the FDNPP accident. WG 30 was extremely focused and very collaborative in the sharing of current information as it was acquired during seasonal cruises undertaken by each of the PICES member countries in the North Pacific, thereby expediting the international dissemination of Fukushima monitoring data. The products of WG 30 include two major workshops, an invited PICES-SCOR collaborative review article and over 30 scientific articles in international, peer-reviewed journals and an outreach brochure for the general public.

WG 30's primary accomplishments and research findings are described in this report. The group promoted research through coordinated communications, exchanges of sampling and analytical methodologies, laboratory visits and the organization of meetings to discuss and publish results. The principal thrust of the collaborative research was on radionuclide transport in the ocean, ocean–atmospheric exchange of radioactivity, radionuclide uptake in sediments and marine biota and impacts on marine food webs and ecosystems. A range of different types of modeling studies were also reported, including radionuclide transport models, fate models and radiological dose and risk assessment models. Model testing and evaluation was enhanced by the fact that the FDNPP accident represents the largest point source discharge of radioactivity into the marine environment that has ever occurred, thereby providing an unusually strong input signal whose far field features were particularly amenable to model validation using experimental data provided in WG 30.

As the end of WG 30's term approached, it became clear that the Working Group members had profited significantly from the international cross-fertilization of ideas, data sharing and cultural exchanges that are supported and encouraged under the auspices of the PICES. It also became clear that the FDNPP accident is unlikely to be the last nuclear-related incident in the Pacific Ocean, with potentially deleterious impacts on marine ecosystems. Within the next decade over 30 new nuclear reactors will begin operations in Asia. Furthermore, there are numerous other possible sources and mechanisms for the discharge of radioactivity into the environment that may emerge in the next few years. This report can be used as a guide for the quick establishment of radioactivity monitoring and assessment programs and the efficient development of international research collaborations in the event of a future nuclear accident or large-scale radioactivity discharge in the North Pacific region.

1 Background

On March 11, 2011, a magnitude 9 earthquake struck off the east coast of Japan resulting in an enormous tsunami that caused massive damage and loss of life on the Japanese coastline. The tsunami inundated the Fukushima Dai-ichi Nuclear Power Plant (FDNPP) on the east coast of Honshu causing a loss of coolant that resulted in core damage due to melting of the fuel rods and a large release of radioactivity to the environment. The FDNPP accident was rated at the highest level of 7 on the International Nuclear and Radiological Event Scale (INES) and was the worst accident at a nuclear power plant since the Chernobyl disaster in 1986.

Radioactivity releases from the FDNPP accident represent the largest unplanned discharges of radioactivity that have occurred directly into the ocean (Buesseler *et al*., 2011; Charette *et al*., 2013; Castrillejo *et al*., 2015). The initial discharges occurred from the venting and explosive releases of gases and volatile radionuclides to the atmosphere with greater than 80% being deposited in the ocean. Subsequent, smaller direct discharges to the ocean occurred during emergency cooling efforts as a result of run-off over land, enhanced flow of contaminated groundwater, and the leakage of water from the reactor buildings. Estimates of the total discharge of the most widely studied radionuclide, the cesium isotope ^{137}Cs, have varied from 3 to 30 PBq, but recent and more precise estimates tend to converge on a range of 15 to 20 PBq (Aoyama *et al*., 2016; Buesseler *et al*., 2017). The total ^{137}Cs discharge comprises direct oceanic inputs of 3 to 5 PBq and another 10 to 15 PBq of ^{137}Cs that were released to the atmosphere and deposited over a broad region of the ocean northeast of Fukushima. These discharges from the FDNPP represent about 25% of the total input of 69 PBq delivered to the North Pacific in the 1950s and 1960s from atmospheric nuclear weapons tests (Aoyama *et al*., 2016).

Although the ocean has a great capacity to dilute and disperse radioactive materials due to its large volume and complex current systems, the long half-life radionuclides such as ^{137}Cs and strontium isotope ^{90}Sr will remain in the marine environment for many years, potentially affecting humans and marine organisms via biological uptake, transfer through the food chain and subsequent exposure of tissues to ionizing radiation. In order to better evaluate the impact of the FDNPP accident on the marine environment in the North Pacific, the Working Group on *Assessment of Marine Environmental Quality of Radiation around the North Pacific* (WG 30) was established in 2013 under the auspices of the Marine Environmental Quality (MEQ) committee, and co-chaired by Prof. Yusheng Zhang (the People's Republic of China) and Prof. Kathryn A. Higley (USA). During its term, WG 30 undertook a range of activities intended to illuminate the environmental consequences of the accident, including workshop development, information exchange, radiological risk assessment, joint field activities and inter-institutional communication and data sharing. The results, conclusions and recommendations associated with the individual national monitoring activities and joint collaborations through WG 30 are outlined in the following report. These are followed by appendices 1 to 6 pertaining to terms of reference, membership, publications and other products produced by the Working Group.

2 Monitoring the Coastal Waters of Japan

2.1 Environmental monitoring strategies

The 2011 accident at the FDNPP of the Tokyo Electric Power Company (TEPCO) focused concerns on radioactivity contamination of the environment and the general radiological safety of the public. An environmental radioactivity survey had been initiated in the 1950s and the monitoring program which extended to coastal waters has been maintained to the present time. For the marine environment, three long-term monitoring projects have been maintained, as described below. Radioactivity survey data obtained by these monitoring systems are archived and posted to publicly available websites (see below). These historical data provide background levels for the radionuclides and can be used to evaluate relationships between levels of radioactivity in environmental phases and those in marine organisms. Based on these established monitoring systems, the Japanese government was able to rapidly establish an updated monitoring program specifically for the radionuclides leaked by the FDNPP accident. The Ministry of Education, Culture, Sports and Technology (MEXT) and beginning in 2012, the Nuclear Regulation Agency (NRA), played critical roles in operating the marine environmental radioactivity monitoring program, and the Fisheries Agency of Japan (JFA) assumed the role for the monitoring of marine organisms.

2.1.1 Environmental radioactivity surveys in Japan

Radioactivity and radiation surveys have been conducted by the Japanese government since the 1950s to monitor fallout radioactivity from nuclear weapons tests in the atmosphere. The concentrations of the cesium isotope ^{137}Cs and strontium isotope ^{90}Sr were measured in a wide range of environmental samples such as rain and dry fallout, airborne dust, fresh water, soil, seawater and sea sediment, and in food such as rice, milk, powdered milk, vegetables, shellfish and seaweeds. The results of the monitoring are published in the report, “Radioactivity Survey Data in Japan” every year and are available through the website of “Environmental Radioactivity and Radiation in Japan” (https://www.kankyo-hoshano.go.jp/). The archived data for the period from 1957 to the present are also available from the database on the website, hereafter referred to as ERRJ (Environmental Radioactivity and Radiation in Japan) database.

2.1.2 Marine environmental radioactivity surveys for nuclear power plants

NRA and the Marine Ecology Research Institute (MERI) have conducted monitoring projects on environmental radioactivity levels in the waters surrounding nuclear power plants in Japan since the 1980s (Kusakabe *et al*., 2013). Seawater, sediments and marine organisms are collected each year at fifteen nuclear power stations and analyzed for artificial radionuclides such as ^{137}Cs and ^{90}Sr. The data are available from the ERRJ database.

2.1.3 Monitoring by the Fisheries Agency of Japan and the Japan Fisheries Research and Education Agency

A third long-term monitoring program has been carried out by the Fisheries Agency of Japan (JFA) and the Japan Fisheries Research and Education Agency (FRA) since 1957 on radionuclides in fisheries products in Japan. This program was initially organized to confirm the effects of atmospheric nuclear weapons tests and has been maintained to the present day to ensure the radiological safety of seafood. In this program marine organisms (fish, cephalopods, crustaceans, shellfish and seaweeds) and environmental samples (seawater, sea sediment and sinking particles) are subjected to gamma ray measurements, beta ray measurements for ^{90}Sr, and further analyses for other radionuclides. Marine organisms, sediments and seawater are collected on oceanographic cruises in marine waters off Japan and the results of the sampling expeditions and radionuclide analyses are reported annually to JFA.

2.1.4 Enhanced monitoring of radionuclides following the FDNPP accident

Following the FDNPP accident, several actions were taken to enhance radioactivity monitoring. MEXT initiated a new radioactivity program off the east coast of Japan designed to monitor the distribution and concentrations of radionuclides in the marine environment. The first offshore survey by a research vessel was implemented on March 23, 2011. Thereafter, MEXT updated the monitoring plan several times and continued the *in-situ* surveys. The main purpose of the monitoring was to evaluate the radiological safety of the marine environment for human exposure. TEPCO was initially responsible for the monitoring of radionuclides in the environment and marine organisms in the harbor of FDNPP and surrounding coastal regions. However, in October 2011, MEXT revised the monitoring plan with TEPCO and a wide range of agencies and published a new version: “Future Plan of Sea Area Monitoring” (MEXT[1]) which lowered radionuclide detection limits in order to better determine the long-term influence of relatively low levels of radionuclide contamination in the marine environment.

Although the relevant government organization was changed from MEXT to NRA in 2012, the basic monitoring framework for marine environmental radioactivity has been maintained to the present. Actions were also taken with regard to the protection of food following the nuclear accident. The Ministry of Health, Labour and Welfare (MHLW) notified prefectural governments to survey commercial food for radioactivity in order to prevent the public distribution of contaminated products. JFA also began the radioactivity monitoring of fisheries products which has continued to the present. The inspection results are published in near real-time on the JFA’s website:[2] and MHLW’s website.[3]

2.2 Seawater

Marine organisms take up radionuclides by intake from food and directly from seawater. The concentrations of radionuclides in seawater are critical data for an evaluation of radioactive contamination of marine organisms. In this Section, the ambient levels and changes in the concentrations of major radionuclides, radiocesium, radioiodine and radiostrontium in seawater are described for time periods before and after the FDNPP accident.

---

[1] https://radioactivity.nsr.go.jp/en/contents/1000/339/24/1000_1020.pdf
[2] https://www.jfa.maff.go.jp/e/index.html
[3] https://www.mhlw.go.jp/english/topics/2011eq/index_food_radioactive.html

2.2.1 Pre-accident monitoring around Japan

Environmental radioactivity data collected during the long history of environmental monitoring in Japan have tended to focus on the long-lived fallout radionuclides ^{137}Cs and ^{90}Sr and much of these data for the period 1963 to present are available from the ERRJ database website. Time series changes in radionuclide concentrations in surface seawater (0–100 m depth) in Japan coastal waters are shown in Figure 2.1. The slow but steadily decreasing trends in radionuclide concentrations are observed for the period from 1963 to 2010 for both ^{137}Cs and ^{90}Sr. The sources of most radionuclides were nuclear weapons tests that were undertaken in the period from the 1940s to the 1970s (UNSCEAR, 2000). Fitting an exponential approximate curve to the data gives apparent half-lives of 18 years for the decrease in ^{137}Cs concentrations and 19 years for the decrease of ^{90}Sr concentrations in surface seawater for the period from 1991 to 2010. Both estimates are shorter than the radioactive decay half-lives of 30.1 years for ^{137}Cs and 28.8 years for ^{90}Sr, indicating that ocean mixing represents an important removal process for these radionuclides, in addition to that of radioactive decay (Oikawa *et al*., 2013b).

A significant peak of ^{137}Cs concentration in 1986 is apparent in the time series which reflects fallout from the Chernobyl accident. The highest value observed in 1986 is 51.8 Bq/m^3 and is about 14 times higher than the background level (3.7 Bq/m^3 for 1985). ^{134}Cs and ^{131}I were also detected in a few samples in 1986.

Statistical characteristics of ^{137}Cs and ^{90}Sr concentration data in seawater are shown in Figure 2.2 for 10-years periods from 1991 to 2000 and 2001 to 2010. The frequency distribution of ^{137}Cs and ^{90}Sr concentration data can be approximated by a lognormal distribution. The changes in mean and standard deviation between the two 10-year periods are consistent with the decreasing trend at half-life of 20 years. In addition, the mean ratio of ^{137}Cs concentration to ^{90}Sr is about 1.4, in agreement with estimated values for global fallout (UNSCEAR, 2000). These results provide a robust analysis of very stable seawater concentrations of ^{137}Cs and ^{90}Sr concentrations prior to the FDNPP accident.

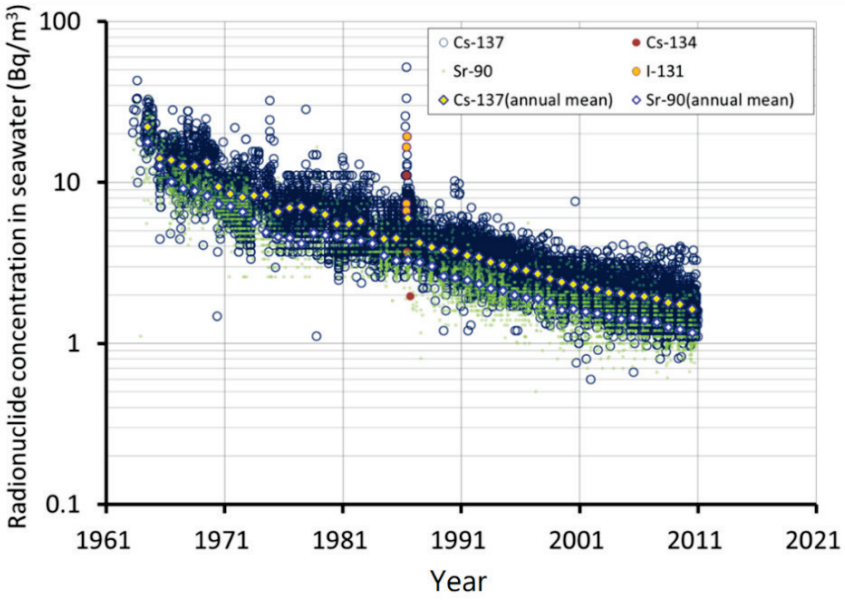

Fig. 2.1 Time series for radionuclide concentrations in Japan coastal waters prior to the FDNPP accident. The data excluding ND (not detected) were plotted.

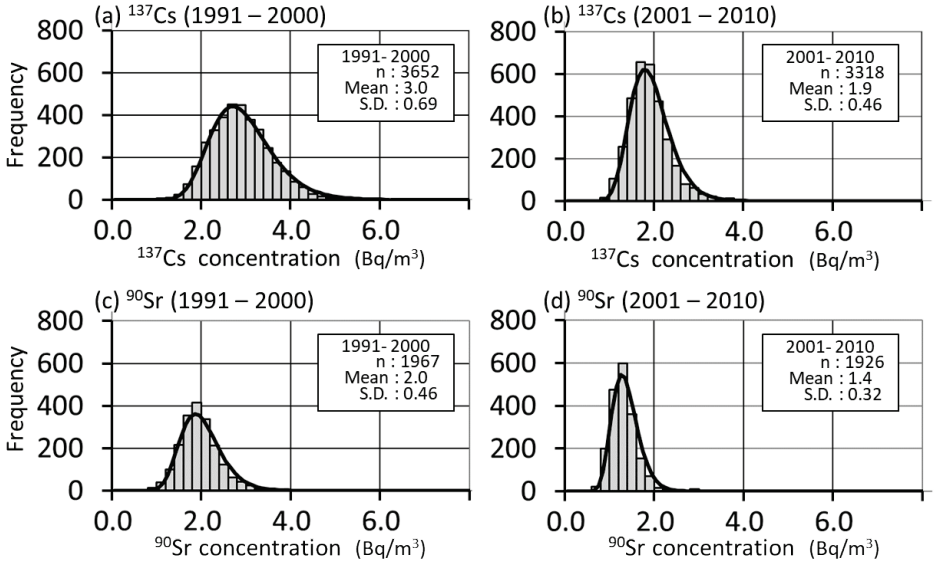

Fig. 2.2 Frequency distributions of seawater ^{137}Cs and ^{90}Sr concentrations in waters surrounding Japan with lognormal distribution curve.

To confirm the level of the radionuclide concentration before the FDNPP accident in the offshore area of East Japan, we summarized the ^{137}Cs and ^{90}Sr concentration data off the coast of Fukushima and adjacent prefectures in East Japan. The time series of annual mean ^{137}Cs and ^{90}Sr concentrations are shown in Figure 2.3. The decreasing trends are obvious, and the half-lives are in the range 16–18 years during the period 1991 to 2010. In Table 2.1, the 10-year means of ^{137}Cs and ^{90}Sr concentrations for 1991–2000 and 2001–2010 are shown. These values are equivalent to the average value estimated from the data for the whole waters surrounding Japan indicated in Figure 2.2, and this reflects the spatial homogeneity in distribution of seawater radiocesium concentration around Japan.

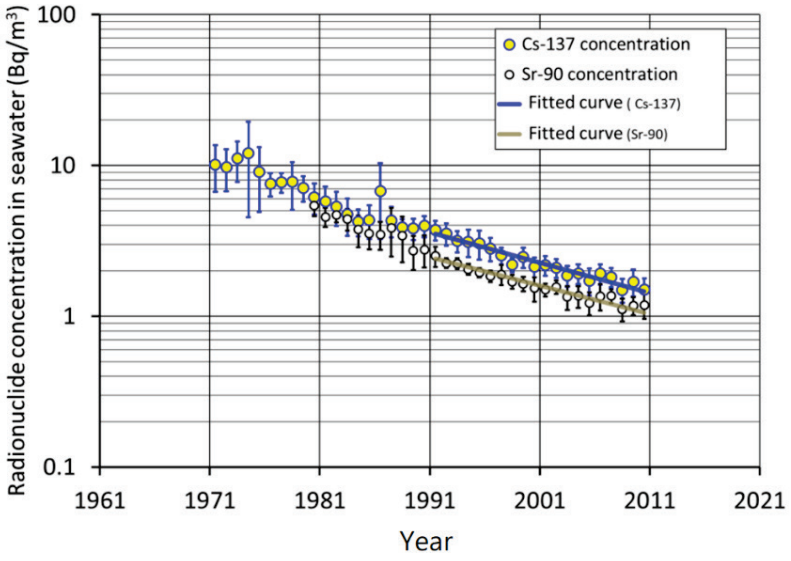

Fig. 2.3 Time series of annual mean ^{137}Cs and ^{90}Sr concentrations in seawater off East Japan (Fukushima and adjacent prefectures) before the FDNPP accident. Vertical bars indicate standard deviations.

Table 2.1 Statistics of radionuclide concentrations in seawater off East Japan (Fukushima and adjacent prefectures) for the 10-year periods from 1991 to 2000 and 2001 to 2010.

	^{137}Cs		^{90}Sr	
Period	**1991–2000**	**2001–2010**	**1991–2000**	**2001–2010**
Number of data	401	276	215	218
Average (Bq/m^3)	3.0	1.8	2.0	1.3
Standard Deviation (Bq/m^3)	0.72	0.36	0.36	0.24
Range (min–max) (Bq/m^3)	1.1–5.0	1.0–2.9	0.8–4.1	0.85–2.3

2.2.2 Post-accident monitoring around the FDNPP

Enhanced monitoring at the FDNPP site was initiated soon after the March 11, 2011 accident at the stations off East Japan and the monitoring data were published by NRA.[4] Time series measurements of ^{137}Cs levels at stations within the red rectangle in Figure 2.4 are combined with long-term seawater monitoring data by MERI in Figure 2.5. The FDNPP accident was clearly characterized by the short-term direct release of water to the ocean contaminated with ^{131}I and radiocesium (^{137}Cs and ^{134}Cs). The direct leakage of ^{137}Cs was estimated as 3.5 PBq and the highest seawater concentration (> 6 × 10^7 Bq/m^3) was observed at the coast near the FDNPP (Tsumune *et al*., 2012). This value was seven orders of magnitude higher than the pre-accident levels. Seawater concentrations of ^{137}Cs declined quickly following the accident owing to ocean mixing and transport in the dynamic coastal regime off East Japan, and within several years ^{137}Cs levels in the offshore area had begun to approach pre-2000 ocean fallout levels (Figure 2.5).

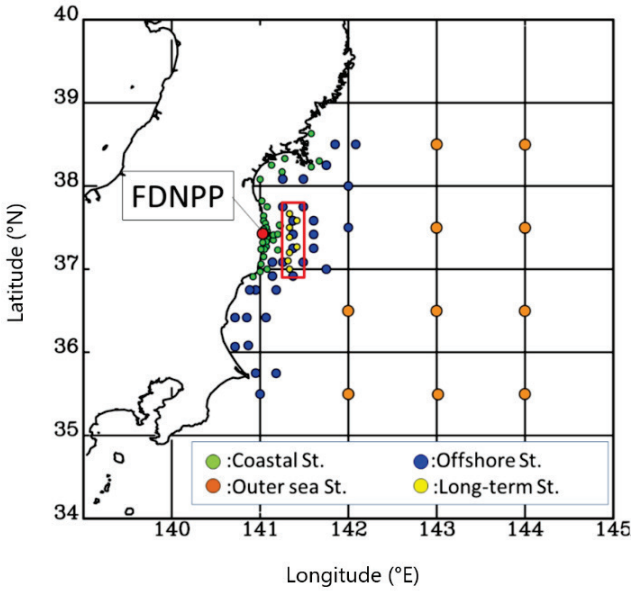

Fig. 2.4 Current monitoring stations where ^{137}Cs concentrations in seawater were measured with detection limit of 1 Bq/m^3 in the waters around Fukushima. Red rectangle indicates the offshore area selected in this report for evaluating the long-term changes.
See https://radioactivity.nsr.go.jp/en/contents/13000/12664/24/274_s_20170428.pdf.

[4] http://radioactivity.nsr.go.jp/en/

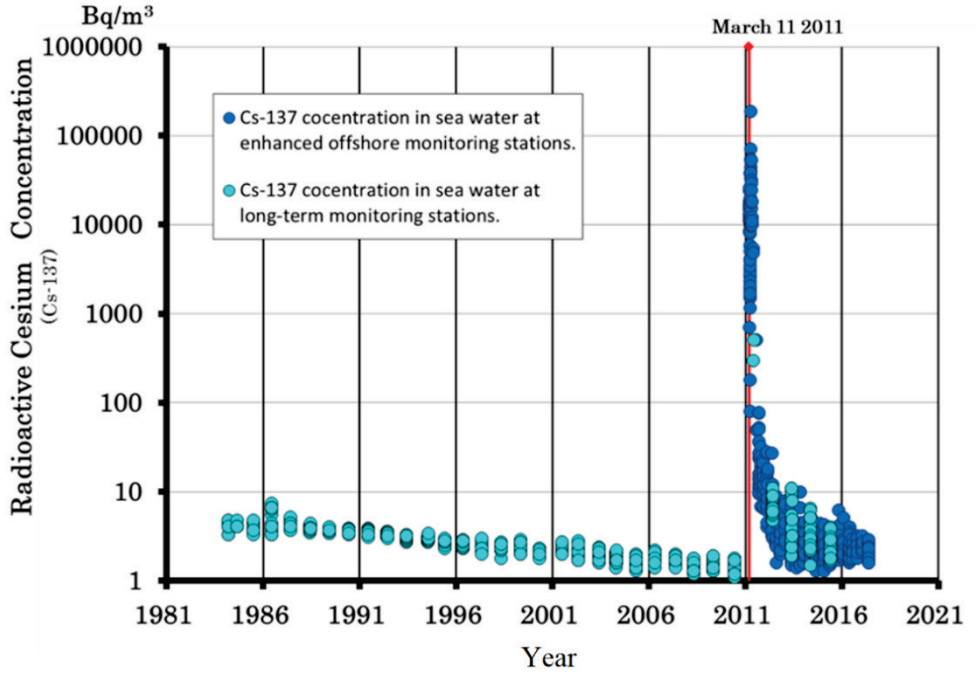

Fig. 2.5 Combined historical and post-accident (from red rectangle region in Figure 2.4) time series monitoring results for ^{137}Cs in seawater off Fukushima fitted with normal distribution curves.

2.2.3 Coastal dispersion of radiocesium

FDNPP-derived radiocesium was initially dispersed southward along the coast, and then eastward into the North Pacific in the strong Kuroshio Extension. The most significant changes in ^{134}Cs and ^{137}Cs concentrations in surface seawater were observed during the first six months of 2011 (Oikawa *et al*., 2013a). Just off the FDNPP site the ^{134}Cs and ^{137}Cs concentrations reached a maximum in the middle of April 2011 of up to 10^8 Bq/m^3 and thereafter rapidly decreased (Figure 2.6). Aoyama *et al*. (2012) reported the results of the weekly seawater monitoring of ^{134}Cs and ^{137}Cs collected at Hasaki, 180 km south of the FDNPP site. The maximum radiocesium concentration at Hasaki was observed in June 2011 of up to 2000 Bq/m^3, a delay of two months from the corresponding maximum value observed near the FDNPP site (Figure 2.6). This delay in the timing of maximum values observed between the FDNPP site and Hasaki may be due to the anticyclonic eddy restricting the southward transport of the FDNPP-derived radiocesium. The radiocesium in Hasaki decreased with time, and an apparent half-life of radiocesium was reported as 60 days (Aoyama *et al*., 2012).

One hundred kilometers north of the FDNPP site, time-series monitoring of radiocesium was conducted in Sendai Bay (Figure 2.6a). The maximum concentration of ^{137}Cs of 2700 Bq/m^3 was observed in June 2011 and subsequently decreased with time (Kaeriyama *et al*., 2015). The apparent half-life of ^{137}Cs in Sendai Bay was estimated as 120 days (Kaeriyama, 2015). FRA and the Fukushima Prefectural Fisheries Experimental Station began weekly monitoring of radiocesium in seawater at Onahama (Figure 2.6a) 35 km south of the FDNPP site in May 2012 (Kaeriyama *et al*., 2015; Kaeriyama, 2017). The concentration of ^{137}Cs and its temporal changes are roughly comparable with those of adjacent stations of NRA monitoring. A regional ocean model with only direct release source accurately simulated the spatio-temporal changes of radiocesium in the coastal area off Fukushima and adjacent prefectures (Masumoto *et al*., 2012; Miyazawa *et al*., 2012, 2013; Tsumune *et al*., 2012, 2013). Although the regional ocean models with atmospheric deposition have large uncertainties, the difficulty in precise estimates of the atmospheric deposition onto the coastal area off Fukushima and adjacent prefectures remains unresolved.

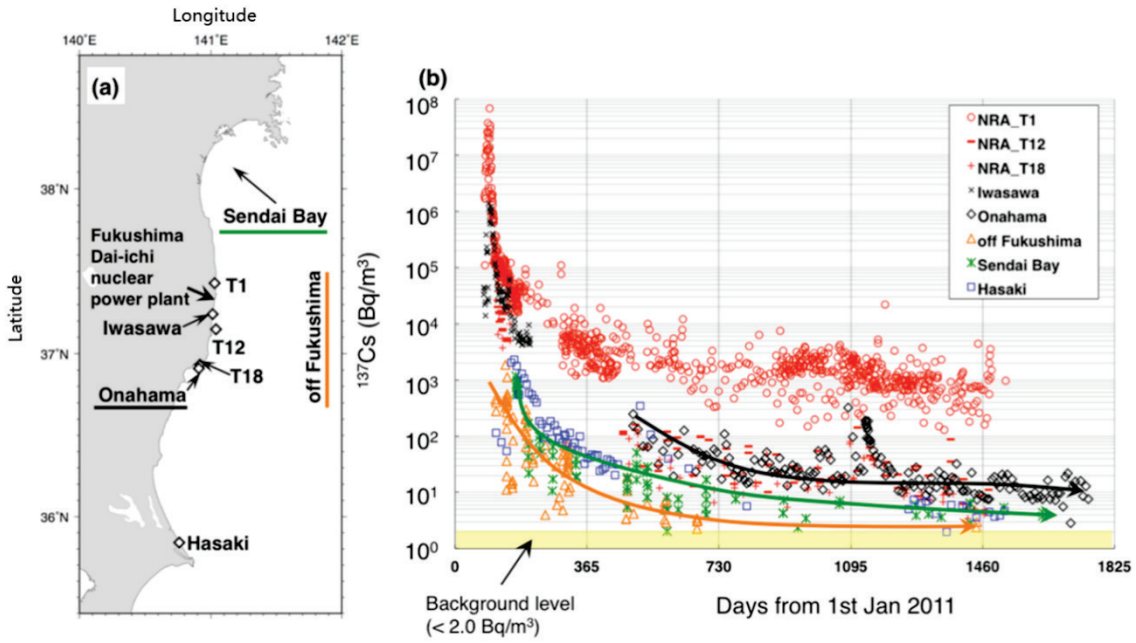

Fig. 2.6 (a) Coastal monitoring locations for radiocesium near the Fukushima Dai-ichi Nuclear Power Plant site and (b) temporal change in ^{137}Cs concentration in seawater. Data were cited from Aoyama *et al.* (2012, 2016), Kaeriyama (2015, 2017), Kaeriyama *et al.* (2015) and NRA (http://radioactivity.nsr.go.jp/en/). Modified from Kaeriyama (2017).

2.3 Sediment

Radionuclide levels in marine sediments may have an influence on the benthic ecosystem through the uptake of radioactivity through benthic food consumption by demersal fishes. Monitoring results from Japanese waters indicate that radionuclide levels in marine sediments are generally several orders of magnitude greater than in demersal fish suggesting that the radionuclides contained in sediment are not major sources for marine organisms. However, the increased radionuclide concentrations in sediments following the FDNPP accident may cause public concern. Monitoring of sediment levels of radioactivity is also an important issue for public communication and assurance.

2.3.1 Pre-accident monitoring around Japan

By using the sea sediment data extracted from the ERRJ database, time-series changes in sea sediment radiocesium concentrations are shown in Figure 2.7 with annual means and medians for ^{137}Cs. Boxplots for each 5-year period from 1981 to 2010 are also shown in Figure 2.8. A decreasing trend of ^{137}Cs is clearly seen and the apparent half-life time estimated for annual means is about 24 years during the period 1991 to 2010. The apparent half-life is longer than that for the ^{137}Cs concentration in seawater, possibly owing to the strong bonding between ^{137}Cs and soil which causes a delay in diffusion. It is also the obvious characteristic that there are large differences between means and medians (Figure 2.7 and Figure 2.8). The difference reflects the structure of a long tail in the high concentration region of frequency distribution (Figure 2.9), and is thought to be caused by the differences in the quality of the sea sediment among the sampling areas (Oikawa *et al.*, 2013b).

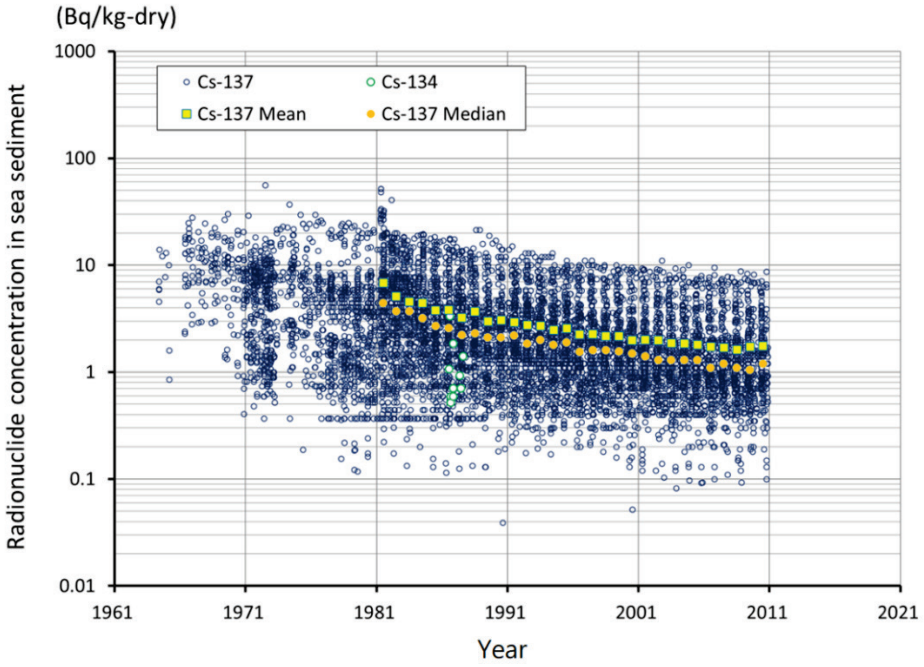

Fig. 2.7 Changes of the radionuclide concentrations in sea sediment around Japan before the FDNPP accident. The data excluding ND (not detected) were plotted.

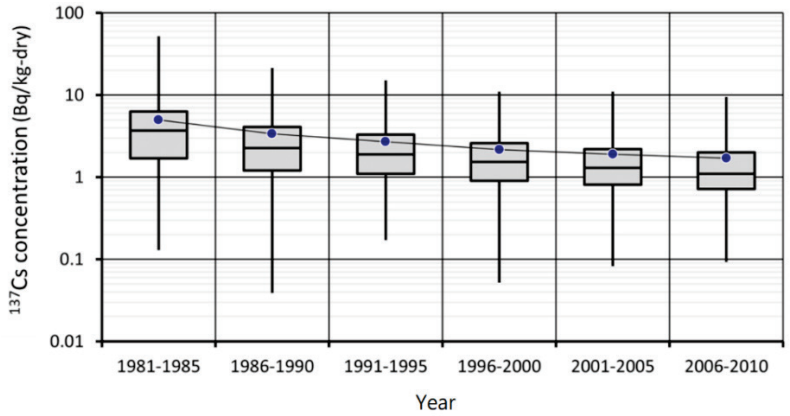

Fig. 2.8 Boxplots of ^{137}Cs concentrations in sea sediment around Japan for each 5-year period from 1981 to 2010. Vertical bars indicate minimum–maximum ranges. Full blue circles indicate 5-year means.

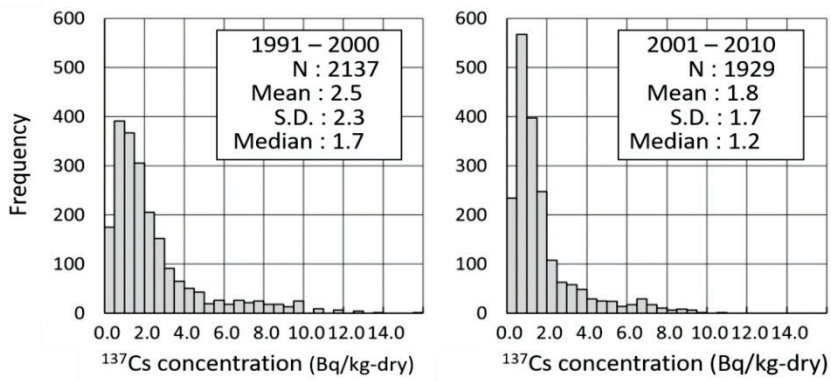

Fig. 2.9 Frequency distribution of ^{137}Cs concentrations in sea sediment in waters surrounding Japan.

2.3.2 Post-accident monitoring around the FDNPP

A wide range of sediment studies have been carried out following the FDNPP accident (Kusakabe *et al.*, 2013; Otosaka and Kobayashi, 2013; Thornton *et al.*, 2013; Ambe *et al.*, 2014; Black and Buesseler, 2014; Otosaka and Kato, 2014). These studies have shown that the inventory of radiocesium stored in the marine sediments in the Fukushima coastal regime within 2 years after the accident was less than a few percent of the total inventory of radiocesium initially discharged from the FDNPP. The distribution of ^{137}Cs in surface sediments in the Fukushima coastal regime based on surveys in 2012–2014 is illustrated in Figure 2.10.

The radiocesium concentration in the surface sediment does not decrease monotonically with the distance from the coast but is particularly high in the areas along the shore and near the 100-m water depth. This feature reflects the transport pathway of radiocesium-contaminated bottom water from the FDNPP over several months after the accident and the cesium adsorption response, depending on the particle size of the sediment (Ambe *et al.*, 2014). This result also shows that the distribution of radiocesium in surface sediments was largely determined in the early stages of the accident and varied little thereafter.

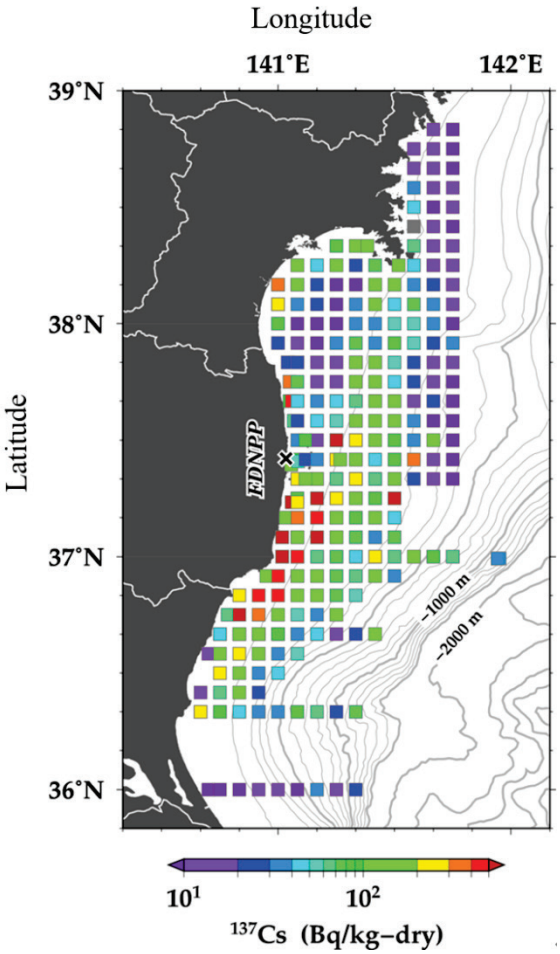

Fig. 2.10 Composite map of ^{137}Cs concentrations in surface sediment (0–1 cm depth) measured in surveys during 2012–2014.

The distribution of ^{137}Cs in surface sediments in 2015 is illustrated in Figure 2.11. The ^{137}Cs signal had decreased by about 45% on average from 2013, for an average reduction rate of about 25% per year. This decay rate is much higher than that of the physical radioactive decay of ^{137}Cs (2.3% per

year). A relatively large declining trend was observed in the surface layer of the sediment, in the coastal zone and/or the northern area from the FDNPP. Long-term flow field monitoring in the coastal area of Fukushima Prefecture reported that southward transport was dominant for suspended particles in the bottom layer in this area. This result suggests that part of the radiocesium deposited in the coastal area around Fukushima was gradually transported southward to the shelf slope by horizontal flow of particle-bound radiocesium (Yagi *et al.*, 2015). Another study indicated that the concentration in the surface layer also decreased by the relatively rapid downward mixing of radiocesium due to the activity of benthos (Black and Buesseler, 2014).

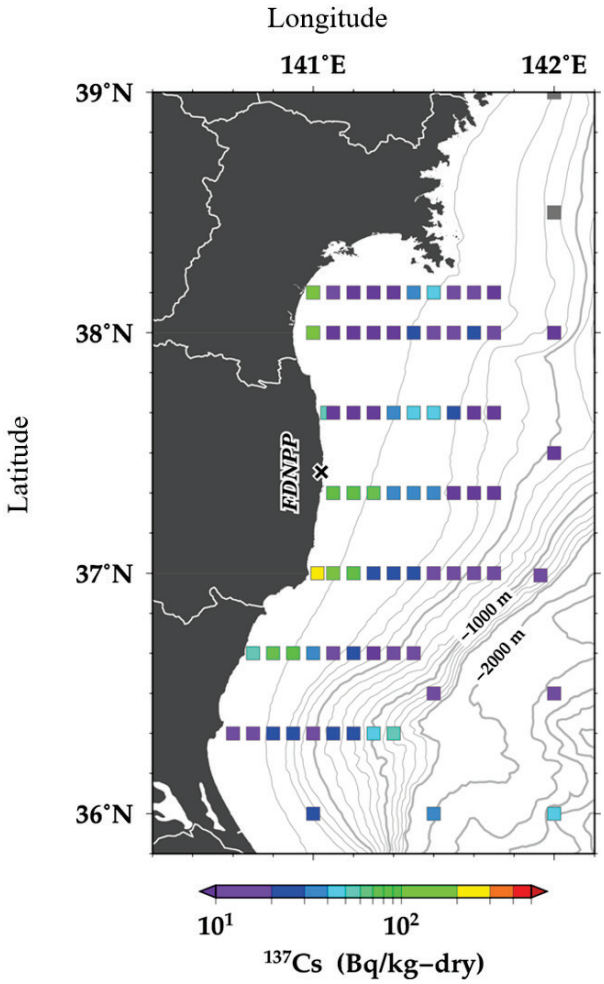

Fig. 2.11 Composite map of ^{137}Cs concentrations in surface sediment (0–1 cm depth) measured in surveys during 2015. Gray tiles indicate that the ^{137}Cs concentrations at these points are less than the detection limit (about 2–3 Bq/kg-dry).

In a study evaluating radiocesium content for each fraction of sediment sampled in 2012 (Ono *et al.*, 2015), about 20% of the radiocesium was distributed in the organic matter fraction (*i.e.*, available for organisms). The radiocesium in these fractions could be gradually eluted into seawater, and translocated to the lithogenic fraction (radiocesium on minerals) or diffuse out of the coastal area with seawater (*e.g.*, Wada *et al.*, 2013). Those results mean that the influence of the radiocesium in sea sediment on marine organisms on the sea floor is steadily decreasing both in a quantitative and qualitative manner.

2.4 Biota

The concentration of radionuclides in marine organisms reflects uptake from seawater and prey consumption. The distribution of radionuclides in marine biota is strongly dependent on the structure of the marine ecosystem. The relationship of contamination of marine organisms to environmental contamination represented a quasi-stable state prior to the FDNPP accident, but this changed to an unstable state after the FDNPP accident as illustrated by the monitoring data.

2.4.1 Pre-accident radionuclide levels in biota around Japan

Time series measurements of ^{134}Cs and ^{137}Cs concentrations in marine fish in Japanese coastal waters are shown in Figure 2.12. The data were extracted from the ERRJ database and ND (not detected) data were excluded. Fitting an exponential curve to the annual means for the period 1991–2010, the apparent half-life of decreasing trend was estimated as approximately 20 years. ^{134}Cs derived from the Chernobyl accident was detected in marine fish only in the period from 1986 to 1988.

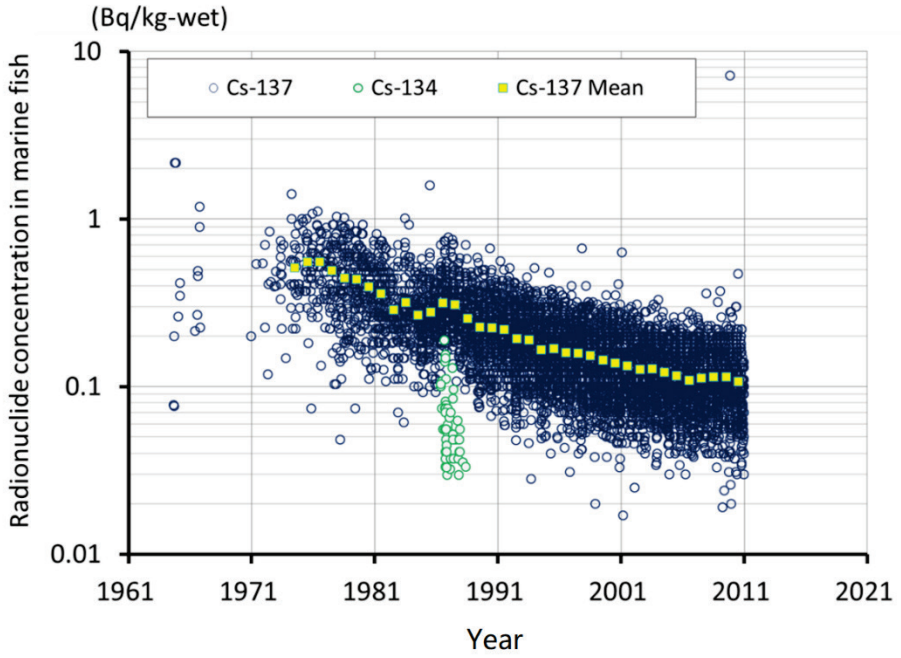

Fig. 2.12 Time series for radionuclide levels in marine fish around Japan before the FDNPP accident. The data excluding ND (not detected) were plotted.

In order to understand statistical characteristics of ^{137}Cs concentration data, the frequency distributions of ^{137}Cs concentration data for the 10-year periods from 1991–2000 and 2001–2010 are shown in Figure 2.13. In both periods, it is clear that the distribution can be approximated by lognormal distributions, and this suggests that the decrease of radioactive concentration in marine fishes is progressing stably. The 10-year mean of ^{137}Cs concentration for the period from 2001–2010 is estimated to be 0.12 Bq/kg-wet (Figure 2.13), and the ratio to the seawater ^{137}Cs concentration (1.9 Bq/m^3, Figure 2.2) is estimated to be about 60. This is included in the known range of concentration factor (CF) for marine fish (Kasamatsu, 1999; IAEA, 2004).

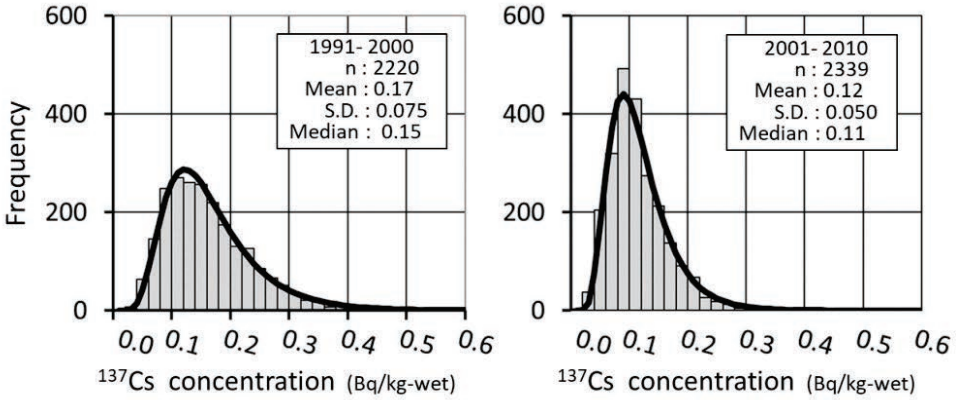

Fig. 2.13 Frequency distribution of ^{137}Cs concentrations in marine fishes with lognormal distribution curve.

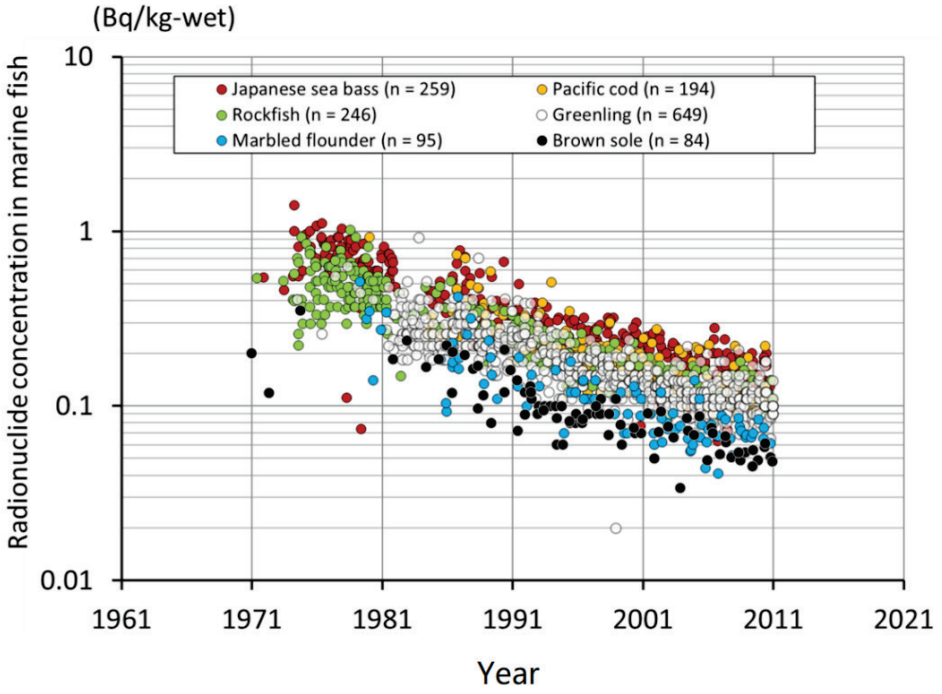

Fig. 2.14 Time series for ^{137}Cs concentrations in six marine fish species. The data excluding ND (not detected) were plotted.

The ^{137}Cs concentration data for six fish species, Japanese seabass (*Lateolabrax japonicus*), Pacific cod (*Gadus macrocephalus*), rockfish (*Sebastes cheni*), greenling (*Hexagrammos otakii*), marbled flounder (*Pseudopleuronectes yokohamae*) and brown flounder (*Pseudopleuronectes yokohamae*), are displayed in Figure 2.14. Although all of the species showed a steady decreasing trend of ^{137}Cs concentration, the levels are different by species. In addition, the boxplots of each fish species for the period from 2001 to 2010 are shown in Figure 2.15 and the CFs are in the range from 30 to 100 (Table 2.2). These comparisons clearly indicate that strong ichthyophagous fish species (Japanese seabass, Pacific cod) have higher ^{137}Cs concentrations and benthos-feeding fish species (marbled flounder, brown sole) have lower ^{137}Cs concentrations, as pointed out by previous studies (Kasamatsu, 1999).

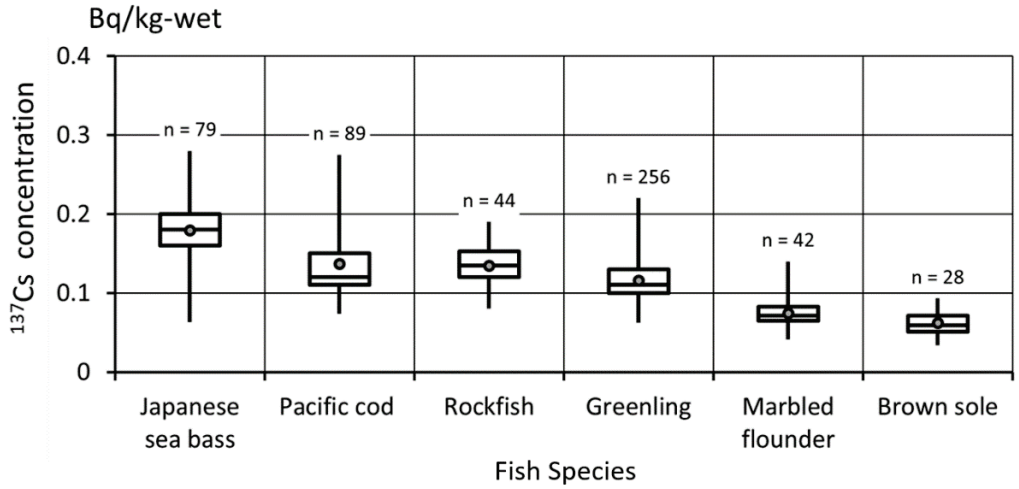

Fig. 2.15 Boxplots of ^{137}Cs concentrations for six fish species from 2001–2010. Vertical bars indicate minimum–maximum ranges. Full grey circles indicate means of the 10-year period.

Table 2.2 Statistics for ^{137}Cs concentrations in seawater, for six fish species from 2001– 2010.

	No. of data	Average	Range (min–max)	Ratio to seawater
Seawater (Bq/m^3)	3318	1.9	0.6–4.1	1
Japanese seabass (Bq/kg-wet)	79	0.18	0.063–0.26	95
Pacific cod (Bq/kg-wet)	89	0.14	0.074–0.28	74
Rockfish (Bq/kg-wet)	44	0.13	0.080–0.19	68
Greenling (Bq/kg-wet)	256	0.12	0.062–0.22	64
Marbled flounder (Bq/kg-wet)	42	0.074	0.041–0.14	39
Brown sole (Bq/kg-wet)	28	0.062	0.034–0.093	33

2.4.2 Post-accident radionuclide levels in biota

Enhanced monitoring of marine biota (invertebrates, fishes, seaweeds) was begun immediately after the FDNPP accident, both within Fukushima Prefecture and throughout Japan (JFA, 2017). TEPCO also began the monitoring of marine organisms collected both in the harbor and within a 20-km zone extending outward from the FDNPP (TEPCO, 2017). Detailed sampling methods and measurement procedures for radiocesium and radiostrontium isotopes in marine products are described elsewhere (Wada *et al*., 2013, 2016; Shigenobu *et al*., 2014; JFA, 2017; Miki *et al*., 2017).

The total ^{137}Cs released into the atmosphere from the FDNPP accident and the amount of ^{137}Cs deposited on the ocean surface from the atmosphere was estimated to be approximately 13–20 PBq and 7.6–15 PBq, respectively (Aoyama *et al*., 2013; Kobayashi *et al*., 2013), which indicates that most of the ^{137}Cs was released into the ocean. In early April 2011, a leak of wastewater occurred which interacted with the ruptured nuclear fuel rods resulting in additional large releases of radioactivity estimated to be 3.5 PBq for ^{137}Cs (Tsumune *et al*., 2012).

Although major released radioactive materials were ^{131}I, ^{134}Cs and ^{137}Cs, two kinds of radiostrontium, ^{89}Sr (50.5 days) and ^{90}Sr (28.8 years) were also released from the FDNPP into the environment. The initial levels of ^{134}Cs and ^{137}Cs were approximately equal to each other (Chino *et al*., 2011), whereas the activity ratio of the ^{89}Sr/^{90}Sr from the reactor core inventory on March 11,

2011 was estimated to be 11.5 (Povinec *et al*., 2012). The total ^{90}Sr released into the atmosphere from the FDNPP accident was estimated to be approximately 0.14 PBq (Povinec *et al*., 2012), about a factor of 100 lower than the ^{137}Cs, owing to its lower volatility than for cesium. The ^{137}Cs/^{90}Sr activity ratio at the beginning of the FDNPP accident and the amount of ^{137}Cs directly released into the ocean indicated that the inventory of ^{90}Sr in the wastewater was about 0.04 PBq (Povinec *et al*., 2012). The monitoring by the Japanese government and TEPCO did not generally include radiostrontium measurements because the released amount was small, and the analytical method is more complex and time-consuming than the analytical method for radiocesium. However, the Japanese government and TEPCO have regularly published data on ^{90}Sr concentrations in some marine fishes (Miki *et al*., 2017).

The biota monitoring data have been published periodically on the JFA website (JFA, 2017), which involved 87,234 inspection results by the end of December 2016. In addition, many independent studies about marine organisms have been carried out by using these monitoring data since the FDNPP accident (Wada *et al*., 2013, 2016; Iwata *et al*., 2013; Tateda *et al*., 2013, 2015, 2017). The monitoring results indicate that the concentration of radiocesium in marine organisms has decreased in all areas since the accident. The results showed that more than 57% of inspected marine fish samples off Fukushima Prefecture were over the Japanese regulatory limit (100 Bq/kg-wet for radiocesium) in the period immediately following the FDNPP accident (April–June 2011). This percentage gradually declined and has remained at 0% since April 2015 (Figure 2.16).

Although evaluating current and future risks for food items is generally difficult, a statistical model has shown that the risks for fisheries products exceeding the Japanese regulatory limit was extremely low (Okamura *et al*., 2016). In fact, more than 99% of current results of the monitoring research off Fukushima are below 10 Bq/kg-wet for radiocesium (Figure 2.17).

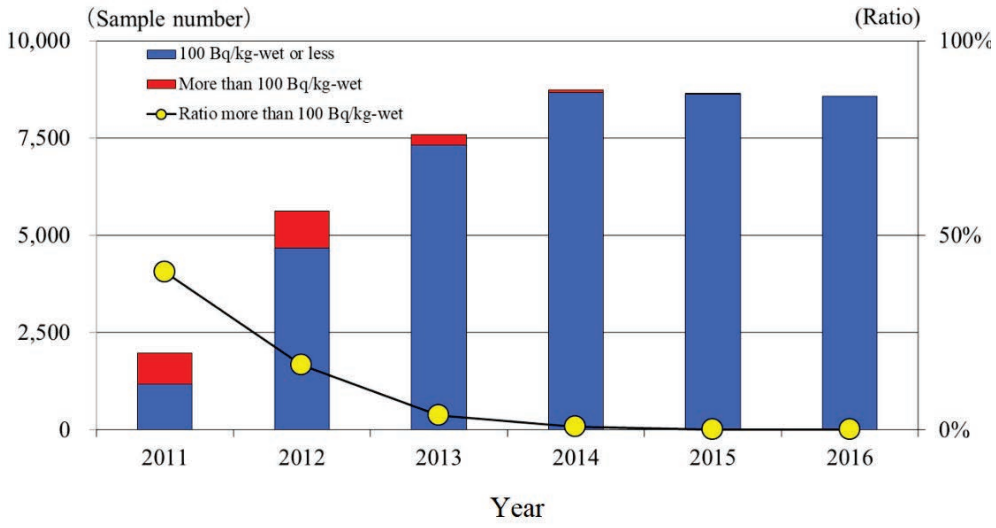

Fig. 2.16 Time series results for marine organisms showing quantities of samples having ^{137}Cs levels over the regulatory limit off Fukushima (JFA, 2017).

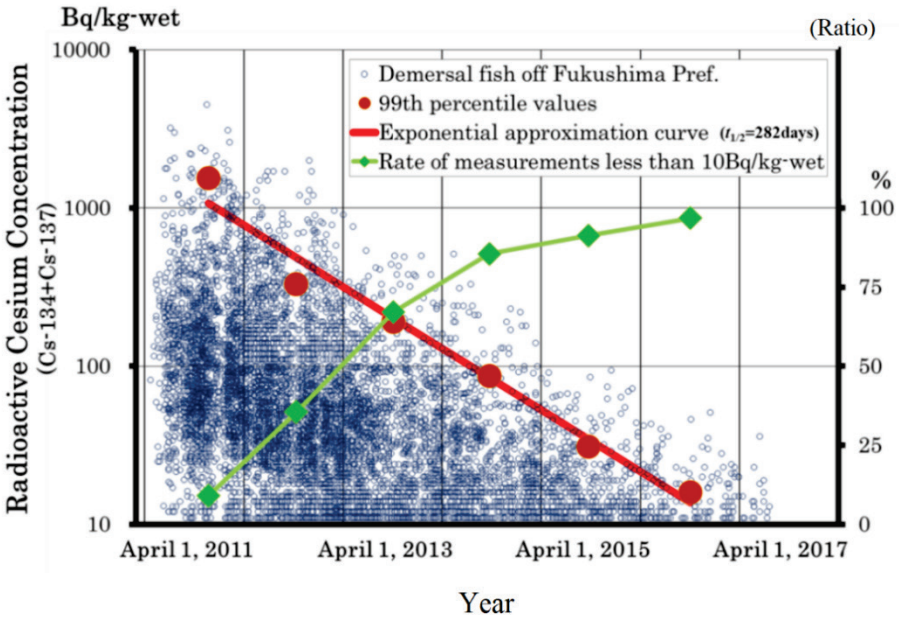

Fig. 2.17 Time series of radio cesium concentrations (^{134}Cs + ^{137}Cs) in demersal fish sampled off Fukushima following the FDNPP accident.

As noted in the previous Sections, radiocesium levels declined rapidly in seawater following the FDNPP accident and as a result, concentrations in pelagic fishes, invertebrates and seaweeds also decreased quickly because their radiocesium concentrations depend strongly on those in seawater. On the other hand, radiocesium concentrations in demersal fishes declined slowly (Buesseler *et al.*, 2012). The time series for radiocesium concentrations in demersal fishes off Fukushima Prefecture (Figure 2.17) is consistent with a half-life for radiocesium in these fishes of about 280 days. Some studies suggested that the slow decline of radiocesium in demersal fishes resulted from continuing contamination of their food source (benthic infauna) from sediments (Buesseler, 2012; Tateda *et al.*, 2013, 2015; Wada *et al.*, 2013; Sohtome *et al.*, 2014; Wang *et al.*, 2016). Previous research indicated that the bioavailability of radiocesium from contaminated sediment is typically low (Fowler and Fisher, 2005) because of the strong interaction of cesium with clay minerals (Comans and Hockley, 1992). However, some studies after the FDNPP accident reported the presence of organically bound radiocesium, which could be more bioavailable (Otosaka and Kobayashi, 2013; Ono *et al.*, 2015). On the other hand, year-class related differences in radiocesium concentration in some demersal fish species (*e.g.*, Pacific cod, and Japanese flounder, *Paralichthys olivaceus*) have been reported (Kurita *et al.*, 2015; Narimatsu *et al.*, 2015). The 2010 year-class and older fish had relatively higher concentrations of radiocesium than 2011 year-class and younger fish. The comparison of radiocesium concentrations among year-classes indicates that these fish species, especially those born after 2011 (after the FDNPP accident), incorporated only a small amount of radiocesium from the surrounding environment and the benthic food web. These studies concluded that the 2010 year-class and older fish with higher concentrations of radiocesium might have been contaminated mainly during the first few months after the FDNPP accident.

Ongoing sources of radiocesium to the ocean are known to be the FDNPP site, rivers and groundwater beneath some sand beaches (Sanial *et al.*, 2017). The ongoing releases of ^{137}Cs from the FDNPP harbor were estimated to be 3 TBq/y for the summer of 2012 (Kanda, 2013). Since the concentration of ^{137}Cs in the harbor decreased by a factor of 5 between 2013 and 2016, the present-day releases of ^{137}Cs from the FDNPP harbor are estimated to be about 0.6 TBq/y. The other sources, groundwater below the sandy beaches and rivers, are similar in magnitude to those from the FDNPP (Sanial *et al.*, 2017). However, the monitoring results have shown a continuing

decrease in the concentration of radiocesium in marine organisms (JFA, 2017; TEPCO, 2017), indicating that these ongoing sources are not a public health issue for Japan.

On August 1, 2012, 25,800 Bq/kg-wet of radiocesium (^{134}Cs = 9,800 Bq/kg-wet, ^{137}Cs = 16,000 Bq/kg-wet) was detected in the muscle tissue of two greenlings (*Hexagrammos otakii*) caught approximately 20 km north of the FDNPP. Although TEPCO had carried out an intensive investigation in a 20 km area from the FDNPP, similarly contaminated fish had not previously been caught. Shigenobu *et al*. (2014) estimated that the probability of similarly contaminated greenlings being found off the coast of Fukushima is exceedingly low. By contrast, heavily contaminated marine fishes were frequently caught in the FDNPP harbor (Fujimoto *et al*., 2015). The averages of ^{137}Cs concentrations in seawater collected from the Unit 1–4 intake canals of the FDNPP for June–August 2011 and April–September 2012 were calculated as 305 to 1,650 Bq/L and 17.1 to 209 Bq/L, respectively (Kanda, 2013). The CF for ^{137}Cs between the 25,800 Bq/kg-wet (^{137}Cs = 16,000 Bq/kg-wet) specimens and seawater around the Unit 1–4 intake canals for June–August 2011 and April–September 2012 ranged from 9.70 to 52.5 and from 76.6 to 936, respectively. The range of CF for June–August 2011 is consistent with previous findings in which the range of the CF for ^{137}Cs between demersal fish species and seawater around Japan was 15 to 54 (Tagami and Uchida, 2013). Accordingly, the radiocesium concentration in seawater within the FDNPP harbor before April–September 2012 was sufficient to contaminate greenlings at a level of 25,800 Bq/kg-wet. These results strongly suggest that the heavily contaminated greenlings caught approximately 20 km north of the FDNPP had incorporated their inventory of radiocesium within or close to the FDNPP harbor immediately after the accident before moving offshore. TEPCO now prevents fishes from entering and leaving the FDNPP harbor by using nets and other techniques (TEPCO, 2017). Afterward, greenlings having comparable concentrations with the greenlings caught on August 1, 2012 have never been detected outside of the port in the following monitoring programs.

Before the FDNPP accident, the main sources of ^{90}Sr in the North Pacific Ocean off Japan were global and from close-in radioactive fallout following atmospheric nuclear bomb tests and the Chernobyl Nuclear Power Plant accident (Bowen *et al*., 1980). The ^{90}Sr concentration in marine fishes of the North Pacific Ocean off Japan was 0.025 ± 0.021 Bq/kg-wet for the two decades prior to the FDNPP accident (Miki *et al*., 2017). The total ^{90}Sr released into the atmosphere from the FDNPP accident was estimated to be approximately 0.14 PBq (Povinec *et al*., 2012), a factor of 100 lower than the ^{137}Cs inputs (Aoyama *et al*., 2013; Kobayashi *et al*., 2013), and the amount of ^{90}Sr in the wastewater was estimated to be approximately 0.04 PBq. TEPCO published the data of ^{90}Sr concentrations in marine fishes, collected within a 20-km radius from the FDNPP (TEPCO, 2017). Most of the ^{90}Sr measurements were lower than 2.0 Bq/kg-wet. Since the FDNPP-derived ^{90}Sr in the marine environment was lower than for ^{137}Cs and the value of CF for radiostrontium in marine fishes is also lower (IAEA, 2004), then the concentrations of ^{90}Sr in marine fishes were expected to be lower than those of ^{137}Cs (Miki *et al*., 2017). The influence of the FDNPP accident on ^{90}Sr in marine fishes was limited to the area off Fukushima and was smaller than that on ^{137}Cs (Karube *et al*., 2016; Miki *et al*., 2017). Although high concentrations of ^{90}Sr were detected in the fishes caught within the FDNPP harbor, the mean ^{137}Cs/^{90}Sr activity ratio was close to 300 (Fujimoto *et al*., 2015).

2.5 Summary

Pre-accident levels of radioactivity in the marine environment off the east coast of Japan were evaluated using monitoring data collected during several different types of programs. The radioactivity environment was governed mainly by the influence of radionuclide fallout from atmospheric nuclear weapons tests in the last century. The short-term direct input of a large quantity of radioactivity from the FDNPP accident resulted in a non-equilibrium state of the marine ecosystem, particularly with regard to radiocesium. The enhanced monitoring of radionuclides implemented shortly after the accident revealed that radioactivity levels in the water and marine organisms were rapidly decreasing to levels typical of pre-accident conditions. Presently, no marine samples have been analyzed with concentrations above the Japanese radiological safety limit of 100 Bq/kg-wet, indicating that the commercial harvesting of Japanese marine fish and biota is now permitted.

3 Monitoring Results in the Northwest Pacific Ocean

3.1 Atmospheric radioactivity

The atmospheric pathway played a significant role in the wide geographic dispersion of radioactivity on a short time scale following the FDNPP accident. The atmospheric radioactivity derived from the accident was widely measured around the world (Masson *et al*., 2011; Achim *et al*., 2012; Biegalski *et al*., 2012; Bossew *et al*., 2012; Hirose, 2012; Kim *et al*., 2012; Long *et al*., 2012; Thakur *et al*., 2012; Tupin *et al*., 2012; Huh *et al*., 2013). A number of models were developed to simulate the temporal–spatial distribution of air concentrations and depositions of radionuclides derived from the accident and a comparison of different models was conducted by the World Health Organization (Draxler *et al*., 2015).

Although many studies on atmospheric radioactivity derived from the FDNPP accident were carried out, a bottom-up investigation on atmospheric radioactivity to understand its behaviors and radiological impacts was limited. In the study, the amount and composition of atmospheric radioactivity derived from the accident was collected as comprehensively as possible and compared with global fallout and the Chernobyl nuclear accident (CNA). The atmospheric impacts of the FDNPP accident were assessed from three perspectives, including natural background of radionuclide spectrometry, concentration limits from national standards, and radiological protection. The conceptual scheme of Fukushima-derived radionuclides with physical and physicochemical insights was discussed and illustrated to understand their fate in the atmosphere.

3.1.1 Atmospheric radioactivity derived from the FDNPP accident

The most critical radionuclides discharged to the atmosphere from the FDNPP accident were ^{131}I, ^{134}Cs, and ^{137}Cs (source terms of 60–390 PBq, 15–20 PBq, and 5–50 PBq, respectively) owing to their potential for providing high radiological doses to humans. Although the FDNPP accident was rated at the highest level in terms of potential radiological impact, the total amount of radioactivity (excluding radioactive noble gases) released into the environment was estimated to be 520 PBq, which was about 10% of that of the Chernobyl nuclear accident (Livingston and Povinec, 2002; Steinhauser *et al*., 2014) and less than 1% of global fallout (UNSCEAR, 2008). The quantity of ^{85}Kr and ^{133}Xe released from the FDNPP accident was larger than that of the CNA but was considered relatively insignificant from a radiological protection perspective owing to their low bioavailability and weak β energy. A comparison of radionuclide inputs among the FDNPP accident, CNA and global fallout is outlined in Table 3.1.

Table 3.1 Comparison of radionuclides among the FDNPP accident, CNA and global fallout (Unit: 10^{15}Bq).

	Fukushima Nuclear Accident		Chernobyl Nuclear Accident		Global Fallout	
	Atmosphere	**Ocean**	**Atmosphere**	**Ocean**	**Atmosphere**	**Ocean**
^{131}I	160[a]	11[g]	1760[i]			
^{137}Cs	15[a]	4[g]	85[i]	16[l]	950[i]	600[l]
^{90}Sr	0.14[b]	1[h]	10[i]		600[i]	380[l]
^{133}Xe	(1.2–1.5) × 10^{4}[c]		(2–6) × 10^{3}[j]			
^{85}Kr	44.1[d]		33[d]		5000[d]	
$^{239+240}$Pu	(1–2.4) × 10^{-6}[e]		0.1[k]		10[i]	
Total radioactivity[m]	520[f]		5300[k]		712,920[i]	

[a] Povinec *et al*., 2013a; [b] Povinec *et al*., 2013b; [c] Bowyer *et al*., 2011; Stohl *et al*., 2012b; [d] Ahlswede *et al*., 2013; [e] Zheng *et al*., 2012; [f] Steinhauser *et al*., 2014; [g] Kawamura *et al*., 2011; [h] Povinec *et al*., 2012; [I] UNSCEAR, 2008; [j] Ginzburg and Reis, 1991; [k] Livingston and Povinec, 2002; [l] IAEA, 2005; [m] Total radioactivity was not included radioactive noble gas.

Radioiodine was widely measured in the atmosphere after the FDNPP accident due to its highly fission yield, mobility, bioavailability and enhanced concentration in the human thyroid (Steinhauser *et al*., 2012). The total radioiodine concentration, including gas and particle phases, was underreported relative to the particulate radioiodine (Masson *et al*., 2011). ^{131}I and ^{132}I were widely reported in the northern hemisphere after the FDNPP accident, with half-lives of 8.04 days and 2.3 hours, respectively (Gudelis *et al*., 2013; Leppänen *et al*., 2013; Khan *et al*., 2014). Although the half-life of ^{132}I was short, its parent radionuclide with the relatively long half-life of ^{132}Te would support ^{132}I in the atmosphere. The atmospheric activity of total ^{131}I was conservatively assumed to be 10^{-2} Bq/m^3 while that of ^{132}I was about 10^{-4} Bq/m^3 according to global radioactive monitoring in the atmosphere (Masson *et al*., 2011, 2013; Thakur *et al*., 2013). Despite concern from a radiological perspective, the rapid decay and dispersion of radioiodine in the atmosphere meant that these isotopes quickly became insignificant as a human health issue.

The peak value of total atmospheric radioactivity derived from the FDNPP accident was mainly from radioactive noble gases in the early phase of the accident. These levels were about two orders of magnitude higher than the radioactive background of the atmosphere in Japan and comparable to natural radioactivity in other countries. The time scale for atmospheric radioactivity derived from the FDNPP accident to be globally dispersed was about 20 days (Hernández-Ceballos *et al*., 2012). Due to radioactive decay, atmospheric dilution and deposition, the total radioactivity derived from the FDNPP accident one month later was dominated by $^{134+137}$Cs at levels of less than 1 mBq/m^3, which was about four orders of magnitude lower than that of natural radioactivity levels in the atmosphere. Consequently, the radioactivity from the FDNPP accident, which lasted for a short period of time and was comparable to the natural radioactivity background of the atmosphere in the early stages of the accident, is considered to have had little impact on human health.

In this study, only the submersion and inhalation exposure pathways were considered for the atmospheric radionuclides derived from the FDNPP accident. The dose conversion factors for specific radionuclides were obtained from the No. 119 report of the International Commission on Radiological Protection (ICRP, 2012). The annually effective dose of natural radioactive noble gases, excluding radon and its progenies, is estimated at 8.07 nSv. The effective doses of radioactive noble gas and radionuclides derived from the FDNPP accident for the global public were 11.1 nSv and

59.6 nSv, respectively. The annual effective dose of naturally occurring radionuclides, excluding radon and its progenies, is about 53.7 μSv, which is several hundred times higher than the effective dose from the FDNPP accident. Meanwhile, the effective dose rate of radon and its progenies is about 1.2 mSv/y, contributing to about 50% of natural effective dose rate of 2.4 mSv/y in the world (Kónya and Nagy, 2012). The effective dose rate limiting for the public was 1 mSv/y by ICRP and several national standards, which was about four orders of magnitude higher than the total effective dose from the FDNPP accident.

3.1.2 FDNPP radionuclides as tracers of atmospheric processes

Although the atmospheric impacts of the FDNPP accident were not significant from a radiological perspective, Fukushima-derived radionuclides could be applied to trace atmospheric processes. The atmospheric behaviors of specific radionuclides derived from the FDNPP accident were variable. After the accident, the volatile radionuclides, including radioactive noble gases (^{85}Kr,^{131}Xe,^{133}Xe,^{133m}Xe), radiotellurium (^{129m}Te/^{129}Te, ^{132}Te), radioiodine (^{131}I,^{132}I), radiocesium (^{134}Cs,^{136}Cs,^{137}Cs), ^{35}S, and ^{140}Ba/^{140}La were preferentially released into the atmosphere and globally dispersed (Masson *et al*., 2011; Priyadarshi *et al*., 2011; de Vismes Ott *et al*., 2013; Thakur *et al*., 2013; Khan *et al*., 2014; Nitta *et al*., 2014). Other volatile radionuclides with short half-lives, semi-volatile and refractory radionuclides in aerosols were only observed in Japan, such as ^{3}H, ^{59}Fe, ^{86}Rb, ^{95}Zr/^{95}Nb, ^{99}Mo/^{99m}Tc, $^{103+106}$Ru, ^{110m}Ag, ^{113}Sn, ^{125}Sb, ^{127m}Te/^{127}Te, ^{129}I, ^{133}I, ^{236}U, ^{239}Np, ^{238}Pu, $^{239+240}$Pu, ^{241}Pu, ^{241}Am, ^{242}Cm and $^{243+244}$Cm (Kanai, 2012; Shozugawa *et al*., 2012; Doi *et al*., 2013; Matsumoto *et al*., 2013; Priyadarshi *et al*., 2013; Saegusa *et al*., 2013; Xu *et al*., 2013; Shinonaga *et al*., 2014). Other radionuclides such as ^{141}Ce, ^{144}Ce and ^{147}Pm were not observed in the environment after the FDNPP accident, while they were reported after the CNA (Buesseler *et al*., 1990).

The elevated levels of radioactivity lasted for a short time in the atmosphere and then declined owing to radioactive decay, atmospheric dilution and dry/wet deposition. The distinct behaviors of radionuclides in the atmosphere depended on the source term characteristics, including source magnitude and source height, meteorological conditions, atmospheric circulation on different temporal–spatial time scales and the physical and physicochemical properties of specific radionuclides.

The behavior of Fukushima-derived radionuclides followed the large-scale atmospheric circulation (Figure 3.1). The volatile radionuclides derived from the FDNPP accident were detected in the northern hemisphere and southern hemisphere within 20 days and one month after the accident, respectively (Orr *et al*., 2013; Thakur *et al*., 2013). Most of the radioactivity from the FDNPP accident was transported eastward by the westerlies and much of it was deposited in the North Pacific Ocean.

The vertical structure of the atmosphere governed the transport of radionuclides from the FDNPP accident which was carried through the planetary boundary layer and upper troposphere with velocities of 3 m/s and 22 m/s, respectively (Hong *et al*., 2012; Huh *et al*., 2012). The planetary boundary layer is the zone in which most human activity takes place at the base of the atmosphere. Most aerosols were measured at ground level, excluding some stations at high mountain elevations situated in the free troposphere (Evrard *et al*., 2012; Huh *et al*., 2012; Tositti *et al*., 2012; López-Pérez *et al*., 2013). The westerly winds rapidly transported the radionuclides from the FDNPP accident in the northern hemisphere with a speed between 50–70 km/h at a height of 5000 m (Masson *et al*., 2011; Hernández-Ceballos *et al*., 2012; Povinec *et al*., 2013a). Vertical exchange among the lower stratosphere, free troposphere and planetary boundary layer would then govern radioactivity levels in each phase. The vertical structure of the atmosphere modified from Wallace and Hobbs (2006) is illustrated in Figure 3.2.

The physicochemical properties of each isotope also influence their specific atmospheric pathway. The inert radioactive noble gases (^{85}Kr, ^{133}Xe) are conservatively transported in the atmosphere and are affected only by atmospheric dilution and physical decaying (Stohl *et al*., 2012a; Nitta *et al*., 2014). In contrast, particle reactive radionuclides, such as radiocesium and radiotellurium, are rapidly adsorbed on aerosols and subject to scavenging and dry/wet deposition in addition to subsequent resuspension by wind action (Igarashi *et al*., 2003; Kaneyasu *et al*., 2012).

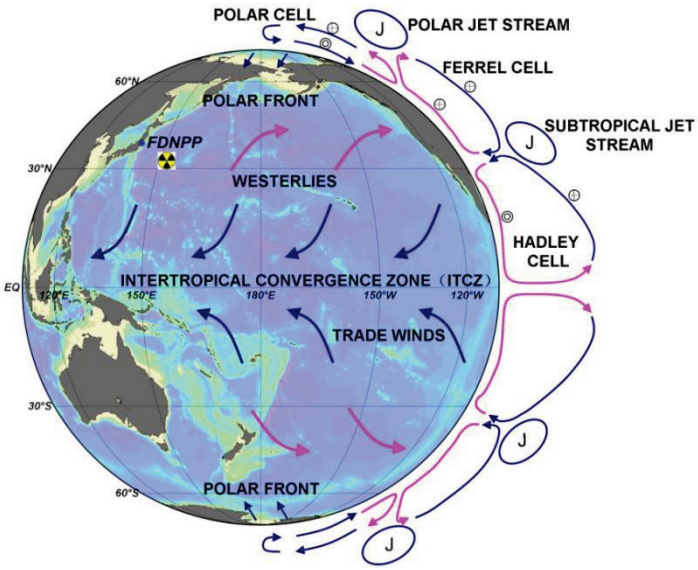

Fig. 3.1 Large-scale zonal and meridian circulation of the atmosphere.

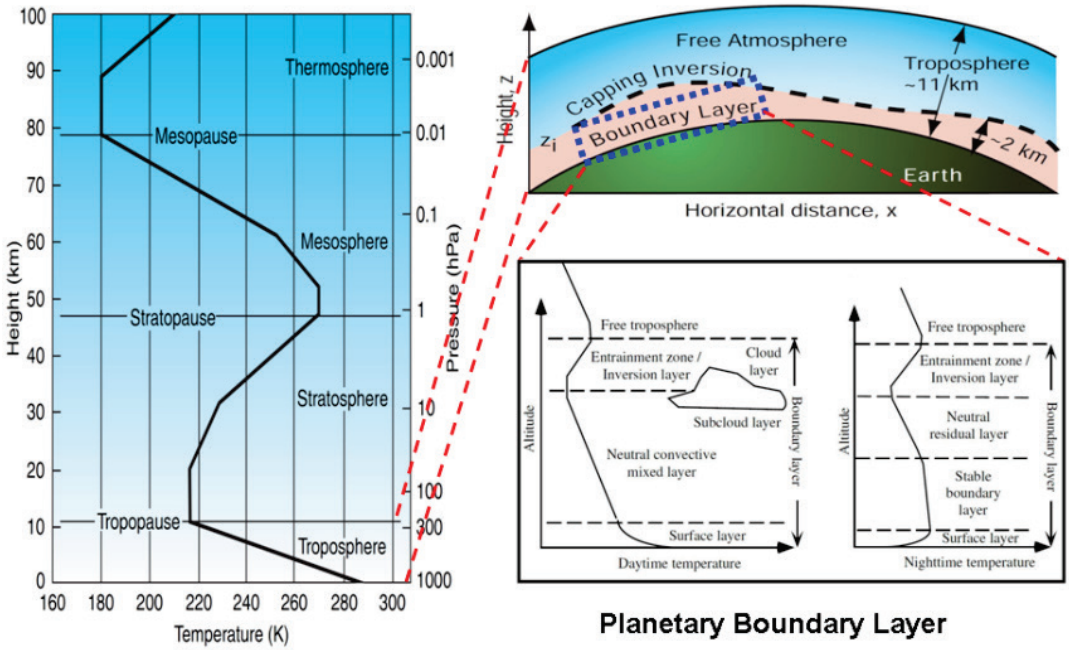

Fig. 3.2 Vertical structure of the atmosphere, including the planetary boundary layer. Modified from Wallace and Hobbs (2006).

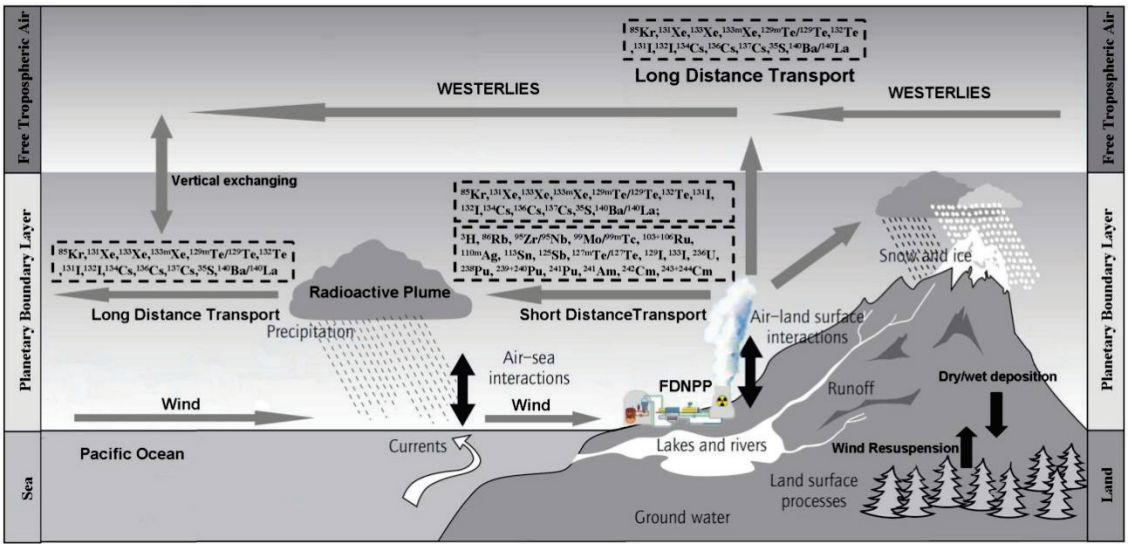

Fig. 3.3 Conceptual scheme of Fukushima-derived radionuclides in the atmosphere.

The physicochemical properties of some radionuclides, such as radioiodine, are complicated with multivalence. Transfer between gas and particulate phases by radioiodine occurs during its transport in the atmosphere (Mietelski *et al*., 2014), with generally 70% of the total radioiodine residing in the gas phase (Masson *et al.*, 2011). The dispersion of Fukushima-derived radionuclides in the atmosphere by these processes is illustrated in Figure 3.3.

3.1.3 Summary

The most critical radionuclides discharged to the atmosphere from the FDNPP accident were ^{131}I, ^{134}Cs, and ^{137}Cs (source terms of 60–390 PBq, 15–20 PBq and 5–50 PBq, respectively) owing to their potential for providing high radiological doses to humans. Although the FDNPP accident was rated at the highest level in terms of potential radiological impact, the total amount of radioactivity (excluding radioactive noble gases) released into the environment was estimated to be 520 PBq, which was about 10% of that of the Chernobyl nuclear accident (Livingston and Povinec, 2002; Steinhauser *et al*., 2014) and less than 1% of global fallout (UNSCEAR, 2008). The peak value of total atmospheric radioactivity derived from the FDNPP accident was mainly from radioactive noble gases in the early phase of the accident. These levels were about two orders of magnitude higher than the radioactive background of the atmosphere in Japan and comparable to natural radioactivity in other countries.

Due to radioactive decay, atmospheric dilution and deposition, the total radioactivity derived from the FDNPP accident one month after the FDNPP accident was dominated by $^{134+137}$Cs at levels of less than 1 mBq/m^3, which was about four orders of magnitude lower than that of natural radioactivity levels in the atmosphere. Consequently, the atmospheric radioactivity release from the FDNPP accident, which lasted for a short period of time and was comparable to the natural radioactivity background of the atmosphere in the early stages of the accident, is considered to have had little impact on human health.

The effective doses of radioactive noble gas and radionuclides derived from the FDNPP accident for the global public were 11.1 nSv and 59.6 nSv, respectively. The annual effective dose of naturally occurring radionuclides, excluding radon and its progenies, is about 53.7 μSv, which is several hundred times higher than the effective dose from the FDNPP accident. The effective dose rate limiting for the public was 1 mSv/y by ICRP and several national standards, which was about four orders of magnitude higher than total effective dose from the FDNPP accident.

3.2 Monitoring results from Japan

In addition to coastal monitoring proximal to Fukushima, FRA established an offshore program for the collection of seawater samples in a broad region of the western North Pacific (Figure 3.4) soon after the FDNPP accident. Kaeriyama (2015, 2017) and Kaeriyama *et al*. (2016) summarized the results of this and other work on the oceanic dispersion of radiocesium derived from the accident. The most important pathway of FDNPP-derived radiocesium in the North Pacific is surface dispersion to the east in the region north of the Kuroshio Extension (Figure 3.5). The other important pathway of FDNPP radiocesium is intrusion into the mode waters. The elevation of radiocesium in seawater in adjacent seas (*e.g*., East China Sea, Okhotsk Sea and Bering Sea, *etc*.) immediately after the FDNPP accident was small or negligible (Kim *et al*., 2012; Ramzaev *et al*., 2013; Kaeriyama, 2015).

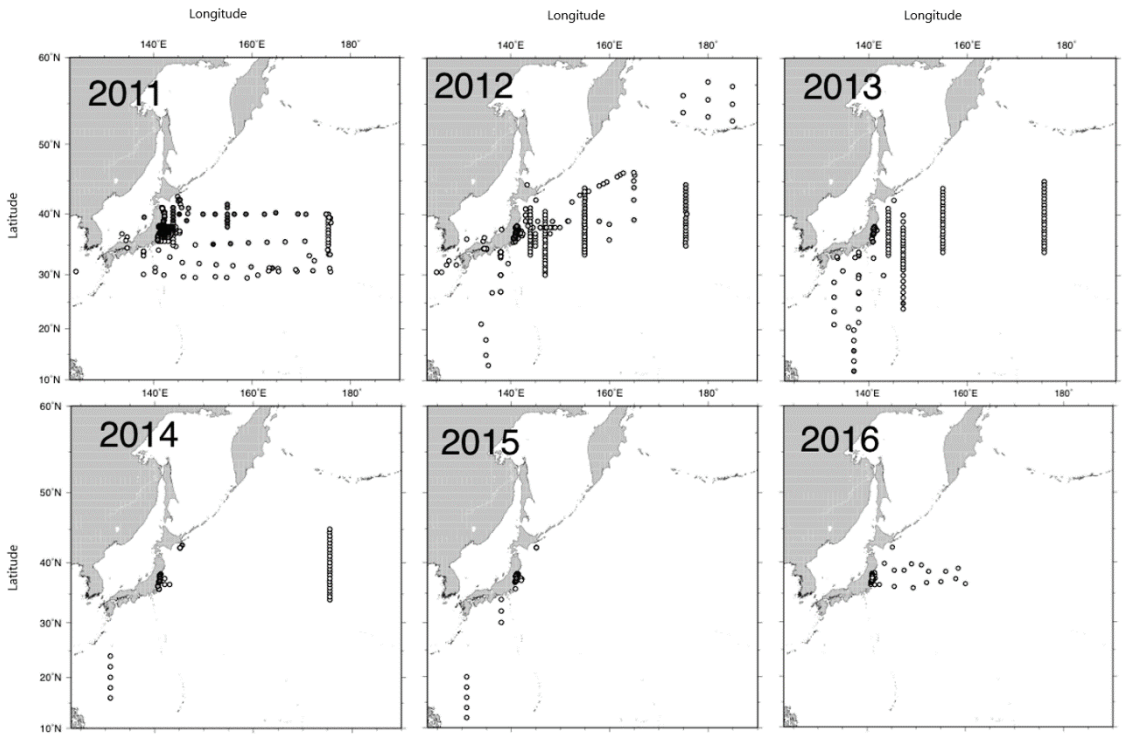

Fig. 3.4 FRA sampling locations of seawater for measurements of ^{134}Cs and ^{137}Cs in each year during 2011–2016.

3.2.1 Surface dispersion

Measurements of radiocesium in the North Pacific east of Japan in 2011–2013 (Figure 3.5), combined with particle tracking experiments (Figure 3.6), showed that the FDNPP-derived radiocesium had been dispersed eastward into the central North Pacific following the FDNPP accident. High ^{134}Cs and ^{137}Cs concentrations of more than 10 Bq/m^3 were observed in the area in the northern part of the Kuroshio Extension (144°E and 155°E) in July 2011, in the area 147–175°E around 40°N in October 2011, and in the northern part of the Kuroshio Extension in the central area (155°E and 175°30′E) in July 2012. In the mid-latitude region, around 40°N, high concentrations of ^{137}Cs more than 50 Bq/m^3 were observed in the western–central North Pacific during July–December 2011. From the temporal changes of the ^{134}Cs concentration Aoyama *et al.* (2013)

estimated the eastward speed of the FDNPP-derived radiocesium plume as 8 cm/s, which was consistent with flow velocities estimated from Argo float data. The main inventory of this FDNPP-derived radiocesium was located in the central part of the North Pacific until about December 2012 (Kaeriyama *et al*., 2013; Kumamoto *et al*., 2014). Subsequently, concentrations of ^{137}Cs off the east coast of Japan (except for the coastal region of the FDNPP site) markedly decreased owing to the absence of continuing large inputs from FDNPP.

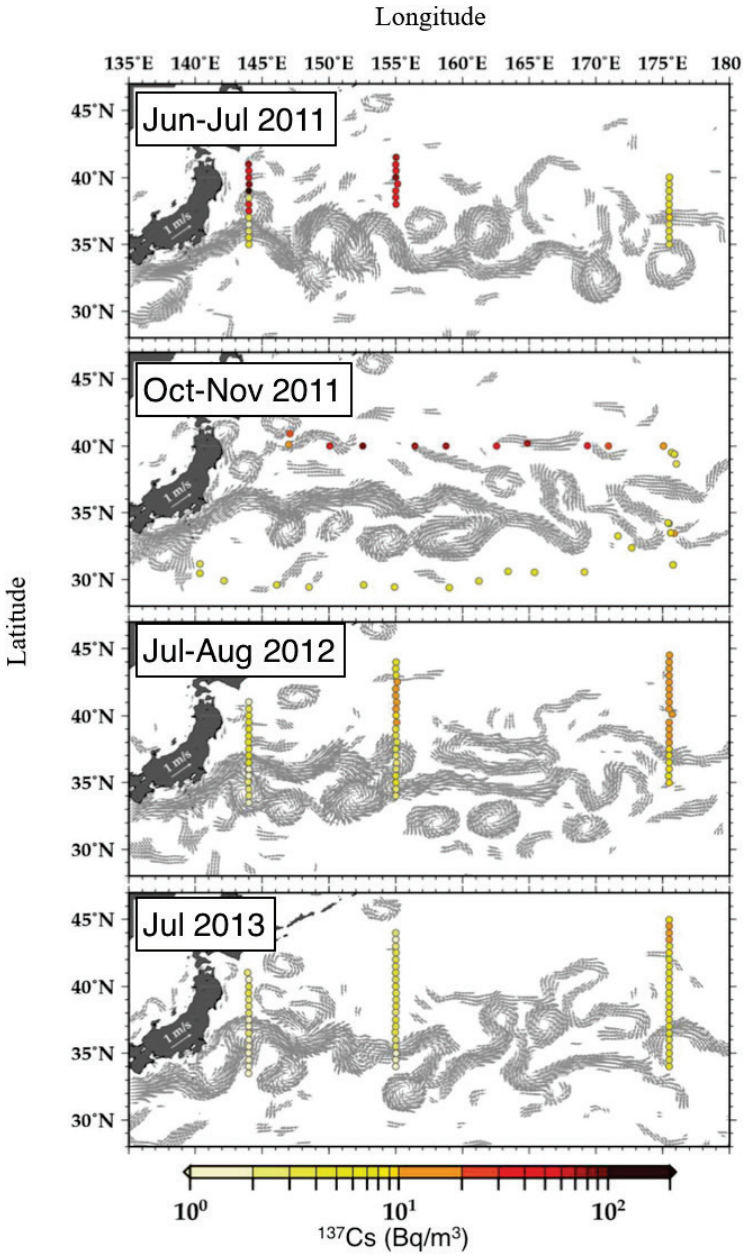

Fig. 3.5 Sampling locations for surface seawater in the western and central North Pacific. Closed circles indicate the sampling stations. Color of the closed circles indicates the concentration of ^{137}Cs in the surface seawater. Gray arrows indicate the estimated temporal mean velocity vectors of the Kuroshio Extension. Modified from Kaeriyama (2015).

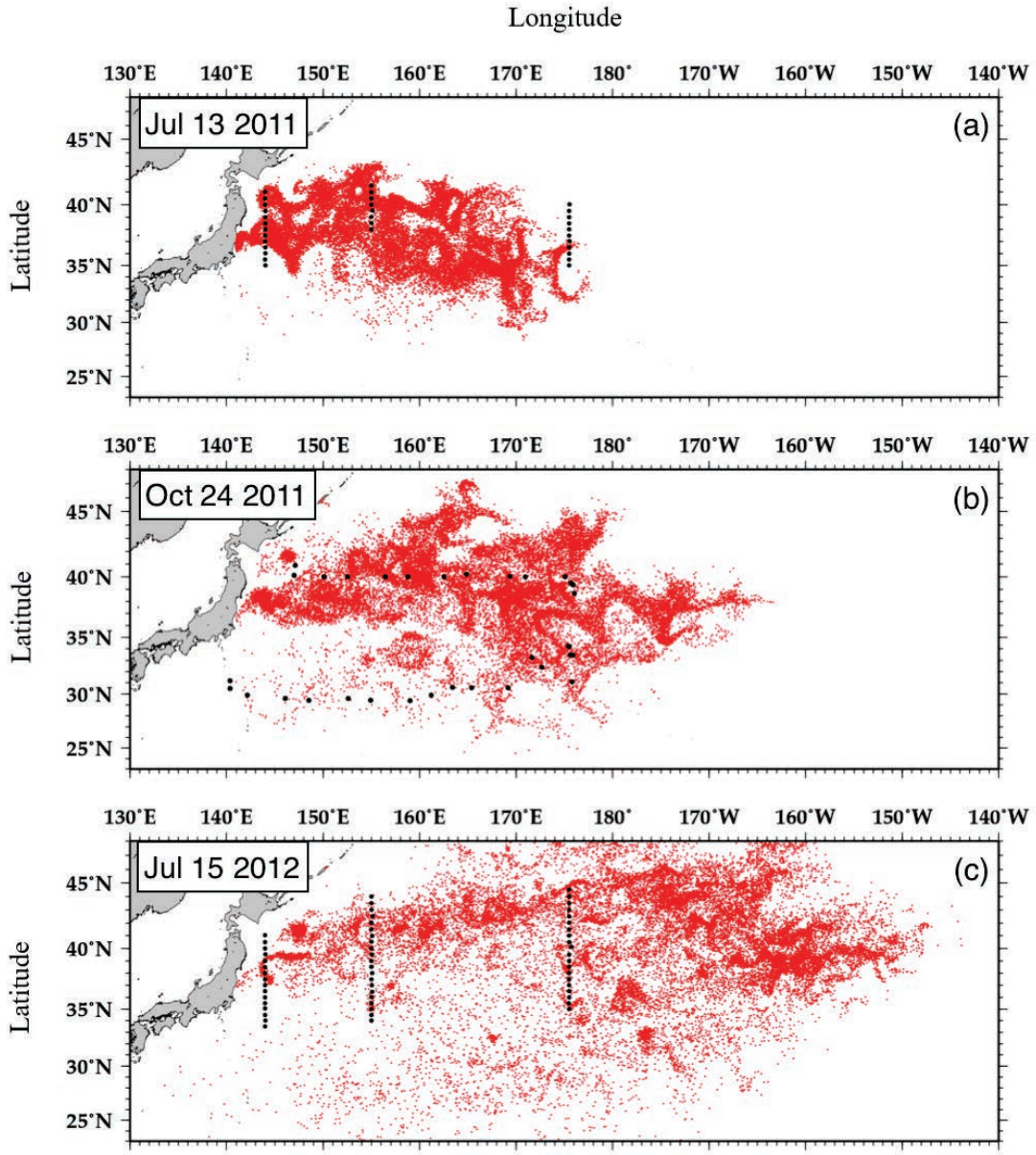

Fig. 3.6 Results of particle tracking experiments at the median date of each sampling period. Closed red circles indicate pseudo-particles. Closed black circles indicate sampling locations for radiocesium measurement. Modified from Kaeriyama *et al*. (2013).

3.2.2 Intrusion into mode waters

Aoyama *et al.* (2008) reported two sub-surface peaks of ^{137}Cs derived from nuclear weapons tests at the potential density ranges of 25.0–25.6 σ_θ and 26.0–26.6 σ_θ in the Subtropical Mode Water (STMW) and Central Mode Water (CMW). After the FDNPP accident, subsurface intrusion of FDNPP-derived radiocesium associated with these mode waters has been further reported (Kumamoto *et al*., 2014; Kaeriyama, 2015; Men *et al*., 2015; Yoshida *et al*., 2015; Aoyama *et al*., 2016; Kaeriyama *et al*., 2016). Kumamoto *et al*. (2014) reported the appearance of a subsurface peak of Fukushima-derived radiocesium at a water depth of 300 m within STMW along 149°E during December 2011–February 2012, in the subtropical region quite far south of the FDNPP and just south of the Kuroshio Extension. This means that the FDNPP-derived radiocesium had been intruded into the subsurface water mass (mode water) soon after the accident, probably during the

late winter of 2011 (March–April 2011). In a vertical cross-section of ^{137}Cs in STMW formation areas (147°E and 155°E transects) during October–November 2012, Kaeriyama *et al*. (2016) revealed that most of the FDNPP-derived radiocesium occurred in two mode waters (STMW and CMW) rather than in the surface water in the northern area of Kuroshio Extension (Figure 3.7). They also estimated the total amount of ^{134}Cs within the STMW, decay-corrected to April 2011 to be 4.2 ± 1.1 PBq, corresponding to 22–28% of the total amount of ^{134}Cs released to the Pacific Ocean. Kumamoto *et al*. (2014) estimated the total amount of ^{134}Cs in STMW during December 2011–February 2012 to be 6.0 PBq, which intruded into the STMW during March and April 2011. Since STMW is lighter than CMW, it outcropped into the surface layer during the next winter season, bearing in mind that the volume of STMW varies year to year (Oka *et al*., 2015). The estimated value of 4.2 PBq of ^{134}Cs in STMW by Kaeriyama *et al*. (2016) probably represents the result of two winter–spring periods of deep mixing (March–April 2011 and February–April 2012) as well as one period of outcropping in the surface water during the second winter–spring time interval (February–April 2012).

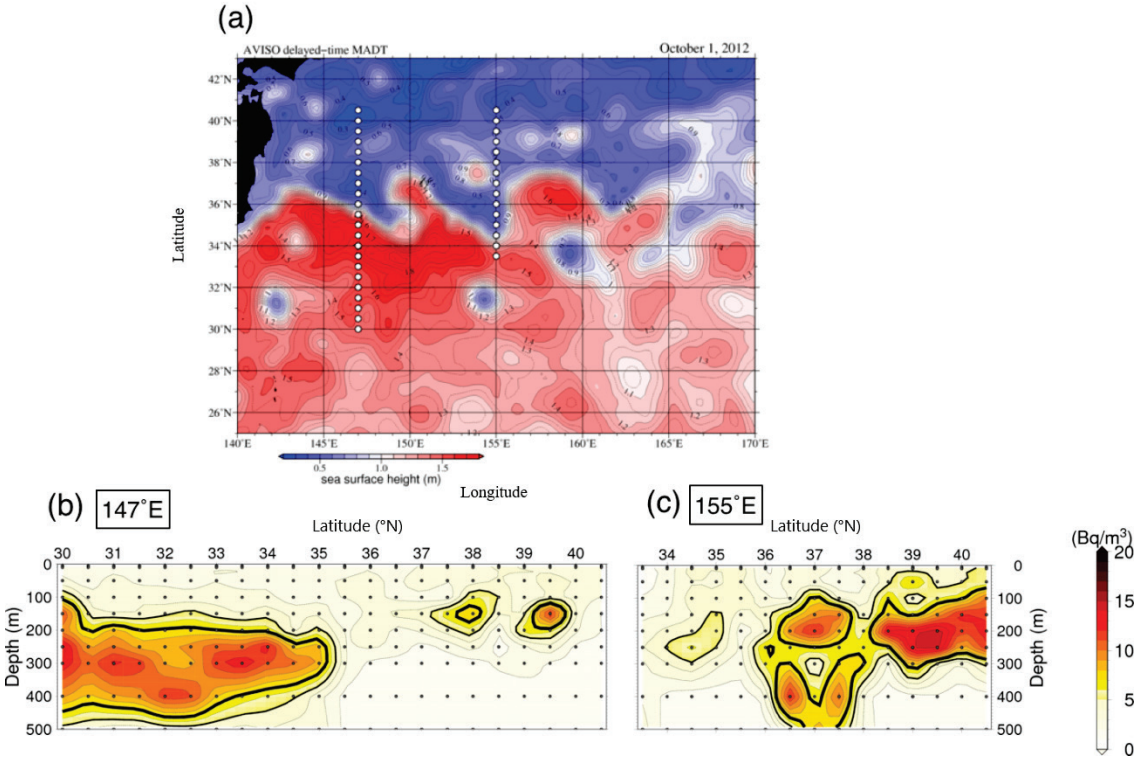

Fig. 3.7 (a) Sampling locations (closed white circles) for radiocesium measurements during October and November 2012 along the 147°E and 155°E transects. Background of the map is sea surface height distribution on October 1, 2012. Vertical cross-section views of ^{137}Cs (b) along 147°E, and (c) along 155°E. Black dots show locations for radiocesium measurements. Bold lines indicate ^{137}Cs activity isolines of 5 Bq/m^3 and 7 Bq/m^3, respectively. Modified from Kaeriyama *et al*. (2016).

In the downstream region of the STMW (12–30°N, 135–138°E), Kaeriyama (2015) reported the temporal change of FDNPP-derived radiocesium during August 2011 and March 2013 at stations indicated in Figure 3.8. Vertical profiles of ^{134}Cs and ^{137}Cs (Figure 3.9) typically exhibited subsurface peaks at the 300 m depth level at which STMW was distributed. The southernmost location (Sta. A04 in Figure 3.8) at which FDNPP-derived ^{134}Cs was measured (1.5−6.8 Bq/m^3) was 18°N, 135°E (September 2012).

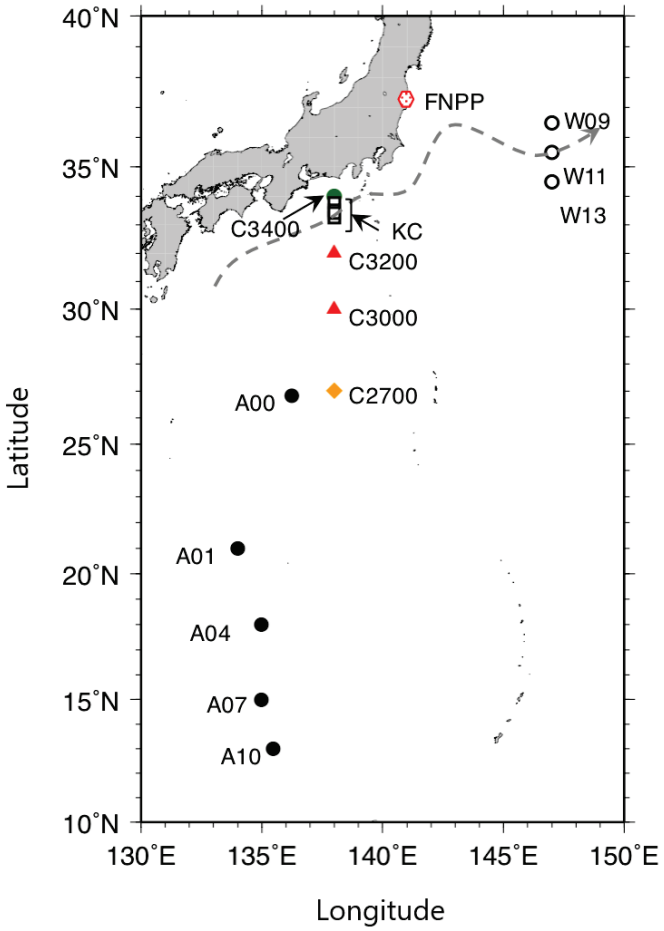

Fig. 3.8 Sampling locations for radiocesium measurements during August 2011 and March 2013.

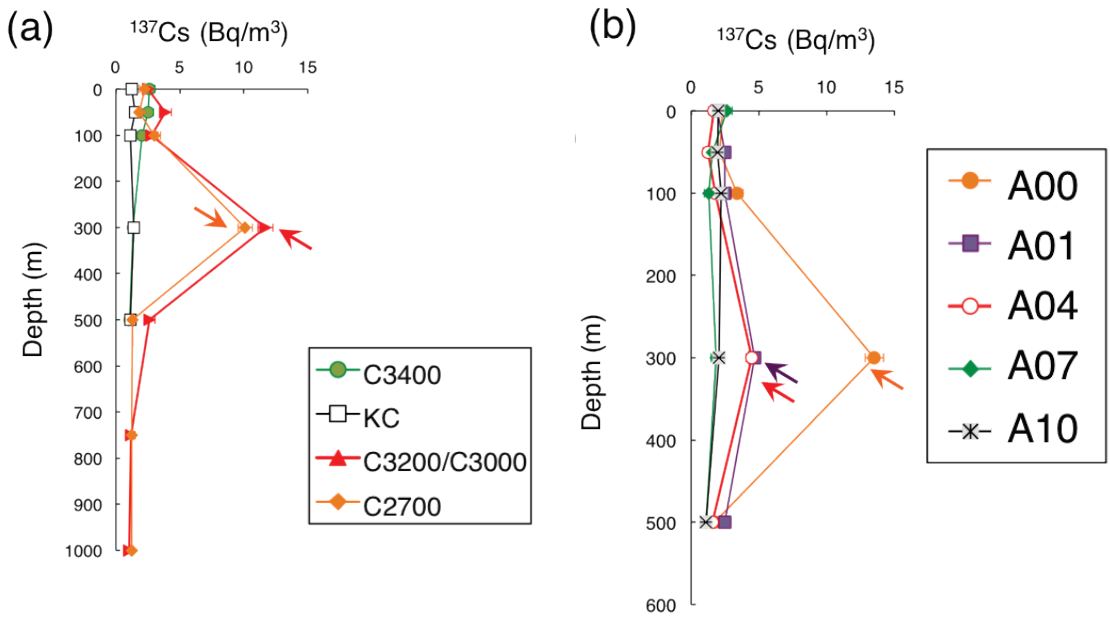

Fig. 3.9 Vertical profiles of ^{137}Cs at (a) four stations along 137°E in August 2012 and (b) five stations around 135°E in September 2012. Arrows indicate the detection of ^{134}Cs. Error bars indicate counting error ($\pm 1\sigma$). Modified from Kaeriyama *et al*. (2014).

The seasonal changes in the ^{137}Cs inventory within the 0–500 m depth range (Figure 3.10) showed an increase in the inventory following the second winter season (December 2011–April 2012). Kaeriyama *et al*. (2014) suggest that the FDNPP-derived radiocesium in STMW had intruded into the subtropical area following the second winter season after the FDNPP accident. In the formation area of CMW, Aoyama *et al*. (2016) reported FDNPP-derived radiocesium in both STMW and CMW along the 165°E transect during June 2012. Most of the FDNPP-derived radiocesium (more than 80% of the water column inventory) had been distributed in the CMW at the 165°E transect location. Kaeriyama *et al*. (2016) also reported FDNPP-derived radiocesium in CMW north of the Kuroshio Extension along 155°E during October–November 2012. The subsurface penetration pathways of FDNPP-derived radiocesium have not yet been fully clarified. The subsurface radiocesium in mode waters derived from the FDNPP accident should probably be monitored in the future because it represents a significant fraction of the total FDNPP input to the North Pacific (Aoyama *et al*., 2016; Kaeriyama *et al*., 2016).

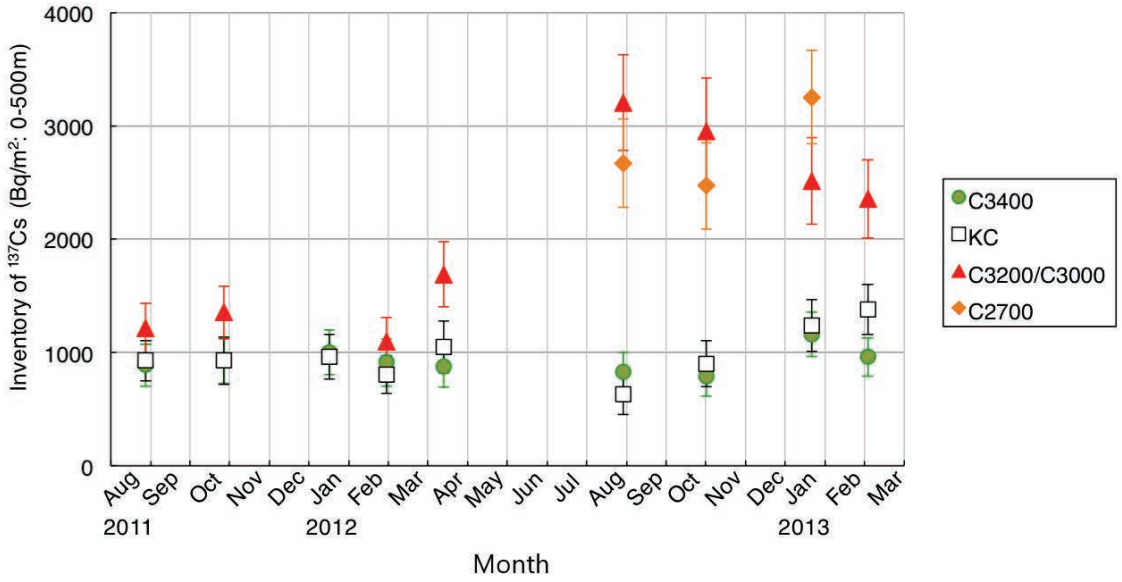

Fig. 3.10 Water column inventories of ^{137}Cs between 0 and 500 m water depths along 137°E from August 2011– March 2013. Modified from Kaeriyama *et al*. (2014).

3.3 Monitoring results from the People's Republic of China

To understand the transport of radioactive pollutants released from the FDNPP accident in the Northwest Pacific and their potential impact, 10 monitoring cruises were conducted by the State Oceanic Administration (SOA) of the People's Republic of China from 2011–2015 (one cruise every half year). The sampling stations of each cruise are shown in Figure 3.11 with more than 400 stations being occupied. ^{134}Cs and ^{137}Cs were measured using an AMP (ammonium phosphomolybdate) coprecipitation-γ spectrometry method (Men *et al*., 2015; Yu *et al*., 2015) while ^{90}Sr was measured by a Bis (2-ethylhexyl) phosphate (HDEHP) extraction-β counting method.

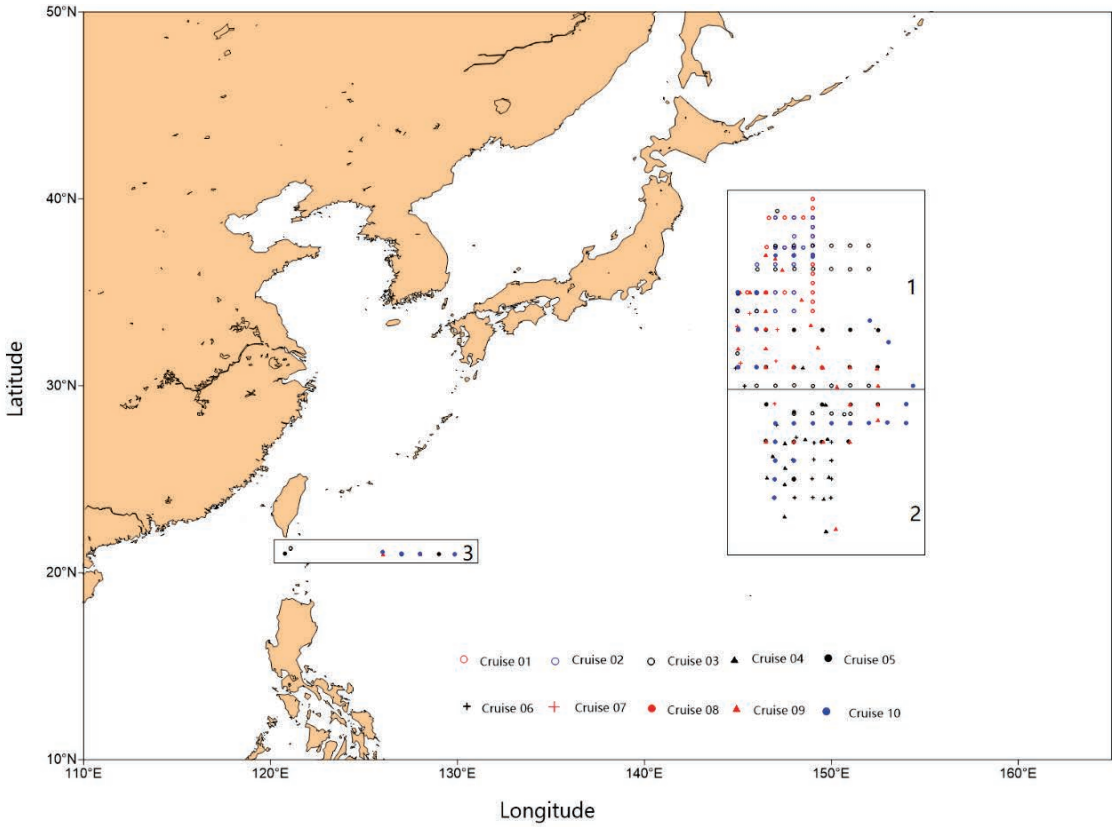

Fig. 3.11 Sampling stations for State Oceanic Administration (SOA) cruises in the Northwest Pacific during 2011–2015.

3.3.1 Environmental setting

The two main current systems in the Northwest Pacific oceanic region are the Kuroshio Current extension distinguished by high temperatures and salinities and the Oyashio Current by low temperatures and salinities (Shimizu *et al*., 2001). The Oyashio Current, flowing southward along the east coast of Japan, joins with the northward Kuroshio Current at 35°N and flows eastward into the North Pacific. The monitoring region was located to the east of the Japanese Exclusive Economic Zone, mainly on the northern side of the Kuroshio Extension which is on the main pathway for the eastward transport of the FDNPP radioactivity discharge plume.

The monitoring region's average surface dynamic topography during June and July of 2011, calculated geostrophic flows and the sampling stations of seawater and biota are shown in Figure 3.12. The surface dynamic topography data were quasi-real-time multi-source integrated altimetry data from TOPEX/Poseidon, Jason and ERS1/2 satellites provided by AVISO (www.aviso.oceanobs.com/). The spatial resolution of the data was 1/3º and the time resolution was 7 days, with a correction for tides and sea level pressure. The dynamic topography was established according to the method proposed by Livingston and Povinec (2002) using satellite altimetry data combined with climatological temperature and salinity data (WOA01). At the main axis of the Kuroshio Extension, the flow velocity attained values over 100 cm/s, while the flow velocity was much lower at the cyclonic and anti-cyclonic mesoscale eddies proximal to the Kuroshio Extension.

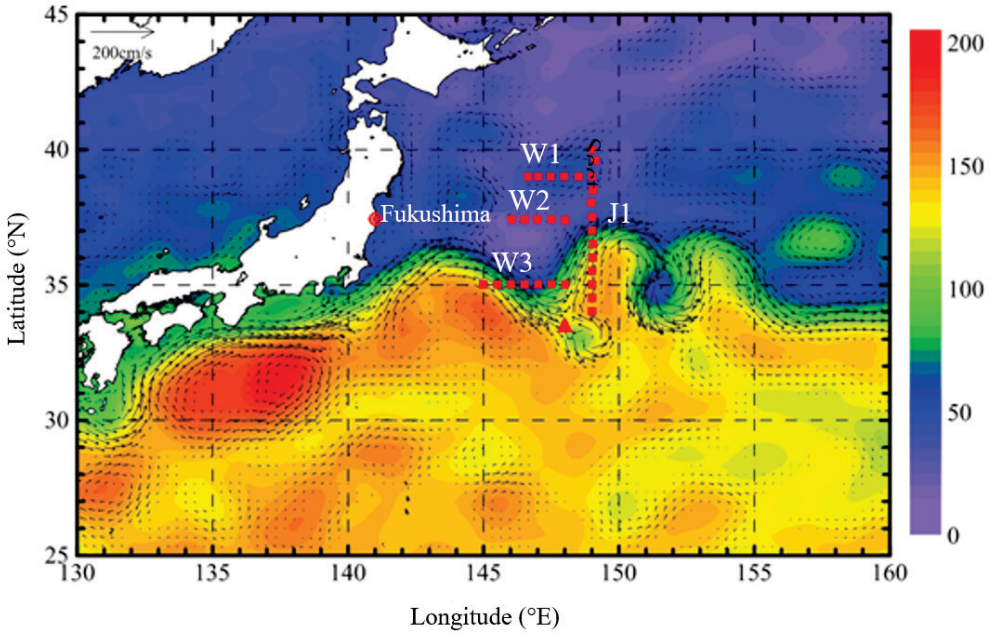

Fig. 3.12 Map of surface dynamic topography (cm), geostrophic flows (black arrows) and the sampling stations (solid red squares for seawater and solid red triangle for biota). Geostrophic flow velocities below 10 cm/s not shown.

3.3.2 Seawater

Radionuclide results from water depths 0 – 50 m

^{137}Cs and ^{134}Cs are two of the most important radioactive contaminants released from a nuclear power plant accident due to their large fission yield and relatively long half-lives (30.2 years and 2.1 years, respectively). Nuclear weapons testing and the Chernobyl Nuclear Power Plant accident in the last century have been the largest sources for ^{137}Cs in the marine environment (IAEA, 2004). From 2000 to 2010, the radioactivity of ^{137}Cs in surface seawater near Japan ranged from 0.04 to 3.4 Bq/m^3 (average 1.7 ± 0.6 Bq/m^3 (n = 961)) in this region (IAEA, 2004). ^{90}Sr is another important radionuclide released from a nuclear accident because of its relatively long half-life (28.6 years) and high affinity for the bones of biota. Atmospheric weapons testing and the Chernobyl nuclear accident also released large amounts of ^{90}Sr into the marine environment. The pre-Fukushima background activity of ^{90}Sr in surface seawater in the Northwest Pacific was 0.01 to 2.6 Bq/m^3 (average = 1.2 ± 0.4; n = 871; IAEA (2004)).

Results from the FDNPP accident showed that the levels of ^{137}Cs and ^{134}Cs in the upper 50 m ranged from 1 to 826 Bq/m^3 and 1 to 757 Bq/m^3, respectively. The median values of these two radionuclides' radioactivity were both in the 35–55 Bq/m^3 range. About 65% of the data was less than 100 Bq/m^3, while only 1% of ^{137}Cs data was more than 800 Bq/m^3, and 1% of ^{134}Cs data was more than 700 Bq/m^3. ^{137}Cs and ^{134}Cs activity data were distributed in similar patterns (Figure 3.13).

The horizontal distribution pattern for ^{134}Cs in surface seawater shown in Figure 3.14 was similar due to their equivalent biogeochemical behavior. Both of the ^{137}Cs and ^{134}Cs activities were higher in the surface seawater at the middle and east of section W2 (along 37.4°N) than in the other areas. The largest value was observed at station W2-7 (148.0°E, 37.4°N). The lateral distribution patterns were similar at depths of 20 m and 50 m as in surface water.

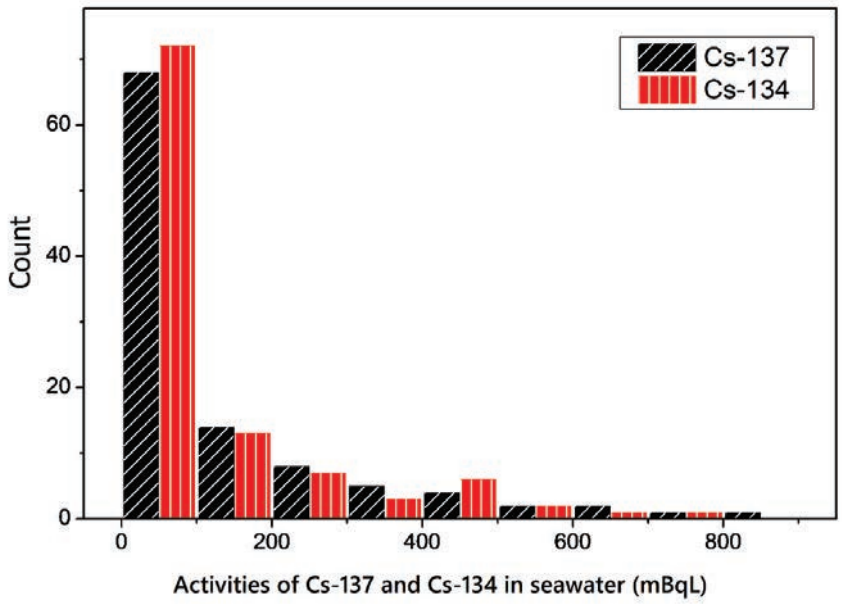

Fig. 3.13 Histogram of ^{137}Cs and ^{134}Cs activities in seawater in the Northwest Pacific off Japan during June–July 2011.

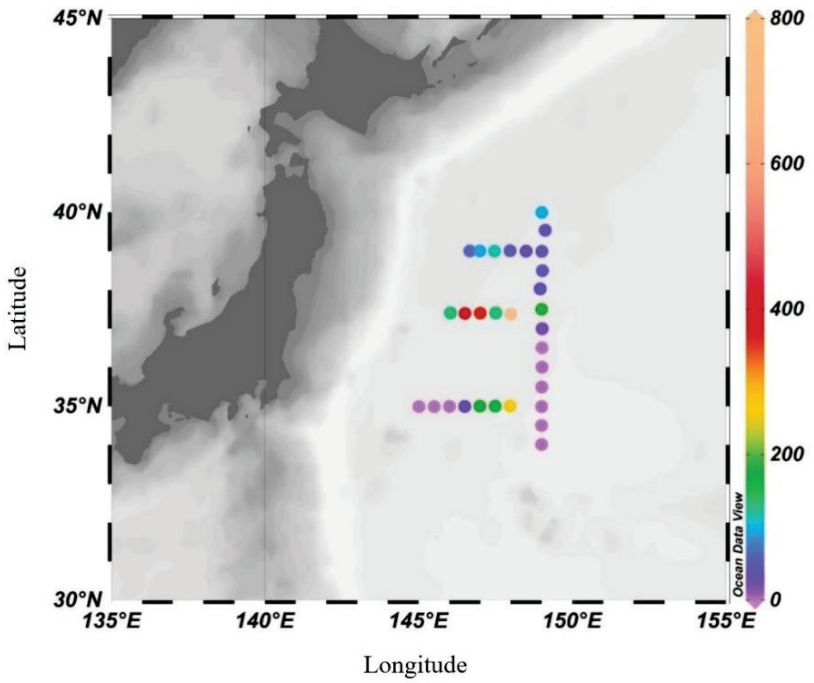

Fig. 3.14 Horizontal distribution of ^{134}Cs (Bq/m^3) in surface seawater in the Northwest Pacific off Japan during June–July 2011.

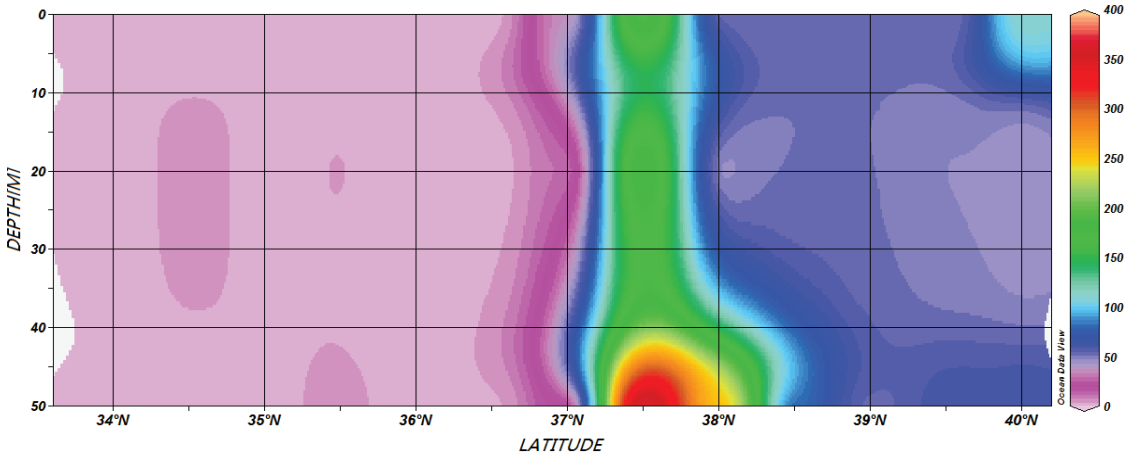

Fig. 3.15 Distribution of ^{137}Cs activity (Bq/m^3) in surface seawater on section J4.

The profile of ^{137}Cs activity in seawater at section J4 (Figure 3.15) showed that activity was higher at the northern side of the Kuroshio Extension (35°N) than that at the southern side, revealing the Kuroshio Extension's barrier effect on transport of the FDNPP accident radionuclides. However, a portion of the radionuclides was transported southward across the Kuroshio Extension by the North Pacific Mode Water (Men *et al.*, 2015).

The ^{134}Cs activity was decay-corrected to the date of the accident, March 11, 2011, and plotted against ^{137}Cs activity in Figure 3.16. The slope of the linear fit was 0.983, very close to the typical FDNPP accident-derived ^{134}Cs/^{137}Cs ratio of 1 (Masson *et al.*, 2011; Buesseler *et al.*, 2012; Merz *et al.*, 2013), indicating that virtually almost all of the measured radioactivity was derived from the accident.

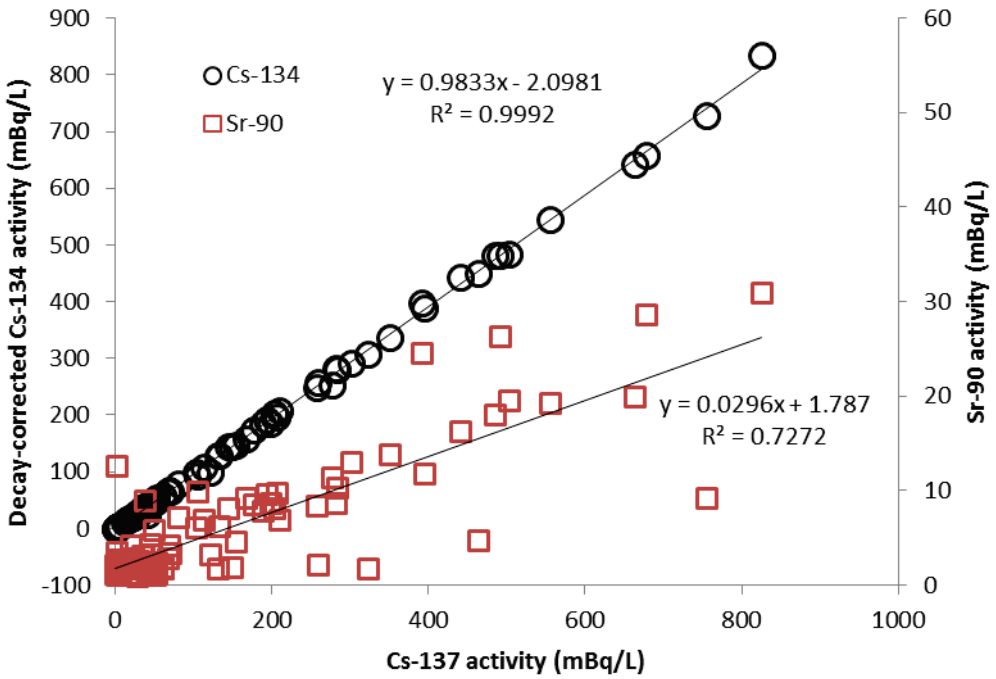

Fig. 3.16 Decay-corrected ^{134}Cs and ^{90}Sr activities plotted against ^{137}Cs activity.

Owing to the complicated and laborious analytical method for ^{90}Sr, the radioactivity of ^{90}Sr in seawater was widely evaluated after the FDNPP accident (Povinec *et al.*, 2012; Casacuberta *et al.*, 2013). The seawater ^{90}Sr activity in the monitoring region ranged from 1 to 31 Bq/m^3, and the median was 2 Bq/m^3. At the depth of 0 m, 20 m and 50 m, all the minimum activities of ^{90}Sr were 1 Bq/m^3. The maximum activities of ^{90}Sr at these depths were 31 Bq/m^3, 26 Bq/m^3 and 29 Bq/m^3, and the medians were 2 Bq/m^3, 2 Bq/m^3 and 3 Bq/m^3, respectively. The distribution pattern of ^{90}Sr was similar to that of ^{137}Cs and ^{134}Cs. The activities of ^{90}Sr were also higher at the middle and eastern part of section W2, with the highest value observed at station W2-7.

The measured ^{90}Sr activity plotted against ^{137}Cs activity in Figure 3.16 shows the slope of the linear fit was 0.029, comparable with the $^{90}Sr/^{137}Cs$ ratio (0.01–0.02) reported by Buesseler (2012) and Periáñez *et al.* (2013). The R^2 of the linear fit of 0.727 is lower than that of the $^{134}Cs/^{137}Cs$ linear fit, probably because of the difference between the biogeochemical behavior of Sr and Cs in addition to differences in the timing of the Sr and Cs releases. Compared with the background data noted above, the observed highest ^{90}Sr activity (31 Bq/m^3) was as much as 26 times the average background and the observed median ^{90}Sr activity was twice the average background activity. In addition to ^{134}Cs, ^{137}Cs and ^{90}Sr, other radionuclides such as ^{110m}Ag, ^{58}Co and ^{60}Co were analyzed, but the results were below the detection limits (0.36 Bq/m^3, 0.36 Bq/m^3 and 0.41 Bq/m^3 for ^{110m}Ag, ^{58}Co and ^{60}Co, respectively).

Radionuclide results from water depths > 50 m

Deep seawater samples were collected during May–June 2012. During theses cruises, a total of 52% of the surface samples contained ^{134}Cs. However, that amount increased to 70% and 69% at the 100-m and the 200-m layers, respectively. Generally, ^{134}Cs was detectable as far south as 21°N and as far east as 152°E (Fig. 3.17) while ^{137}Cs was measurable at all sampling stations (see Figure 3.12). From the surface to a depth of 200 m, the activities of ^{137}Cs and ^{134}Cs increased with depth increment. In the region near Taiwan Island, ^{134}Cs was not detectable at the surface or at the 100-m water depth layer. However, at a depth of 200 m ^{134}Cs was detectable at a relatively high level of 1.99 ± 0.23 Bq/m^3 at a location (21°N, 126°E), which is about 550 km away from the southernmost point of Taiwan Island.

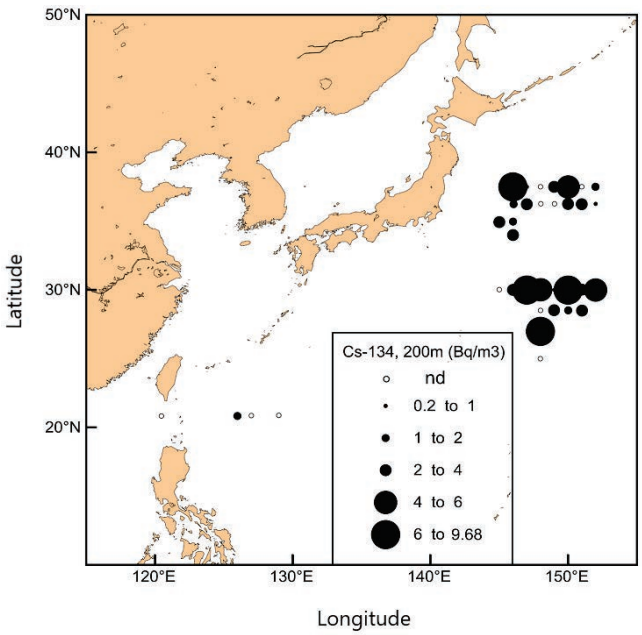

Fig. 3.17 Distributions of ^{134}Cs at 200-m depth in the Northwest Pacific Ocean in May–June 2012.

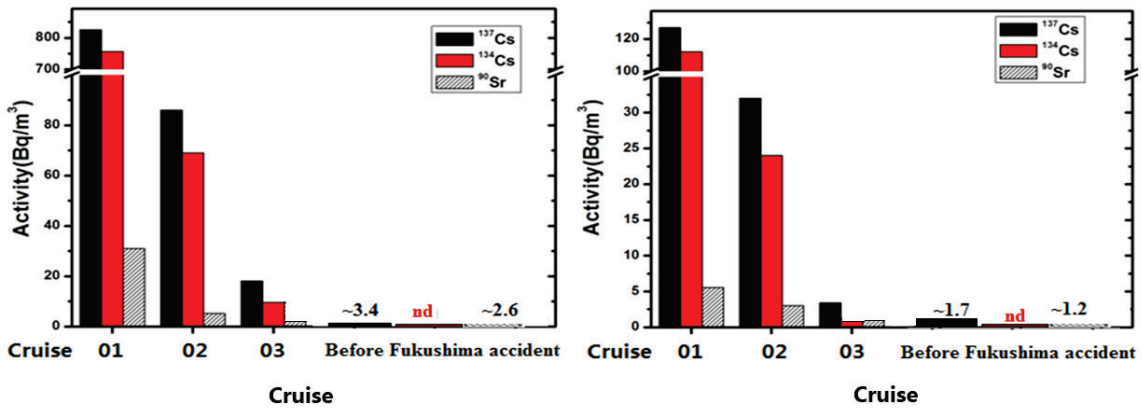

Fig. 3.18 Variations in the highest activities (left) and the average activities (right) in the Northwest Pacific during cruises 1–3 (see Figure 3.11) in 2011–2012 compared to the pre-FDNPP accident results.

The highest and average activities of ^{137}Cs, ^{134}Cs and ^{90}Sr for 2011–2012 are compared to the pre-accident values in Figure 3.18. The highest activities (~800 Bq/m^3) were measured approximately 400–800 km away from Fukushima. The values of the highest activities for each radionuclide decreased by almost 10 times during each successive cruise, thereby illustrating the rapid dilution and dispersion of the Fukushima plume in the waters of the North Pacific. Nevertheless, Northwest Pacific waters were still significantly contaminated by Fukushima radioactivity even as much as one year after the accident.

The highest ^{137}Cs and ^{134}Cs levels were measured in the 200-m layer (the deepest sampling depth) during these cruises. These results are consistent with Kumamoto *et al*. (2014) determinations that radioactive contaminants can descend to a depth of 200 m through surface cooling and vertical mixing in the winter. Kumamoto *et al*. (2014) also noted that ^{134}Cs penetrated to a depth of approximately 300 m between 35°N and 40°N along the 149°E meridian in January–February 2012, suggesting that similar transport resulting from the formation and subduction of STMW occurred in the regions discussed above. To the south of the Kuroshio Extension between 30°N and 35°N, STMW is formed and penetrates to a depth of approximately 400 m (25.6 δ_Θ) in late winter (Figure 3.19). The STMW then spreads to the nearly subtropical front through advection over the Kuroshio recirculation region (Suga and Hanawa, 1990, 1995). The discharge of ^{134}Cs from the FDNPP accident into the North Pacific Ocean occurred mainly in March 2011, when STMW was just being formed. Therefore, the ^{134}Cs that arrived at the south of the Kuroshio Extension was most likely immediately mixed vertically to depths of 300–400 m. The ^{134}Cs in newly formed STMW then began to spread southward to approximately 20°N along subsurface isopycnals (25.0–25.6 δ_Θ; Kumamoto *et al*., 2014). It only took 14–15 months for the Fukushima-derived nuclear wastes to be transported from the high latitude area (~37°N) to the low latitude area (~21°N).

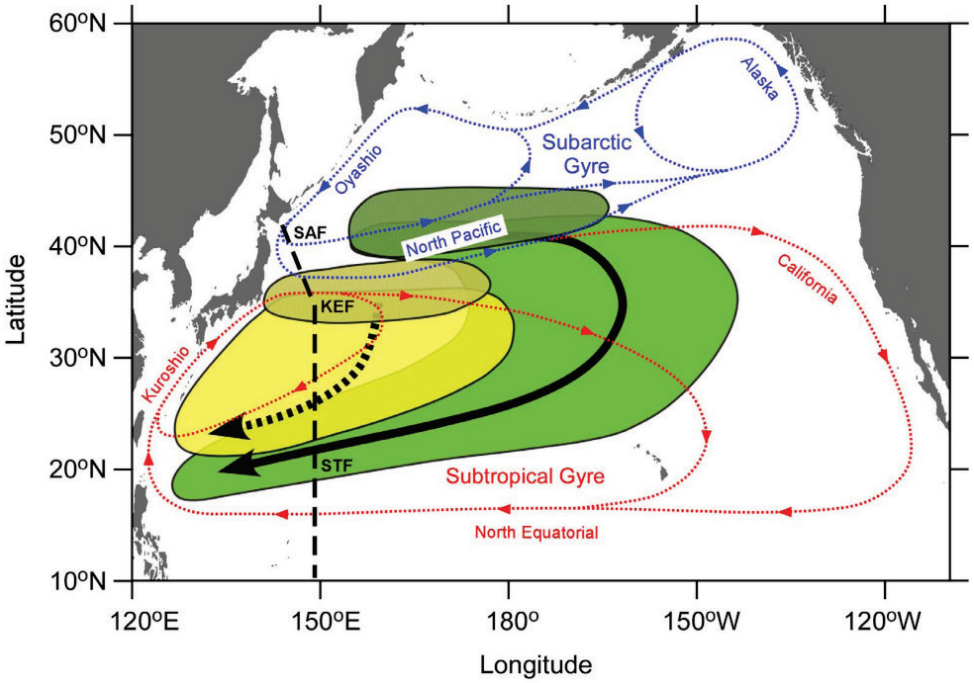

Fig. 3.19 Schematic view of the formation and subduction of mode waters in the North Pacific. Yellow and yellow-shaded ellipses indicate spreading and formation areas, respectively, of Subtropical Mode Water (STMW; 25.0–25.6 δ_θ). Green and green-shaded areas indicate spreading and formation areas, respectively, of Central Mode Water (CMW; 26.0–26.6 δ_θ), which is denser than STMW. The thick broken and solid arrows show the spreading directions of STMW and CMW, respectively. The blue and red dotted lines are surface water currents of the subarctic and subtropical gyres, respectively. SAF, KEF, and STF indicate the subarctic, Kuroshio Extension, and subtropical fronts along the observational line, respectively. From Kumamoto *et al*. (2014). With permission of Creative Commons CC BY license.

Temporal variation of seawater radioactivity

The monitoring region in the Northwest Pacific was separated into the following 3 areas (see Figure 3.11): area 1 is in east of Japan, area 2 is in southeast of Japan and area 3 is in southeast of Taiwan Island.

For area 1, the temporal variations of the highest activities of ^{137}Cs (825.49 Bq/m^3) and ^{134}Cs (756.86 Bq/m^3) are shown in Figure 3.20 and Figure 3.21. The radionuclide concentrations decreased by an order of magnitude for each cruise for the first three cruises owing to the rapid dispersion of the contamination. Beginning with the fourth cruise, the radiocesium concentrations decreased slowly, with some small variability.

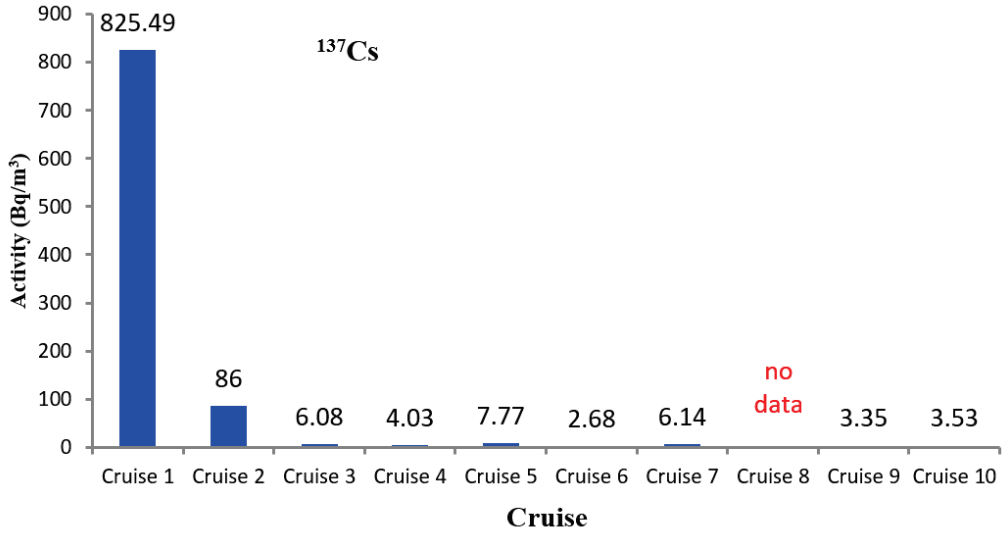

Fig. 3.20 Temporal variation of the highest ^{137}Cs activities in area 1 from 2011–2015. Samples were not collected in this area in Cruise 8.

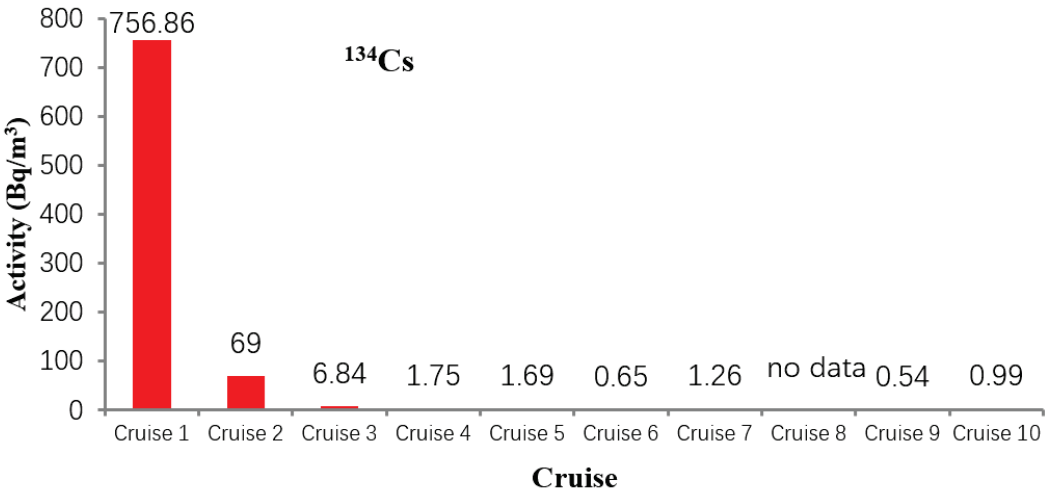

Fig. 3.21 Temporal variation of the highest ^{134}Cs activities in area 1 from 2011–2015. Samples were not collected in this area in Cruise 8.

The temporal variations of ^{137}Cs and ^{134}Cs activities in area 2 (Figure 3.22 and Figure 3.23) show the highest levels on the third cruise, probably owing to delayed contaminant transport into this area from area 1. Radiocesium levels generally declined after the third cruise, with some small degree of variability.

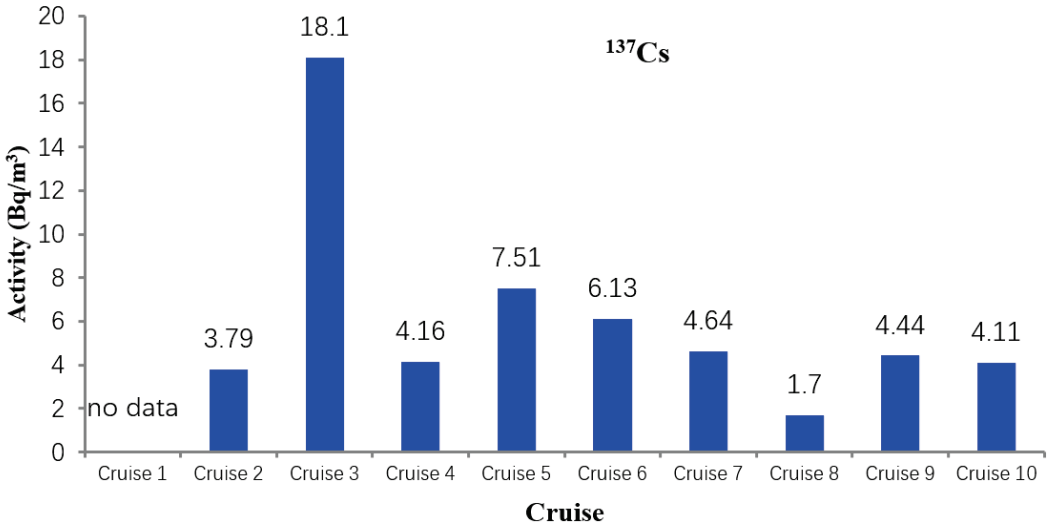

Fig. 3.22 Temporal variation of the highest ^{137}Cs activities in area 2 from 2011–2015. Samples were not collected in this area in Cruise 1.

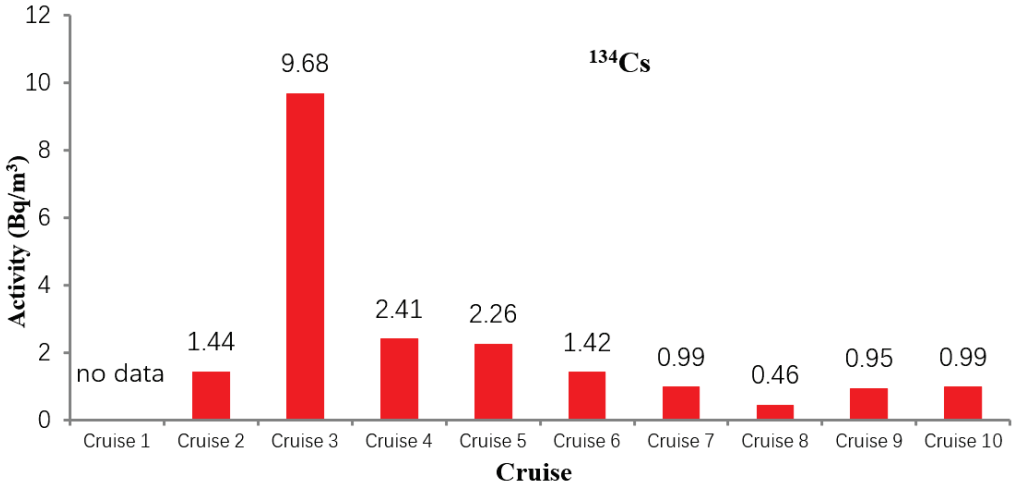

Fig. 3.23 Temporal variation of the highest ^{134}Cs activities in area 2 from 2011–2015. Samples were not collected in this area in Cruise 1.

For area 3, the temporal variations of the highest ^{137}Cs and ^{134}Cs activities are the highest (Figure 3.24 and Figure 3.25). The changes of radiocesium concentrations in this area have been previously discussed and are related to the transport of Fukushima contaminants by the subduction and transport of North Pacific STMW into the area.

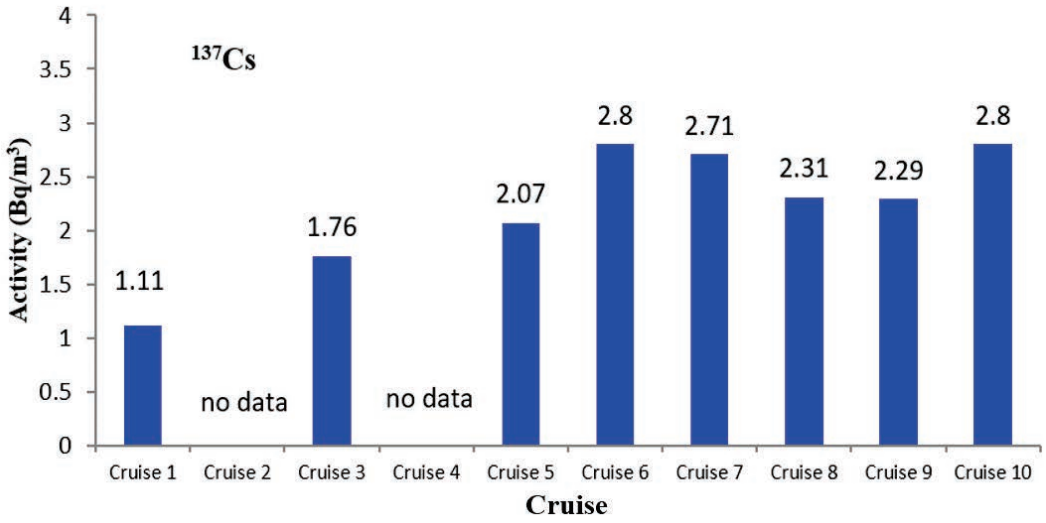

Fig. 3.24 Temporal variation of the highest ^{137}Cs activities in area 3 from 2011–2015. Samples were not collected in this area in Cruises 2 and 4.

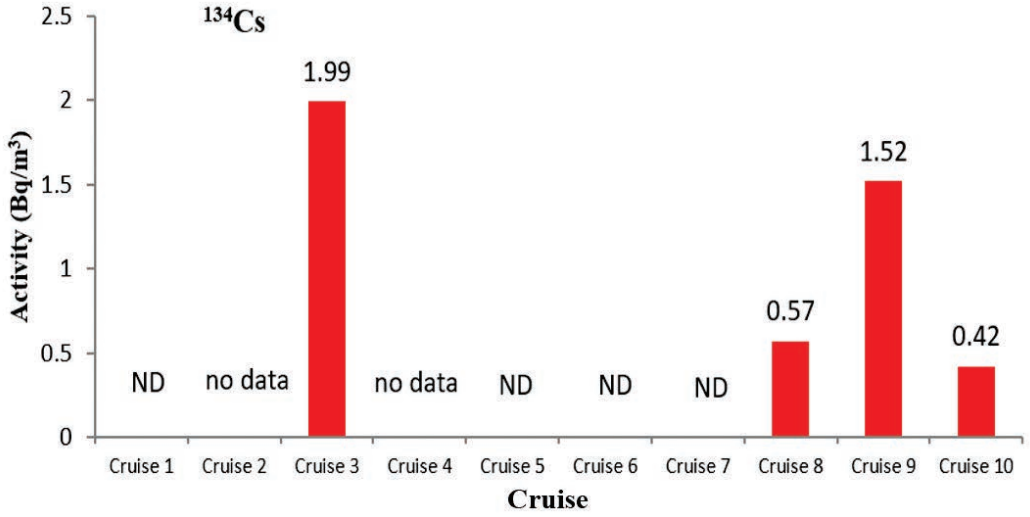

Fig. 3.25 Temporal variation of the highest ^{134}Cs activities in area 3 from 2011–2015. ND = not detected. Samples were not collected in this area in Cruises 2 and 4.

3.3.3 Biota

A wide range of biota samples (squid, mackerel, grouper, *etc*.) were collected on the ten cruises between 2011 and 2015. The activities of various artificial and natural radionuclides were measured for these biota samples using standard gamma ray procedures and reported in units of Bq/kg$_{\text{wet weight}}$. The following study looked at the radioactivity levels and dose rates of the neon flying squid in November 2011.

Squid radioactivity levels and dose assessment in November 2011

Ommastrephes bartramii (neon flying squid) is a migratory squid species of the class Cephalopoda that is commercially important for human consumption, and common in the Pacific Ocean and circumglobally in temperate and tropical waters. It feeds near the surface on small fish and is thus a potential accumulator of radiocesium *via* diet and water pathways. Moreover, cephalopods have a

strong capability to accumulate silver in their bodies (Miramand and Bentley, 1992; Bustamante *et al*., 2004) and would potentially indicate uptake of the short-lived ^{110m}Ag (0.70-year half-life) released from the FDNPP accident. Similarly, the presence of ^{134}Cs (2.1-year half-life) in samples would also indicate a pathway from FDNPP releases. Therefore, specimens captured at locations in the North Pacific may serve as bio-indicators of the presence, strength and transport of the radioactive signal from the FDNPP accident.

This study assessed samples of *O. bartramii* obtained from the Northwest Pacific in November 2011 for a range of artificial and natural radionuclides (^{134}Cs, ^{137}Cs, ^{110m}Ag, ^{238}U, ^{226}Ra and ^{40}K). The radiological dose rates and relevant risk levels were determined for the squid, as well as potential dose rates to human consumers of squid seafood. Consistent with international efforts to compile transfer data, CRs (wholebody-to-water and wholebody-to-tissue) were calculated and reported, including those for different age classes of squid.

Materials and methods

Sample collection and analytical procedure

Thirteen composite samples of *O. bartramii* with a total weight of 126.2 kg were obtained by bait fishing in open waters in the Northwest Pacific. Six sampling locations were selected in the area of 34°–39°N to 145°–149°E to investigate eastward deposition and oceanic migration pathways of radionuclide releases from the FDNPP accident (Figure 3.26). To ensure the sample mass was sufficient to reach minimum detectable activity (MDA) levels for key radionuclides, composite samples were made with multiple specimens from the same sampling site. For those sites with enough sample mass, the *O. bartramii* specimens were divided into different composite categories according to their body weight. Specimens with body mass less than 1 kg were categorized as “small”, those between 1 kg and 2 kg were categorized as “medium” and those more than 2 kg were categorized as “large”. The samples were frozen at –18°C on board for transport to the laboratory for subsequent analysis.

O. bartramii samples were dissected into muscle and gut tissues after thawing, dried at 50°C and ashed at 450°C. The fresh weight and ash weight of the composite samples were recorded. The ash was sealed in cylindrical 75 mm diameter containers, and then subjected to high-purity germanium (HPGe) spectrometry for detection of gamma-emitting radionuclides.

Gamma rays from artificial radionuclides (^{134}Cs, ^{137}Cs, ^{110m}Ag, ^{58}Co, ^{60}Co, ^{54}Mn and ^{65}Zn) and natural radionuclides (^{40}K, ^{226}Ra and ^{238}U) were analyzed using a planar HPGe detector (Model BE6530 with Multi Channel Analyzer Lynx system; Canberra Packard, USA). Detection efficiencies for the geometry used were 2.7885% and 2.4476%, for ^{137}Cs and ^{110m}Ag, respectively. The counting time for each sample was 24 hours. Genie 2000 software was used to analyze the respective peaks in the energy spectrum. The concentrations were corrected for decay to the initial date of the nuclear accident on March 12, 2011, when the first hydrogen explosion occurred in Unit 1 of the FDNPP (Wakeford, 2011).

Dose assessment

The ERICA Assessment Tool (version 1.2) (Brown *et al*., 2008) was used in Tier 2 assessment to evaluate the radiological risk to squid from the study areas in 2011 (Fig. 3.26). The ERICA Tool includes the capability to specify organism sizes, and in this study, average mass (1.3 kg) and dimensions (ellipsoid equivalent of 0.3, 0.1 and 0.085 m length, width and height, respectively) from the specimens were used to calculate dose rates. The dimensions of the average *O. bartramii* happen to be very similar to the standard ERICA “pelagic fish” and therefore, the dose rates are very similar as calculated by ERICA. The measured activity concentrations in the whole-body of

^{137}Cs, ^{134}Cs, ^{110m}Ag, ^{226}Ra and ^{238}U in the samples were used as dose calculation input. The maximum tissue activity concentrations were used for a more conservative result. As *O. bartramii* are migratory, their radionuclide tissue levels represent an integrated accumulation from recently traversed areas in the open ocean area. The exact migratory routes are not known. Therefore, the external dose rates to the squid were calculated using the average of water radioactivity levels in the study capture region (average of samples across all sampling locations). Use of the average is reasonable in this instance as the external dose rates for artificial radionuclides were much smaller than internal dose rates and therefore, variable water activity concentrations had little influence on overall dose results. For internal dose rates to squid, the dose conversion coefficients (DCCs) were calculated within the ERICA Tool. The occupancy factors were 100% in water, and weighting factors of internal low beta, internal beta/gamma and internal alpha were set as 3, 1 and 10, respectively.

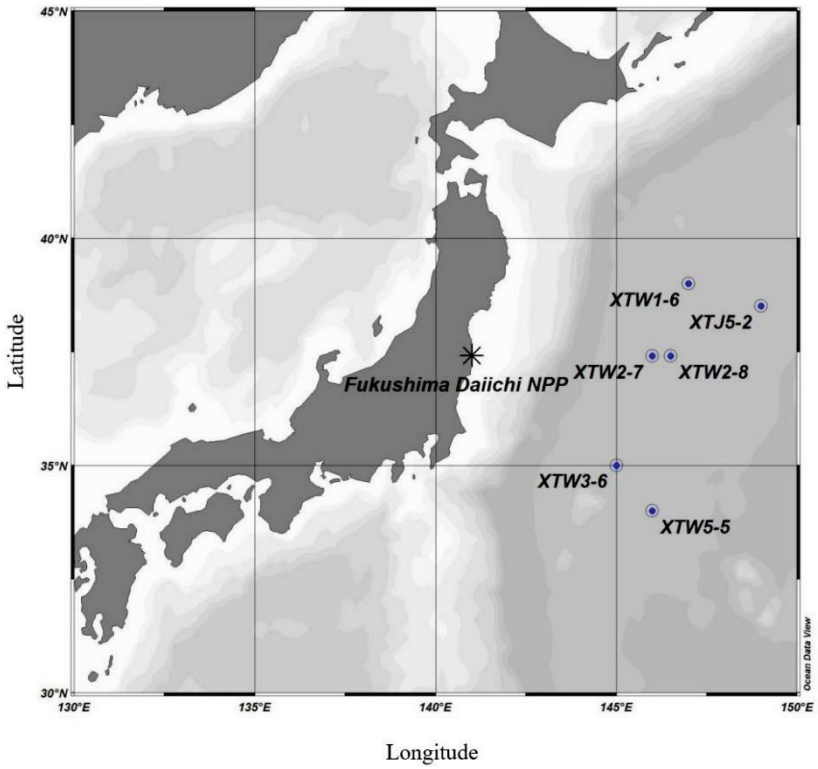

Fig. 3.26 Map of sampling sites for *Ommastrephes bartramii* (neon flying squid) obtained in 2011.

Dose from ingesting squid by human consumers

Committed effective doses (Sv) to human consumers of squid were estimated using standard exposure-to-dose conversion factors (DCFs) for ingestion from the ICRP Compendium of dose coefficients based on ICRP Publication 60 (ICRP, 1991). Key DCFs are 1.30E-08 and 1.90E-08 Sv/Bq for ^{137}Cs and ^{134}Cs (DCFs provided in the supplemental). The factors are multiplied by intake (*e.g.*, kg/yr) to obtain committed effective doses to the consumer. In this study, the annual intake rate of seafood by an adult consumer is assumed to be 20 kg/yr (consistent with world per capita fish and related seafood consumption (FAO, 2016). As a conservative assumption, the entire 20 kg/yr for a hypothetical consumer is assumed to be sourced from the squid of the study area east of the FDNPP (in practice, only a small percentage of seafood diet would be sourced from this region). As most dose-to-human consumers of seafood typically come from the natural radionuclide ^{210}Po

(~89%; Johansen *et al*., 2015), the seafood ingestion dose rates here included ^{210}Po using conservative generic data for marine seafood (Hosseini *et al*., 2010; Carvalho, 2011).

Whole-body concentration ratios

The water-to-organism whole-body Concentration Ratio CR_{WB} (in L/kg) used here is defined as:

$$CR_{WB:Water} = \frac{Whole\text{-}Body\ Activity\ Concentration\ (fresh\ mass)\ (Bq/kg\text{-}wet)}{Water\ Activity\ Concentration\ (Bq/L)}. \quad (1)$$

The whole-body activity of a radionuclide was estimated using a mass balance approach (Yankovich *et al*., 2010) to reconstruct the amount of radionuclide in the whole-body of the squid. The whole-body to tissue concentration ratio (dimensionless) was estimated as:

$$CR_{WB:Tissue} = \frac{\sum[Tissue_t\ Activity\ Concentration\ (fresh\ mass)\cdot Tissue_t\ fresh\ mass\ fraction]}{Tissue_t\ Activity\ Concentration\ (fresh\ mass)}. \quad (2)$$

Results and discussion

Description of specimens

In total, 98 *O. bartramii* specimens were obtained from 6 stations. The mass of the specimens ranged from 118 g to 2551 g with an average of 1347 g. Sixty percent of the specimens weighed from 701 g to 1700 g. The trunk length of the specimens ranged from 115 mm to 440 mm, on average 333 mm. Seventy-five percent of the specimens had a length greater than 290 mm (adult size) suggesting that the majority of the specimens were hatched in winter of 2010 or spring in 2011 and had been living for 8 to 11 months (Wang and Chen, 2005). Combining the estimated age of the squid and assuming residence in the general area east of Fukushima Prefecture, it can be inferred that most *O. bartramii* specimens had been accumulating radionuclides since the FDNPP accident, while a minor proportion (the small size category) were likely to have been hatched after the accident and had shorter exposure times.

Activity concentrations and CRs in squid

The activity levels of radionuclides in Table 3.2. indicate that all *O. bartramii* size classes had accumulated radionuclides from FDNPP releases as indicated by ^{134}Cs and ^{110m}Ag. The squid specimens had a strong capability to concentrate Ag in their bodies. The maximum activity of ^{110m}Ag in the whole body of *O. bartramii* was up to 9 Bq/kg, as compared to that in water which was below the MDA of 0.22 Bq/m^3, indicating a maximum concentration factor that is higher than 4×10^4. The mean CRs for ^{110m}Ag were calculated as $>2.95 \times 10^4 \pm 9.84 \times 10^3$ L/kg (Table 3.3) using the MDA as the activity of seawater in Equation (1).

Although this estimate is with large uncertainties because of using MDA of ^{110m}Ag as the water concentration, these Ag data provide new insights for international researchers and fill a gap as the relevant international database (Wildlife Transfer Parameter Database[5]) and IAEA Technical Reports Series No. 422 (IAEA, 2004) which have entrees for Ag uptake in the mollusk category (3.6×10^4 and 6×10^4, respectively), but none specifically for squid (cephalopods).

[5] www.wildlifetransferdatabase.org

The mean CR_{WB} values for ^{134}Cs and ^{137}Cs in *O. bartramii* were 5.57 (± 2.59 SD) and 6.33 (± 2.80 SD), respectively. These values are similar to previously published mean concentration factors for Cs in cephalopods ranging from 9 to 14 (IAEA, 1978, 2004; Ishii *et al*., 1978; Suzuki *et al*., 1978). The slightly lower CR_{WB} in this study is well within the range of expected variation, which can be very high for water-to-organism CR values (*e.g*., reported CRs for ^{137}Cs in marine fish range over nearly an order of magnitude, Beresford, 2010). The activity concentration of ^{137}Cs in the research area reached a maximum of ~600 Bq/m^3 in June 2011 and soon decreased to below 100 Bq/m^3 (Aoyama *et al*., 2016). Considering the temporal change of radiocesium in seawater and its relatively short biological half-life (~70 days) in marine organisms in this study, the CR calculation used mean ^{134}Cs and ^{137}Cs seawater activity concentrations (35.1 and 36.2 Bq/m^3, respectively) from this study's November 2011 sampling, which were similar to the ~50 Bq/m^3 reported for July–December timeframe from the same open ocean area (Kaeriyama, 2017).

The results also showed that both ^{134}Cs and ^{137}Cs were concentrated mainly in the muscle of the squid. Cesium behaves similarly to potassium in biota, and it tends to be distributed to the muscle tissue. These results for the open ocean and real-world conditions are consistent with previous laboratory results of 80+ % accumulation in the muscle and head of cuttlefish after only 8 hours of exposure to water (Bustamante *et al*., 2004). In contrast, for Ag, the open ocean squid had 95% Ag in the gut *vs*. muscle. This result was also consistent with the laboratory cuttlefish which had 98% Ag in the gut following a single spiked feeding and 29 day depuration (Bustamante *et al*., 2004). From the same study, within the gut, accumulation of Ag is dominantly in the digestive gland.

The smallest squid samples had the highest concentration factors for ^{134}Cs, ^{137}Cs, ^{110m}Ag and ^{238}U (Figure 3.27, Table 3.2). The higher accumulation occurred in the smaller size class despite their inferred shorter exposure times (shorter lifespan) as compared with the larger size class. These results are consistent with observed Cs depuration rates in juvenile cephalopods (*Sepia officinalis*) being approximately four times slower than that of adults, with however, both being relatively fast (adult cuttlefish biological half-life of 16 days for Cs and 9 days for Ag, Bustamante *et al*., 2004). This previous study suggests the radiocesium accumulation and depuration in *O. bartramii* is relatively rapid and that our results, therefore, primarily reflect recent (approximately several months) exposure rather than longer-term accumulation.

The levels of activity for ^{58}Co, ^{60}Co, ^{54}Mn and ^{65}Zn in the samples were all below the MDA (0.22 mBq/g-ash).

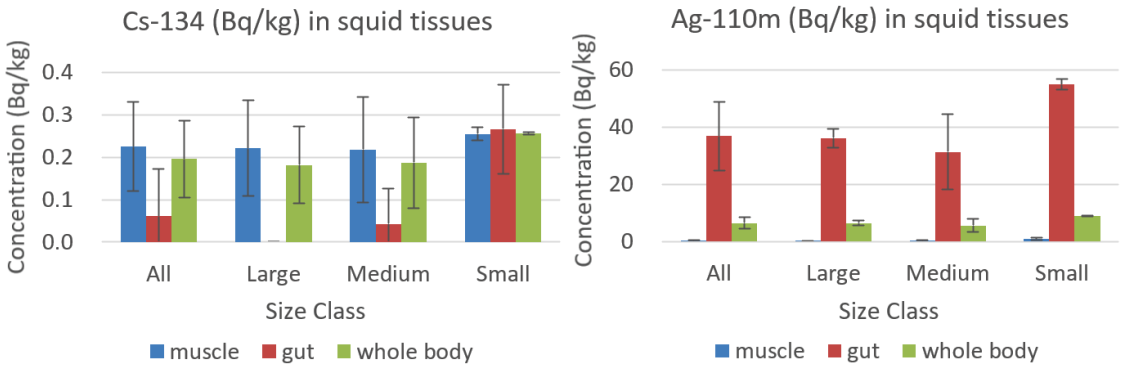

Fig. 3.27 Activity concentrations of ^{134}Cs (left) and ^{110m}Ag (right) in *O. bartramii* tissues.

Whole-body: muscle and whole-body: gut concentration ratios

Most of the non-human biota radiation dose assessing models focus on estimation of dose rates using the whole-body activity concentrations of radionuclides (Brown *et al*., 2008). However, muscle tissue (*vs*. whole-body) is measured in most monitoring programs which typically focus on seafood tissues consumed by humans. Therefore, there exists a need for whole-body:tissue concentration ratios that allow for estimation of whole-body concentrations from commonly measured tissue data (Yankovich *et al*., 2010).

The whole-body: muscle and whole-body: gut concentration ratios for radionuclides in *O. bartramii* samples are listed in Table 3.3. For many radionuclides, the tissue-specific concentration values for the small squids tend to be higher than those for large squids. The uncertainty of the whole-body: gut CRs for ^{137}Cs and ^{134}Cs are relatively high because of the relatively low level and large activity range of radiocesium in the gut samples. The CRs presented here are calculated for the non-equilibrium conditions following the FDNPP accident. This issue is somewhat compensated for by focusing on radionuclides that are taken up relatively quickly, and by using the average activity concentrations over their relatively short lifespan of the squid. Equilibrium conditions are generally not achieved in natural systems and our results, like all CRs, should be considered in context. Further research is necessary to obtain a better estimation the biokinetics of uptake in squid and of the whole-body: gut CRs for ^{137}Cs and ^{134}Cs.

Table 3.2 Statistics of radionuclide levels in composite squid samples (Bq/kg-wet).

Size	Tissues*	^{137}Cs		^{134}Cs		^{110m}Ag		^{40}K		^{226}Ra		^{238}U	
		Range	Average	Range	Average	Range	Average	Range	Average	Range	Average	Range	Average
All (n = 13)	M	0.10–0.46	0.27±0.12	0.06–0.39	0.22±0.10	0.06–1.29	0.36±0.33	56.29–94.80	76.05±9.40	ND–0.07	0.03±0.03	0.16–1.77	0.59±0.44
	G	ND**–0.33	0.05±0.10	ND–0.34	0.06±0.11	8.10–56.27	36.85±12.02	9.72–72.37	53.03±15.77	ND–0.89	0.28±0.28	ND–26.89	5.40±7.60
	WB	0.08–0.38	0.23±0.10	0.05–0.31	0.20±0.09	1.70–9.04	6.49±1.97	53.67–88.09	72.13±8.45	ND–0.17	0.07±0.05	0.27–5.32	1.35±1.40
Large (n = 5)	M	0.13–0.46	0.26±0.13	0.09–0.39	0.22±0.11	0.06–0.36	0.24±0.13	67.62–94.80	80.55±11.49	ND–0.07	0.04±0.03	0.33–0.94	0.63±0.26
	G	ND	ND	ND	ND	32.25–40.50	36.14±3.19	49.57–58.88	53.00±3.66	ND–0.68	0.24±0.27	ND–7.89	2.61±3.22
	WB	0.11–0.38	0.21±0.11	0.08–0.31	0.18±0.09	5.53–7.78	6.54±0.83	64.55–88.09	75.76±9.86	ND–0.15	0.07±0.06	0.54–2.09	0.97±0.63
Medium (n = 6)	M	0.10–0.41	0.27±0.14	0.06–0.34	0.22±0.12	0.06–0.46	0.25±0.19	56.29–78.78	72.30±8.12	ND–0.05	0.02±0.02	0.16–0.86	0.40±0.28
	G	ND–0.13	0.03±0.05	ND–0.21	0.04±0.08	8.10–45.85	31.40±13.05	9.72–67.73	47.80±21.18	ND–0.53	0.18±0.19	ND–10.44	3.05±3.84
	WB	0.08–0.35	0.23±0.12	0.05–0.29	0.19±0.11	1.70–8.09	5.61±2.31	53.67–73.94	68.16±7.56	ND–0.11	0.04±0.04	0.27–2.45	0.86±0.80
Small (n = 2)	M	0.21–0.34	0.27±0.09	0.24–0.27	0.25±0.02	0.65–1.29	0.97±0.45	73.26–78.88	76.07±3.97	ND–0.05	0.02±0.03	0.41–1.77	1.09±0.97
	G	0.20–0.33	0.27±0.09	0.19–0.34	0.27±0.11	53.64–56.27	54.95±1.86	65.30–72.37	68.83±4.99	0.44-0.89	0.67±0.32	12.00–26.89	19.45±10.53
	WB	0.21–0.34	0.27±0.09	0.25–0.26	0.26±0.00	8.90–9.04	8.97±0.10	73.13–76.76	74.95±2.57	0.07-0.17	0.12±0.07	2.21–5.32	3.76±2.19

* Tissues: M – muscle, G – gut, WB – whole body.

**ND: level was below the minimum detectable activity.

Table 3.3 Concentration ratios (CRs) for radionuclides in *O. bartramii* in 2011 conditions following the FDNPP accident.

CR*	Size	^{137}Cs	^{134}Cs	^{110m}Ag	^{40}K	^{226}Ra	^{238}U
WB-M	All	0.93 ± 0.28	0.94 ± 0.30	41.87 ± 39.49	1.04 ± 0.28	2.75 ± 1.60	2.36 ± 1.36
	Large	0.82 ± 0.01	0.82 ± 0.01	38.89 ± 30.21	0.94 ± 0.01	2.42 ± 1.69	1.64 ± 0.79
	Medium	0.85 ± 0.03	0.86 ± 0.06	47.90 ± 50.29	0.96 ± 0.01	2.00 ± 1.53	2.35 ± 1.20
	Small	1.00 ± 0.00	1.01 ± 0.07	10.30 ± 4.67	0.99 ± 0.02	3.58	4.22 ± 1.73
WB-G	All	2.59 ± 2.50	2.29 ± 2.44	0.18 ± 0.02	1.30 ± 0.18	0.33 ± 0.29	0.24 ± 0.03
	Large	NA**	NA	0.18 ± 0.01	1.43 ± 0.18	0.50 ± 0.43	0.28 ± 0.01
	Medium	4.15 ± 4.15	3.54 ± 3.54	0.18 ± 0.02	1.25 ± 0.12	0.24 ± 0.09	0.24 ± 0.01
	Small	1.03 ± 0.01	1.04 ± 0.40	0.16 ± 0.00	1.09 ± 0.12	0.17 ± 0.02	0.19 ± 0.01
WB-W***	All	6.33 ± 2.80	5.57 ± 2.59	>2.95 ± 8.94E+3	6.17 ± 0.71	14.66 ± 11.92	37.97 ± 39.39
	Large	5.90 ± 2.91	5.18 ± 2.60	>2.97 ± 3.76+3	6.42 ± 0.84	16.35 ± 12.46	27.34 ± 17.89
	Medium	6.30 ± 3.17	5.33 ± 3.04	>2.55± 1.05E+4	5.89 ± 0.69	9.56 ± 9.40	24.11 ± 22.43
	Small	7.52 ± 2.52	7.29 ± 0.06	>4.08 ± 4.50E+2	6.35 ± 0.22	25.76 ± 15.07	106.09 ± 61.85

* CR: WB-M – whole-body to muscle concentration ratios, WB-G – whole-body to gut concentration ratios, WB-W – whole-body to water concentration ratios.
** NA: Data are not available because radioactivity of specific radionuclides in at least one tissue was below MDA.
*** Values were calculated using mean ^{134}Cs and ^{137}Cs seawater activity concentrations of 35.1 and 36.2 Bq/m^3, and the MDA of ^{110m}Ag in seawater (0.22 Bq/m^3).

Dose rates for squid

The internal radiological dose rates to *O. bartramii* from artificial radionuclides (^{110m}Ag, ^{134}Cs and ^{137}Cs) were collectively much higher than the external dose rates (Figure 3.28). This is consistent with the observed accumulation of radionuclides inside the squid body as compared with that in the surrounding seawater. The internal dose rates from FDNPP-associated artificial radionuclides were lower, by two orders of magnitude, than those from the natural radionuclides measured in this study. From these radionuclides, only approximately 1.4% of the total dose rate is estimated to have come from the FDNPP releases. The total dose rate for *O. bartramii* is 0.15 μGy/h from the study radionuclides, and increases to approximately 0.61 μGy/h when adding ^{210}Po, a natural radionuclide and significant dose contributor in marine organisms (using a conservative generic marine value of 15 Bq/kg-fresh mass and 0.001 Bq/L in squid and seawater, respectively, based on Carvalho (2011) and Hosseini *et al*. (2010). These dose rates are much lower than the most conservative screening benchmark dose rate of 10 μGy/h (Garnier-Laplace *et al*., 2008). The dose calculations used the measured activity concentrations in *O. bartramii* (not CRs), and the calculated dose rates represent a point in time (November 2011) with likely higher doses prior to, and lower doses following the sampling date. However, the relatively low values, indicating a more detailed (*e.g*., pulse-dynamic uptake) dose calculation, is not necessary in this case. Overall, results indicate that the radioactive releases from the FDNPP accident would not have a significant adverse effect on *O. bartramii* individuals or populations living in the study area.

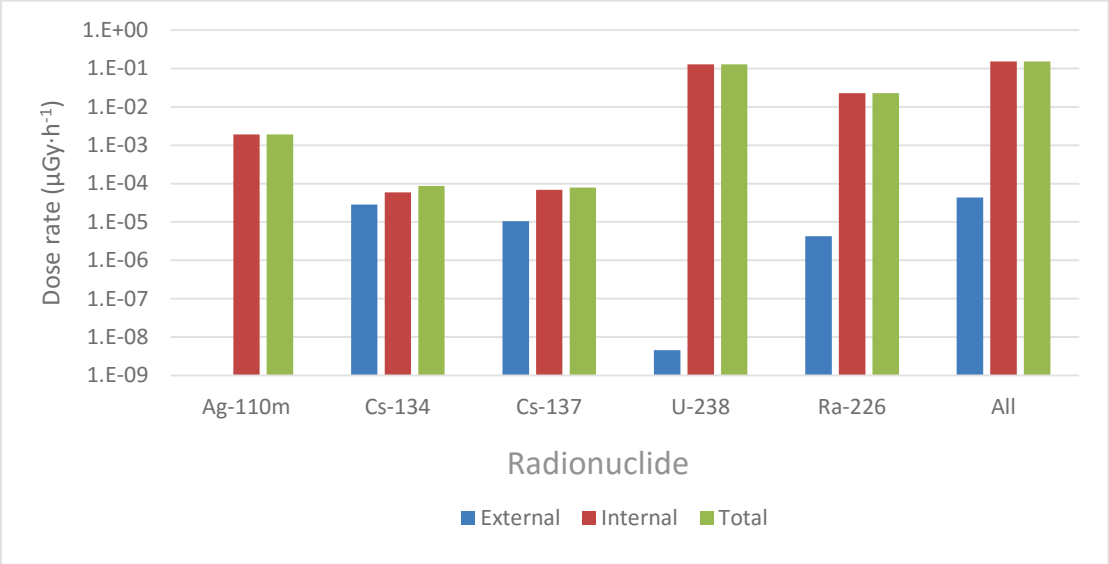

Fig. 3.28 Dose rates (μGy/h) from measured radionuclides for *O. bartramii* samples.

Dose rates for human consumers of seafood

From the radionuclides measured in edible squid tissue (muscle), a committed effective ingestion dose of 0.01 mSv (median; minimum = 0.007 mSv, maximum = 0.014 mSv) would have occurred to a hypothetical human consumer of 20 kg/yr of squid from the study area (based on *O. bartramii* captured in November 2011). The doses calculated here are hypothetical and are intended to be conservative overestimates, given the unrealistic assumption that all of the consumer's yearly seafood came from the study area. If consumption of ^{210}Po (from natural background) is also included, the total dose increases to 0.30 mSv, with almost all derived from ^{210}Po (Table 3.4). Of this dose (including ^{210}Po), less than 0.1% is estimated to have been sourced from the FDNPP. This is consistent with previous findings that natural radionuclides provided far greater dose rates to

potential consumers of Pacific tuna (Fisher *et al*., 2013), and even for seafood sourced within a few kilometers of the FDNPP in 2013 (Johansen *et al*., 2015). The dose contribution from the FDNPP releases for squid consumption of this study are far below the 1 mSv per year recommended constraint for prolonged exposure to the public from nuclear facility releases (ICRP, 1999).

Table 3.4 Ingestion dose estimates to human consumers of the squid in this study (Sv/y based on 20 kg consumption of study squid).

	Minimum (Sv/y)	Median (Sv/y)	Maximum (Sv/y)	This study* (%)
^{40}K	6.98E-06	9.43E-06	1.18E-05	3.12
^{110m}Ag	3.36E-09	2.02E-08	7.22E-08	0.01
^{134}Cs-	2.28E-08	8.36E-08	1.48E-07	0.03
^{137}Cs-	2.60E-08	7.02E-08	1.20E-07	0.02
^{226}Ra-	NA**	1.68E-07	3.92E-07	0.06
^{238}U-	1.44E-07	5.31E-07	1.59E-06	0.18
^{310}Po***	1.44E-05	2.92E-04	1.08E-03	96.59

* Based on median activity concentration values this study (Table 3.2 data, average of all sizes).
** NA = Data not available.
** ^{210}Po from generic published data (Hosseini, *et al*., 2010; Carvalho, 2011).

Summary

Elevated levels of ^{134}Cs and ^{110m}Ag from the FDNPP accident were found in the squid (*O. bartramii*) samples collected in the Northwest Pacific in November 2011. This study filled a gap in international transfer data by providing concentration ratios for several key NPP-associated radionuclides in the whole-body and tissues of cephalopods. The Concentration Ratio for ^{110m}Ag in squid was found to be as high as 4×10^4 L/kg in the smallest samples, with a mean value of 2.95×10^4 L/kg in all the samples, indicating that squid was a good bioindicator for ^{110m}Ag from the FDNPP accident. The radiological dose contribution from the FDNPP releases for squid living in the study area, and for human consumers of these squid, were both far below the recommended dose limits. By comparison, natural radionuclides, particularly ^{210}Po, provide orders of magnitude greater dose rates.

Temporal variation of squid radioactivity

The variations of three FDNPP accident-derived radionuclides in *O. bartramii* are shown in Figure 3.29. ^{134}Cs and ^{110m}Ag were detected on the first seven cruises, indicating contamination from the FDNPP accident, but thereafter were undetectable. Due to the high mobility of squids, different sampling areas and different life stages, it is challenging to determine exactly how the radionuclide levels varied in squid, but levels in all of the detected marine organisms clearly decreased with time.

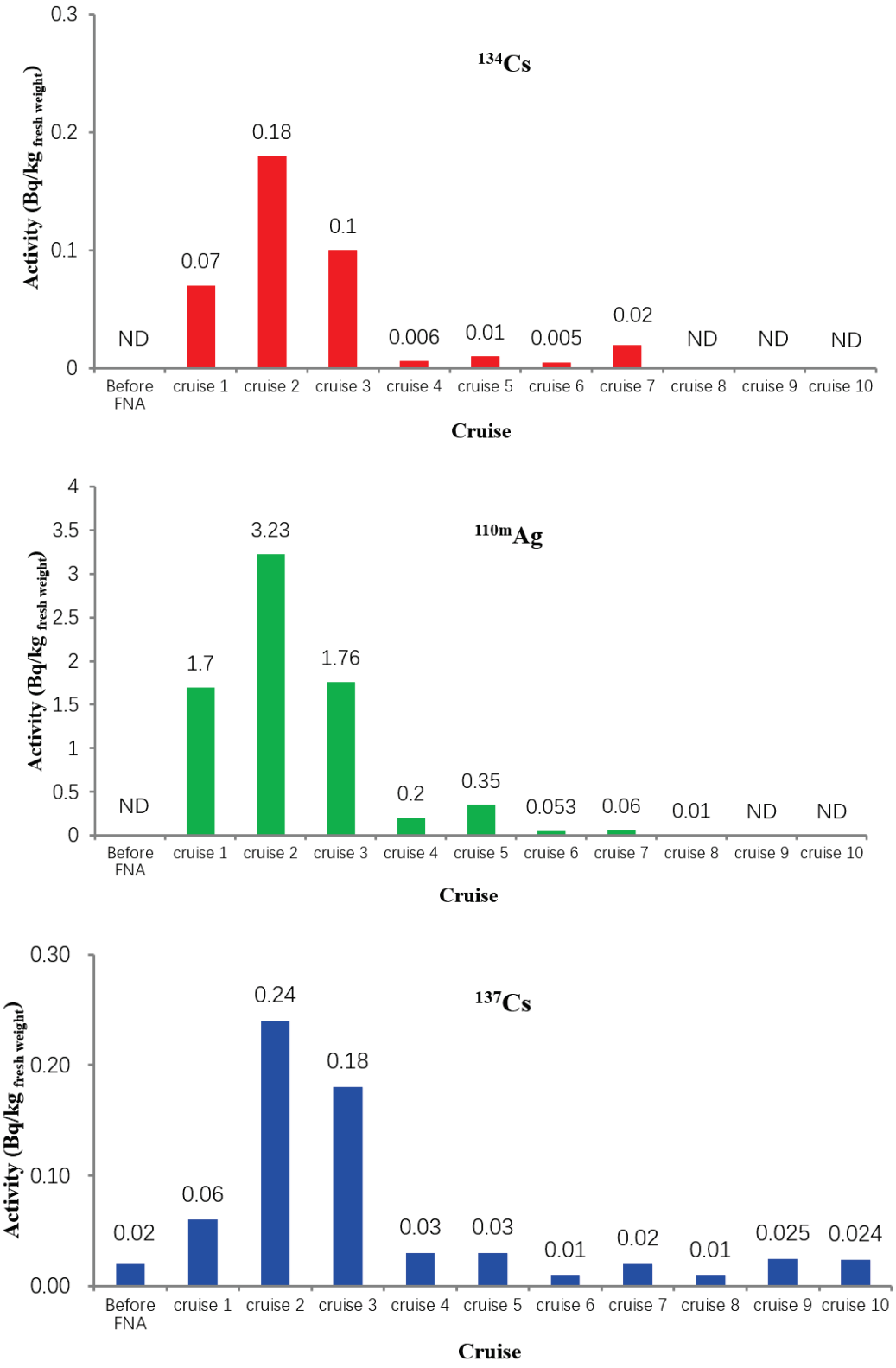

Fig. 3.29 Variations of three radionuclide concentrations in *O. bartramii*.before the FDNPP accident, and after (2011–2015). ND = not detected.

3.3.4 Coastal monitoring

Seawater, marine organism and sediment samples were collected in Chinese coastal waters in 2011–2015 and analyzed for a range of radionuclides discharged during the FDNPP accident.

The activity of ^{134}Cs in coastal seawater samples varied from below the MDL (minimum detection limit, 0.20 Bq/m^3) to 0.98 Bq/m^3. Detectable levels of ^{134}Cs were found in 11 out of 146 coastal samples, indicating that a small amount of ^{134}Cs was transported from the FDNPP accident site to the coastal waters of China.

Sediment samples were collected with a grab sampler from coastal waters and analyzed for ^{90}Sr and gamma emitting radionuclides (*e.g.*, ^{137}Cs, ^{134}Cs, ^{58}Co, ^{60}Co, ^{54}Mn, *etc.*). The radioactivity levels of ^{137}Cs and ^{90}Sr in all the sediment samples were within the background levels determined before the FDNPP accident and the radioactivity levels of other artificial radionuclides such as ^{134}Cs, ^{58}Co, ^{60}Co and ^{54}Mn were all below the detection limit.

In total, 12 biota samples, including algae, fish and mollusks, were obtained in coastal waters. All the samples were analyzed for ^{90}Sr and gamma emitting radionuclides (*e.g.*, ^{134}Cs, ^{58}Co, ^{60}Co and ^{54}Mn, *etc.*). The radioactivity levels of ^{137}Cs and ^{90}Sr in biota samples were within the background level before the FDNPP accident and the radioactivity levels of ^{134}Cs, ^{58}Co, ^{60}Co and ^{54}Mn in biota samples were all below the detection limit.

3.3.5 Summary

To investigate the impact of the FDNPP accident, ten monitoring cruises were conducted by the Third Institute of Oceanography from 2011 to 2015 (one cruise every half year) during which ^{137}Cs, ^{134}Cs, ^{110m}Ag, ^{90}Sr and other artificial radionuclides were measured at more than 400 stations. In May–June 2011, monitoring results showed elevated activities of ^{137}Cs, ^{134}Cs and ^{90}Sr in the surface seawater of the Northwest Pacific. The highest activity for ^{137}Cs (826 Bq/m^3, 485 times higher than the average background), was observed at the area/station 615 km from Fukushima. Similar activity levels of ^{134}Cs were measured in surface seawater samples, confirming that the monitoring area was impacted by the FDNPP accident contamination. The highest activity of ^{90}Sr in seawater samples was 31 Bq/m^3, 25 times higher than the background level. In the samples of squid, ^{134}Cs and ^{110m}Ag were detected, indicating the radioactive release was concentrated by the marine organisms.

In May–June 2012, it was observed that the activities of the artificial radionuclides ^{137}Cs, ^{134}Cs and ^{90}Sr in the seawater of the Northwest Pacific decreased with time. During the third monitoring cruise, ^{134}Cs was found in 63.7% of the samples while 32.9% of the ^{137}Cs data were higher than the highest value measured before the FDNPP accident (3.4 Bq/m^3). The western North Pacific was clearly affected by the accident as much as one year later. ^{134}Cs was measured as far south as 21°N and as far east as 152°E. From the surface to deep water, the activities of ^{137}Cs and ^{134}Cs increased with increasing depth. At a depth of 200 m, both ^{137}Cs and ^{134}Cs had the highest values. ^{134}Cs was found at a depth of 200 m at the station which is 550 km away from the southernmost point of Taiwan Island. The formation and subduction of Subtropical Mode Water (STMW) is a reasonable explanation for this observation. STMW is formed and penetrates to a depth of approximately 400 m (25.6 δ_Θ) south of the Kuroshio Extension between 30°N and 35°N in late winter before spreading to the nearly subtropical front through advection over the Kuroshio recirculation region. The radioactive contaminants were injected into the deep water (300–400 m) and transported to approximately 20°N along subsurface isopycnals (25.0–25.6 δ_Θ). Based on an analysis of potential vorticity, depth, salinity, temperature, potential density and time scale, it has been shown that only the seawater at a depth of 200 m at that station near Taiwan Island represents STMW.

Monitoring results by China indicate that by 2015 ^{134}Cs and ^{137}Cs levels in the Northwest Pacific had decreased with time by several orders of magnitude following the 2011 FDNPP accident. The ten cruises also confirmed a similar level of radioactivity decreases in marine organisms.

Marine radioactivity levels in seawater, sediments and biota were also monitored in the coastal waters of China from 2011 to 2015. ^{134}Cs from the FDNPP accident was detected in 11 of 146 seawater samples, indicating a small amount of the radioactive release was transported to the coastal waters of China. However, the maximum radioactivity level of ^{134}Cs was 0.98 Bq/m^3, well-below the Chinese national regulatory limit for ^{134}Cs in seawater, and radioactivity levels for other detected radionuclides were either within the background levels or less than the detection limits. Therefore, the radiological impact on the ecological environment was small in the monitored waters of China during this period.

3.4 Monitoring results from the Republic of Korea

The Korea Institute of Nuclear Safety (KINS) and National Institute of Fisheries Science (NIFS) have carried out Marine Environmental Radioactivity Surveys (MERS) at permanent stations in Korean coastal regions biannually since 1994. Following the FDNPP accident, the government of the Republic of Korea immediately organized an emergency response system, and the sampling frequencies and areas for the monitoring surveys were enhanced. Among other activities, KINS announced on March 28, 2011, that it was the first agency to detect an artificial radioactive nuclear species, such as ^{131}I emanating from the FDNPP accident. At the government level, the “Plan for Strengthening Environmental Radiation Monitoring by Stage” program was established and converted to an emergency radiation monitoring system for the whole country. A broad range of seawater, sediments and marine biological samples (14 species of fish, 6 kinds of shellfish, 3 kinds of seaweed) were collected in coastal waters during each survey and analyzed for radionuclides. The monitoring results, titled “Marine Environmental Radioactivity Survey” have been published annually (KINS, 2011, 2012, 2013, 2014, 2015, 2016).

3.4.1 Seawater

Surface seawater samples were collected at 21 stations of Korean coastal waters biannually until 2011, at 21–22 stations quarterly during 2012–2013 and at 32 stations quarterly from 2014, and analyzed for a range of radionuclides using standard radiochemical and radioanalytical techniques. Time series measurements for ^{137}Cs, ^{3}H, ^{239,240}Pu and ^{90}Sr are shown in Figure 3.30 for the time period of 1994–2015. Although there are fluctuations in the concentration values, there is an overall decrease with time. The concentrations of radionuclides in the surface seawater of the coastal sea of Korea since 2011 are consistent with levels measured during the 5 years (2006–2010) prior to the FDNPP accident, indicating that there had been minimal transport of contamination to Korean coastal waters (Tables 3.5 and 3.6).

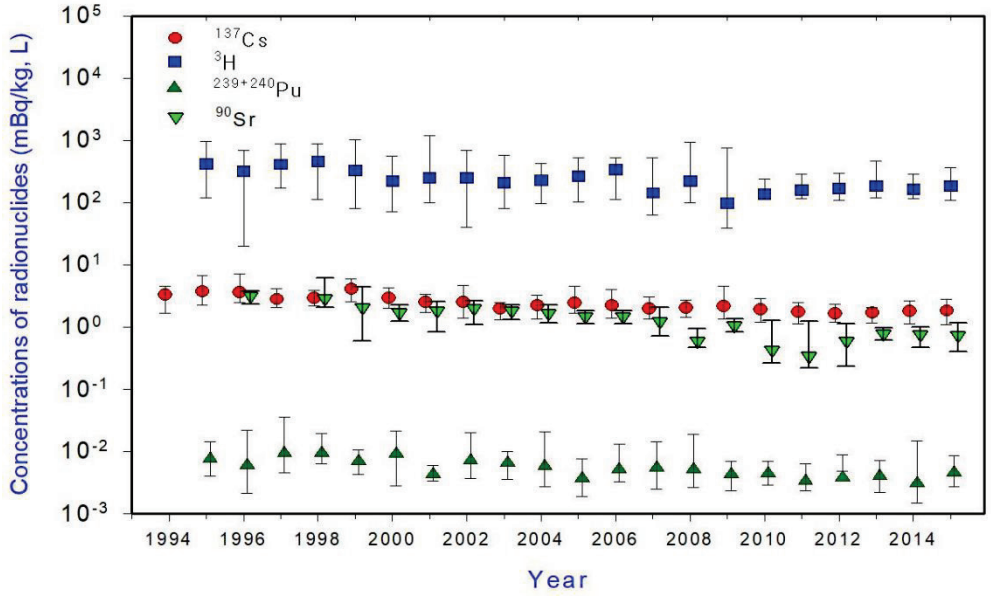

Fig. 3.30 Time series measurements for ^{137}Cs, ^{3}H, ^{239,240}Pu and ^{90}Sr in surface seawater from Korean coastal regimes.

Table 3.5 Time series concentrations of ^{3}H in the surface waters of the coastal sea of Korea.

Year	^{3}H (Bq/L)	
	Average ± SD	Range
2006–2010	0.203 ± 0.131	<0.0376–0.743
2011	0.160 ± 0.046	<0.116–0.286
2012	0.169 ± 0.053	<0.107–0.294
2013	0.190 ± 0.089	<0.120–0.458
2014	0.152 ± 0.044	<0.115–0.285
2015	0.185 ± 0.072	<0.109–0.360
2016	0.184 ± 0.052	<0.110–0.301

Table 3.6 Concentrations of ^{137}Cs, ^{90}Sr and ^{239,240}Pu in the surface waters of the coastal sea of Korea.

Year	^{137}Cs (mBq/L)		^{90}Sr (mBq/L)		$^{239+240}$Pu (μBq/L)	
	Average ± SD	Range	Average ± SD	Range	Average ± SD	Range
2006–2010	2.02 ± 0.37	<1.19–4.04	0.60 ± 0.43	<0.266–2.05	4.91 ± 2.26	2.21–18.0
2011	1.17 ± 0.27	<1.13–2.49	0.33 ± 0.29	<0.227–1.24	3.39 ± 0.95	2.30–6.36
2012	1.64 ± 0.28	1.18–2.29	0.56 ± 0.39	<0.239–1.13	3.76 ± 1.94	2.05–11.5
2013	1.69 ± 0.23	<1.16–<2.07	0.77 ± 0.11	0.61–0.97	4.01 ± 1.46	2.20–7.20
2014	1.78 ± 0.36	1.13–2.63	0.75 ± 0.13	0.46–1.00	3.11 ± 2.70	1.48–14.6
2015	1.81 ± 0.44	1.09–2.77	0.73 ± 0.23	0.40–1.15	4.62 ± 1.41	2.68–8.46
2016	1.69 ± 0.34	<1.04–2.55	1.10 ± 0.26	0.67–1.77	4.63 ± 1.49	2.86–8.85

3.4.2 Sediment

Surface sediments were collected from 15 MERS monitoring stations on an annual basis using grab samplers that collected the upper 5 cm of sediment.

Average concentrations of ^{137}Cs, ^{90}Sr and $^{239+240}$Pu in surface sediments (Table 3.7) were 1–3 Bq/kg, 0.1–0.2 Bq/kg and 0.4–0.5 Bq/kg, respectively, both during 2006–2010 and following the FDNPP accident, during 2011–2016. These results indicate that the FDNPP accident had no detectable impact on sediments in coastal waters of Korea.

Table 3.7 Concentrations of ^{137}Cs, ^{90}Sr and $^{239+240}$Pu in surface sediments in the coastal sea of Korea.

Year	^{137}Cs (Bq/kg·dry)		^{90}Sr (Bq/kg·dry)		$^{239+240}$Pu (Bq/kg·dry)	
	Average ± SD	Range	Average ± SD	Range	Average ± SD	Range
2006–2010	1.81 ± 1.05	<0.502–5.78	–	<0.169	0.528 ± 0.306	0.096–1.20
2011	2.59 ± 1.38	<0.804–4.71	0.182 ± 0.092	<0.096–0.318	0.414 ± 0.34	0.102–1.12
2012	2.05 ± 0.97	<1.01–4.3	–	<0.202	0.428 ± 0.287	0.137–0.836
2013	1.92 ± 1.03	<0.781–3.9	–	<0.086	0.406 ± 0.304	0.075–0.841
2014	2.05 ± 0.94	<0.946–4.45	0.088 ± 0.014	<0.080–0.117	0.493 ± 0.297	0.120–0.865
2015	1.92 ± 0.83	<0.854–3.84	–	<0.100	0.484 ± 0.293	0.086–0.870
2016	1.59 ± 0.65	<0.741–2.97	0.171 ± 0.044	<0.127–0.242	0.542 ± 0.461	0.048–1.36

Dash indicates less than minimum detected activity.

3.4.3 Biota

Marine biota, including fish, shellfish and seaweed were collected by NIFS biannually at the MERS monitoring stations of Korean coastal waters and subsequently analyzed by KINS for radionuclides. Results of these analyses revealed that over the period from 2011 to 2016 the concentrations of ^{137}Cs, ^{90}Sr and $^{239+240}$Pu in the fish samples were very similar to values obtained over the 5 years (2006–2010) prior to the FDNPP accident in 2011 (Table 3.8, Figures 3.31–3.33).

Table 3.8 Concentrations of ^{137}Cs, ^{90}Sr and $^{239+240}$Pu in marine fish in the coastal sea of Korea.

Year	^{137}Cs (mBq/kg·fresh)		^{90}Sr (mBq/kg·fresh)		$^{239+240}$Pu (mBq/kg·fresh)	
	Average ± SD	Range	Average ± SD	Range	Average ± SD	Range
2006–2010	87.2 ± 32.9	<14.5–184	37.5 ± 3.90	<20.1–43.3	0.132 ± 0.102	0.003–0.810
2011	107 ± 34.0	55.3–175	15.2 ± 8.20	<7.03–36.1	0.968 ± 0.801	0.223–2.91
2012	260 ± 629	31.6–2432	–	<18.4	–	<0.043
2013	73.8 ± 38.7	23.2–159	6.42 ± 3.05	<3.77–10.7	0.011 ± 0.003	<0.008–0.011
2014	101 ± 64.9	42.8–285	6.22 ± 1.24	<4.68 ~ 7	0.017 ± 0.006	0.009–0.014
2015	89.5 ± 38.4	39.9–172	–	<8.73	–	<0.633
2016	67.9 ± 31.1	<33.0–119	19.3 ± 3.5	<14.2–23.6	–	<0.221

Dash indicates less than minimum detected activity.

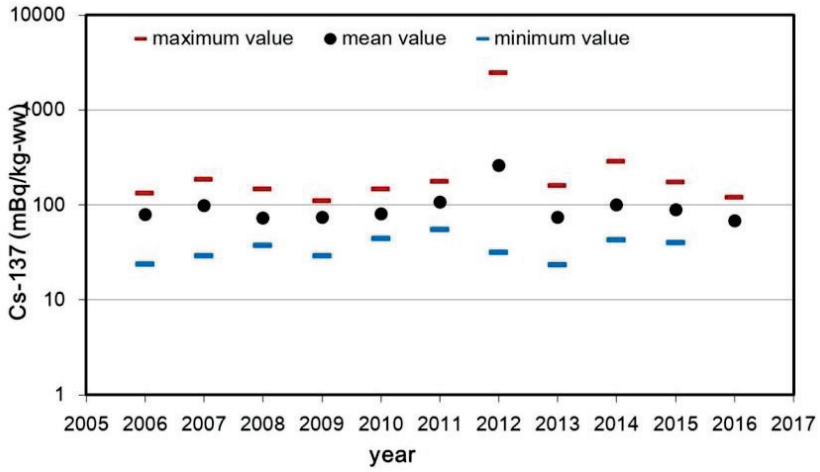

Fig. 3.31 Time series for ^{137}Cs concentrations (mBq/kg-fresh) in fish from the coastal waters of Korea.

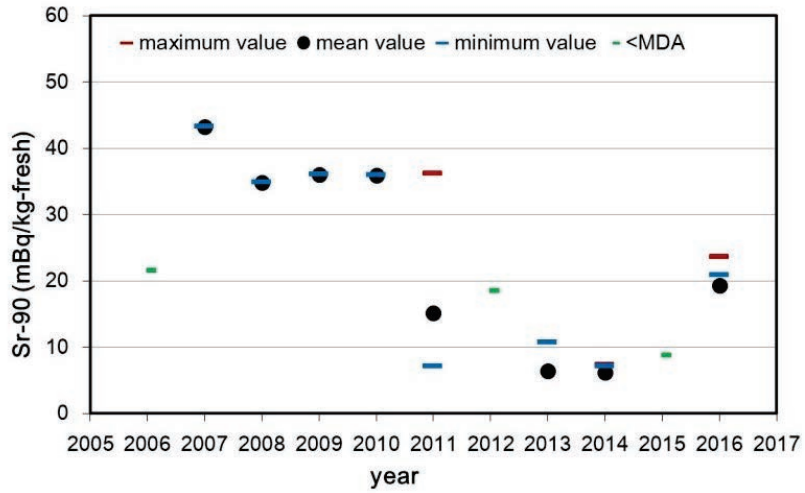

Fig. 3.32 Time series for ^{90}Sr concentrations (mBq/kg-fresh) in fish from the coastal waters of Korea. MDA denotes minimum detected activity.

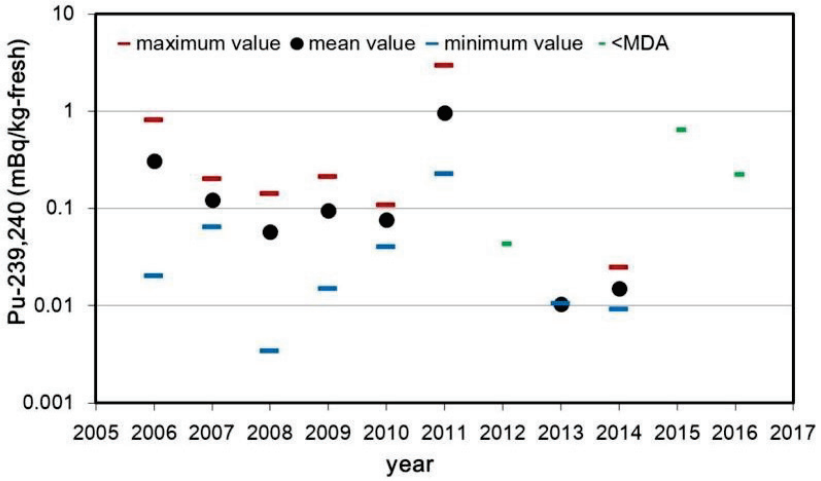

Fig. 3.33 Time series for $^{239+240}$Pu concentrations (mBq/kg-fresh) in fish from the coastal waters of Korea. MDA denotes minimum detected activity.

The concentrations of ^{137}Cs in shellfish were in the range of 55–175 mBq/kg·fresh in 2011 and in the period 2012 to 2016, ^{90}Sr reached its lowest level of <5.3 mBq/kg·fresh (2015) and $^{239+240}$Pu was in the range of 0.16~20.1 mBq/kg·fresh (Table 3.9, Figures 3.34–3.36).

Table 3.9 Concentrations of ^{137}Cs, ^{90}Sr and $^{239+240}$Pu in shellfish from the coastal sea of Korea.

Year	^{137}Cs (mBq/kg·fresh)		^{90}Sr (mBq/kg·fresh)		$^{239+240}$Pu (mBq/kg·fresh)	
	Average ± SD	Range	Average ± SD	Range	Average ± SD	Range
2006–2010	87 ± 33	<14.5–184	–	<29.7	6.65 ± 4.07	0.39–28.60
2011	107 ± 34	55–175	–	<7.11	8.22 ± 10.30	2.23–20.1
2012	–	30.3	–	<13.1	3.98 ± 3.88	1.39–8.45
2013	–	<43.6	–	<8.70	1.91 ± 1.03	1.28–3.09
2014	–	<37.1	–	<6.44	1.47 ± 0.94	0.16–2.26
2015	–	<36.7	–	<5.28	1.54 ± 0.97	0.778–2.63
2016	–	<20.2	–	<8.75	1.39 ± 0.82	0.261–2.18

Dash indicates less than minimum detected activity.

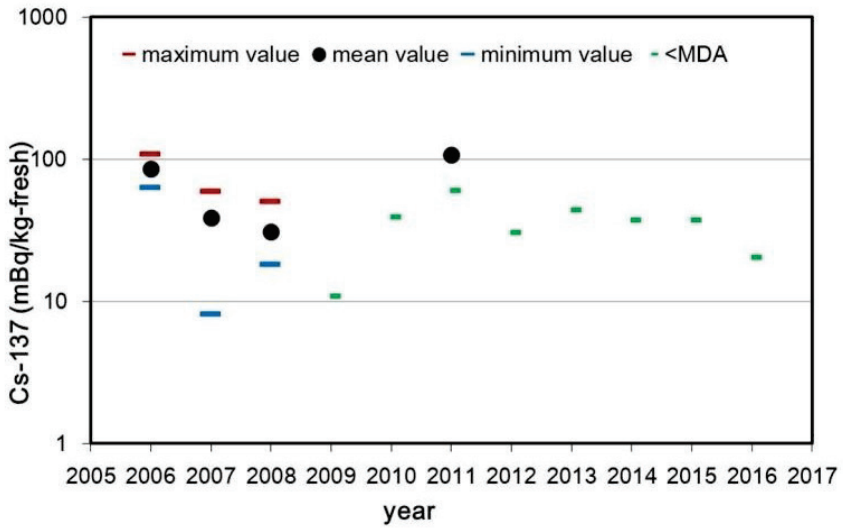

Fig. 3.34 Time series for ^{137}Cs concentrations (mBq/kg-fresh) in shellfish from the coastal waters of Korea. MDA denotes minimum detected activity.

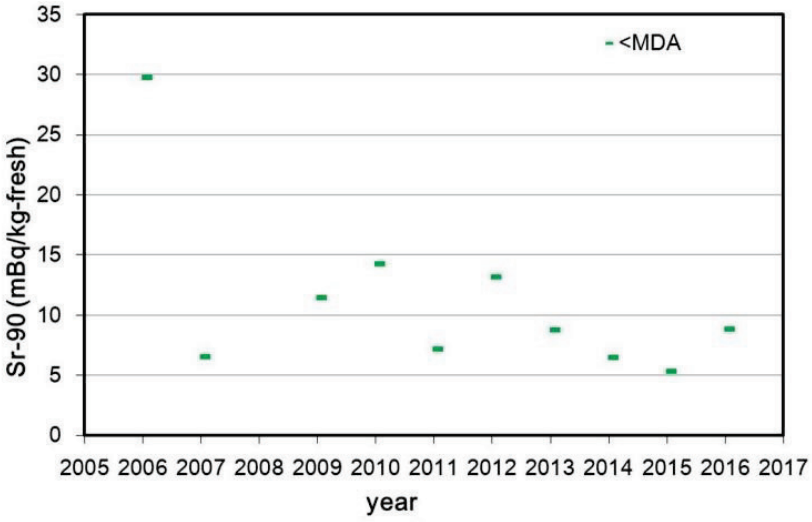

Fig. 3.35 Time series for ^{90}Sr concentrations (mBq/kg-fresh) in shellfish from the coastal waters of Korea. MDA denotes minimum detected activity.

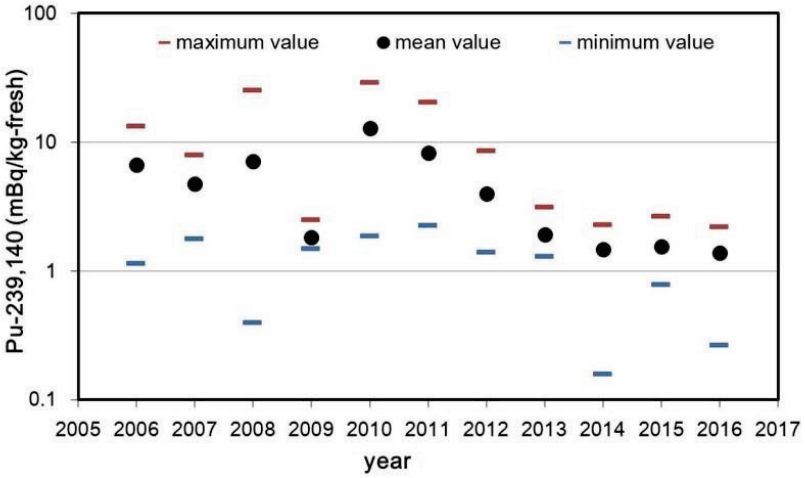

Fig. 3.36 Time series for $^{239+240}$Pu concentrations (mBq/kg-fresh) in shellfish from the coastal waters of Korea. MDA denotes minimum detected activity.

^{137}Cs concentrations in seaweed were all below the MDA (<59.9 mBq/kg·fresh) while ^{90}Sr and $^{239+240}$Pu levels were 7.2–28.7 mBq/kg·fresh and 0.232–2.63 mBq/kg·fresh in the period from 2011 to 2016, respectively (Table 3.10, Figures 3.37–3.39).

Table 3.10 Concentrations of ^{137}Cs, ^{90}Sr and $^{239+240}$Pu in seaweed from the coastal sea of Korea.

Year	^{137}Cs (mBq/kg·fresh)		^{90}Sr (mBq/kg·fresh)		$^{239+240}$Pu (mBq/kg·fresh)	
	Average ± SD	Range	Average ± SD	Range	Average ± SD	Range
2006–2010	–	<14.5–<52.4	26.8 ± 18.7	11.7–47.8	3.16 ± 1.41	0.21–9.79
2011	–	<14.1	18.3 ± 10.8	7.2–28.7	0.86 ± 0.39	0.51–1.28
2012	–	<59.9	–	<20.8	1.82 ± 0.07	1.74–1.86
2013	–	<35.2	13.2 ± 3.8	10.1–17.4	0.868 ± 0.528	0.264–1.24
2014	–	<47.9	–	<8.6	0.233 ± 0.010	0.232–0.233
2015	–	<48.0	–	<11.9	2.30 ± 0.42	2.00–2.60
2016	–	<28.4	–	<22.3	2.35 ± 0.28	2.07–2.63

Dash indicates less than minimum detected activity.

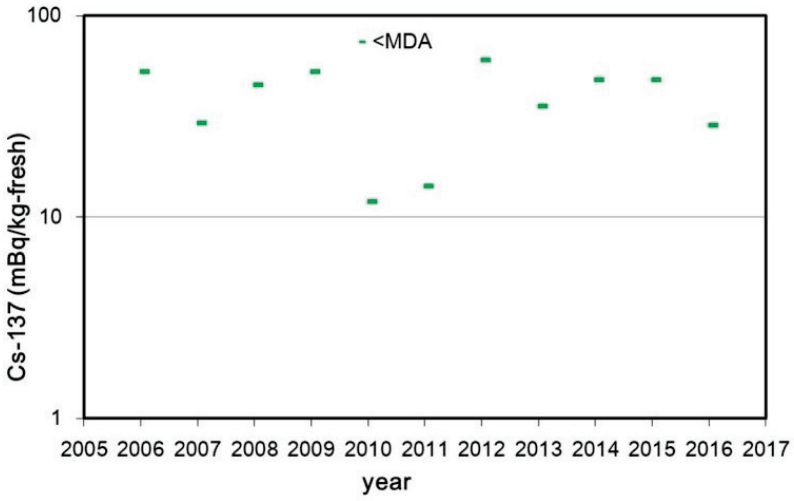

Fig. 3.37 Time series for ^{137}Cs concentrations (mBq/kg-fresh) in seaweed from the coastal waters of Korea. MDA denotes minimum detected activity.

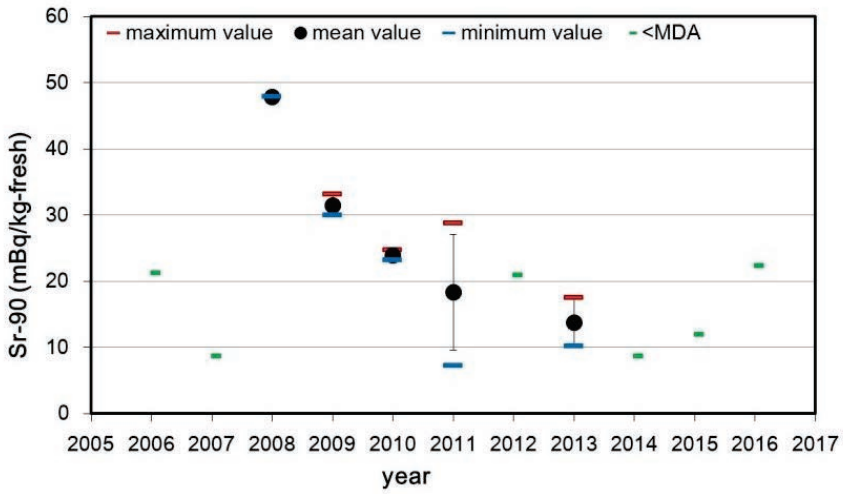

Fig. 3.38 Time series for ^{90}Sr concentrations (mBq/kg-fresh) in seaweed from the coastal waters of Korea. MDA denotes minimum detected activity.

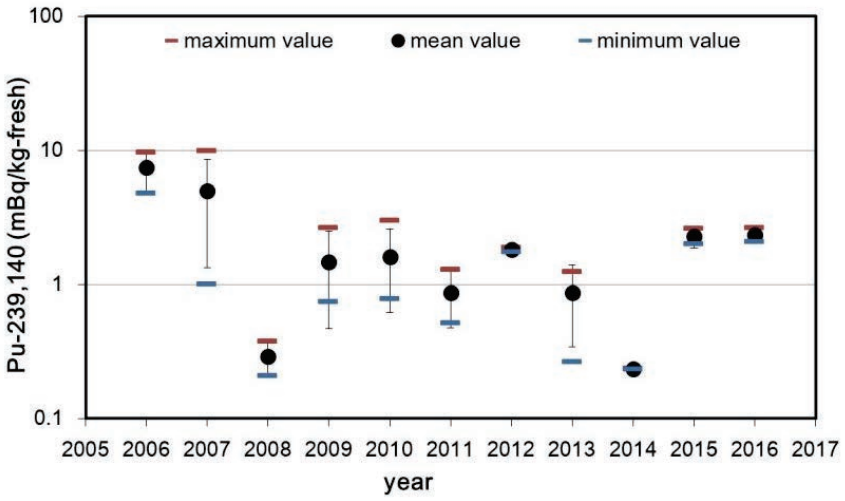

Fig. 3.39 Time series for $^{239+240}$Pu concentrations (mBq/kg-fresh) in seaweed from the coastal waters of Korea. MDA denotes minimum detected activity.

The concentrations of ^{137}Cs, ^{90}Sr and $^{239+240}$Pu in the marine biota, including fish, shellfish and seaweed collected in the coastal waters of Korea during 2011–2016 were similar with those before the FDNPP accident. However, the concentration of ^{137}Cs in a sample of the mullet (*Mugil cephalus*) captured along the eastern coast in 2012 was found to be 2,432 ± 32 mBq/kg·fresh, which was ten times higher than annual average concentrations in fish measured during 2006–2011. The concentration of ^{134}Cs in this sample was 1,719 ± 28 mBq/kg·fresh, and the radioactivity ratio of ^{134}Cs/^{137}Cs calculated at the time of the FDNPP accident (March 2011) coincides closely with the release ratio of the accident source radiocesium (^{134}Cs/^{137}Cs = 1).

3.4.4 Summary

Monitoring of radionuclides in coastal waters of Korea has continued on a regular basis since 1994. Seawater samples have been collected biannually and quarterly at 21–32 stations off the coast of Korea. Sediments were collected at 16 stations once a year, and marine biota including more than 20, 6 and 6 samples for fish, shellfish and seaweed, respectively, also were monitored. The concentrations of ^{137}Cs, ^{3}H, ^{90}Sr and $^{239+240}$Pu were analyzed and assessed in the seawater while biota and sediment samples were analyzed for ^{137}Cs, ^{90}Sr and $^{239+240}$Pu. On March 11, the government of the Republic of Korea established an emergency response system to respond to the accident of the FDNPP in Japan. On March 28, 2011, KINS announced that it was the first agency to detect an artificial radioactive nuclear species, such as ^{131}I emanating from the FDNPP accident. At the government level, the “Plan for Strengthening Environmental Radiation Monitoring by Stage” program was established and converted to an emergency radiation monitoring system for the whole country. In order to promptly confirm the possibility of radioactive materials released to the atmosphere and to the sea into the surrounding waters in Korea, the marine environmental radioactivity survey was enhanced with increased sampling frequency and geographic area for seawater and fish samples.

During 2011–2016, ^{3}H, ^{137}Cs, ^{90}Sr and $^{239+240}$Pu levels in the surface waters of the coastal sea of Korea had values varying from <0.107 to 0.458 Bq/L, from <1.04 to 2.77 mBq/L, from <0.239 to 1.77 mBq/L and from 1.48 to 14.6 μBq/kg, respectively. The levels of radionuclide concentrations in the surface seawater of the coastal sea of Korea since 2011 are consistent with levels obtained over the past 5 years (2006–2010) before the FDNPP accident in Japan.

The concentrations of ^{137}Cs, ^{90}Sr and $^{239+240}$Pu in surface sediments of the coastal sea of Korea over the period of 2011 to 2016 were in the ranges <0.741–4.71 Bq/kg·dry, <0.080–0.318 Bq/kg·dry and 0.048–1.36 Bq/kg·dry, respectively. The levels of concentrations of radionuclides in the surface sediment of the coastal sea of Korea since 2011 are consistent with the concentrations (^{137}Cs: <0.502–5.78 Bq/kg·dry, ^{90}Sr: <0.169 Bq/kg·dry and $^{239+240}$Pu: 0.096–1.20 Bq/kg·dry) obtained over the past 5 years (2006–2010) before the FDNPP accident, indicating negligible influence of this accident on sediment regimes in Korean coastal waters.

The concentrations of ^{137}Cs, ^{90}Sr and $^{239+240}$Pu in marine biota, including fish, shellfish and seaweed collected from the coastal waters of Korea during 2011–2016 were similar to those measured before the FDNPP accident. However, the concentration of ^{137}Cs in the mullet (*Mugil cephalus*) captured along the eastern coast in 2012 was found to be 2,432 ± 32 mBq/kg·fresh, which was ten times higher than annual average concentrations in fish measured during 2006–2011. The concentration of ^{134}Cs in this sample was detected as 1,719 ± 28 mBq/kg·fresh, and the radioactivity ratio of ^{134}Cs/^{137}Cs calculated at the time of the FDNPP accident (March 2011) coincides closely with the release ratio of the accident source Cs (^{134}Cs/^{137}Cs = 1).

4 Monitoring Results in the Northeast Pacific Ocean from Canada

The plume of radioactivity discharged into the ocean from the FDNPP accident dissipated rapidly in the energetic coastal waters off Japan under the influence of jet-like currents, tidal currents and mesoscale eddies (Tsumune *et al*., 2013), but a significant remnant was transported eastward by extensions of the Oyashio and Kuroshio systems (Figure 4.1). The Kuroshio formed a boundary between contaminated surface waters to the north and unaffected waters to the south (Buesseler *et al*., 2012) while the eastward progression of the FDNPP plume was driven by the North Pacific and higher latitude Subarctic Current. The latter bifurcates as it approaches North America, diverging into the northward-flowing Alaska Current and the southward-flowing California Current (Figure 4.1). The leading edge of the plume advanced at an average speed of 7–8 km/day (Aoyama *et al*., 2016) that is consistent with drifter-based estimates of the horizontal spread of the FDNPP plume (Rypina *et al*., 2013, 2014) and comparable to zonal geostrophic current velocities in the core of the North Pacific Current (Cummins and Freeland, 2007).

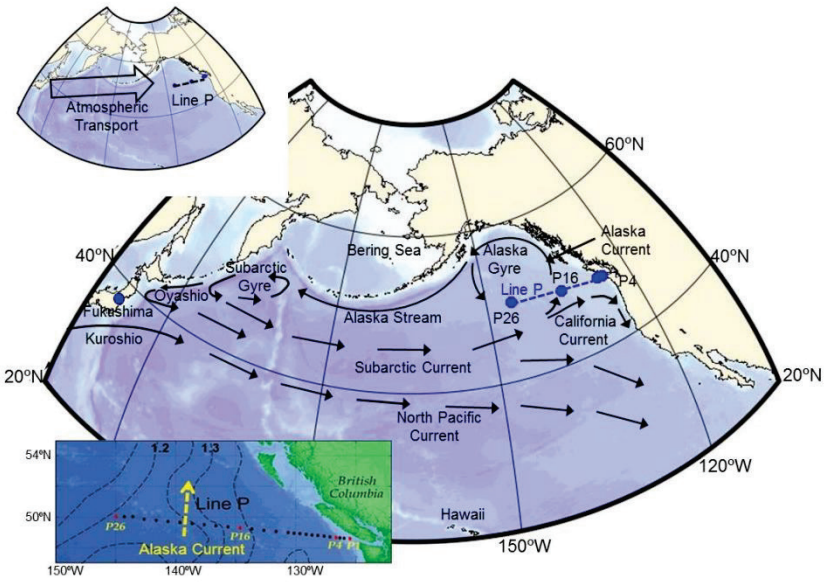

Fig. 4.1 Current systems transported oceanic discharges of radioactivity from the FDNPP accident (dark blue symbol) eastward across the Pacific and northward across Line P at the eastern edge of the Alaska gyre. Upper inset: Open arrow illustrates general northeastward direction for transport of atmospheric discharges of FDNPP accident radioactivity. Lower inset: Positions of stations illustrated for Line P. Dashed curves are streamlines whose values (cm) represent the average dynamic height field for 2002–2012, indicating strong northward flow in the Alaska Current (yellow arrow).

Ocean circulation models predicted that the major component of the FDNPP accident (hereinafter also termed 'Fukushima') radioactivity plume would be almost entirely transported from the

western to eastern North Pacific in the 5 years following the accident and that the highest levels would be first observed off the British Columbia (BC) coast (Behrens *et al*., 2012; Rossi *et al*., 2013). Accordingly, a Canadian monitoring program for the sampling and analysis of seawater for Fukushima radioactivity in the offshore regime was initiated shortly after the accident (Smith *et al*., 2015). Subsequently, a second inshore monitoring program called InFORM (Integrated Fukushima Ocean Radionuclide Monitoring Network) was established that employed citizen scientists to collect biota and seawater samples and monitor the arrival and progress of the signal along the coast. Close collaboration was established between the Canadian monitoring program and the USA crowd sourcing program established at the Woods Hole Oceanographic Institution (WHOI). The results outlined in these studies are being used to evaluate ecosystem impacts of Fukushima radioactivity in the Canadian marine environment, delineate water circulation patterns and flow velocity time scales in the eastern North Pacific and provide insight into the accuracy of global circulation model simulations of Fukushima tracer dispersion.

4.1 Protocols

The sampling program for the monitoring of the Fukushima radioactivity plume in the eastern North Pacific was anchored by ten missions between June 2011 and February 2017 on the CCGS *John P. Tully* on Line P, three (2014, 2015 and 2016) expeditions of the CCGS *Sir Wilfrid Laurier* in the eastern North Pacific and the USA 2014 R/V *Point Sur* and 2015 CLIVAR-P16N cruises. Sample collection in coastal systems was carried out through crowd sourcing programs using citizen scientists in Canada and the USA with results posted to the websites of InFORM (https://fukushimainform.ca/) and WHOI (http://www.ourradioactiveocean.org/), respectively. In the offshore sampling program, large volume (≅ 60 L) water samples were collected to depths of 1,000 m and then passed through potassium cobalt ferrocyanide (KCFC) resin columns to selectively extract Cs isotopes from seawater. Column extraction efficiencies are generally greater than 96% as determined using spiked yield tracers with resin columns arranged in series (Smith *et al.*, 1990). The isotopes ^{137}Cs and ^{134}Cs were subsequently measured on the oven-dried KCFC resins in the laboratory using high purity Ge well detectors. All data were decay corrected to the time, April 6, 2011, of maximum discharges from the FDNPP accident, following Buesseler *et al*. (2011). Detection limits for ^{137}Cs and ^{134}Cs were generally 0.10 Bq/m^3 and 0.13 Bq/m^3, respectively. Detector efficiencies were measured using National Institute of Standards and Technology (NIST) and National Bureau of Sciences (NBS) calibration standards (*e.g*., NBS 4350B river sediment) and IAEA reference materials. Hydrographic results for the Line P cruises are available at http://linep.waterproperties.ca.

Coastal water samples were collected monthly by citizen scientists supported by InFORM at a wide range of nearshore locations along the BC shoreline. A 20 L water sample was passed through a 5-milliliter column of potassium-nickel-hexacyanoferrate resin for cesium extraction. Column extraction efficiencies were determined using spiked yield tracers, and were generally greater than 96%. The radio-cesium measurement was subsequently performed by gamma spectrometry using a high purity germanium well-detector. The USA open ocean sampling program involved the collection of 20 L seawater samples which were filtered, acidified with nitric acid and spiked with stable Cs after which radiocesium was extracted using a KNiFC-PAN ion-exchange resin (Breier *et al*., 2016). Resins were dried and gamma counted using methodologies similar to those outlined above. Stable Cs was measured using ICP (inductively coupled plasma) mass spectrometry to determine and correct for resin extraction efficiencies.

Between 2014 and 2016, nearly 400 fish samples (primarily salmon species) were collected. Samples were donated, for the most part, by First Nations communities from more than 10 rivers in BC and Yukon. The samples were frozen and measured in a well-defined counting geometry using a

high purity germanium detector (6 h of counting time, each). Samples showing the highest concentration of radio cesium in this screening phase were then freeze-dried and re-measured for an extended period of time (2 weeks). Regional and annual averages of ^{137}Cs were obtained by summing the gamma spectra of all the results from each region and/or year.

The monitoring of Fukushima radioactivity is simplified by the fact that the initial ^{134}Cs/^{137}Cs activity ratio in Fukushima-derived radioactivity was 1 (Buesseler *et al*., 2011). Owing to its short half-life ($T_{1/2}$ = 2.1 y), any residual ^{134}Cs in atmospheric fallout from nuclear weapons tests or the Chernobyl nuclear accident has decayed in contrast to ^{137}Cs ($T_{1/2}$ = 30 y) for which there is still a measurable weapons tests fallout background. The detection of ^{134}Cs in seawater is therefore an unequivocal "fingerprint" indicator of contamination from Fukushima, which is the only large-scale contributor of radioactivity to the Pacific Ocean besides weapons tests fallout. The measured ^{134}Cs concentration decay corrected to April 6, 2011, is therefore equivalent to the ^{137}Cs concentration at the time of the accident and will hereafter be termed the "Fukushima ^{137}Cs" concentration, as distinguished from the background weapons tests "fallout ^{137}Cs" and "total ^{137}Cs (= Fukushima plus fallout ^{137}Cs)" concentrations.

4.2 Offshore water

Radionuclide measurements on Line P intercepted the plume of Fukushima radioactivity advancing along the southern and eastern edges of the Alaska Gyre (Figure 4.1). Sta. P4 is situated over the continental slope at a water depth of 1,300 m while Sta. P26, located at a depth of 4,250 m, anchors Line P offshore near the southwestern boundary of the Alaska Gyre. Water depth profiles of ^{137}Cs measured at Stas. P4 and P26 at depths up to 1,000 m in June 2011, three months after the accident, were consistent with weapons tests fallout profiles having surface water background levels of 1–2 Bq/m^3, indicating that Fukushima radioactivity transported by ocean currents had not yet arrived in the eastern North Pacific. The first observations of the Fukushima signal were measurements of low levels of ^{134}Cs in the upper 100 m at Sta. P26 in June 2012 (Smith *et al*., 2015). By June 2013,^{134}Cs from Fukushima was detectable in surface water at most stations sampled on Line P at levels of about 1–2 Bq/m^3 (decay corrected to time of the Fukushima accident), thereby providing the first evidence for the arrival of the Fukushima radioactivity plume in western North American continental waters. In 2013, ^{134}Cs was detectable to a depth of 100 m of the water column, matching the maximum depth of the winter mixed layer in the eastern North Pacific at Sta. P26 (Thomson and Fine, 2009).

The June 2013, Line P section for total ^{137}Cs (Fukushima plus fallout ^{137}Cs) is illustrated in Figure 4.2 (upper left panel). Through February and August 2014, total ^{137}Cs concentrations in surface water at the western end of Line P (Stas. P16–P26) increased steadily to levels greater than 5 Bq/m^3, while much smaller ^{137}Cs increases were observed at the eastern end of Line P proximal to the continental shelf (Figure 4.2). During 2014, ^{137}Cs levels began to increase at water depths of 150–200 m that extend well below the surface mixed layer, particularly on the western end of Line P. These observations indicate that Fukushima ^{137}Cs had been injected into the pycnocline upstream of Line P in the western North Pacific where winter mixed layer depths are much deeper. Rainfall and freshwater inputs from the coast maintain a much more surface stratified regime in the Northeast Pacific. Between August 2014 and February 2015, the ^{137}Cs plume began to advance shoreward and to descend to depths below 200 m. By August 2015 the total ^{137}Cs plume had progressed to the eastern side of Line P and by February 2016 had increased in concentration to values in excess of 8 Bq/m^3 at central locations (Figure 4.2).

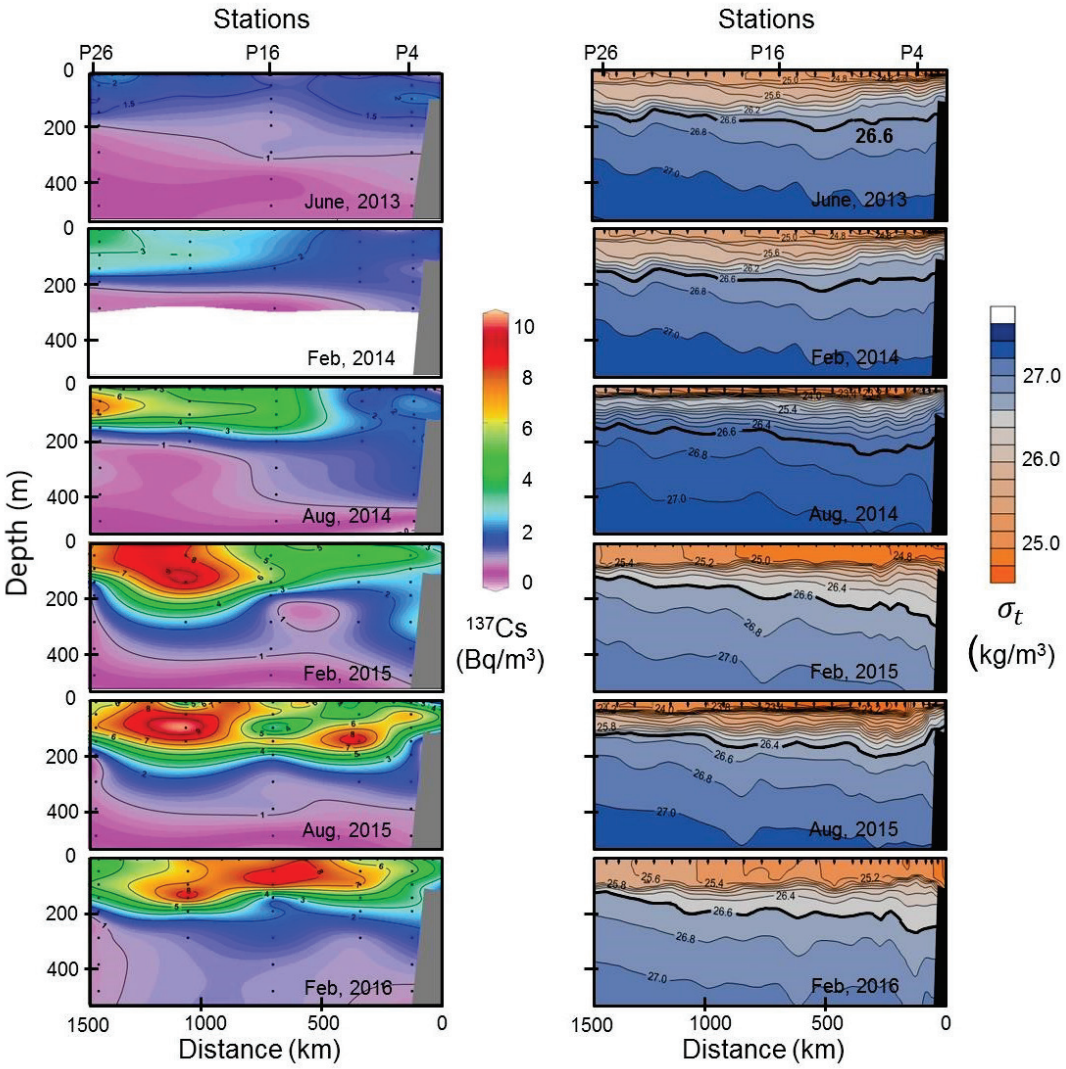

Fig. 4.2 (Left panel) Time series of total ^{137}Cs sections showing the progressive arrival of the Fukushima signal on Line P between June 2013 and February 2016. (Right panel) Time series of density (σ_t) surfaces on Line P with the bolded 26.6 isopycnal that outcrops in the western North Pacific.

Line P density sections illustrated in Figure 4.2 (right hand panel) exhibit features associated with processes that govern ^{137}Cs transport. The eastward deepening of the Fukushima ^{137}Cs signal on Line P over time reflects tracer spreading with minimal diapycnal mixing in a shoreward direction owing to ^{137}Cs concentration gradients on the large-scale, downward tilting isopycnal surfaces. The σ_t = 26.6 kg/m^3 isopycnal (bolded in Figure 4.2) corresponds to North Pacific Intermediate Water (NPIW) that outcrops in regions northeast of Japan that also received significant atmospheric inputs of Fukushima fallout (Aoyama *et al*., 2013). NPIW is formed on time scales of 1 to 2 years (Simizu *et al*., 2004) by winter mixing in the subarctic gyre of the northwestern Pacific (Figure 4.1) and takes 5 to 7 years to flow along the 26.5–26.8 isopycnals (at water depths of 100–200 m) to Sta. P26 on Line P (Ueno and Yasuda, 2003). These values are similar to transit time inferences of Whitney *et al*. (2007) for NPIW flow based on minimum AOU (Apparent Oxygen Utilization) measurements at Sta. P26. The eastward spreading of Fukushima ^{137}Cs in the NPIW from the subarctic gyre to Line P could explain the arrival of Fukushima ^{137}Cs at depths of 100–200 m at Sta. P26 by 2014 if these spreading rates were somewhat faster than previously reported.

Subsurface transport of the Fukushima signal has been extensively documented in the northwestern Pacific. In 2013, Yoshida *et al*. (2015) measured Fukushima ^{137}Cs at 600 m depth near the 26.5 isopycnal surface on a 30°N longitudinal transect near 180° which they hypothesized may be the result of Fukushima isotopes being directly discharged into the ocean near the NPIW formation region and transported to the mid depth subtropical gyre following NPIW pathways. Fukushima ^{137}Cs has also been observed (Yoshida *et al*., 2015; Aoyama *et al*., 2016; Kaeriyama *et al*., 2016) in several mode waters, including Central Mode Water (CMW) and Subtropical Mode Water (STMW) formed in subduction areas north and south, respectively, of the Kuroshio (Oka and Qiu, 2012). The southernmost (25–30°N) region of subduction, where STMW forms ($\sigma_t \cong 25$ kg/m^3), likely entrained only the fallout portion of Fukushima ^{137}Cs since the direct release occurred farther north. However, subduction zones for lighter CMW (LCMW, $\sigma_t \cong 26$ kg/m^3 formed within 30–37.5°N) and denser CMW (DCMW, $\sigma_t \cong 27$ kg/m^3 formed within 37.5–45°N) are sufficiently far north that ^{137}Cs can be entrained into the interior ocean from both direct releases and atmospheric deposition (Aoyama, *et al*., 2016). It is therefore likely that tracer transport in CMW also contributes to Fukushima ^{137}Cs inventories below depths of 100 m on Line P.

At smaller, continental shelf scales, an additional factor that influences ^{137}Cs distributions on Line P is upwelling over the BC continental slope and outer shelf caused by the prevailing alongshore, southward winds during summer months. This process is reflected in density sections in Figure 4.2 by upward tilting isopycnals adjacent to the shelf break that were observed on August cruises. Upwelling is accompanied by a weak seaward flow in the surface Ekman layer and by a strong surface-intensified southeastward flow associated with the wind-induced shelf-break current centered near the 200 m depth contour. Eddies and lateral turbulent mixing associated with these currents transport fresher, subsurface coastal water over the shelf which tends to have lower ^{137}Cs concentrations derived mainly from weapons tests fallout and thereby prevents the surface Fukushima radionuclide plume from reaching nearshore regions. In addition, the mixing of recently upwelled waters (having low ^{137}Cs levels from weapons tests fallout) with the offshore plume (higher ^{137}Cs levels from Fukushima), followed by subduction and subsequent re-circulation into the coastal upwelling can produce subsurface tracer maxima proximal to the shelf as observed in the ^{137}Cs panels (Figure 4.2) for August 2014 and 2015. The deeper Fukushima ^{137}Cs signal below depths of 300 m in each panel represents a residual weapons tests fallout signal that has accumulated over previous years by ocean interior transport on isopycnal surfaces.

The eastward advance of the Fukushima ^{137}Cs signal in surface water along Line P is illustrated in Figure 4.3 by an Hovmöller diagram (time *vs.* distance from the coast) for mean Fukushima ^{137}Cs in the upper 150 m. The slope of a given iso-concentration boundary (white dashed lines) represents the inverse of the inshore flow velocity of the Fukushima signal. During 2013–2014, the Fukushima signal advanced eastward at a speed of 6.6 km/day between Stas. P26 and P15, based on the 1–3 Bq/m^3 iso-concentration curves (Figure 4.3). However, further eastward, advance from Sta. P15 to Sta. P4 occurred at a much slower rate of 0.8 km/day (Figure 4.3). The principal component of the Fukushima plume arrived at Line P in 2014–2015 during which the eastward transport rate of the Fukushima signal on the western end of Line P decreased slightly, but the same slow flow rate of 0.8 km/day was observed eastward from Sta. P15.

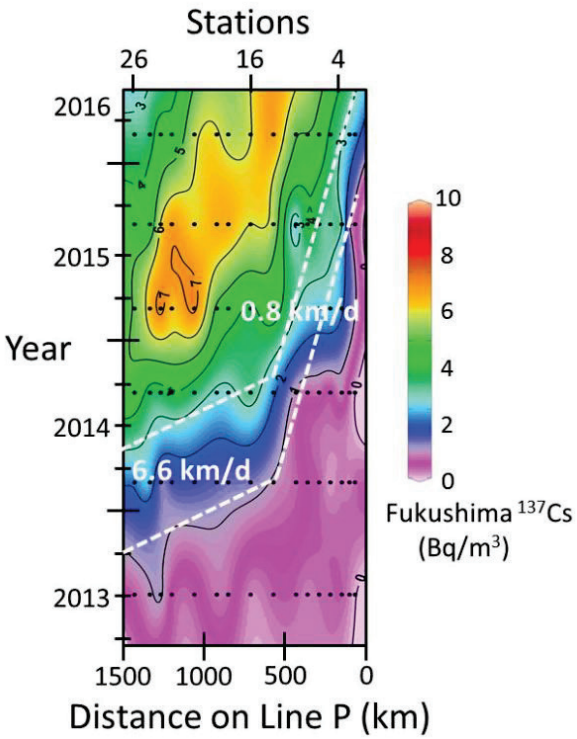

Fig. 4.3 The landward transport of the Fukushima tracer signal is illustrated by a Hovmöller diagram (time *vs.* distance) of mean Fukushima ^{137}Cs concentrations (Bq/m^3) in the upper 150 m along Line P. The value of the slope of a given iso-concentration boundary (white dashed lines) gives the reciprocal of the inshore spreading velocity of the Fukushima signal along Line P.

The Fukushima ^{137}Cs plume took about 2 years to be transported 6,000 km across the Pacific Ocean in the North Pacific Current to Sta. P26 at a speed of 7 km/day (Aoyama *et al.*, 2016) and then advanced eastward across the Alaska Current from Sta. P26 to Sta. P15 at 5–7 km/day. However, the continued progression of the signal eastward from Sta. P15 to the continental shelf occurred at the sharply reduced rate of 0.8 km/day. There are several factors contributing to this reduced flow rate in the onshore transport of the tracer signal. Line P is situated in the vicinity of the bifurcation of the North Pacific Current, where the large-scale circulation diverges into the northward flowing Alaska Current and the southward flowing California Current (Figure 4.1). These flows are subject to pronounced variability on inter-annual to decadal time scales. Time-averaged streamlines representing the mean dynamic height field for 2002–2012 calculated from Argo float data[6] are illustrated in Figure 4.1 (inset). The mean streamlines are concentrated on the western end of Line P (seaward of Sta. P15), which on average intercepts the northward geostrophic transport of the Alaska Current with flow speeds of 5–10 km/day. The streamlines diverge markedly on the eastern end of Line P, which lies generally within the bifurcation zone. The flow in this region is highly variable and mean currents are weak and difficult to define (Cummins and Freeland, 2007). Indeed, this region with strong seasonal variability constitutes the transition zone between the quasi-permanent coastal upwelling to the south (California coast) and the dominant downwelling to the north. The decreasing ^{137}Cs tracer levels in the surface mixed layer eastward along Line P (Figure 4.2) therefore represent a transition from higher levels in the northward flowing core of the Fukushima tracer plume to lower levels in the weaker transitional flow field of the bifurcation zone.

[6] http://www.meds-sdmm.dfo-mpo.gc.ca/isdm-gdsi/argo/canadian-products/index-eng.html

This slower eastward flow of the Fukushima signal onto the shelf is illustrated by the reduced spreading velocity between Sta. P15 and Sta. P4 inferred from the ^{137}Cs iso-concentration curves in Figure 4.3.

A second factor in the onshore flow of the Fukushima ^{137}Cs signal is related to the large-scale atmospheric circulation in 2013–2015. This factor is addressed in Figure 4.4, where the left-hand time series panels show areal time series distributions for total ^{137}Cs (Fukushima plus weapons tests fallout ^{137}Cs) in surface water between 2013 and 2016 for samples collected in the offshore and coastal monitoring programs (InFORM and WHOI) noted in the Section above. The right-hand panels (Figure 4.4) show sea surface temperature (SST) anomalies for the same geographical regions and sampling time frames.

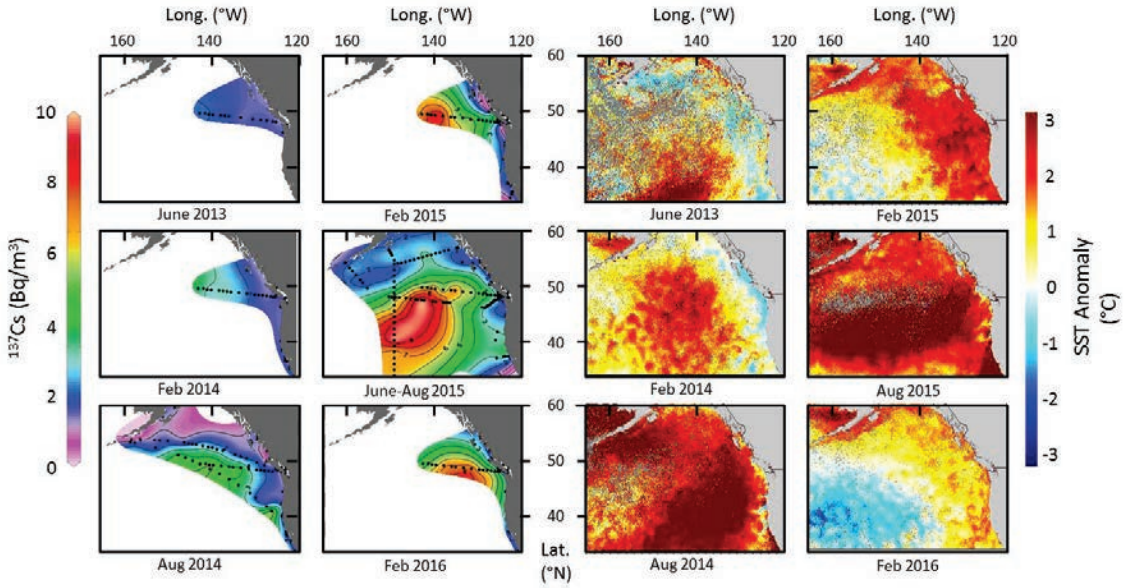

Fig. 4.4 (Left two columns) ^{137}Cs surface water distributions for June 2013 to February 2016 showing spatial evolution of the Fukushima plume as it nears the coastline. (Right two columns) SST anomaly distributions (http://coastwatch.pfel.noaa.gov/data.html) for same time period outlining the development of the warm "blob" which occupies the same water masses as the Fukushima tracer patch.

During the winter of 2013–2014, a large pool of unusually warm water was observed in the south central Gulf of Alaska (Bond *et al.*, 2015). Within the topmost 300 feet (91 m) of the ocean, temperatures were as much as 2.5°C (4.0°F) above average in February 2014, creating a warm sea surface temperature (SST) anomaly that became popularly known as the warm "blob" (Bond *et al.*, 2015). The SST anomaly had its origins in the preceding winter of 2012–2013, but its signature became considerably stronger in 2013–2014, as illustrated by the area of the high SST anomalies (departures from the 1981–2010 mean) which, in February 2014, intersected the western end of Line P and extended southward to 35°N (Figure 4.4, right hand panels). The formation of the SST anomaly was related to an overlying region of unusually persistent and record-high atmospheric pressure that for the winter of 2013–2014 hovered over the eastern North Pacific, deflecting the storm track northward away from the West Coast (Hartmann, 2015). With the ridge in place, the West Coast's typical northwest winds, which produce mechanical mixing and upwelling, slackened, thereby allowed the surface layer water to retain large quantities of heat (Figure 4.4, February and August 2014 SST panels). During the winter of 2014–2015, the high atmospheric pressure system weakened and the SST anomaly shifted southward and evolved into a configuration known as the

Arc Pattern (Di Lorenzo and Mantua, 2016). The high atmospheric pressure ridge had completely dissipated by the winter of 2015–2016 resulting in a return of the normal storm track and the usual pattern of surface layer mixing, giving the relatively even areal SST distribution evident in the February 2016 panel of Figure 4.4.

The ^{137}Cs signal became an incidental proxy radiochemical tracer for the warm SST anomaly or "blob". The areal distribution of total ^{137}Cs derived from surface water measurements for August 2014 (Figure 4.4) outlines the northern component of a large pool of water labelled by ^{137}Cs levels in excess of 5 Bq/m^3 that is nearly spatially congruent with the spatial configuration of the SST anomaly. Despite this large offshore signal, Fukushima ^{137}Cs was not observed in August 2014 in seawater collected at the coastal stations operated by the InFORM and WHOI monitoring programs. However, as the ridge of anomalously high atmospheric pressure over the Northeast Pacific began to dissipate during the winter of 2014–2015, partly in response to weak El Niño-like warming along the equator (Di Lorenzo and Mantua, 2016), both warm SST anomaly water and Fukushima ^{137}Cs sporadically and concurrently reached the Canadian coastline (February 2015 SST panel, Figure 4.4) as first observed at Ucluelet, BC, in February 2015.[7] By August 2015, Fukushima ^{137}Cs had been detected at multiple locations along the Canadian and the USA coastlines as the SST anomaly pattern broadened and shifted southeastward. By February 2016, the high atmospheric pressure ridge had dissipated and both the anomalously warm water and the Fukushima ^{137}Cs signal had spread southward along the USA coastline to California.[8]

4.3 Model simulation

Various global ocean circulation models (Behrens *et al*., 2012; Rossi *et al*., 2013; Aoyama *et al*., 2016) have been used to simulate the long-term spreading of the Fukushima signal across the North Pacific Ocean. The Rossi *et al.* (2013) model used Lagrangian particles within the regional eddy-resolving Ocean General Circulation Model for the Earth Simulator (OFES) to evaluate multi-decadal transport of the Fukushima plume along surface and subsurface pathways. They projected the arrival of the Fukushima plume at Sta. P26 on Line P to occur in early 2014, in general agreement with the present observations (Figure 4.2). In addition, their simulated ^{137}Cs concentrations after correction (Rossi *et al*., 2013) exhibited a good fit with data measured along the International Date Line (180°) in 2012 (Aoyama *et al*., 2013).

The Rossi *et al*. (2013) simulations of the Fukushima ^{137}Cs time series sections on Line P are compared to the experimental results in Figure 4.5. The model simulations are in agreement with experimental observations with two key exceptions. First, the model predicts that the leading edge of the Fukushima signal would be initially observed centrally on Line P near Sta. P16 (Figures 4.5 and 4.6). The experimental results (Figures 4.4–4.6) reveal that the eastward spreading signal actually first encountered Line P at the westernmost station, Sta. P26. A possible factor explaining this discrepancy is that the Rossi *et al*. (2013, 2014) simulation assumed that radioactivity releases occurred solely by direct discharges from the FDNPP into the ocean. Measurements by Aoyama *et al*. (2013) in April–June 2011 of ^{137}Cs levels >10 Bq/m^3 at locations between 40°N and 50°N in the North Pacific were too distant from Fukushima to be explained by surface current transport, and confirm the presence of a more northerly atmospheric transport pathway for Fukushima fallout that was not included in the simulation of Rossi *et al*. (2013, 2014). The initial rapid advance of the Fukushima signal through the atmosphere and its concurrent deposition in the surface ocean is probably responsible for its arrival at Sta. P26 earlier than predicted by model simulations.

[7] https://fukushimainform.ca/about/informal-e-news-archives/

[8] http://www.ourradioactiveocean.org/

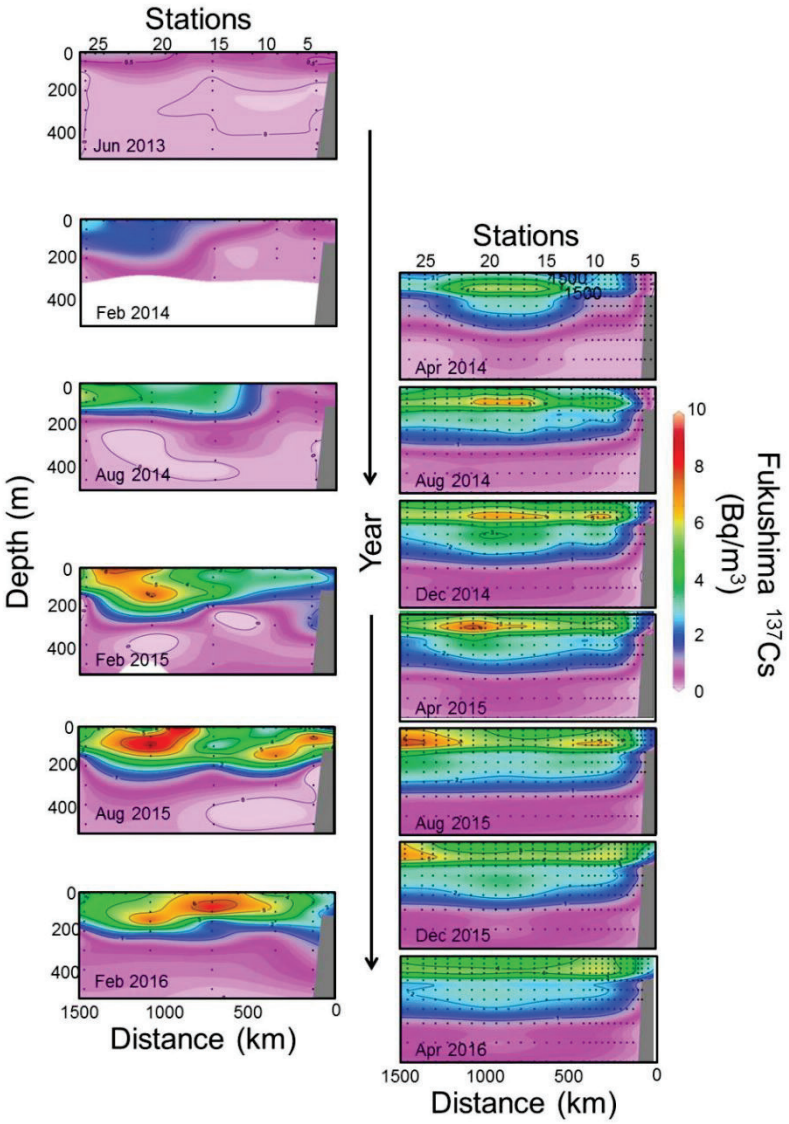

Fig. 4.5 (Left panel) Line P time series sections for Fukushima ^{137}Cs. (Right panel) ^{137}Cs time series simulations for Line P determined from the Rossi *et al*. (2013, 2014) model are generally consistent with the main features of the measured results.

The second model–data discrepancy stems from model simulations showing the descent of the Fukushima signal to 300 m depth by the time it arrives on Line P (Figure 4.5), in contrast to the experimental results indicating negligible transport of Fukushima ^{137}Cs had occurred below 250 m by 2016. This inconsistency derives from model predictions of more rapid eastward spreading of Fukushima ^{137}Cs along the deeper isopycal surfaces at 300 m ($\sigma_t \cong$ 26.8–26.9 kg/m^3) than has actually been observed. This result may also stem from the adoption by Rossi *et al*. (2013, 2014) of a tracer input function neglecting atmospheric discharges and assuming that releases were solely into the ocean off Fukushima. In the model simulation, the subsequent eastward flow of the Fukushima ^{137}Cs signal across the Pacific at 40°N would encounter various subduction areas (Oka *et al*., 2012) facilitating incorporation into the pycnocline. However, the more northern atmospheric pathway actually followed by much of the tracer signal would have encountered different subduction regimes. These results indicate that the magnitude of ^{137}Cs subduction in mode waters (LCMW, DCMW and STMW) was probably over-estimated by the model (*i.e*., positive bias at depths spanning 200–400 m).

Line P time series for mean surface mixed layer (0–150 m) Fukushima ^{137}Cs concentrations at Stas. P4, P16 and P26 are compared with the results of the model simulation of Rossi *et al*. (2013, 2014) in Figure 4.6. As noted above, the Rossi *et al*. (2014) time series for Fukushima ^{137}Cs slightly lags the measured values at the westernmost location, Sta. P26. However, the model is in good agreement with the measured Fukushima ^{137}Cs time series at the shelf edge location, Sta. P4, where confounding factors such as the early atmospheric delivery of Fukushima ^{137}Cs and enhanced stratification associated with warm SST anomalies may have had minimal impact. On average, ^{137}Cs levels measured on Line P (Stas. P4, P16, P26; Figure 4.6) in 2015–2016 appear to be leveling off. According to the Rossi *et al*. (2014) model, Line P surface water ^{137}Cs concentrations should be close to their maxima in 2015–2016 and will begin to decline during 2017–2018.

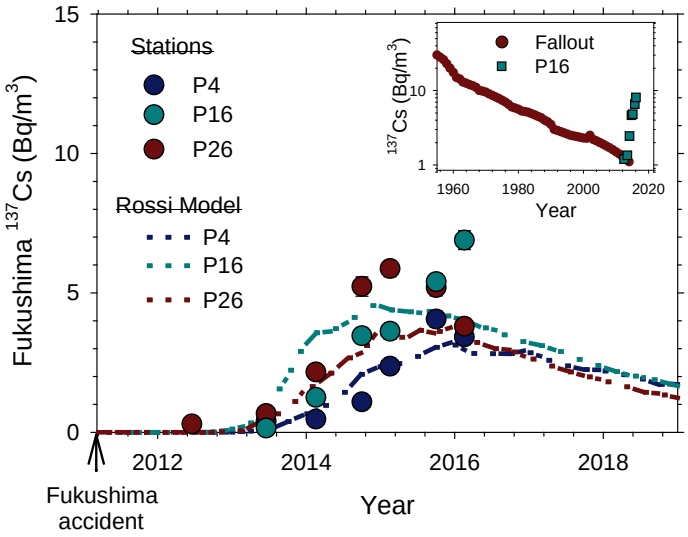

Fig. 4.6 Time series for mean measured Fukushima ^{137}Cs concentrations in the upper 150 m at Stas. P4, P16 and P26 on Line P are compared to model simulations of Rossi *et al*. (2014). (Inset) ^{137}Cs time series for fallout in the North Pacific and total ^{137}Cs (fallout plus Fukushima) in the upper 150 m at Sta. P16.

Given that the ^{137}Cs weapons tests fallout background averaged 1.5 Bq/m^3 in surface water on Line P, levels of Fukushima ^{137}Cs of about 7 Bq/m^3 measured on Line P in 2016 can be viewed as increasing the weapons tests fallout background by a factor of about 5. Comparison with the history of atmospheric fallout in surface water in the North Pacific (inset, Figure 4.6) indicates that total ^{137}Cs values (Fukushima plus weapons tests fallout ^{137}Cs) of 8.5 Bq/m^3 measured at Sta. P16 have returned ^{137}Cs levels in specific water masses such as the Alaska Current to those fallout levels that prevailed during the early 1970s. However, these concentrations of ^{137}Cs in the Northeast Pacific Ocean are well below Canadian guidelines for drinking water quality for which the maximum acceptable concentration (MAC) of ^{137}Cs in drinking water is 10,000 Bq/m^3 and do not represent a radiological threat to human health or the environment (Fisher *et al*., 2013).

4.4 Coastal water

The Fukushima InFORM network is a partnership between academic, government, private organizations and citizen scientists designed to monitor the arrival of Fukushima-derived radioactivity (^{134}Cs and ^{137}Cs) in Canadian coastal waters. Beginning in 2014, the 5-year monitoring effort has captured the initial arrival and peak of the radionuclide signal in the Northeast Pacific and

provided scientifically sound information on the coastal distribution of radioactivity in biota and seawater. The transparent public communication of results from this program informs public health, industry and oceanographic research.

Citizen scientists in 16 communities along the BC coast have collected monthly water samples at locations indicated in Figure 4.7 since October 2014. Since the main component of the Fukushima radioactivity plume arrived in Canadian waters in 2015, there has been a trend of increasing ^{137}Cs levels by an average factor of 2 above fallout background levels (Figures 4.8 and 4.9) which is expected to increase by an additional few Bq/m^3 in the next few years. The largest increases in ^{137}Cs by a factor of 3 appear to have occurred in northern regions, probably owing to the proximity of the northward flowing Alaska Current which carries the main inventory of Fukushima radioactivity. Smaller increases in ^{137}Cs have occurred in the Strait of Georgia where onshore flow is somewhat restricted by the large freshwater outflow from the Fraser River. As noted above, these nearshore concentrations of ^{137}Cs in seawater are orders of magnitude below Canadian guidelines for drinking water quality (MAC of ^{137}Cs in drinking water is 10,000 Bq/m^3) and do not represent a radiological threat to human health or the environment. The regional distribution of Fukushima radioactivity along the BC coast reflects local circulation and mixing processes, and the time constants associated with the spreading of the signal are mainly influenced by estuarine circulation processes at the mouths of the major river systems.

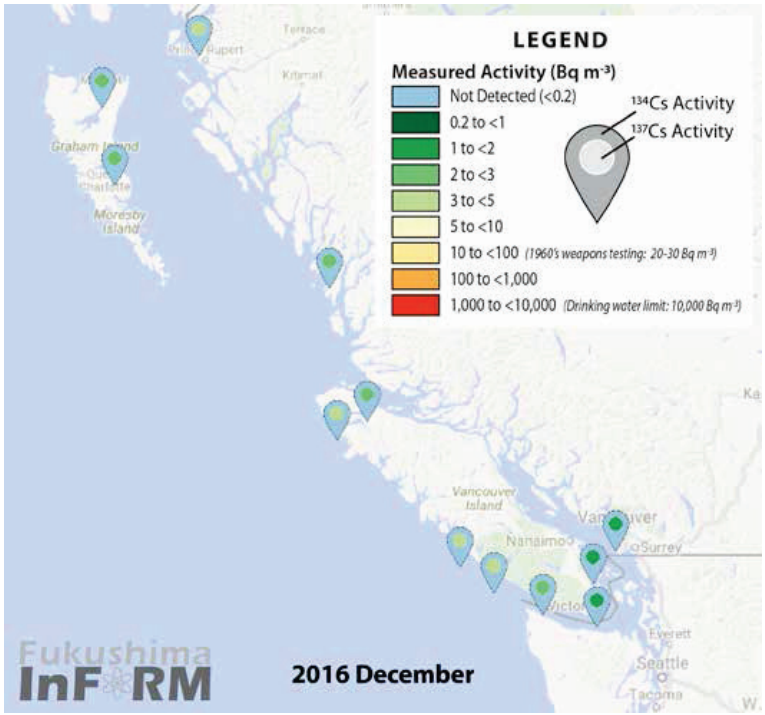

Fig. 4.7 Radioactivity levels for seawater samples collected along the BC coast in December 2016 showing slightly elevated ^{137}Cs levels (above fallout levels of about 1.5 Bq/m^3) along the seaward coast of Vancouver Island and at Prince Rupert in the north, but no detectable measurements of ^{134}Cs, indicating that Fukushima radioactivity is present at only very low levels.

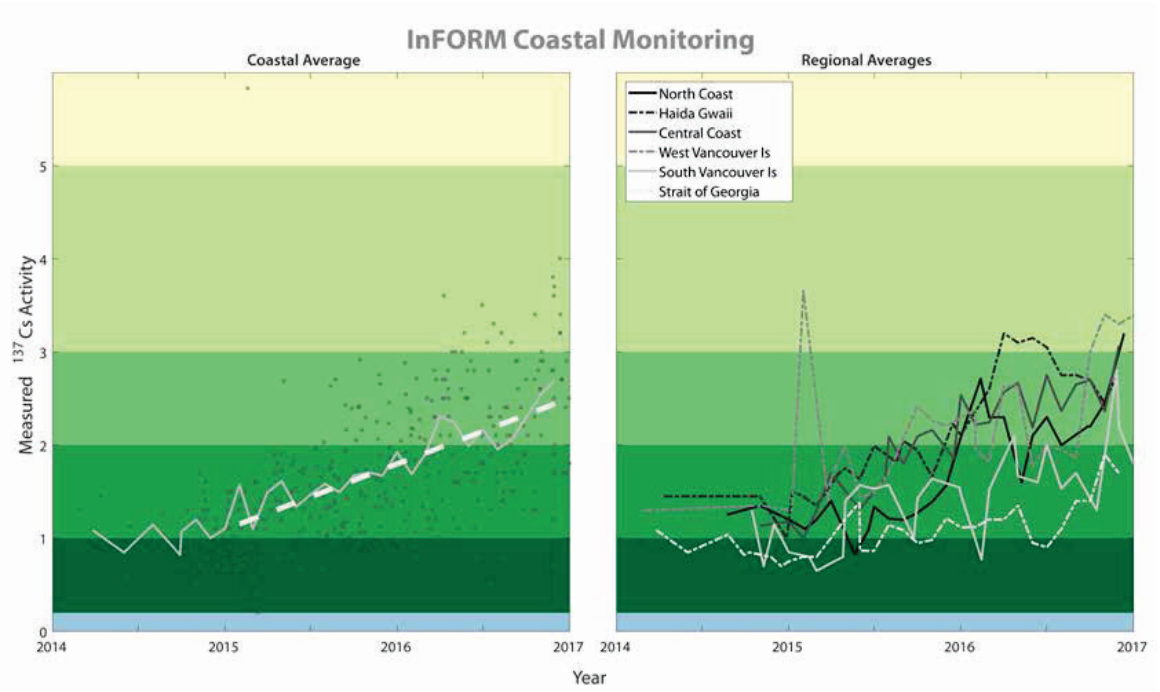

Fig. 4.8 (Left) Increase in ^{137}Cs levels in seawater at coastal stations (2014–2017). (Right) Regional averages of ^{137}Cs levels increased as much as a factor of 3 during 2014–2017.

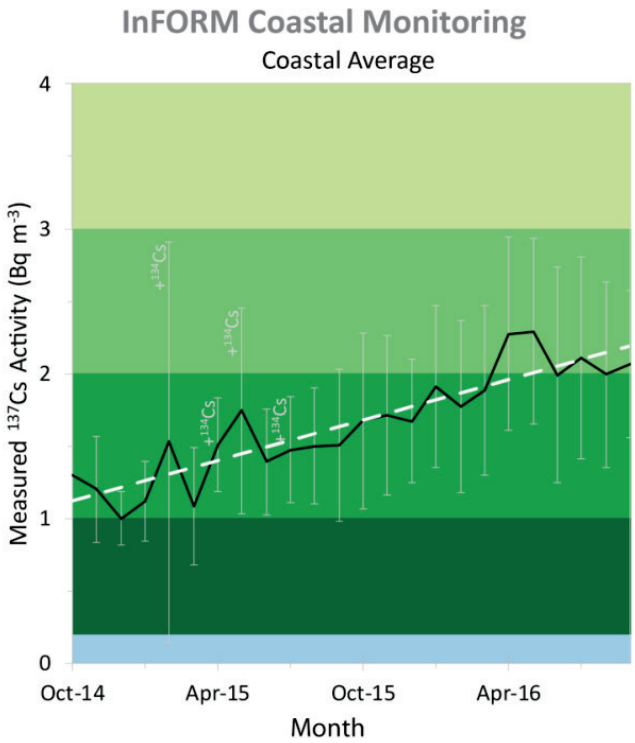

Fig. 4.9 Average increase in ^{137}Cs measured in all seawater samples increased by a factor close to 2 during 2014–2016 on the BC coastline.

The increase in ^{137}Cs levels in northern BC is delineated in Figure 4.10 where it is observed that Haida Gwaii levels were consistently higher than those on the mainland except during the winter. One question that arises is if this signal is due to seasonally reversing mean flows in Hecate Strait or to the influence of low radioactivity freshwater input from coastal rivers. Further, if contamination is entering through Dixon Entrance, the question remains as to how is this water transiting to Sandspit? These are issues that will be addressed as the Fukushima radionuclide plume clears the BC coastline during the next few years.

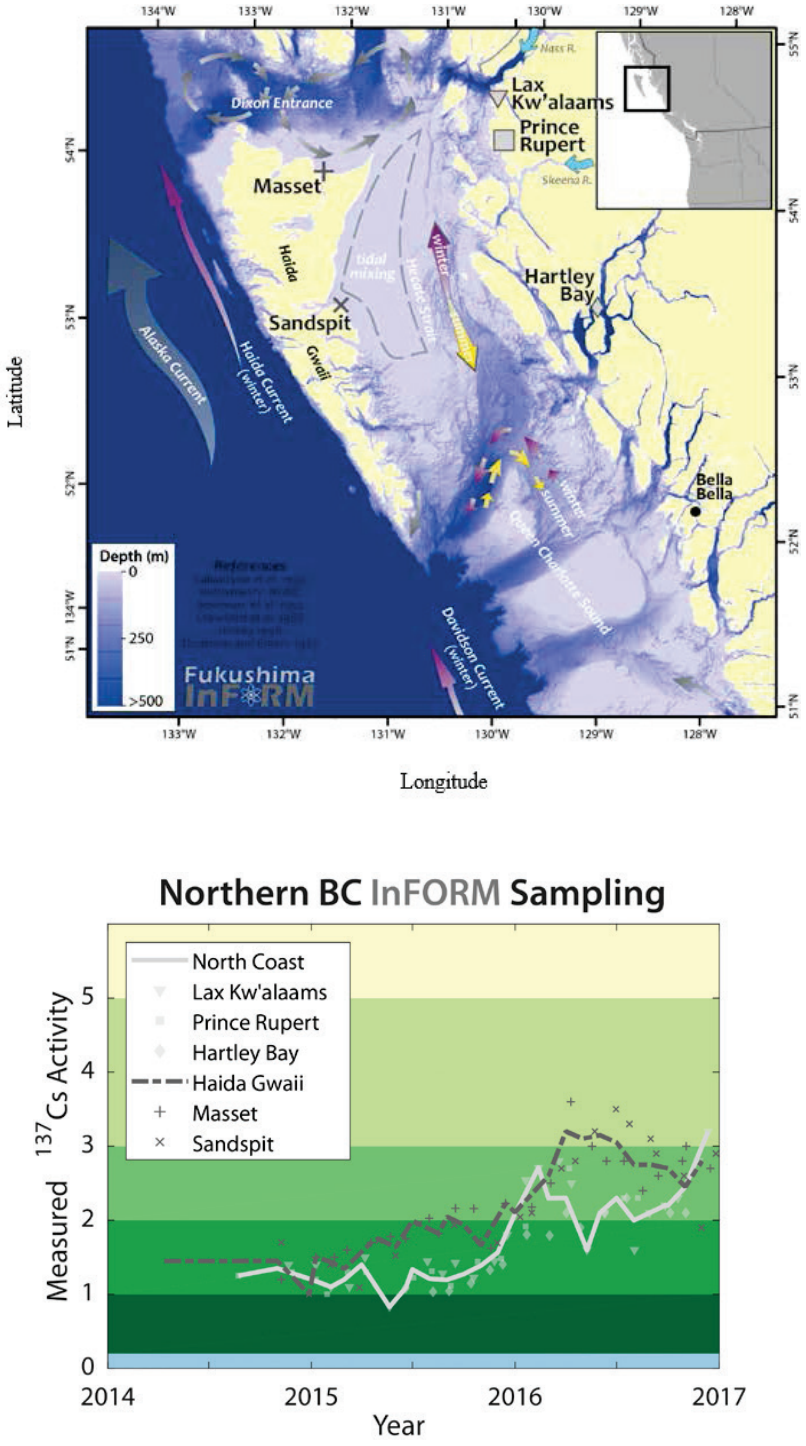

Fig. 4.10 (Top) Sampling locations in northern BC; (bottom) ^{137}Cs levels at northern BC locations increased markedly for 2014–2017.

4.5 Biota

There is widespread interest in the levels of contamination of salmon from the FDNPP accident because this is an important resource for First Nations and also a $600 million industry. Approximately 400 salmon, many donated by First Nations in BC and Yukon, have been collected from locations indicated in Figure 4.11 and analyzed for radionuclides since 2014. The average concentrations of ^{137}Cs were determined to be 0.21 (±0.02) Bq/kg, 0.19 (±0.01) Bq/kg and 0.18 (±0.02) Bq/kg (wet weight) for 2014, 2105, and 2016, respectively. The maximum concentration of ^{137}Cs recorded in an individual InFORM sample was 0.55 (+0.03) Bq/kg (wet weight) which is approximately 1,400 times lower than the national and international action level of 1,000 Bq/kg. One salmon collected in 2015 exhibited a measurable level of ^{134}Cs of 0.07 Bq/kg, indicating the presence of Fukushima radioactivity at extremely low and barely detectable levels. ^{210}Po levels of 1–3 Bq/kg were also measured in this fish, because this natural radionuclide ($T_{1/2}$ = 138 days) generally provides a much greater radiological dose to humans through consumption of seafood compared to doses from fallout levels of artificial radionuclides. Shellfish samples collected from British Columbia's main aquaculture regions in 2016 showed no detectable levels of ^{137}Cs (MDC ~0.2 Bq/kg).

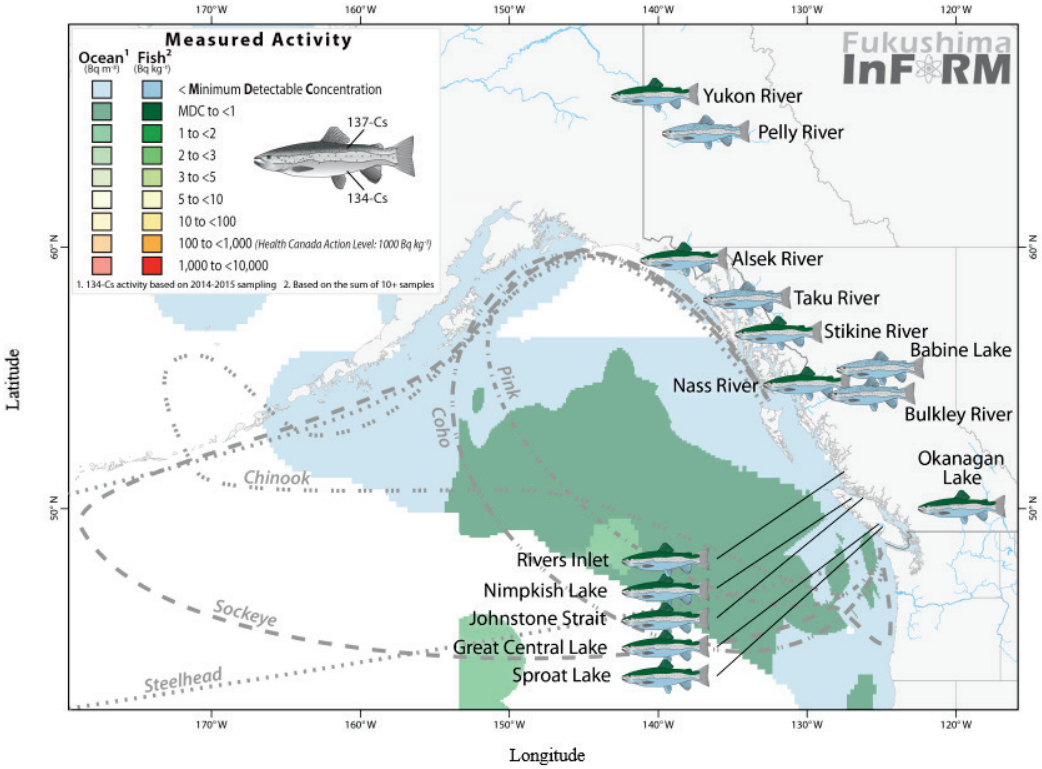

Fig. 4.11 ^{137}Cs levels measured in salmon illustrated for samples collected at various locations in BC waters.

4.6 Summary

The Fisheries and Oceans Canada Fukushima monitoring program has provided the principal sustained time series record for the large-scale transport of the Fukushima radioactivity plume from the western to the eastern North Pacific Ocean between 2011 and 2016. The Fukushima ^{137}Cs signal was initially observed on Line P in June 2012, 15 months after the accident and had fully spread onto the BC continental shelf by June 2013. The signal continued to increase through February 2015 to levels in excess of 6 Bq/m^3 at Sta. P26 on the western end of Line P, but increased much more slowly on the eastern end of Line P at Sta. P4. This decoupling in the transport of the Fukushima signal to the different sections of Line P was promoted by an anomalously high atmospheric pressure system positioned over this region in 2013–2014 that deflected storm tracks and interfered with circulation and convective mixing in the ocean. This resulted in both the offshore pooling of Fukushima radioactivity and the development of unusually high surface temperatures in a large region that became known as “the blob”. Slackening of atmospheric pressures in 2015 resulted in the dispersion of the blob and the spreading of the Fukushima signal onto the continental shelf that has been observed by coastal monitoring by the InFORM program. Comparison of the Line P time series with model simulations suggests that ^{137}Cs concentrations will be approaching their maximum levels in 2016–2017 and will then begin to gradually decline. Measurements of total ^{137}Cs levels (Fukushima + fallout) of 8–10 Bq/m^3 on Line P have returned ^{137}Cs levels to those typical of fallout in the North Pacific in the early 1970s, but are well below levels posing a threat to human health or the environment.

Coastal monitoring of seawater and biota has been conducted in Canada under the auspices of the InFORM program. ^{137}Cs levels in samples of coastal seawater collected by citizen scientists have increased by a factor of 2–3 since the initiation of monitoring in 2014. These increases in radionuclide levels are most pronounced in northern BC at locations proximal to the northward flowing Alaska Current which transports the major inventory of Fukushima radioactivity. Average concentrations of ^{137}Cs measured in salmon are about 0.2 Bq/kg while only one of 400 salmon samples had detectable levels of ^{134}Cs. These levels are well below the Canadian action level for ^{137}Cs of 1,000 Bq/kg and represent a negligible radiological threat to human consumption of seafood. Shellfish samples collected from BC’s main aquaculture regions in 2016 showed no detectable levels of ^{137}Cs. This work has revealed that FDNPP accident-derived radionuclides represent useful tracers to study water circulation in the Northeast Pacific Ocean, but do not represent a radiological threat to human health or the environment.

5 Environmental Radioactivity Models

A total of six radioactivity modeling-related works have been reported by WG 30 members through presentations in workshops and business meetings. Modeling works described in this Section can be divided into two parts, namely, marine radioactivity transport modeling and fate modeling. For the transport modeling, two regional models and one global model are described, while for the marine radioactivity fate model, three versions of the northwestern Pacific Ocean marine radioactivity fate models are described. Some detailed features of models are summarized in Table 5.1.

Table 5.1 Summary of modeling details reported in PICES marine radioactivity sessions.

Contributing organizations	Model types in terms of radioactivity behaviors	Model types in terms of model configuration	Source of radioactivity
KIOST, IMMSP, FIO	Transport model	Regional unstructured model	Atmospheric and direct releases to ocean
FRA, Japan	Transport model of contaminated bottom	Regional finite difference model with a series of downscaling	Initial field of bottom contamination
FIO, KIOST	Transport model	Global finite difference model	Atmospheric and direct releases to ocean
KIOST, IMMSP, FIO	Fate model with pelagic food chain	Regional box model with 1 to 3 vertical layers	Global fallout, atmospheric and direct releases to ocean
KIOST, IMMSP, FIO	Fate model with pelagic and benthic food chains	Regional box model with 1 to 3 vertical layers	Global fallout, atmospheric and direct releases to ocean
KIOST, IMMSP, FIO	Fate model with multi-organ fish module ver.1	Regional box model with 1 to 3 vertical layers	

KIOST – Korea Institute of Ocean Science and Technology; IMMSP – Institute of Mathematical Machine and System Problems, Ukraine; FIO – First Institute of Oceanography, the People's Republic of China; FRA – Japan Fisheries Research and Education Agency

5.1 Transport models

5.1.1 KIOST-IMMSP-FIO regional transport model

KIOST (Korea Institute of Ocean Science and Technology) researchers reported a sophisticated regional model with applications to future hypothetical accidents in the Yellow Sea and East China Sea as well as to the 2011 FDNPP accident which is under development jointly with researchers from IMMSP (Institute of Mathematical Machine and System Problems), Ukraine, and FIO (First Institute of Oceanography), the People's Republic of China (Jung *et al.*, 2015). This study is funded by KIOST and FIO as well as CKJORC (China–Korea Joint Ocean Research Center). As seen in Figure 5.1, radionuclides in the sea can exist in dissolved and particulate forms within bottom

sediments as well as in the water column, although modelers usually consider the transport of dissolved radionuclides in the water column. The ultimate goal is the development of a new three-dimensional radionuclide transport model applicable to coastal waters with complex circulation patterns and high turbidity of cohesive and non-cohesive sedimentary origin.

The present model is composed of multi-scale circulation, waves and suspended sediment modules in a manner similar to other modeling systems. For the simulation of the circulation and wavefields, the hydrodynamic numerical model SELFE (semi-implicit Eulerian–Lagrangian finite-element, Zhang and Baptista, 2008) that solves Reynolds stress averaged Navier–Stokes (RANS) equations and the wave action transport equation on the unstructured grids has been used. For the case of the suspended sediment module, the original SELFE code was extended to a model applicable to a mixture of cohesive and non-cohesive sedimentary regimes through the implementation of a flocculation model for the determination of settling velocities of cohesive flocs. The radioactivity module has some more distinct features. The model calculates the concentration of radionuclides in bed sediments and pore water as well as in dissolved and particulate phases in the water column. The two-step reaction model is adopted to consider the phase change between dissolved and particulate radionuclides. The transfer of activity between the water column and the pore water in the upper layer of the bottom sediment is governed by diffusion processes. The phase exchange between dissolved and particulate radionuclides is written in terms of the desorption rate and distribution coefficients for the water column and bottom deposit. The distribution coefficients are inversely proportional to the sediment particle size.

The application of the model to the FDNPP accident was made with a consideration of a single bed layer of 2 cm thickness. The radionuclide inputs by direct release and atmospheric deposition in the model domain were 3.5 PBq and 2.5 PBq, respectively. Meteorological forcing at the sea surface was specified using Era-Interim data, while the open boundary condition was defined using Hybrid Coordinate Ocean Model (HYCOM) results. Figure 5.2 shows the computed distribution of bottom inventory of ^{137}Cs at the end of June 2011. It is seen that the bottom contaminated region is aligned along the coastal sea region with highest values near the FDNPP. The model result appears to be similar to that of Min *et al*. (2013). Comparison with measurements by Black and Buesseler (2014) shows favorable agreement although the comparison is not valid in a strict sense due to the time differences between model results and measurements. It is expected that the longer time integration of the model with realistic time-varying model inputs will have to be performed to obtain better agreement. Some information on the distribution of dissolved ^{137}Cs can be seen in the model inter-comparison report prepared by the Science Council of Japan (2014).

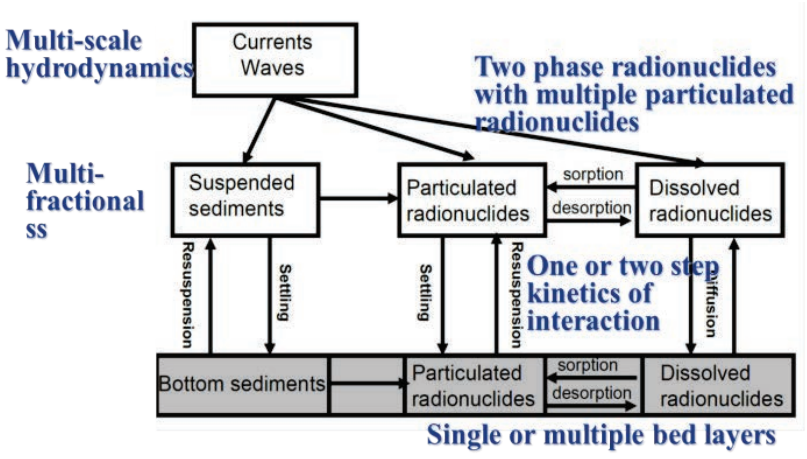

Fig. 5.1 Processes considered in the marine radioactive transport model under development.

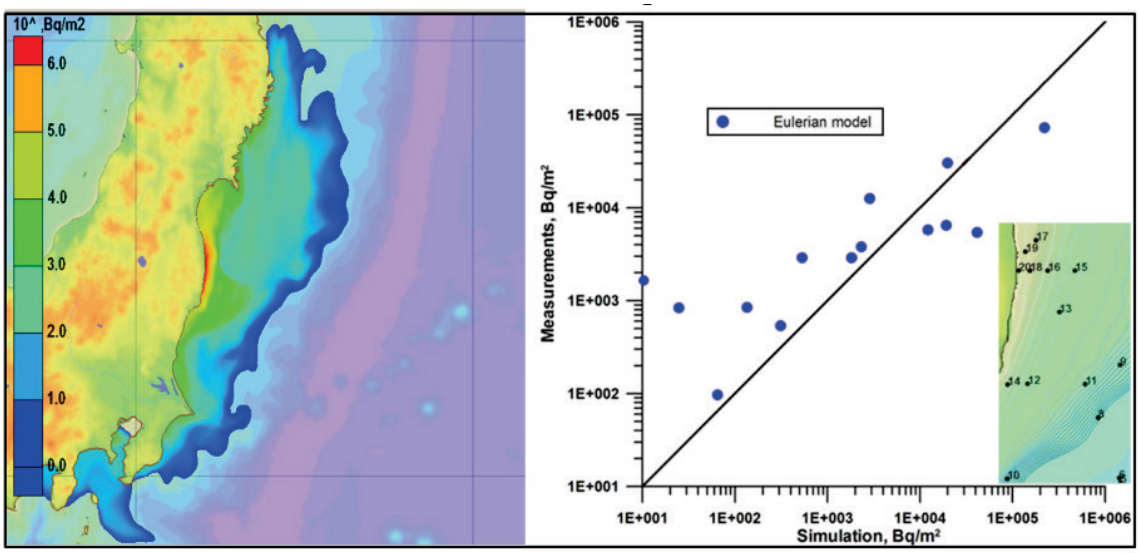

Fig. 5.2 Model results of ^{137}Cs bottom contamination: (left) horizontal distribution of ^{137}Cs bottom inventory, (right) comparison results with measurements shown in Black and Buesseler (2014) at selected points off the FDNPP site.

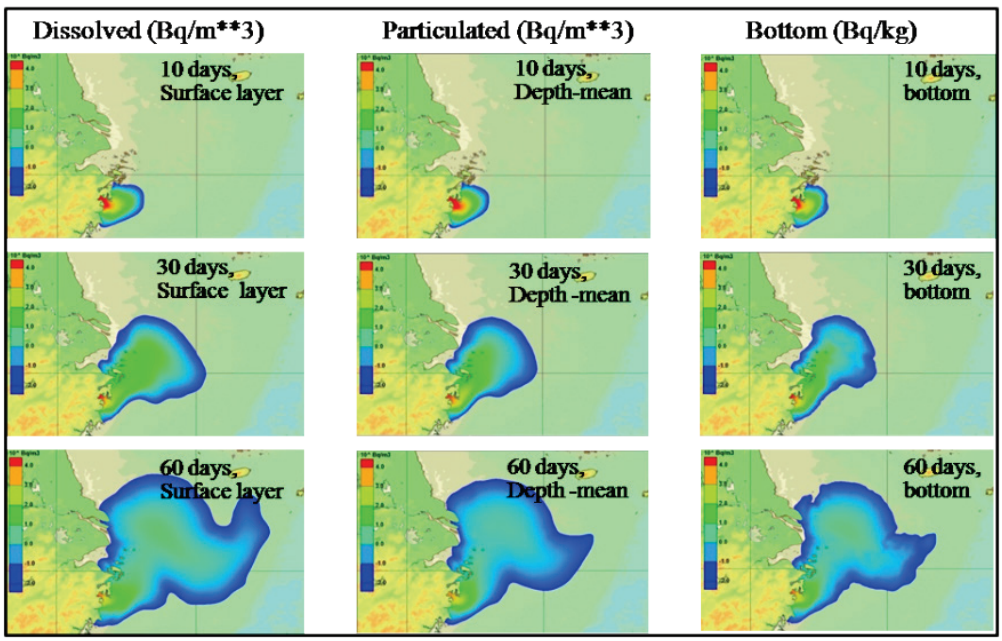

Fig. 5.3 Time evolvement of horizontal distribution of dissolved (sea surface), particulate (depth-mean) and bottom-deposited (bottom surface) ^{137}Cs concentrations computed with a hypothetical release from the Sanmen Nuclear Power Plant, China.

Following application to the FDNPP accident, the model was applied to the Yellow and East China seas. Figure 5.3 shows the dissolved, particulate and sea bottom concentrations computed using a hypothetical release scenario from the Sanmen Nuclear Power Plant located south of Hangzhou Bay. It was assumed that 1 PBq of ^{137}Cs was released to the coastal sea region over 14 days. It is noted that unlike the case of the FDNPP accident, the particulate and bottom sediment phases include considerable quantities of radioactivity contamination, mainly because the turbidity level is high. In the case of FDNPP accident, the correct simulation of coastal circulation was found to be critical as described in the Science Council of Japan report (2014), while for the Yellow Sea and East China

Sea the correct simulation of suspended sediment concentration is essential to assess the behavior of the released radioactivity materials.

Further refinement of the model, including multi-layers in the bottom sediments, is underway. For model validation, the model was tested in a laboratory experiment by Smith *et al*. (2000). A 1DV (one-dimensional vertical) model was set up for the test. The upper 2 cm water layer initially contained 10 kBq of ^{134}Cs in a sediment core of 10 cm in length. The simulation was performed for the 1D configuration with 1 mm resolution where the upper 2 cm layer is filled with corresponding levels of contaminated water. Model validation results are shown in Figure 5.4 along with the configuration of the multi-layers within the bottom sediment. Reasonable agreement was obtained between model and experimental results.

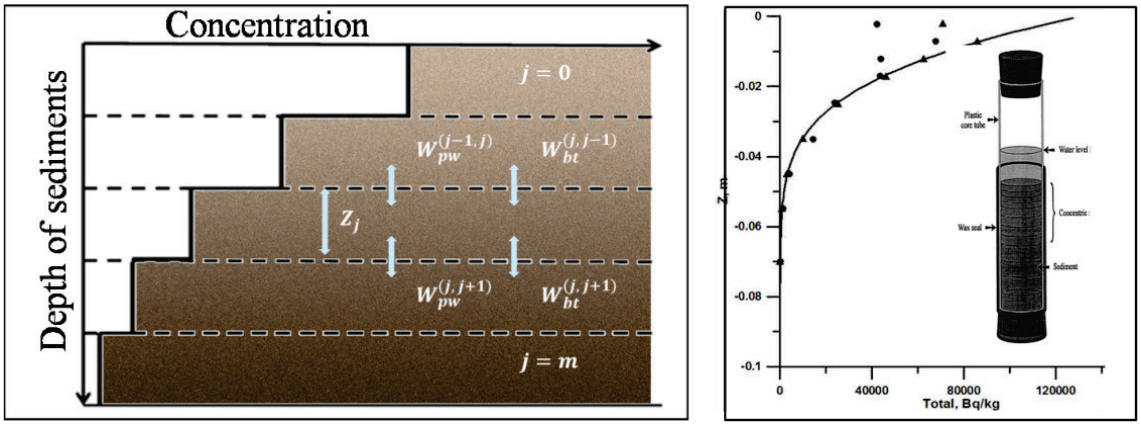

Fig. 5.4 Initial testing of the model equipped with multi-layers within bottom sediments: (left) configuration of a 1DV (one-dimensional vertical) model, (right) comparison between computed and measured profiles of ^{134}Cs.

Application of the model with sediment multi-layers to the FDNPP is underway. Preliminary results (not shown) indicate that to validate the concentration profile within the bottom sediment is a formidable task, due partly to computing burden and partly because the measured profiles show substantial time and space variability as noted by Buesseler *et al*. (2017). The variability might be due to various reasons, one of which is the presence of strong bioturbation effects. For this reason, a parameterization of bioturbation effects has recently been included in the model. The model will be applied to the Yellow and East China seas where serious concerns have been raised with regard to nuclear safety because a total of about 300 nuclear units are expected to be sited in this region by 2030.

5.1.2 FIO-KIOST global transport models

This work was led by researchers from FIO cooperatively with researchers from KIOST, with funding from FIO and CKJORC. The circulation part of the model is based on the Princeton Ocean Model (POM). The model domain covers the region of 78ºS–65ºN, 0–360ºE with a horizontal resolution of 0.5°. Twenty-one vertical sigma layers are used with finer resolutions in the upper layers, taking into account the presence of wind-induced Ekman layers and the thermocline. The topography of the model is based on Etopo5. A cyclic boundary condition is used for the east and west boundaries, and solid walls are set to southern and northern boundaries. The circulation model is forced by the monthly climatology of surface wind stress and net heat fluxes from the Comprehensive Ocean-Atmosphere Data Set (COADS; da Silva *et al*., 1994) with a resolution of

1° × 1°. After a 20-year spin-up, the outputs for March 11, 2011, are stored as the initial fields for the calculation of ^{137}Cs transport released due to the FDNPP accident. The radioactivity module was added following the approach proposed by Tsumune *et al*. (2003). After a 20-year spin-up of circulation, the ^{137}Cs discharge from the FDNPP, both the direct release and atmospheric deposition, is introduced into the model to simulate its transport from March 2011 to March 2041.

The source conditions initially considered in Zhao *et al*. (2015) were 5 PBq (5×10^{15} Bq) for the amount of ^{137}Cs deposited at the sea surface on the Japanese coastal sea, that is, the localized atmospheric fallout, and 3.5 PBq for the direct release. Recently Zhao *et al*. (2016) considered the global-scale atmospheric fallout based on the results in the report by the Science Council of Japan (2014). Figure 5.5 shows part of the horizontal distribution at the near surface computed using the localized atmospheric source plus direct release and global atmospheric fallout plus direct release.

Figure 5.6 shows a comparison between the Canadian observations at two selected stations (P26 and P4) and model results by Zhao *et al*. (2016) and Behrens *et al*. (2012). Computed ^{134}Cs concentrations are also included for a reference. It is noted that despite the poor resolution, the Zhao *et al*. (2016) model produces reasonable agreement with observations that are somewhat better than that by Behrens *et al*. (2012). The Zhao *et al*. (2016) model predicted that the maximum concentration of ^{137}Cs at P26 would occur in 2016, earlier than the prediction by Behrens *et al*. (2012) and in much better agreement with the measured results.

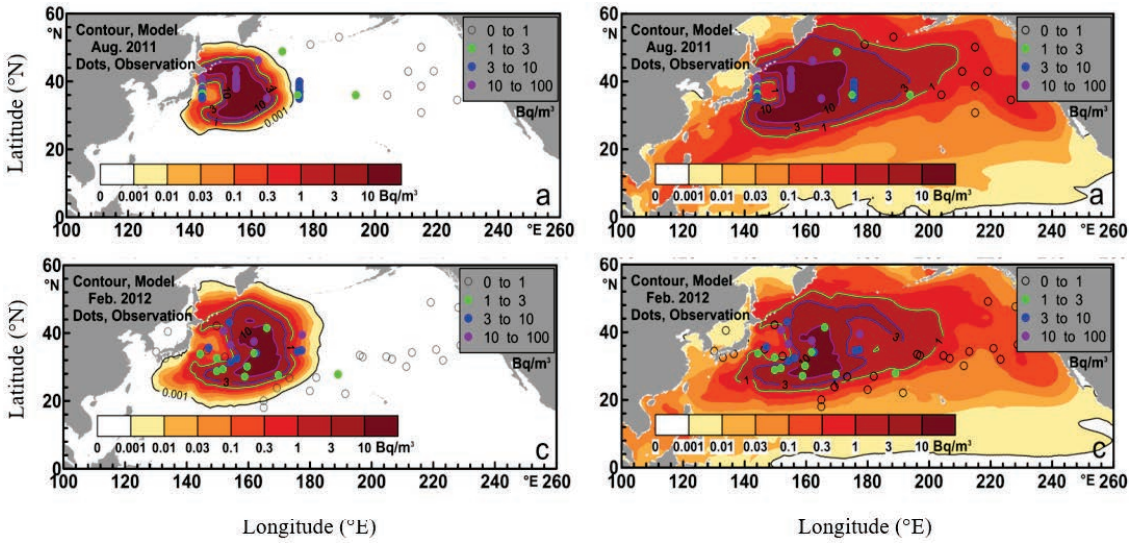

Fig. 5.5 Horizontal distribution of FDNPP accident-derived ^{137}Cs at the near surface computed with: (left) localized atmospheric fallout plus direct release, (right) global-scale atmospheric fallout plus direct release. Left diagrams from Zhao *et al*. (2015). Reprinted with permission of Springer Nature; right diagrams from Zhao *et al*. (2016).

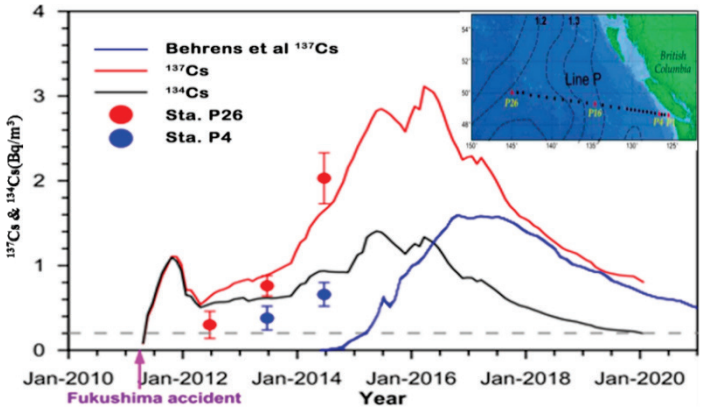

Fig. 5.6 Model validation results at two stations located on the Canadian Line P. Extracted from Zhao *et al.* (2016).

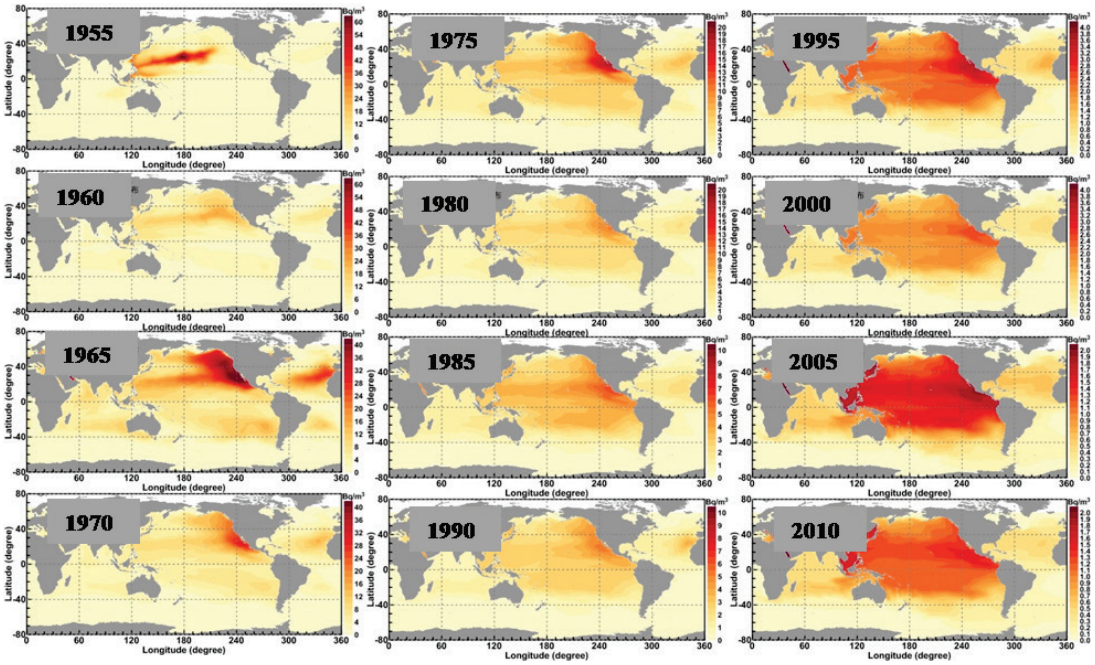

Fig. 5.7 Horizontal distribution of ^{137}Cs due to global fallout from atmospheric nuclear weapons tests. Drawn based on Zhao *et al.* (2016).

In addition to the application of the global model to the FDNPP accident, Zhao *et al.* (2015) also reported long-term integration results, taking into account the global fallout due to nuclear weapons tests over the period of about 1945 to 2010, as illustrated in Figure 5.7.

5.2 Fate models

5.2.1 KIOST-IMMSP-FIO fate model: Pelagic food chain

KIOST researchers reported a series of developments of marine fate models which can be used to assess the transfer of accidently released radioactivity materials to marine organisms in the northwestern Pacific Ocean. The models have been developed jointly with researchers from IMMSP (Institute of Mathematical Machine and System Problems), Ukraine, and FIO (First Institute of

Oceanography), the People's Republic of China. The basic framework of the models is based on the Poseidon model (Lepicard *et al*., 2004) which describes the marine environment as a system of compartments (or boxes) for water column, bottom sediment and biota. Figure 5.8 shows the configuration of boxes for the northwestern Pacific Ocean. More than 170 boxes were allocated on the horizontal plane to cover the main body of the northwestern Pacific region, while near the FDNPP a coastal box with a smaller size is placed to compare results with observation data. A number of boxes can be considered in the vertical direction to represent water column and bottom sediment. In practice, after a set of initial model testing, a single layer was allocated for the shallow water region, while three layers were used for the deep-water region. For the bottom sediment, three layers were considered. The averaged advective and diffusive water fluxes between compartments were specified using 10-year period (2000–2009) results from the Regional Ocean Modeling System (ROMS). The marine radioactivity studies reported in this report are unique in that the model included the radioactivity releases due to the FDNPP accident as well as the global fallout.

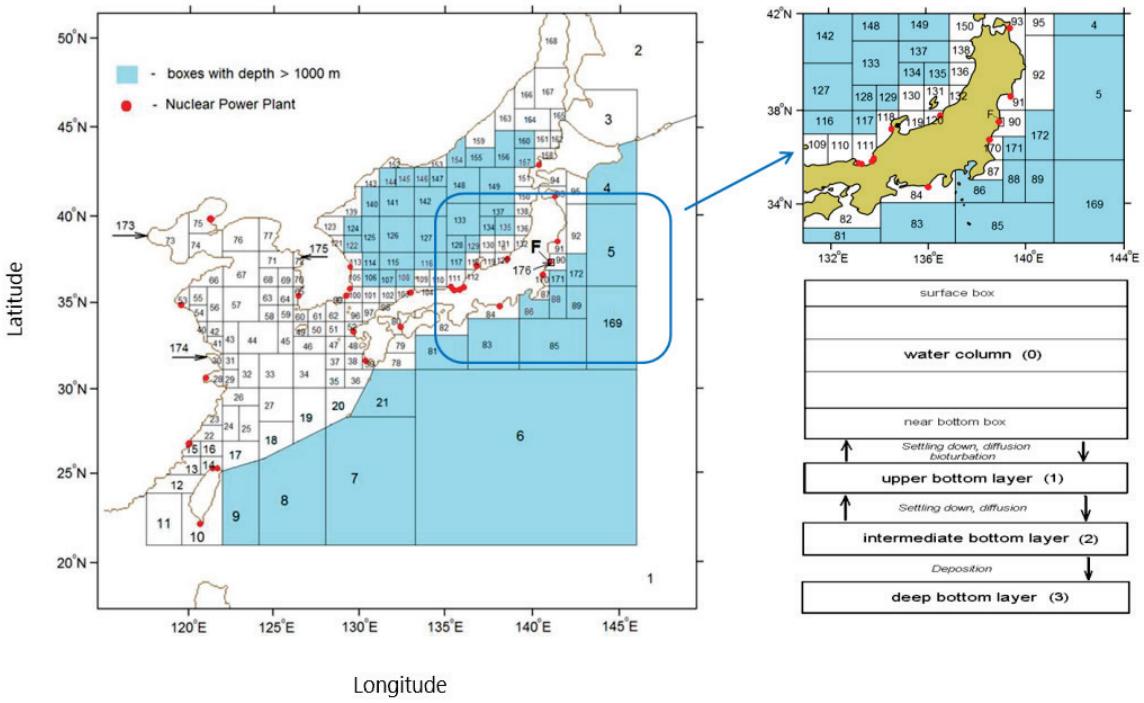

Fig. 5.8 Configuration of horizontal compartments (boxes) and vertical layers for the northwestern Pacific Ocean. Drawn, based on Maderich *et al*. (2014b) and Bezhenar *et al*. (2016).

The radionuclide concentration for each compartment is determined by either an algebraic equation or a set of differential equations, including the temporal variation of concentration, the exchange with adjacent compartments and with the suspended and bottom sediment, radioactive sources and decay. The exchange between the water column boxes is described by fluxes of radionuclides due to advection, sediment settling and turbulent diffusion processes. Details of the customization to the northwestern Pacific Ocean are given by Maderich *et al*. (2014a, b) and Bezhenar *et al*. (2016).

Two studies were initially carried out using the original POSEIDON-R model with applications to ^{137}Cs and ^{90}Sr, respectively (Maderich *et al*., 2014a, b). Figure 5.9 displays the marine food chain considered for the transfer of radioactivity materials which is composed of 9 state variables. In detail, seawater, bottom sediment, phytoplankton, zooplankton, algae, mollusks, crustacean, non-piscivorous and piscivorours fishes were considered. For convenience, the model is called BURN-POSEIDON.

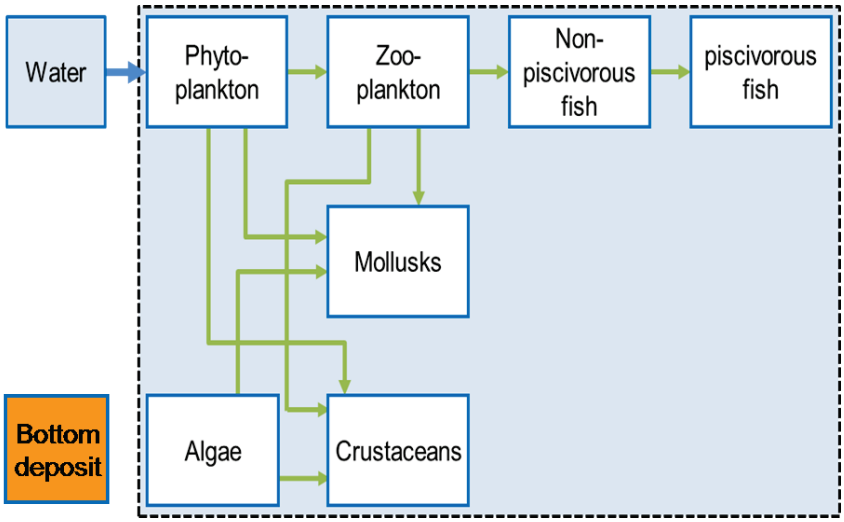

Fig. 5.9 Pelagic marine food chain with transfer paths of radioactive materials used in BURN-POSEIDON.

To determine the concentration in phytoplankton and algae, a concentration factor approach was used, while the concentrations in other marine species were dynamically calculated using a time-dependent differential equation with source and loss terms. In addition to the releases from the FDNPP accident as well as the global fallout, the leakage through the groundwater flow from the FDNPP was considered as an additional source.

Figure 5.10 shows the computed and observed concentrations of ^{137}Cs in seawater and piscivorous fish in the coastal box with a radius of 15 km. Validation using various observations in the northwestern Pacific Ocean before and after the FDNPP accident showed that the simulated ^{137}Cs results are in good agreement with observations. It is noted that use of the dynamic approach produces a time delay in the occurrence of the maximum value, compared with the concentration factor approach. The BURN-POSEIDON model supports the presence of continuing groundwater discharge.

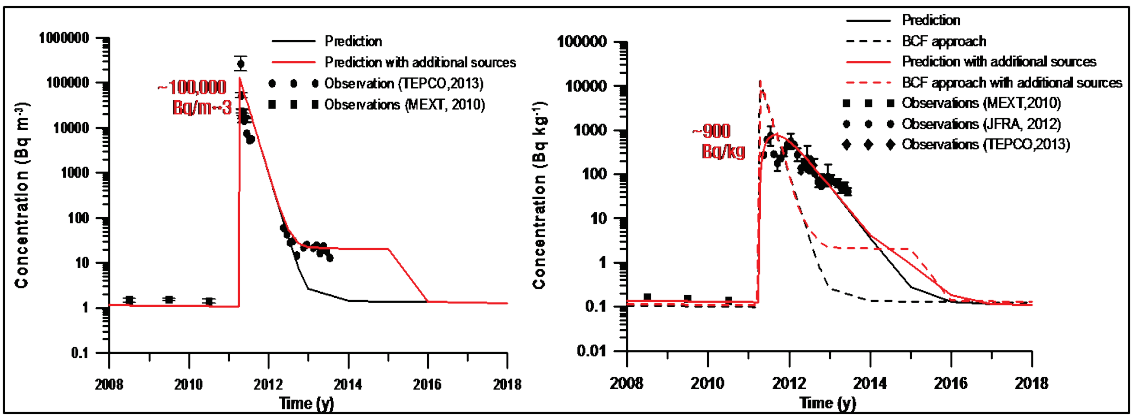

Fig. 5.10 Computed and observed concentration of ^{137}Cs in seawater and piscivorous fish in the coastal box with a radius of 15 km. Results from the concentration factor approach and discharge with/without groundwater discharge are included. Red-colored numbers represent the computed maximum value. Modified from Maderich *et al.* (2014a).

For the case of ^{90}Sr, available observation data were limited compared to ^{137}Cs, and were found to have high time and space variability. For that reason, sensitivity tests were performed with a range of source intensity (Maderich *et al*., 2014b).

5.2.2 KIOST-IMMSP-FIO fate model: Pelagic and benthic food chains

The model developed by Maderich *et al*. (2014a) was improved by introducing a marine benthic food chain to the BURN-POSEIDON. For convenience, the model is called Extended BURN-POSEIDON. The extension of BURN-POSEIDON was motivated by the measurements by the Japanese Agencies over the past four years which showed that relatively high ^{137}Cs concentrations have still been observed in sediments, benthic organisms and demersal fishes in the coastal zone around the FDNPP. These observations indicate the presence of ^{137}Cs transfer pathways from bottom sediments to the marine organisms. For that reason, the dynamic food chain model BURN has been extended to include benthic marine organisms. Figure 5.11 displays the marine food chain considered for the transfer of radioactivity materials which is composed of 13 state variables. The benthic food chain includes transfer from bottom sediments to the deposit feeding invertebrates, demersal fishes and benthic predators. Crustaceans and mollusks and coastal predators play a role in the coupling of the pelagic and benthic food chains. Various researchers have applied benthic food web models to the FDNPP accident (Tateda *et al*., 2013, 2015; Keum *et al*., 2015), but the deposit feeder ingestion is not included as a transfer process in the food chain.

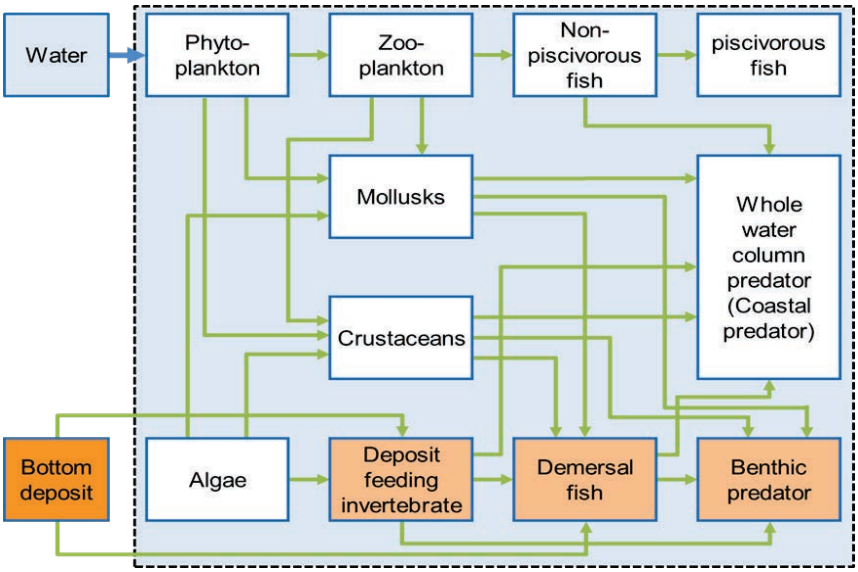

Fig. 5.11 Radioactivity transfer paths in pelagic and benthic marine species used in Extended BURN-POSEIDON. Redrawn from Bezhenar *et al*. (2016).

The model was integrated for the period of 1945–2010 and then for the period of 2011–2020 to assess the radiological consequences of releases of ^{137}Cs from the FDNPP by comparing model results with measurements for the period of 2011–2015. Direct releases to the ocean and atmospheric inputs over the domain were 4 PBq and 8.2 PBq, respectively. Based on the estimation by Kanda (2013) a ^{137}Cs flux of 3.6 TBq/y through groundwater flow was also taken into account.

Figure 5.12 shows some model validation results. Model results show good agreement with measurements. It is noted that in the concentration levels in 2016 are around 10 Bq/kg, about 50 to 60 times higher than those before the FDNPP accident. Model results as well as measurements

support the hypothesis that transfer of radioactivity from bottom deposits through the benthic food chain over a prolonged time period can be an increasingly important factor in the radiological assessment of released radioactivity.

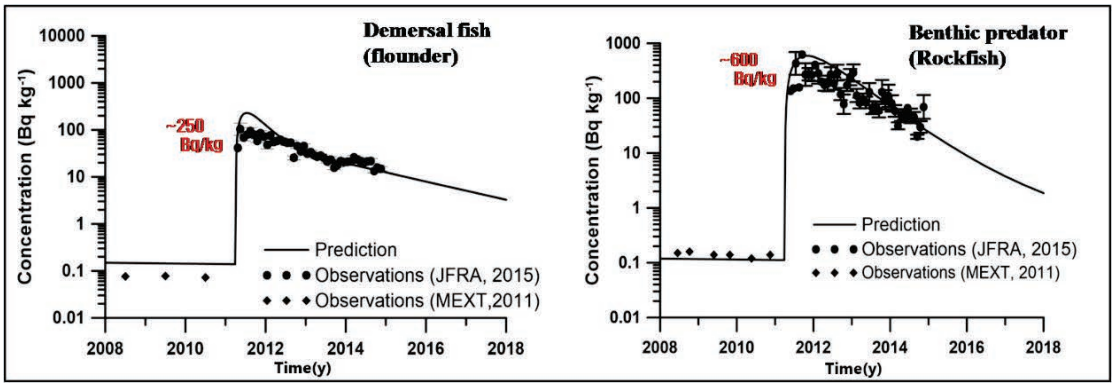

Fig. 5.12 Computed and measured concentration of ^{137}Cs in (left) demersal fish (flounder), (right) benthic predator (Rockfish). Red-colored numbers represent the computed maximum value. Modified from Bezhenar *et al*. (2016).

The model was also successfully applied to the Baltic Sea where the deposition of activity originating from the Chernobyl Nuclear Power Plant accident in 1986 was used to validate the model.

5.2.3 KIOST-IMMSP-FIO fate model: Pelagic and benthic food chains and multi-organ fishes

During the course of applying the Extended BURN-POSEIDON to the FDNPP accident with ^{90}Sr, it was noted that unlike the case of ^{137}Cs, the Extended BURN-POSEIDON underestimated the concentration levels of ^{90}Sr in fishes. Furthermore, its application to the regular releases of ^{60}Co and ^{54}Mn from the Forsmark and Ringhals nuclear power plants in Sweden revealed the same problem. Careful examination led to the conclusion that use of the single-target-tissue model adopted in the Extended BURN-POSEIDON was the main cause. Estimation of the whole body-specific tissue concentration ratios by Yankovich *et al*. (2010) showed that radionuclides such as ^{137}Cs, ^{134}Cs and ^{3}H were transferred to flesh by about 90%, bone by 9% and organs by 1%, radionuclides such as ^{90}Sr, ^{45}Ca, ^{226}Ra, *etc*. were transferred to flesh by about 28%, bone by 52% and organs by 10%, and radionuclides such as ^{60}Co, ^{54}Mn, ^{65}Zn, *etc*. were transferred to flesh by 32–44%, bone by 17–39% and organs by 25–40%. Subsequently, attempts to develop a new radionuclide transfer model for fishes were made.

Figure 5.13 displays the marine food chain considered for the transfer of radioactivity which is composed of 23 state variables. It can be seen that the marine food chain is the same as in the Extended BURN-POSEIDON, but three tissues (flesh, bone and organs) are considered for fishes. To calculate radionuclide concentrations in different tissues of fish simultaneously, three equations without interaction were initially introduced for each of the fish tissues with the use of different values of extraction coefficients in uptake terms and biological half-life in the loss term. Equations for marine species other than fishes were the same as in the Extended BURN-POSEIDON. Summing up the concentrations for flesh, bone and organs multiplied by corresponding fractional factors gives rise to the total concentration accumulated in fishes.

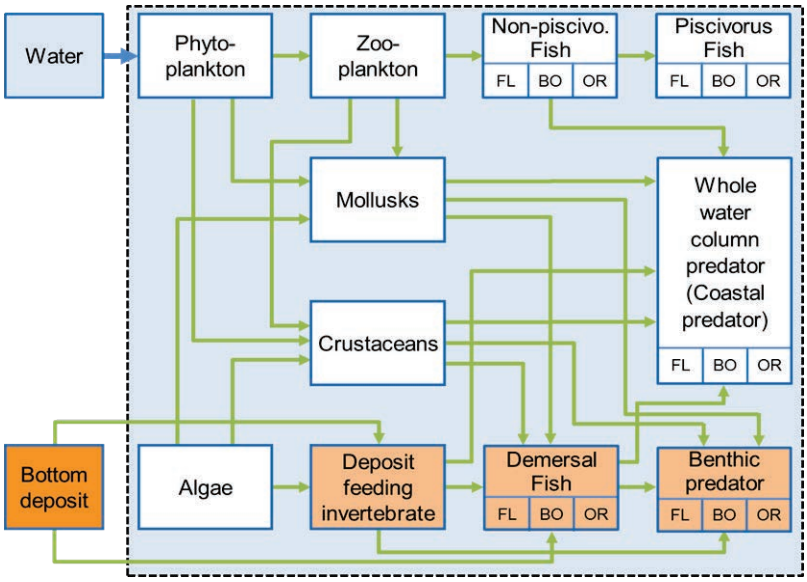

Fig. 5.13 Radioactivity transfer paths in Multi-BURN-POSEIDON. FL, BO and OR represent flesh, bone and organs, respectively. Drawn based on Bezhenar *et al*. (2016).

For the simulation two scenarios were considered for the source intensity, taking into account the lack of information on the real leaks for ^{90}Sr. Scenario 1 considered a constant leak with a release rate of 3 GBq/day and scenario 2 considered a release rate of 30 GBq/day during the period from the middle of 2011 to the end of 2012, 10 GBq/day in 2013 and 3 GBq/day from 2014 to 2015. Figure 5.14 displays preliminary results from the application to the FDNPP accident for the coastal box with size of 4 km by 4 km. The application of the Poseidon model with a multi-tissue approach for the accumulation of radionuclides in fish shows that the results of the modeling agree well with measurements and that both scenarios give acceptable results.

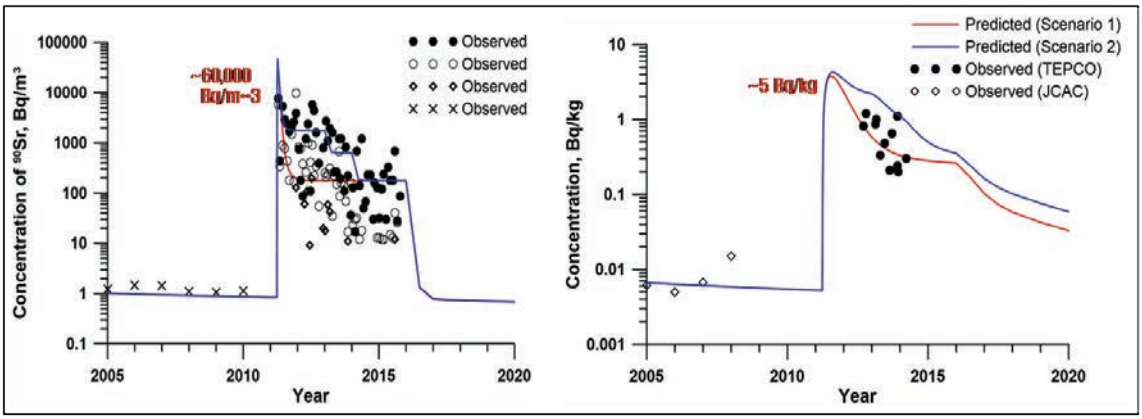

Fig. 5.14 Computed and observed concentrations of ^{90}Sr in: (left) sea water, (right) piscivorous fish. Red-colored numbers represent the computed maximum value.

5.3 Summary

Following the FDNPP accident, a number of modeling experiments associated with the oceanic dispersion of radionuclides have been reported in the scientific literature. It is noted that apart from the independent modeling reports by various researchers, there have been some efforts at carrying out model inter-comparisons. The model inter-comparison programs organized by the IAEA as well as by the Science Council of Japan (SCJ) were typical examples. In late 2011 SCJ initiated the program and published a final report in early September 2014. IAEA organized intercomparisons of ocean dispersion models and marine radioactivity fate models as a part of the MODARIA II (Modelling and Data for Radiological Impact Assessments) program. Phase I covered the period from 2014 to 2016 and phase II is on-going from 2017. MODARIA II model results have been reported through the publication of various papers in international journals. A total of ten international organizations participated in the SCJ inter-comparison of oceanic dispersion models, comparing a total of eleven model results. The model comparison was confined to the dispersion behaviours of dissolved radionuclides in the water column in coastal waters off the FDNPP. It was found that the model results were significantly different from one another, and that circulation played a key role in determining the dispersion patterns. In MODARIA II phase I, up to seven dispersion models and nine biota models were compared. Comparisons in MODARIA II phase I also revealed that significant differences between the results from both dispersion and marine biota models can occur according to the implemented numerical methods and physical processes. In MODARIA II phase, the comparison area is underway with further harmonization of model inputs to investigate why such differences might occur. The model domain is extended to the large area covering almost the entire North Pacific region.

Only a relatively limited number of modelers have contributed to WG 30 activities, reporting three transport models and three versions of marine radioactivity fate models. Unlike the two programs above, no attempt was made to compare model results. However, all modelers provided unique and valuable information. The regional transport models off the FDNPP have reported sophisticated modeling results with emphasis on bottom contamination and the global model has reported a long-term transport of dissolved marine radioactivity in the North Pacific, successfully validating results with observations off the Canadian coast. The development of a series of dynamic fate models has been helpful in understanding the recent technical progress achieved in the modeling of marine radioactivity transfer processes.

6 Dose and Risk Assessment Methodology Improvement

Presently, the international standard for modeling radiation transport and calculating doses to biota uses extraordinarily simple geometry and composition. The International Commission on Radiological Protection (ICRP, 2008) has set a small number of "Reference Animals and Plants" to be used as the basis for protecting a given ecosystem. Whether it is the reference frog, deer, or crab (Figure 6.1), however, the geometry of the organism is nearly identical: a homogenous ellipsoid, uniform in density and in the distribution of any internal radionuclides, with rare exceptions. The most complicated of these models is the reference deer (Figure 6.2). Numerous challenges were raised about deepening the understanding of the impacts of exposure to ionizing radiation on marine biota, including the demand of a voxelized model more accurately representing an organism's body.

Fig. 6.1 Dungeness crab, male (left) and female (right).

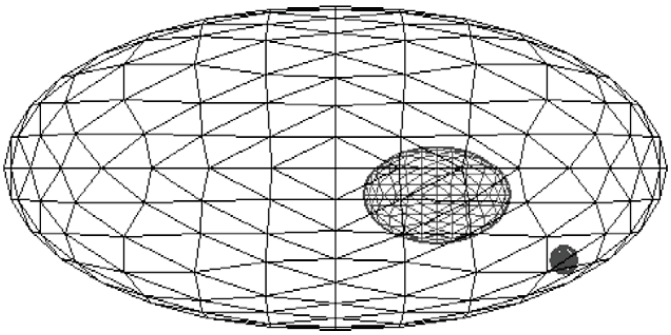

Fig. 6.2 The reference deer, a homogenous ellipsoid except for the liver (larger internal ellipsoid) and testes (smaller, nearly external ellipsoid).

Work by Caffrey (2012) formed the initial basis for this process, with the intention to create a realistic model of the reference crab (a Dungeness adult female), reference flatfish (a sanddab adult) and the reference brown algae (*Fucus vesiculosus*).

6.1 Integrated spatiotemporal modeling

Much of the existing body of knowledge on how radiation impacts a living organism boils down to a relationship between the amount of energy deposited per unit mass of the organism, and the endpoints of concern that arise. Unlike in humans, published endpoints largely average this deposition over the entire body of the organism rather than examining the dose–effect relationship on a per-tissue basis. Ph.D. research by Liu (2017) attempted to stretch this connection deeper, not just to a per-tissue basis, but to a per-cell basis.

The classic paradigm of radiation injury (Figure 6.3) shows the relationship between ionizing events caused by radiation (on time scales of nanoseconds) and ion recombination and free radical production (on time scales of seconds), DNA damage and repair (minutes to hours), and the ultimate outcomes for that damage.

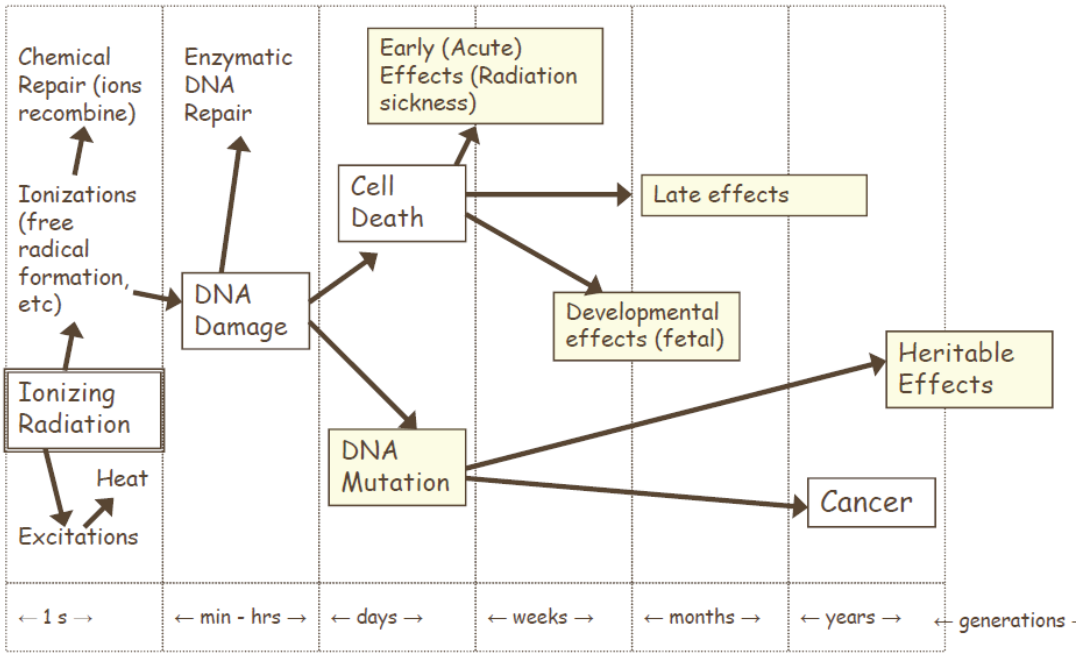

Fig. 6.3 The classic paradigm of radiation injury.

In humans, it is the pathways to mutations that are typically of concern. Only in the cases of radiation ablation or radiation therapy are they relevant to human radiation protection models, as the thresholds managing carcinogenesis are much more restrictive than those that are sufficient to produce early and late effects. However, for protection of wild populations, it is largely acute and late effects, and to lesser degree heritable mutations, that are the primary focus. The issue with addressing these in biota using average-energy-deposition models is that a significant proportion of cell deaths occurs in cells that did not have any radiation interactions at all. This sort of cell death, termed the bystander effect, is not well understood, as it occurs in cells unaffected by the radiation in question, including indirect damage by free radicals.

The model produced by Liu (2017) links a GEANT4-based radiation transport simulation (Figures 6.4 and 6.5) with inter- and extra-cellular DNA damage, repair and signal molecule diffusion, and finally links these through to a cell cycle simulation to track cell growth, apoptosis and necrosis. It is hoped that this model may eventually allow us to better understand the relationships between given doses of radiation and resulting effects in biota by simulating the full degree of cell deaths that produce the early and late effects that can impact an organism's survival in the wild (and, in turn, any population comprised of such individuals). However, there are many quirks to the model's behavior that are not well understood, so it may be some time before a transition might be made to cell-level simulations of radiation effects.

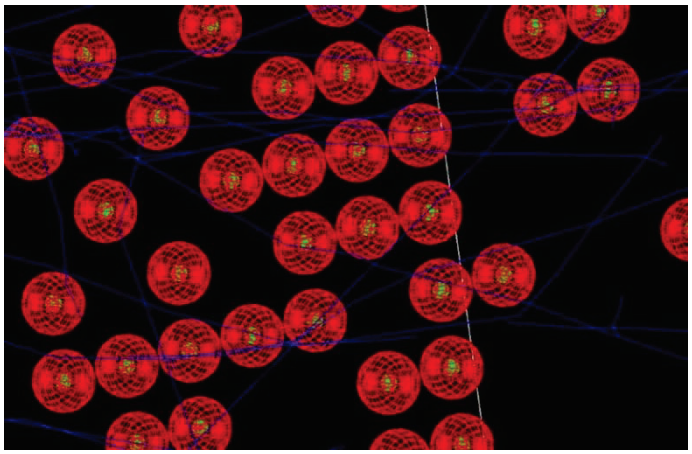

Fig. 6.4 GEANT4-based radiation transport through and around individual cells.

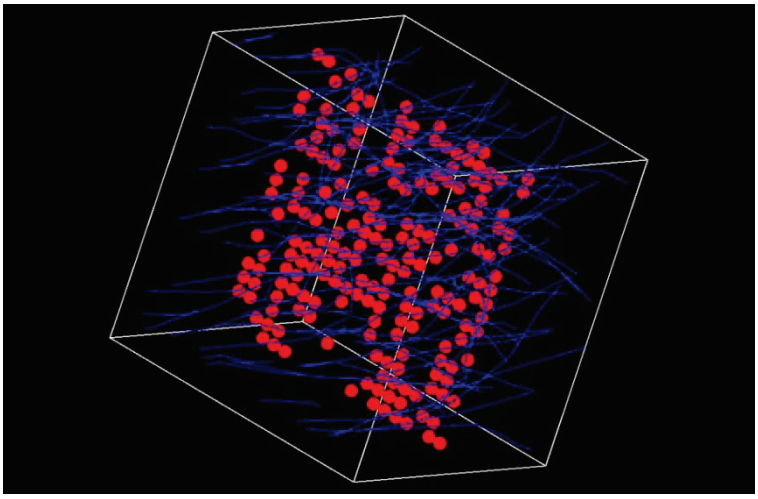

Fig. 6.5 GEANT4 radiation transport through a single layer of cells of interest embedded within a 3D medium.

6.2 *Voxel models*

6.2.1 Crab

A realistic model of the Dungeness crab (Figure 6.6) was produced using CT (computerized tomography) imaging, which allows for the production of a 3D set of images of an organism in the form of individual x-ray slices calculated *via* a Radon transformation. For the crab, this method produced sufficient contrast between the tissues of interest to allow segmenting them slice-by-slice. The resulting model, which is termed a voxel model, is pictured in Figure 6.7. A 'voxel' is essentially the 3-dimensional equivalent to the 'pixel', where each individual voxel is uniform within itself.

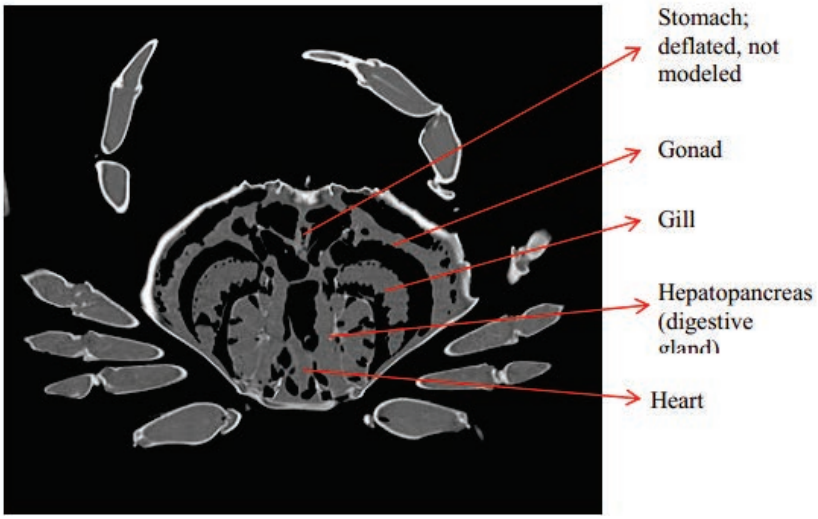

Fig. 6.6 CT slice of an adult male Dungeness crab, with radiologically relevant tissues identified.

Fig. 6.7 Full 3D voxel model of a Dungeness crab, with the heart, gills, gonads and hepatopancreas identified separately from the exoskeleton and muscle tissue. The stomach was deflated, and thus not able to be segmented.

6.2.2 Flatfish

In the case of the reference flatfish (a sanddab), application of the CT technique produced insufficient contrast in the CT images to discern the boundaries between organs (Figure 6.8). An MRI (Magnetic Resonance Imaging) allowed much better contrast between tissue types (Figure 6.9) to allow for some degree of segmentation. However, it too suffered from issues that were not present in the reference crab. First, geometrically speaking, a flatfish is flat. In order to keep the number of slices along the length of the organism manageable, the resulting voxel size only allowed for 27 slices along the shortest axis, and poor resolution of the relatively fine-structured bones (Figure 6.10). Second, the presence of any residual ice crystals inside the sample produces noise and shadows in the resulting image, which would not be an issue using CTs. Therefore, rapid and careful transport of the organism in question to the imaging facility is required to preserve the sample's condition without producing any internal ice crystals in cold storage during transport (see Figure 6.11, MRI of the cervical section of Pacific albacore, for the degree to which noise can vary due solely to ice crystal composition).

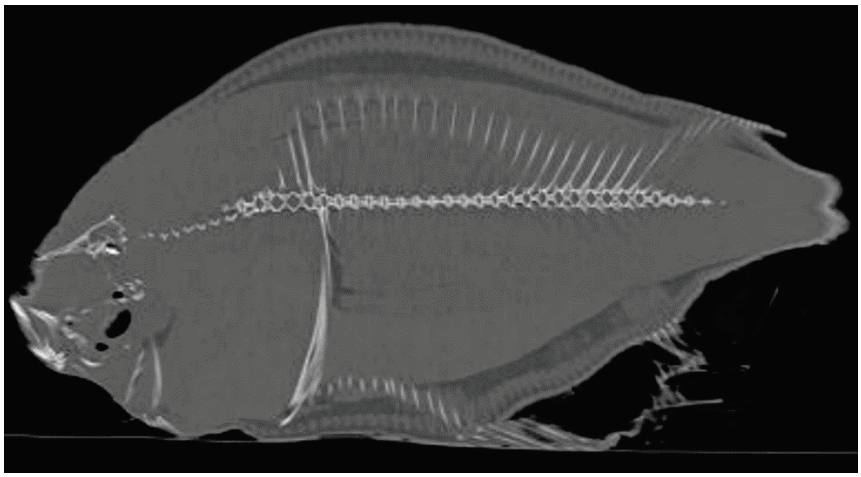

Fig. 6.8 CT slice of the sanddab used for the reference flatfish. Note that it is only bone *versus* soft tissue that can be differentiated from in the image.

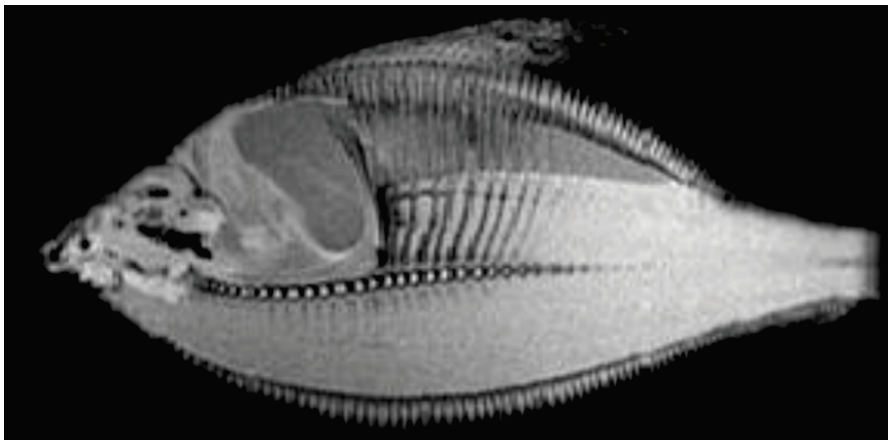

Fig. 6.9 MRI slice of the sanddab used for the reference flatfish.

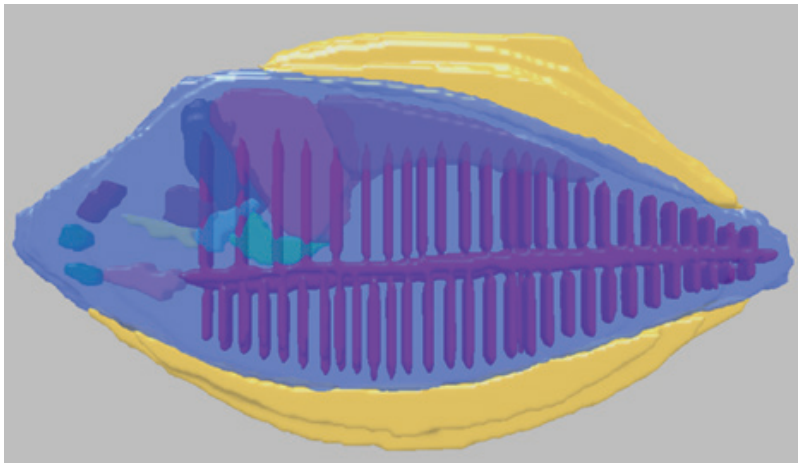

Fig. 6.10 Resulting voxel model of the reference flatfish. Note the voxel size relative to thickness is very evident along the dorsal and ventral fins, and the uneven representation of the bone structures.

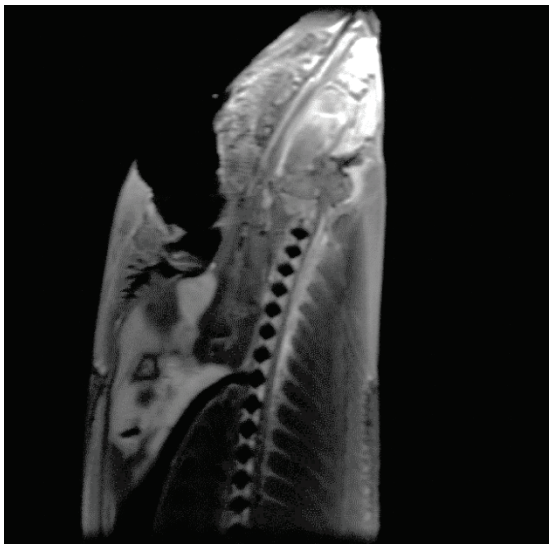

Fig. 6.11 MRI slice of a Pacific albacore, cervical section. Although there is less fine-scale noise than the flatfish MRI, there is significantly more shadowing.

6.2.3 Squid

A voxel model of squid, including trunk, head, arms, pen, stomach, ink sac, liver, gills and other glands was developed with MRI technology by the Third Institute of Oceanography, State Oceanic Administration of the People's Republic of China using a neon flying squid (*Ommastrephes bartramii*) sample obtained from captured in the northwestern Pacific in November 2011. The squid, trunk length of 25 cm, was frozen immediately after catch and was thawed just prior to imaging. This voxel model will be used to further contribute to the estimation of radiation dose rates in marine biota of the same taxon.

Voxelized phantoms are based on tomography, and they show the shape and position of different organs or tissues inside the organism. As a result, voxelized models are much more accurate in describing the geometry of the organism than the currently generally used radiological dose assessment model, which uses ellipsoids to represent the organisms. A voxelized phantom, which substantially improves the precision of the existing geometric phantom for squid, is created using

anatomic data obtained with MRI technology, which has a better resolution on soft tissues compared to CTs. The MRI scanning was performed at the Jimei Hospital in Xiamen, the People's Republic of China. Slice thickness of the individual was 6 mm; in total, 12 slices were utilized in making the model. The resulting pixel matrix was 512 rows by 512 columns. To create the realistic geometry used in the voxel phantom, individual organs were contoured on each slice of the MRI image in a process called segmentation. Segments (Figure 6.12) were hand-drawn after attempts at auto segmentation with the software 3D-DOCTOR resulted in highly irregular surfaces. Not all organs were individually contoured due to the difficulties in distinguishing tiny organs, or those located most proximally. Afterwards, a voxel phantom was created using 3D-DOCTOR.

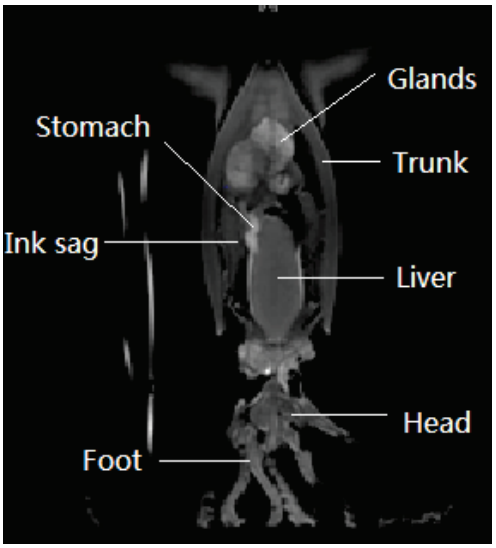

Fig. 6.12 Segmentation of a slice of the squid sample.

Figure 6.13 depicts the voxel phantom constructed in this study using 3D-DOCTOR, which contained 9 segments, including trunk, head, arms, pen, stomach, ink sac, liver, gills and other glands. Work on elemental composition analysis, and particle transport simulations will be done in the near future to calculate the absorbed fractions (AFs) in different tissues, and to further enhance the radiological dose assessment for this species.

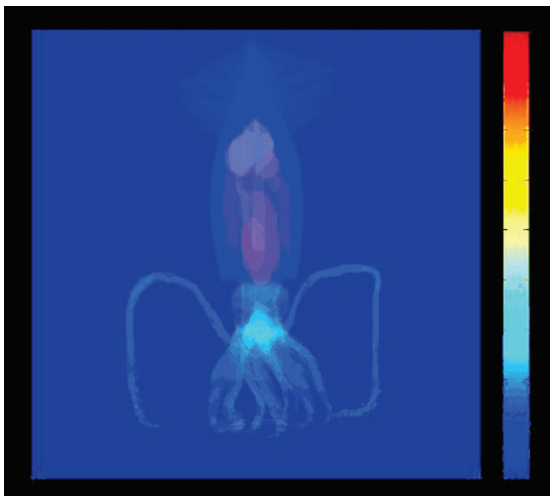

Fig. 6.13 Segment rendering of the voxelized squid model created by 3D-DOCTOR.

6.2.4 Plants

The general pipeline for voxel model generation, first established by Caffrey (2012), has allowed for the creation of models of the reference bee, as well as a beehive, the reference trout, adult and juvenile rabbits, as well as related work on the reference mouse and frog. However, more work is needed on modeling members of the Plant Kingdom.

Initial imaging of the brown seaweed, *Fucus* (Figure 6.14), was done while live and surrounded by seawater to preserve its natural geometry. However, seawater has nearly the same density as the algae, which led to practically no contrast in the CT images. Further, even imaging the seaweed surrounded by air was insufficient to produce contrast of any of the internal structure, including the air bladder. The size of a mature plant for both the reference seaweed and reference pine tree can vary substantially, as can the number and placement of branching structures.

Fig. 6.14 *Fucus* from Yaquina Bay, Oregon, used by Caffrey (2012) for initial models of the reference brown seaweed.

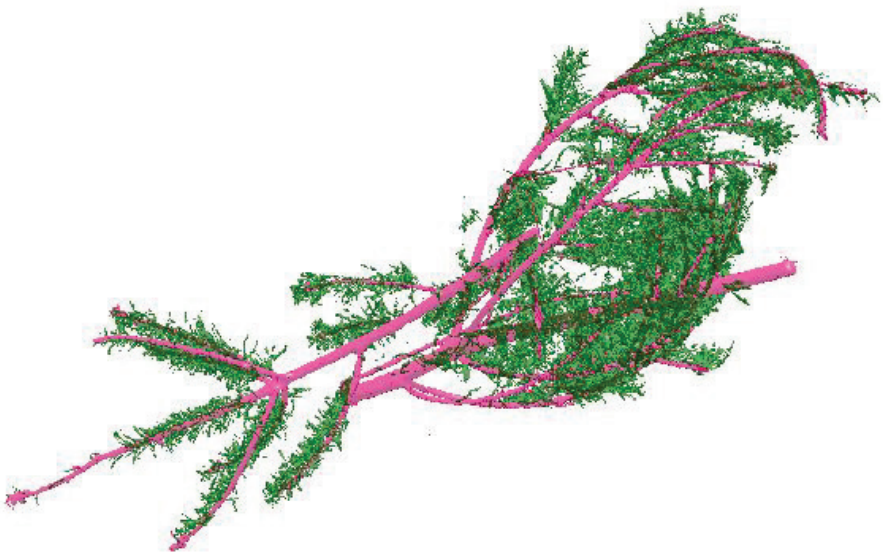

Fig. 6.15 Large and medium branch voxel model subsections for the modular reference pine.

Ongoing work at Oregon State University by Caitlin Condon is aimed at imaging subsections of the three reference plants. By limiting each imaging session to only a subsection of the plant, imaging techniques can be optimized for the structures (and scale of those structures). This modular approach allows for a union between the freedom of a simple geometric model and the accuracy of electromagnetic-based imaging modalities. At the time of this writing, only the reference pine subsections have relevant figures available (see Figure 6.15).

6.3 DICE-CT imaging

Improved imaging for marine biota models has been tested using facilities at Friday Harbor Labs, University of Washington, operated by Adam Summers. Using a Bruker micro-CT, fine-scale images were performed on 24 biota samples that are too small or complex for CTs designed for human or veterinary use. Tissue-based contrast was achieved for these samples through the use of diffusible-iodine contrast-enhanced CTs (DICE-CT). This project was additionally performed to contribute to the #ScanAllFish initiative (https://www.adamsummers.org/scanallfish) which seeks to acquire high resolution micro-CTs of all fish (though more plausibly, many fish).

Samples were fixed in 10% formalin, then stained using a 1% I_2KI aqueous solution. Each organism was then marked with an x-ray opaque marker (see Figure 6.16, marked 'E') to discern each organism after scanning a cylinder packing several specimens into the allowable geometry of the micro-CT used (Figure 6.17).

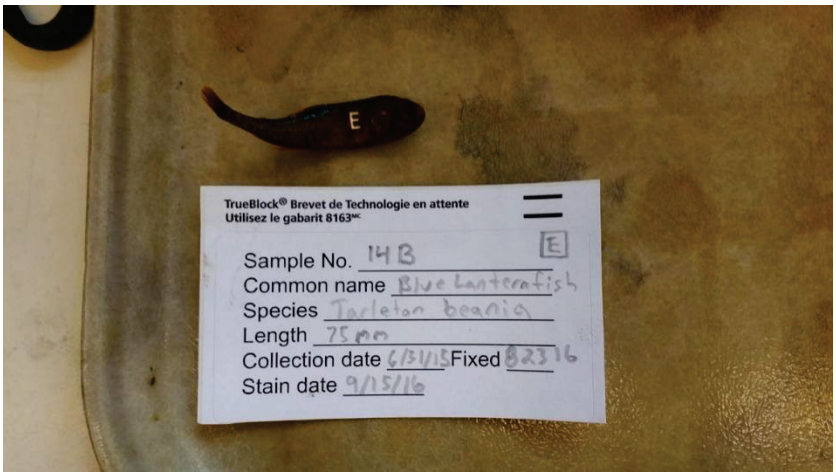

Fig. 6.16 A blue lanternfish, *Tarleton beania*, specimen, following staining with Lugol's solution.

Fig. 6.17 Forage fish (including a butterfish, surf smelt, whitebait smelt, and a squid) 'burritoed' for imaging.

6.4 Polygonal mesh vs. voxel

Ongoing work by Delvan Neville at Oregon State University is seeking to revamp the model creation pipeline currently in use for accurate dose calculations for marine biota (and later, for other biota). The existing voxel model pipeline suffers from some disadvantages: first, the analyst must choose between a large voxel size to allow a manageable number of slices to segment and small voxel size to allow for the imaging and later representation of fine-scale structures, as shown by the reference flatfish model. Second, the software used is proprietary, and is either simply expensive (3D-DOCTOR) or source-controlled (Voxelizer, MCNP). In the case of MCNP (Monte Carlo N-Particle), many scientists who are not based in the U.S. are prohibited from utilizing this pipeline as this code is classified as NOFORN by the United States Government.

Utilizing the fine-structure images collected as part of the #ScanAllFish contribution, progress is being made by Neville on a new pipeline that is both free and open-source, and bypasses the limitations that come with a voxel-based solution by using a surface-mesh based model. This new pipeline uses Slicer (also known as 3D Slicer), an open-source alternative to software like 3D-DOCTOR, and GEANT4, an open-source radiation transport code used both in particle physics and medical physics.

The latter improvement, surface-mesh models rather than voxel models, has already become popular in human dosimetry in recent years (Figure 6.18). A surface-mesh defines the boundaries between two compartments by a collection of connected polygons, typically triangles, rather than by assigning each of a grid of voxels to one compartment or the other. It allows fine-scale structures to be represented without requiring every surface to be segmented to the same level of detail, and does not result in the prohibitively long processing time that comes with modelling particle transport through an exceptionally fine-fixed voxel.

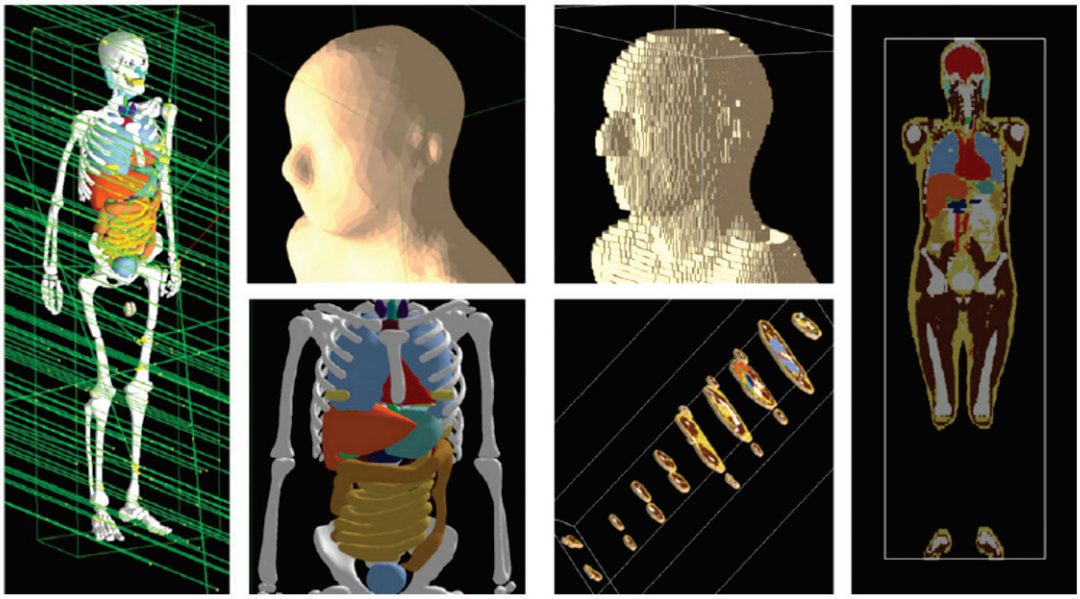

Fig. 6.18 Comparison and contrast of (left) a surface-mesh based model of the human body to (right) a voxel-based model of the human body.

6.5 Summary

In the post-Fukushima Dai-ichi Nuclear Power Plant accident era, marine radio-ecological research in PICES member countries has largely taken the form of North Pacific oceanographic surveys that could append additional radioactivity measurements, or to radio-ecological modelling work that was shifted towards the North Pacific. Radio-ecology work, as a whole in PICES member countries, is largely funded by stakeholders (the general public) either as a result of pressure on overlapping organizations to fund relevant work, or now as a product directly funded by the general public *via* crowd-sourcing. It remains to be seen if there will ever be a substantial state or federal push for strong marine radio-ecology research before another major event occurs, rather than only reacting to that need afterwards.

7 Innovations in Monitoring Devices

7.1 *In-situ underwater Labr$_3$ detector*

An *in-situ* underwater $Labr_3$ detector (Figure 7.1) was developed by the Third Institute of Oceanography and Tsinghua University in the People's Republic of China in order to monitor gamma radioactivity on site in an emergency. Features of this device are that it is light and watertight, has a compact gamma spectrometer and communication unit, and can store data on-site. The resolution of the detector for ^{137}Cs is about 2.6% at 662 keV, the detecting efficiency for ^{137}Cs at 662 keV is about 0.080 ± 0.004 cps/(Bq/L), and the MDA for ^{137}Cs in seawater (at 662keV in one hour) is about 0.35 Bq/L (without the background of itself). This detector can be deployed on a buoy near a nuclear power plant, and the data will be sent back to the control center in real time.

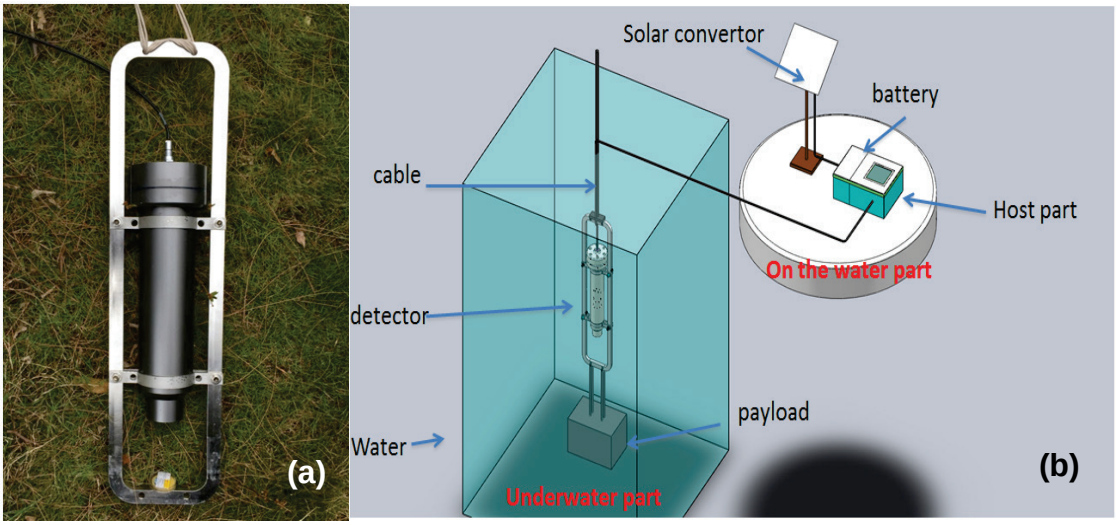

Fig. 7.1 $Labr_3$ detector. (a) Prototype, (b) Layout.

7.2 *Integrated device for radiocesium in seawater*

To improve the pretreatment efficiency of radiocesium in seawater, a prototype machine (Figure 7.2) based on a new design of an integrated device for coprecipitation and filtration was developed by the Third Institute of Oceanography, State Oceanic Administration of the People's Republic of China and tested in the laboratory for its potential and efficiency. Results show that the efficiency of pretreatment of radiocesium can be improved by more than one order of magnitude compared to traditional methods. In addition, results on the effect of settling time show that immediate filtration of solution after reaction will not affect the absorption of AMP (ammonium phosphomolybdate) to radiocesium in seawater.

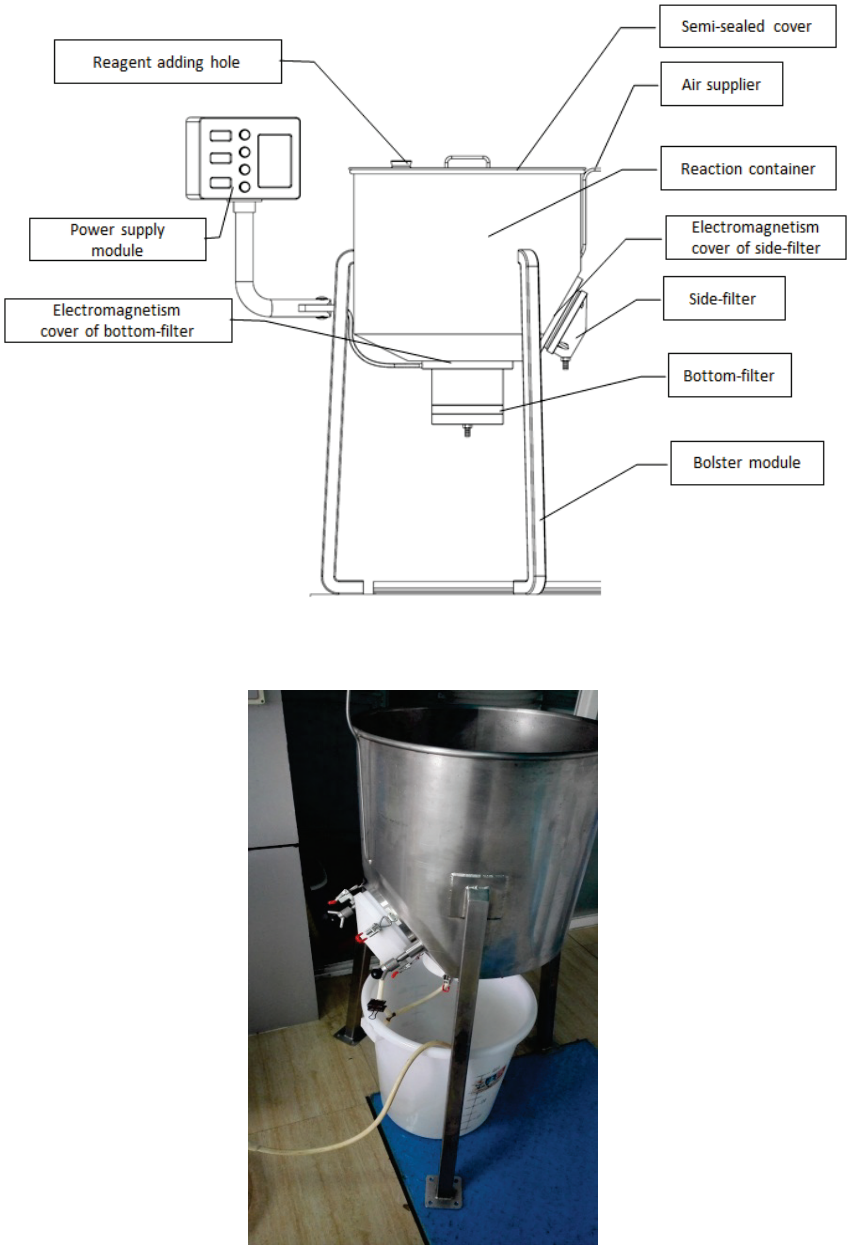

Fig. 7.2 (Top) Schematic of the integrated device; (bottom) Prototype of the device.

8 National Summaries and Conclusions

8.1 Canada

The Fisheries and Oceans Canada Fukushima monitoring program has provided the principal sustained time series record for the large-scale transport of the Fukushima radioactivity plume from the western to the eastern North Pacific Ocean since 2011. The Fukushima ^{137}Cs signal was initially observed on Line P in June 2012, 15 months after the accident and had fully spread onto the BC continental shelf by June 2013. The signal continued to increase through February 2015 to levels in excess of 6 Bq/m^3 at Sta. P26 on the western end of Line P, but increased much more slowly on the eastern end of Line P at Sta. P4. This decoupling in the transport of the Fukushima signal to the different sections of Line P was promoted by an anomalously high atmospheric pressure system positioned over this region in 2013–2014 that deflected storm tracks and interfered with circulation and convective mixing in the ocean. This resulted in both the offshore pooling of Fukushima radioactivity and the development of unusually high surface temperatures in a large region that became known as “the blob”. Slackening of atmospheric pressures in 2015 resulted in the dispersion of the blob and spreading of the Fukushima signal onto the continental shelf.

Comparisons of the Line P time series with model simulations suggests that ^{137}Cs concentrations will approach their maximum levels in 2016–2017 and will then begin to gradually decline. Measurements of total ^{137}Cs levels (Fukushima + fallout) of 8–10 Bq/m^3 on Line P have returned ^{137}Cs levels to those typical of fallout in the North Pacific in the early 1970s, but are well below levels posing a threat to human health or the environment.

^{137}Cs levels in samples of coastal seawater collected by citizen scientists under the InFORM program have increased by a factor of 2–3 since the initiation of monitoring in 2014. These increases in radionuclide levels are most pronounced in northern BC at locations proximal to the northward flowing Alaska Current which transports the major inventory of FDNPP accident radioactivity. Average concentrations of ^{137}Cs measured in salmon are about 0.2 Bq/kg while only one of 400 salmon samples had detectable levels of ^{134}Cs. These levels are well below the Canadian action level for ^{137}Cs of 1,000 Bq/kg and represent a negligible radiological threat to human consumption of seafood. Shellfish samples collected from BC’s main aquaculture regions in 2016 showed no detectable levels of ^{137}Cs. This work has revealed that FDNPP accident-derived radionuclides represent useful tracers to study water circulation in the Northeast Pacific Ocean, but do not represent a radiological threat to human health or the environment.

8.2 Japan

Japan has a long history of monitoring radioactivity in the environment which, prior to 2011, consisted mainly of establishing levels of fallout radioactivity in environmental phases. As a result, there was a large marine radioactivity database to which post-FDNPP accident radioactivity levels could be compared. The FDNPP accident was characterized by the sort-term direct release of water to the ocean contaminated with ^{131}I and radiocesium (^{137}Cs and ^{134}Cs). The direct leakage of ^{137}Cs was estimated as 3.5 PBq and the highest seawater concentration ($> 6 \times 10^7$ Bq/m^3) was observed at the coast near the FDNPP. This value was seven orders of magnitude higher than the pre-accident levels. Seawater concentrations of ^{137}Cs declined quickly following the accident owing to ocean mixing and transport in the dynamic coastal regime off eastern Japan and within several years ^{137}Cs levels had begun to approach pre-2000 ocean fallout levels in the offshore area.

Biota monitoring data for the FDNPP accident involved 87,234 inspection results by the end of December 2016. The monitoring results showed that more than 57% of inspected marine fish samples off Fukushima Prefecture were over the Japanese regulatory limit (100 Bq/kg-wet for radioactive Cs) in the period immediately following the accident (April–June 2011). This percentage gradually declined and has remained at 0% since April 2015.

Ongoing sources of radiocesium from the FDNPP to the ocean are known to be the FDNPP site, rivers and groundwater beneath some sand beaches. The ongoing releases of ^{137}Cs from the FDNPP harbor were estimated to be 3 TBq/y for the summer of 2012 while the concentration of ^{137}Cs in the harbor decreased by a factor of 5 between 2013 and 2016 and the present-day releases of ^{137}Cs from the FDNPP harbor are estimated to be about 0.6 TBq/y. However, the monitoring results have shown a continuing decrease in the concentration of radiocesium in marine organisms, indicating that these ongoing sources are not a public health issue for Japan.

Measurements of radiocesium in the North Pacific east of Japan in 2011–2013, combined with particle tracking experiments, showed that the FDNPP-derived radiocesium had been dispersed eastward into the central North Pacific following the accident. ^{134}Cs and ^{137}Cs concentrations of more than 10 Bq/m^3 were observed in the area in the northern part of the Kuroshio Extension. From the temporal changes of the ^{134}Cs concentration, it was estimated that the eastward speed of the FDNPP-derived radiocesium plume was 8 cm/s which was consistent with flow velocities estimated from Argo float data. After 2012, concentrations of ^{137}Cs off the east coast of Japan (except for the coastal region of the FDNPP site) markedly decreased owing to the absence of continuing large inputs from FDNPP.

Following the FDNPP accident, subsurface intrusion of FDNPP-derived radiocesium associated with STMW and CMW was reported. The total amount of ^{134}Cs within the STMW, decay-corrected to April 2011 to be 4.2 ± 1.1 PBq, corresponded to 22–28% of the total amount of ^{134}Cs released to the Pacific Ocean. In the formation area of CMW, FDNPP-derived radiocesium was observed both in STMW and CMW along the 165°E transect during June 2012 and was in CMW north of the Kuroshio Extension along 155°E during October–November 2012.

8.3 People's Republic of China

Ten monitoring cruises were conducted in the coastal waters of the People's Republic of China and in the Northwest Pacific by the State Oceanic Administration of the People's Republic of China from 2011–2015 in order to understand the transport of radioactive pollutants released from the FDNPP accident and their potential environmental impact. The monitoring results in seawater show that the highest activity of ^{137}Cs measured in the Northwest Pacific in May–June 2011 was 826 Bq/m^3, which was two orders of magnitude higher than fallout background level, while the highest activity of ^{90}Sr was 31 Bq/m^3, which was 25 times higher than the background level. Levels of ^{137}Cs, ^{134}Cs and ^{90}Sr in the Northwest Pacific decreased quickly with time after the accident, but were still elevated compared to the background levels before March 2011.

In general, the activities of ^{137}Cs and ^{134}Cs have decreased quickly with time since late 2011 or 2012, but activities in the Northwest Pacific are still higher than the background levels. ^{134}Cs from the FDNPP accident was found in 11 out of 146 samples collected from coastal waters of China and at a station (at the depth of 200 m) 550 km away from Taiwan Island, indicating that a small amount of ^{134}Cs was transported from the FDNPP accident site to the coastal waters of China. Radioactivity levels in marine organisms attained maximum levels in 2012 and decreased with time thereafter. A marine organism radiological dose assessment shows that the radiological dose to nekton species from the FDNPP accident was far below the recommended dose limits, indicating that there were no significant radiological effects on nekton.

Elevated levels of ^{134}Cs and ^{110m}Ag from the FDNPP accident were found in the squid (*O. bartramii*) samples collected in the Northwest Pacific in November 2011. The study carried out by the WG members from China filled a gap in international transfer data by providing concentration ratios for several key NPP-associated radionuclides in the whole-body and tissues of cephalopods. The Concentration Ratio for ^{110m}Ag in squid was found to be as high as 4×10^4 L/kg in the smallest samples, with a mean value of 2.95×10^4 L/kg in all the samples, indicating that squid was a good bioindicator for ^{110m}Ag from the FDNPP accident. The radiological dose contribution from the FDNPP releases for squid living in the study area, and for human consumers of these squids, were both far below the recommended dose limits. By comparison, natural radionuclides, particularly ^{210}Po, provide orders of magnitude greater dose rates.

8.4 Republic of Korea

Monitoring of radionuclides such as ^{137}Cs, ^{3}H, ^{90}Sr, and $^{239+240}$Pu has been undertaken in sediments seawater and biota in coastal waters of Korea since 1994. Following the FDNPP accident, the government of the Republic of Korea established an emergency response organization system to respond to the accident of FDNPP in Japan. The "Plan for Strengthening Environmental Radiation Monitoring by Stage" program was established and converted to an emergency radiation monitoring system for the whole country. In order to promptly confirm the possibility of radioactive materials released to the atmosphere and radioactive materials released to the sea into the surrounding waters of Korea, the marine environmental radioactivity survey was enhanced with increased sampling frequency for seawater samples and extended sampling areas for seawater and fish samples.

The levels of concentrations of radionuclides (^{3}H, ^{137}Cs, ^{90}Sr and $^{239+240}$Pu) in the surface seawater of coastal sea of Korea since 2011 are consistent with the radionuclide level obtained over the 5 years (2006–2010) prior to the FDNPP accident in 2011. The concentrations of ^{137}Cs, ^{90}Sr and $^{239+240}$Pu in ocean sediments and marine biota, including fish, shellfish and seaweed collected in the coastal waters of Korea during 2011–2016 were also similar to those determined before the FDNPP

accident. However, the concentration of ^{137}Cs in the mullet captured along the eastern coast in 2012 was found to be 2,432 ± 32 mBq/kg·fresh, which was ten times higher than annual average concentrations in fish measured during 2006–2011, indicating that this fish had probably been contaminated off the coast of Japan and subsequently migrated to coastal waters of Korea.

It is noted that a relatively limited number of modelers have contributed to WG 30 activities, reporting three transport models and three versions of marine radioactivity fate models. However, all modelers have provided unique and valuable information. The regional transport models off FDNPP reported sophisticated modeling works with emphasis on bottom contamination and the global model reported a long-term transport of dissolved marine radioactivity in North Pacific, successfully validating results with observations off the Canadian coast. The development of a series of dynamic fate models has been very helpful in understanding the technical progress made in the modeling of marine radioactivity transfer processes.

8.5 United States of America

Integrated spatiotemporal modeling has not only improved the dose–effect relationship from the entire body of an organism to a per-tissue basis, but to a per-cell basis. Improved imaging with tissue-based contrast for 24 marine biota samples was achieved through the use of diffusible-iodine contrast enhanced CTs (DICE-CT). A new pipeline that is both free and open-source, and bypasses the limitations that come with a voxel-based solution by using a surface-mesh based model, is also in progress utilizing the fine-structure images collected as part of the #ScanAllFish contribution.

9 Collaboration between WG 30 and Other Scientific Organizations and PICES Member Countries

9.1 Collaboration with SCOR RiO5 WG

Close collaborations between PICES WG 30 and SCOR WG 146 (Radioactivity in the Ocean, 5 decades later (RiO5)) during the past 3 years included:

- Drs. Kathryn A. Higley and John N. Smith being members of both Working Groups.
- Smith and Higley were co-authors on a joint SCOR-PICES scientific publication: Buesseler, K., Dai, M., Aoyama, M., Benitez-Nelson, C., Charmasson, S., Higley, K., Maderich, V., Masque, P., Oughton, D. and Smith, J.N. 2017. Fukushima Daiichi-derived radionuclides in the ocean: Transport, fate, and impacts. Annual Review of Marine Science 9: 173–203.
- RiO5 WG members, Dr. Michio Aoyama and Dr. Minhan Dai, were invited to give invited presentations on "^{134}Cs and ^{137}Cs in the North Pacific Ocean derived from the TEPCO Fukushima Dai-ichi Nuclear Power Plant accident, Japan in March 2011" and "Sources and inventory of Cesium and Plutonium in China seas", respectively, at the Workshop (W5) on "*Monitoring and assessment of environmental radioactivity in the North Pacific*" organized by WG 30, during the PICES 2015 Annual Meeting in Qingdao, China.
- SCOR RiO5 WG member, Dr. Núria Casacuberta, gave an invited presentation on "Assessment of the distribution of radionuclides (^{137}Cs, ^{134}Cs, ^{90}Sr, ^{129}I, ^{236}U and Pu-isotopes) in the coast off Japan derived from the Fukushima Dai-ichi nuclear accident" at the Workshop (W10) on "*Distribution and risk analysis of radionuclides in the North Pacific*" held by WG 30 during the PICES 2016 Annual Meeting in San Diego, USA.

9.2 Collaboration with IAEA

During its term, WG 30 actively collaborated with the International Atomic Energy Agency (IAEA). In 2013, IAEA consultant, Mr. Ronald Szymczak, was invited to visit the Third Institute of Oceanography, State Oceanic Administration, for a week to perform an expert mission on radioecology study and laboratory QMS. He and Dr. Wen Yu carried out radioecology studies on shrimps during the week, and together they proposed a letter of intent to establish an IAEA Regional Training Centre for Marine Radiochemistry and Radioecology.

In the W5 workshop organized by WG 30 during the PICES 2015 Annual Meeting, Mr. Szymczak, gave an invited presentation on "Asia/Pacific marine ecosystem impacts from the Fukushima Daiichi Nuclear Power Plant accident". Head of Environmental Laboratories of IAEA, Mr. David Osborn was also invited to attend the workshop but was unable to due to administrative reasons.

9.3 Collaboration between PICES member countries

9.3.1 The Republic of Korea and the People's Republic of China

KIOST (Korea Institute of Ocean Science and Technology) researchers participating in WG 30 collaborated with researchers from FIO (First Institute of Oceanography), China, under the financial support of CKJORC (China-Korea Joint Ocean Research Center) located in Qingdao, China. The project, titled "China-Korea cooperation on the development of monitoring and prediction system of marine radionuclides for nuclear safety", was started in December 2011 and finished in November 2017.

KIOST researchers participating in WG 30 also collaborated with researchers from IMMSP (Institute of Mathematical Machine and System Problems), Ukraine, starting in 2011, for the development of marine radioactivity transport and fate models as part of a marine radioactivity-related KIOST major project.

10 Recommendations

The results generated by WG 30 indicate that radioactivity levels in the North Pacific Ocean are presently declining in most phases of the marine ecosystem. However, there are still continuing releases of radioactivity through rivers and groundwater into the ocean both directly from the FDNPP site and from terrestrial regions in which accident-derived radioactivity has been temporarily sequestered.

1. *Post-FDNPP monitoring of radionuclides (^{134}Cs, ^{137}Cs) should be continued in the North Pacific for seawater and biota until levels have reached the pre-2011 baseline fallout levels.*

The complex hydrodynamic current regime of the Northwest Pacific has resulted in the injection of much of the FDNPP accident radioactivity inventory into CMW and STMW waters that are being dispersed southward and eastward by subsurface transport. It is important to keep track of the marine dispersal patterns for this large quantity of artificial radioactivity.

2. *Oceanographic surveillance of the FDNPP radionuclide inventory should be maintained in North Pacific mode waters, both from an environmental radiological perspective and from an ocean tracer perspective.*

Existing radiological policy standards are different among PICES member countries, especially with regard to the long-term environmental and health effects of low radioactive wastes released into the marine environment. With the anticipated, continuing development of the nuclear power industry around the North Pacific, the effects of radioactivity releases on fisheries and the marine ecosystem will become an important environmental issue.

3. *Further collaboration should be continued to examine the influence of long-term, low-level radioactive waste releases from coastal nuclear facilities on fisheries and marine ecosystems.*

The Canadian InFORM program, through government funding, enlisted citizen scientists to collect environmental samples that were analyzed for radioactivity, with the results posted to publicly available websites. The direct engagement of the public in the environmental monitoring was effective in public outreach and in diminishing the spread of false information about environmental threats.

4. *Environmental monitoring for radioactivity can be made significantly more effective in terms of public outreach and education if efforts are made to directly engage the public in some aspect of the surveillance operations.*

11 References

Achim, P., Monfort, M., Le Petit, G., Gross, P., Douysset, G., Taffary, T., Blanchard, X. and Moulin, C. 2012. Analysis of radionuclide releases from the Fukushima Dai-ichi nuclear power plant accident part II. *Pure and Applied Geophysics* **171**: 645–667, https://doi.org/10.1007/s00024-012-0578-1.

Ahlswede, J., Hebel, S., Ross, O., Schoetter, R. and Kalinowski, M.B. 2013. Update and improvement of the global krypton-85 emission inventory. *Journal of Environmental Radioactivity* **115**: 34–42, https://doi.org/10.1016/j.jenvrad.2012.07.006.

Ambe, D., Kaeriyama, H., Shigenobu, Y. and Fujimoto, K. 2014. Five-minute resolved spatial distribution of radiocesium in sea sediment derived from the Fukushima Dai-ichi Nuclear Power Plant. *Journal of Environmental Radioactivity* **138**: 264–275, https://doi.org/10.1016/j.jenvrad.2014.09.007.

Aoyama, M., Hirose, K., Nemoto, K., Takatsuki, Y. and Tsumune, D. 2008. Water masses labeled with global fallout ^{137}Cs formed by subduction in the North Pacific. *Geophysical Research Letters* **35**: L01604, https://doi.org/10.1029/2007GL031964.

Aoyama, M., Tsumune, D., Uematsu, M., Kondo, F. and Hamajima, Y. 2012. Temporal variation of ^{134}Cs and ^{137}Cs activities in surface water at stations along the coastline near the Fukushima Dai-ichi Nuclear Power Plant accident site, Japan. *Geochemical Journal* **46**: 321–325, https://doi.org/10.2343/geochemj.2.0211.

Aoyama, M., Uematsu, M., Tsumune, D. and Hamajima, Y. 2013. Surface pathway of radioactive plume of TEPCO Fukushima NPP1 released ^{134}Cs and ^{137}Cs. *Biogeosciences* **10**: 3067–3078, https://doi.org/10.5194/bg-10-3067-2013.

Aoyama, M., Kajino, M. and Tanaka, T.Y. 2016. ^{134}Cs and ^{137}Cs in the North Pacific Ocean derived from the March 2011 TEPCO Fukushima Dai-ichi Nuclear Power Plant accident, Japan. Part two: estimation of ^{134}Cs and ^{137}Cs inventories in the North Pacific Ocean. *Journal of Oceanography* **72**: 67–76, https://doi.org/10.1007/s10872-015-0332-2.

Behrens, E., Schwarzkopf, F.U., Lübbecke, J.F. and Böning, C.W. 2012. Model simulations on the long-term dispersal of ^{137}Cs released into the Pacific Ocean off Fukushima. *Environmental Research Letters* **7**: 034004, doi:10.1088/1748-9326/7/3/034004.

Beresford, N.A. 2010. The transfer of radionuclides to wildlife. *Radiation and Environmental Biophysics* **49**: 505–508, https://doi.org/10.1007/s00411-010-0325-x.

Bezhenar, R., Jung, K.T., Maderich, V., Willemsen, S., de With, G. and Qiao, F. 2016. Transfer of radiocaesium from contaminated bottom sediments to marine organisms through benthic food chains in post-Fukushima and post-Chernobyl periods. *Biogeosciences* **13**: 3021–3034, https://doi.org/10.5194/bg-13-3021-2016.

Biegalski, S.R., Bowyer, T.W., Eslinger, P.W., Friese, J.I., Greenwood, L.R., Haas, D.A., Hayes, J.C., Hoffman, I., Keillor, M., Miley, H.S. and Moring, M. 2012. Analysis of data from sensitive U.S. monitoring stations for the Fukushima Dai-ichi nuclear reactor accident. *Journal of Environmental Radioactivity* **114**: 15–21, https://doi.org/10.1016/j.jenvrad.2011.11.007.

Black, E.E. and Buesseler, K.O. 2014. Spatial variability and the fate of cesium in coastal sediments near Fukushima, Japan. *Biogeosciences* **11**: 5123–5137, https://doi.org/10.5194/bg-11-5123-2014.

Bond, N.A., Cronin, M.F., Freeland, H. and Mantua, N. 2015. Causes and impacts of the 2014 warm anomaly in the NE Pacific. *Geophysical Research Letters* **42**: 3414–3420, https://doi.org/10.1002/2015GL063306.

Bossew, P., Kirchner, G., De Cort, M., de Vries, G., Nishe, A. and de Felice, L. 2012. Radioactivity from Fukushima Dai-Ichi in air over Europe; Part 1: Spatio-temporal analysis. *Journal of Environmental Radioactivity* **114**: 22–34, https://doi.org/10.1016/j.jenvrad.2011.11.019.

Bowen, V.T., Noshkin, V.E., Vivingston, H.D. and Volchok, H.L. 1980. Fallout radionuclides in the Pacific Ocean: vertical and horizontal distributions, largely from GEOSECS stations. *Earth and Planetary Science Letters* **49**: 411–434, https://doi.org/10.1016/0012-821X(80)90083-7.

Bowyer, T.W., Biegalski, S.R., Cooper, M., Eslinger, P.W., Haas, D., Hayes, J.C., Miley, H.S., Strom, D.J. and Woods, V. 2011. Elevated radioxenon detected remotely following the Fukushima nuclear accident. *Journal of Environmental Radioactivity* **102**: 681–687, https://doi.org/10.1016/j.jenvrad.2011.04.009.

Breier, C., Pike, S.M., Sebestra, F., Tradd, K., Breier, J.A. and Buesseler, K.O. 2016. New applications of KNiFC-PAN resin for broad scale monitoring of radiocesium following the Fukushima Dai-ichi nuclear disaster. *Journal of Radioanalytical and Nuclear Chemistry* **307**: 2193–2200, https://doi.org/10.1007/s10967-015-4421-x.

Brown, J.E., Alfonso, B., Avila, R., Beresford, N.A., Copplestone, D., Pröhl, G. and Ulanovsky, A. 2008. The ERICA Tool. *Journal of Environmental Radioactivity* **99**: 1371–1383, https://doi.org/10.1016/j.jenvrad.2008.01.008.

Buesseler, K.O. 2012. Fishing for answers off Fukushima. *Science* **338**: 480–482, doi:10.1126/science.1228250.

Buesseler, K., Casso, S.A., Hartman, M.C. and Livingston, H.D. 1990. Determination of fission-products and actinides in the Black Sea following the Chernobyl accident. *Journal of Radioanalytical and Nuclear Chemistry* **138**: 33–47, https://doi.org/10.1007/BF02049345.

Buesseler, K., Aoyama, M. and Fukasawa, M. 2011. Impacts of the Fukushima nuclear power plants on marine radioactivity. *Environmental Science and Technology* **45**: 9931–9935, https://doi.org/10.1021/es202816c.

Buesseler, K.O., Jayne, S.R., Fisher, N.S., Rypina, I.I., Baumann, H., Baumann, Z., Breier, C.F., Douglass, E.M., George, J., Macdonald, A.M., Miyamoto, H., Nishikawa, J., Pike, S.M. and Yoshida, S. 2012. Fukushima-derived radionuclides in the ocean and biota off Japan. *Proceedings of the National Academy of Sciences* **109**: 5984–5988, https://doi.org/10.1073/pnas.1120794109.

Buesseler, K., Dai, M., Aoyama, M., Benitez-Nelson, C., Charmasson, S., Higley, K., Maderich, V., Masque, P., Oughton, D. and Smith, J.N. 2017. Fukushima Daiichi–derived radionuclides in the ocean: transport, fate, and impacts. *Annual Review of Marine Science* **9**: 173–203, https://doi.org/10.1146/annurev-marine-010816-060733.

Bustamante, P., Teyssié, J.-L., Danis, B., Fowler, S.W., Miramand, P., Cotret, O. and Warnau, M. 2004. Uptake, transfer and distribution of silver and cobalt in tissues of the common cuttlefish *Sepia officinalis* at different stages of its life cycle. *Marine Ecology Progress Series* **269**: 185–195, doi:10.3354/meps269185.

Caffrey, E.A. 2012. Improvements in the dosimetric models of selected benthic organisms. Master's Thesis. Oregon State University, Corvallis, Oregon, USA, http://ir.library.oregonstate.edu/xmlui/handle/1957/34305.

Carvalho, F.P. 2011. Polonium (^{210}Po) and lead (^{210}Pb) in marine organisms and their transfer in marine food chains. *Journal of Environmental Radioactivity* **102**: 462–472, https://doi.org/10.1016/j.jenvrad.2010.10.011.

Casacuberta, N., Masque, P., Garcia-Orellana, J., Garcia-Tenorio, R. and Buesseler, K.O. 2013. ^{90}Sr and ^{89}Sr in seawater off Japan as a consequence of the Fukushima Dai-ichi nuclear accident. *Biogeosciences* **10**: 3649–3659, https://doi.org/10.5194/bg-10-3649-2013.

Castrillejo, M., Casacuberta, N., Breier, C.F., Pike, S.M., Masqué, P. and Buesseler, K.O. 2015. Reassessment of ^{90}Sr, ^{137}Cs, and ^{134}Cs in the coast off Japan derived from the Fukushima Dai-Ichi nuclear accident. *Environmental Science and Technology* **50**: 173–180, https://doi.org/10.1021/acs.est.5b03903.

Charette, M.A., Breier, C.F., Henderson, P.B., Pike, S.M., Rypina, I.I., Jayne, S.R. and Buesseler, K.O. 2013. Radium-based estimates of cesium isotope transport and total direct ocean discharges from the Fukushima Nuclear Power Plant accident. *Biogeosciences* **10**: 2159–2167, https://doi.org/10.5194/bg-10-2159-201313.

Chino, M., Nakayama, H., Nagai, H., Terada, H., Katata, G. and Yamazawa, H. 2011. Preliminary estimation of release amounts of ^{131}I and ^{137}Cs accidentally discharged from the Fukushima Daiichi nuclear power plant into the atmosphere. *Journal of Nuclear Science and Technology* **48**: 1129–1134, https://doi.org/10.1080/18811248.2011.9711799.

Comans, R.N. and Hockley, D.E. 1992. Kinetics of cesium sorption on illite. *Geochimica et Cosmochimica Acta* **56**: 1157–1164, https://doi.org/10.1016/0016-7037(92)90053-L.

Cummins, P.F. and Freeland, H.J. 2007. Variability of the North Pacific Current and its bifurcation. *Progress in Oceanography* **75**: 253–265, https://doi.org/10.1016/j.pocean.2007.08.006.

Da Silva, A.M., Young, C.C. and Levitus, S. 1994. Atlas of Surface Marine Data 1994. NOAA Atlas NESDIS 6–10, U.S. Government Printing Office, Washington, DC.

de Vismes Ott, A., Gurriaran, R., Cagnat, X. and Masson, O. 2013. Fission product activity ratios measured at trace level over France during the Fukushima accident. *Journal of Environmental Radioactivity* **125**: 6–16, https://doi.org/10.1016/j.jenvrad.2013.02.014.

Di Lorenzo, E. and Mantua, N. 2016. Multi-year persistence of the 2014/15 North Pacific marine heatwave. *Nature Climate Change* **6**: 1042–1047, https://doi.org/10.1038/nclimate3082.

Doi, T., Masumoto, K., Toyoda, A., Tanaka, A., Shibata, Y. and Hirose, K. 2013. Anthropogenic radionuclides in the atmosphere observed at Tsukuba: characteristics of the radionuclides derived from Fukushima. *Journal of Environmental Radioactivity* **122**: 55–62, doi: 10.1016/j.jenvrad.2013.02.001.

Draxler, R., Arnold., D., Chino, M., Galmarini, S., Hort, M., Jones, A., Leadbetter, S., Malo, A., Maurer, C., Rolph, G., Saito, K., Servranckx, R., Shimbori, T., Solazzo, E. and Watawa, G. 2015. World Meteorological Organization's model simulations of the radionuclide dispersion and deposition from the Fukushima Daiichi nuclear power plant accident. *Journal of Environmental Radioactivity* **139**: 172–184, https://doi.org/10.1016/j.jenvrad.2013.09.014.

Evrard, O., Van Beek, P., Gateuille, D., Pont, V., Lefèvre, Lansard, B. and Bonté, P. 2012. Evidence of the radioactive fallout in France due to the Fukushima nuclear accident. *Journal of Environmental Radioactivity* **114**: 54–60, https://doi.org/10.1016/j.jenvrad.2012.01.024.

FAO (Food and Agriculture Organization). 2016. The State of World Fisheries and Aquaculture 2016. Contributing to food security and nutrition for all. Rome. 200 pp.

Fisher, N.S., Beaugelin-Seiller, K., Hinton, T.G., Baumann, Z., Madigan, D.J. and Garnier-Laplace, J. 2013. Evaluation of radiation doses and associated risk from the Fukushima nuclear accident to marine biota and human consumers of seafood. *Proceedings of the National Academy of Sciences* **110**: 10,670–10,675, https://doi.org/10.1073/pnas.1221834110.

Fowler, S.W. and Fisher, N.S. 2005. Radionuclides in the biosphere, pp. 167–203 *in:* Radioactivity in the Environment *edited by* H.D. Livingston, Elsevier, Amsterdam.

Fujimoto, K., Miki, S., Kaeriyama, H., Shigenobu, Y., Takagi, K., Ambe, D., Ono, T., Watanabe, T., Morinaga, K., Nakata, K. and Morita, T. 2015. Use of otolith for detecting ^{90}Sr in fish from the harbor of Fukushima Dai-ichi Nuclear Power Plant. *Environmental Science and Technology* **49**: 7294–7301, https://doi.org/10.1021/es5051315.

Garnier-Laplace, J., Copplestone, D., Gilbin, R., Alonzo, F., Ciffroy, P., Gilek, M., Agüero, A., Björk, M., Oughton, D.H., Jaworska, A., Larsson, C.M. and Hingston, J.L. 2008. Issues and practices in the use of effects data from FREDERICA in the ERICA Integrated Approach. *Journal of Environmental Radioactivity* **99**: 1474–1483, https://doi.org/10.1016/j.jenvrad.2008.04.012.

Ginzburg, H.M. and Reis, E. 1991. Consequences of the nuclear power plant accident at Chernobyl. *Public Health Reports* **106**: 32–40, 352.

Gudelis, A., Gorina, I., Nedveckaitė, T., Kovař, P., Dryak, P. and Suran, J. 2013. Activity measurement of gamma-ray emitters in aerosol filters exposed in Lithuania, in March–April 2011. *Applied Radiation and Isotopes* **81**: 362–365, https://doi.org/10.1016/j.apradiso.2013.03.019.

Hartmann, D.L. 2015. Pacific sea surface temperature and the winter of 2014. *Geophysical Research Letters* **42**: 1894–1902, https://doi.org/10.1002/2015GL063083.

Hernández-Ceballos, M., Hong, G.H., Lozano, R.L., Kim, Y.I., Lee, H.M., Kim, S.H., Yeh, S.-W., Bolívar, J.P. and Baskaran, M. 2012. Tracking the complete revolution of Surface Westerlies over Northern Hemisphere using radionuclides emitted from Fukushima. *Science of the Total Environment* **438**: 80–85, https://doi.org/10.1016/j.scitotenv.2012.08.024.

Hirose, K. 2012. 2011 Fukushima Dai-ichi nuclear power plant accident: Summary of regional radioactive deposition monitoring results. *Journal of Environmental Radioactivity* **111**: 13–17, https://doi.org/10.1016/j.jenvrad.2011.09.003.

Hong, G.H., Hernández-Ceballos, M.A., Lozano, R.L., Kim, Y.I., Lee, H.M., Kim, S.H., Bolívar, J.P. and Baskaran, M. 2012. Radioactive impact in South Korea from the damaged nuclear reactors in Fukushima: evidence of long and short range transport. *Journal of Radiological Protection* **32**: 397, DOI: 10.1088/0952-4746/32/4/397.

Hosseini, A., Beresford, N.A., Brown, J.E., Jones, D.G., Phaneuf, M., Thorring, H. and Yankovich, T. 2010. Background dose-rates to reference animals and plants arising from exposure to naturally occurring radionuclides in aquatic environments. *Journal of Radiological Protection* **30**: 235–264, https://doi.org/10.1088/0952-4746/30/2/S03.

Huh, C.-A., Hsu, S.-C. and Lin, C.-Y. 2012. Fukushima-derived fission nuclides monitored around Taiwan: Free tropospheric versus boundary layer transport. *Earth and Planetary Science Letters* **319**: 9–14, https://doi.org/10.1016/j.epsl.2011.12.004.

Huh, C.-A., Lin, C.-Y. and Hsu, S.-C. 2013. Regional dispersal of Fukushima-derived fission nuclides by East-Asian monsoon: a synthesis and review. *Aerosol and Air Quality Research* **13**: 537–544, https://doi.org/10.4209/aaqr.2012.08.0223.

IAEA (International Atomic Energy Agency). 1978. The radiological basis of the IAEA revised definition and recommendations concerning high-level radioactive waste unsuitable for dumping at sea. IAEA-TECDOC-211, IAEA, Vienna, Austria.

IAEA. 2004. Sediment distribution coefficients and concentration factors for biota in the marine environment. Technical Reports Series No. 422, IAEA Vienna, Austria.

IAEA. 2005. Worldwide marine radioactivity studies (WOMARS): Radionuclide levels in oceans and seas. IAEA-TECDOC-1429, IAEA, Vienna, Austria.

ICRP (International Commission on Radiological Protection). 1991. 1990 Recommendations of the International Commission on Radiological Protection. ICRP Publication 60. Ann. ICRP 21 (1-3).

ICRP. 2008. Environmental Protection - the Concept and Use of Reference Animals and Plants *edited by* C.L. Clement. ICRP Publication 108. Annals of the ICRP, Vol. 38, Nos. 4–6.

ICRP. 2012. Compendium of Dose Coefficients based on ICRP Publication 60. ICRP Publication 119. Annals of the ICRP, Vol. 41, Suppl. 1.

Igarashi, Y., Aoyama, M., Hirose, K., Miyao, T., Nemoto, K., Tomita, M. and Fujikawa, T. 2003. Resuspension: decadal monitoring time series of the anthropogenic radioactivity deposition in Japan. *Journal of Radiation Research* **44**: 319–328, https://doi.org/10.1269/jrr.44.319.

Ishii, T., Suzuki, H. and Koyanagi, T. 1978. Determination of trace elements in marine organisms, 1: Factors for variation of concentration of trace element. *Bulletin of the Japan Society of Scientific Fisheries* **44**: 155–162, https://doi.org/10.2331/suisan.44.155.

Iwata, K., Tagami, K. and Uchida, S. 2013. Ecological half-lives of radiocesium in 16 species in marine biota after the TEPCO's Fukushima Daiichi Nuclear Power Plant accident. *Environmental Science and Technology* **47**: 7696–7703, https://doi.org/10.1021/es400491b.

JFA (Fisheries Agency of Japan). 2017. Results of the monitoring on radioactivity level in fisheries products. http://www.jfa.maff.go.jp/e/inspection/index.html.

JFRA (Japan Fisheries Research Agency). 2012. Results of the inspection on radioactivity materials in fisheries products. http://www.jfa.maff.go.jp/e/inspection/index.html.

JFRA. 2015. Results of the inspection on radioactivity materials in fisheries products. http://www.jfa.maff.go.jp/e/inspection/index.html.

Johansen, M.P., Ruedig, E., Tagami, K., Uchida, S., Higley, K. and Beresford, N.A. 2015. Radiological dose rates to marine fish from the Fukushima Daiichi accident: the first three years across the North Pacific. *Environmental Science and Technology* **49**: 1277–1285, https://doi.org/10.1021/es505064d.

Jung, K.T., Brovchenko, I., Maderich, V., Kim, K.O. and Qiao, F. 2015. Development of a radionuclide transport model applicable to coastal regime with multi-fractional cohesive and non-cohesive sediments. Paper presented at PICES workshop W5 on "*Monitoring and assessment of environmental radioactivity in the North Pacific*" held at PICES-2015 on October 15, Qingdao, China.

Kaeriyama, H. 2015. ^{134}Cs and ^{137}Cs in the seawater around Japan and in the North Pacific, pp. 11–32 *in:* Impacts of the Fukushima Nuclear Accident on Fish and Fishing Grounds *edited by* K. Nakata and H. Sugisaki, Springer, Tokyo, https://doi.org/10.1007/978-4-431-55537-7_2.

Kaeriyama, H. 2017. Oceanic dispersion of Fukushima-derived radioactive cesium: a review. *Fisheries Oceanography* **26**: 99–113, https://doi.org/10.1111/fog.12177.

Kaeriyama, H., Ambe, D., Shimizu, Y., Fujimoto, K., Ono, T., Yonezaki, S., Kato, Y., Matsunaga, H., Minami, H., Nakatsuka, S. and Watanabe, T. 2013. Direct observation of ^{134}Cs and ^{137}Cs in surface seawater in the western and central North Pacific after the Fukushima Dai-ichi nuclear power plant accident. *Biogeosciences* **10**: 4287– 4295, https://doi.org/10.5194/bg-10-4287-2013.

Kaeriyama, H., Shimizu, Y., Ambe, D., Masujima, M., Shigenobu, Y., Fuijimoto, K., Ono, T., Nishiuchi, K., Taneda, T., Kurogi, H., Setou, T., Sugisaki, H., Ichikawa, T., Hidaka, K., Hiroe, Y., Kusaka, A., Kodama, T., Kuriyama, M., Morita, H., Nakata, K., Morinaga, K., Mortia, T. and Watanabe, T. 2014. Southwest intrusion of ^{134}Cs and ^{137}Cs derived from the Fukushima Dai-ichi Nuclear Power Plant accident in the western North Pacific. *Environmental Science and Technology* **48**: 3120–3127, https://doi.org/10.1021/es403686v.

Kaeriyama, H., Fujimoto, K., Ambe, D., Shigenobu, Y., Ono, T., Tadokoro, K., Okazaki, Y., Kakehi, S., Ito, S., Narimatsu, Y., Nakata, K., Morita, T. and Watanabe, T. 2015. Fukushima-derived radionuclides ^{134}Cs and ^{137}Cs in zooplankton and seawater samples collected off the Joban-Sanriku coast, in Sendai Bay, and in the Oyashio region. *Fisheries Science* **81**: 139–153, https://doi.org/10.1007/s12562-014-0827-6.

Kaeriyama, H., Shimizu, Y., Setou, T., Kumamoto, Y., Okazaki, M., Ambe, D. and Ono, T. 2016. Intrusion of Fukushima-derived radiocaesium into subsurface water due to formation of mode waters in the North Pacific. *Scientific Reports* **6**: 22010, https://doi.org/10.1038/srep22010.

Kanai, Y. 2012. Monitoring of aerosols in Tsukuba after Fukushima Nuclear Power Plant incident in 2011. *Journal of Environmental Radioactivity* **111**: 33–37, https://doi.org/10.1016/j.jenvrad.2011.10.011.

Kanda, J. 2013. Continuing ^{137}Cs release to the sea from the Fukushima Dai-ichi Nuclear Power Plant through 2012. *Biogeosciences* **10**: 6107–6113, https://doi.org/10.5194/bg-10-6107-2013.

Kaneyasu, N., Ohashi, H., Suzuki, F., Okuda, T. and Ikemori, F. 2012. Sulfate aerosol as a potential transport medium of radiocesium from the Fukushima nuclear accident. *Environmental Science and Technology* **46**: 5720–5726, https://doi.org/10.1021/es204667h.

Karube, Z., Inuzuka, Y., Tanaka, A., Kurishima, K., Kihou, N. and Shibata, Y. 2016. Radiostrontium monitoring of bivalves from the Pacific coast of eastern Japan. *Environmental Science and Pollution Research* **23**: 17,095–17,104, https://doi.org/10.1007/s11356-016-6878-8.

Kasamatsu, F. 1999. Marine organisms and radionuclides with special reference to the factors affecting concentrations of ^{137}Cs in marine fish. *Radioisotopes* **48**: 266–282, https://doi.org/10.3769/radioisotopes.48.266 (in Japanese).

Kawamura, H., Kobayashi, T., Furuno, A., In, T., Ishikawa, Y., Nakayama, T., Shima, S. and Awaji, T. 2011. Preliminary numerical experiments on oceanic dispersion of ^{131}I and ^{137}Cs discharged into the ocean because of the Fukushima Daiichi nuclear power plant disaster. *Journal of Nuclear Science and Technology* **48**: 1349–1356, https://doi.org/10.1080/18811248.2011.9711826.

Kawamura, H., Kobayashi, T., Furuno, A. and Usui, N. 2014. Numerical simulation on the long-term variation of radioactive cesium concentration in the North Pacific due to the Fukushima disaster. *Journal of Environmental Radioactivity* **136**: 64–75, https://doi.org/10.1016/j.jenvrad.2014.05.005.

Keum, D.-K., Jun, I., Kim, B.-H., Lim, K.-M. and Choi, Y.-H. 2015. A dynamic model to estimate the activity concentration and whole body dose rate of marine biota as consequences of a nuclear accident. *Journal of Environmental Radioactivity* **140**: 84–94, https://doi.org/10.1016/j.jenvrad.2014.11.006.

Khan, A.J., Semkow, T.M., Beach, S.E., Haines, D.K., Bradt, C.J., Bari, A., Syed, U.-F., Torres, M., Marrantino, J., Kitto, M.E. Menia, T. and Fielman, E. 2014. Application of low-background gamma-ray spectrometry to monitor radioactivity in the environment and food. *Applied Radiation and Isotopes* **90**: 251–257, https://doi.org/10.1016/j.apradiso.2014.04.011.

Kim, C.-K., Byun, J.-I., Chae, J.-S., Choi, H.-Y., Choi, S.-W., Kim, D.-J., Kim, Y.-J., Lee, D.-M., Park, W.-J., Yim, S.A. and Yun, J.-Y. 2012. Radiological impact in Korea following the Fukushima nuclear accident. *Journal of Environmental Radioactivity* **111**: 70–82, https://doi.org/10.1016/j.jenvrad.2011.10.018.

KINS (Korea Institute of Nuclear Safety). 2011–2016. Marine Environmental Radioactivity Survey. KINS/ER-092; 7–12.

Kobayashi, T., Nagai, H., Chino, M. and Kawamura, H. 2013. Source term estimation of atmospheric release due to the Fukushima Dai-ichi Nuclear Power Plant accident by atmospheric and oceanic dispersion simulations: Fukushima NPP accident related. *Journal of Nuclear Science and Technology* **50**: 255–264, https://doi.org/10.1080/00223131.2013.772449.

Kónya, J. and Nagy, N.M. 2012. 13 - Environmental Radioactivity, pp. 375–394 *in:* Nuclear and Radiochemistry, Elsevier, Oxford, https://doi.org/10.1016/B978-0-12-391430-9.00013-5.

Kumamoto, Y., Aoyama, M., Hamajima, Y., Aono, T., Kouketsu, S., Murata, A. and Kawano, T. 2014. Southward spreading of the Fukushima-derived radiocesium across the Kuroshio Extension in the North Pacific. *Scientific Reports* **4**: 4276, https://doi.org/10.1038/srep04276.

Kurita, Y., Shigenobu, Y., Sakuma, T. and Ito, S. 2015. Radiocesium contamination histories of Japanese flounder (*Paralichthys olivaceus*) after the 2011 Fukushima Nuclear Power Plant accident, pp. 139–151 *in:* Impacts of the Fukushima Nuclear Accident on Fish and Fishing Grounds *edited by* K. Nakata and H. Sugisaki, Springer, Tokyo, https://doi.org/10.1007/978-4-431-55537-7_11.

Kusakabe, M., Oikawa, S., Takata, H. and Misonoo, J. 2013. Spatiotemporal distributions of Fukushima-derived radionuclides in nearby marine surface sediments. *Biogeosciences* **10**: 5019–5030, https://doi.org/10.5194/bg-10-5019-2013.

Lepicard, S., Heling, R. and Maderich, V. 2004. POSEIDON/RODOS models for radiological assessment of marine environment after accidental releases: application to coastal areas of the Baltic, Black and North Seas. *Journal of Environmental Radioactivity* **72**: 153–161, https://doi.org/10.1016/S0265-931X(03)00197-8.

Leppänen, A.-P., Mattila, A., Kettunen, M. and Kontro, R. 2013. Artificial radionuclides in surface air in Finland following the Fukushima Dai-ichi nuclear power plant accident. *Journal of Environmental Radioactivity* **126**: 273–283, https://doi.org/10.1016/j.jenvrad.2013.08.008.

Liu, R. 2017. Integrated spatial and temporal stochastic model in radiation biology: Design, implementation, and application. Ph.D. Dissertation, Oregon State University, Corvallis, Oregon, USA.

Livingston, H.D. and Povinec, P.P. 2002. A millennium perspective on the contribution of global fallout radionuclides to ocean science. *Health Physics* **82**: 656–668, DOI:10.1097/00004032-200205000-00012.

Long, N.Q., Truong, Y., Hien, P.D., Binh, N.T., Sieu, L.N., Giap, T.V. and Phan, N.T. 2012. Atmospheric radionuclides from the Fukushima Dai-ichi nuclear reactor accident observed in Vietnam. *Journal of Environmental Radioactivity* **111**: 53–58, https://doi.org/10.1016/j.jenvrad.2011.11.018.

López-Pérez, M., Ramos-López, R., Perestelo, N.R., Duarte-Rodriguez, X., Bustos, J.J., Alonso-Pérez, S., Cuevas, E. and Hernández-Armas, J. 2013. Arrival of radionuclides released by the Fukushima accident to Tenerife (Canary Islands). *Journal of Environmental Radioactivity* **116**: 180–186, https://doi.org/10.1016/j.jenvrad.2012.09.011.

Maderich, V., Bezhenar, R., Heling, R., de With, G., Jung, K.T., Myoung, J.G., Cho, Y.K., Qiao, F. and Robertson, L. 2014a. Regional long-term model of radioactivity dispersion and fate in the Northwestern Pacific and adjacent seas: application to the Fukushima Dai-ichi accident. *Journal of Environmental Radioactivity* **131**: 4–18, https://doi.org/10.1016/j.jenvrad.2013.09.009.

Maderich, V., Jung, K.T., Bezhenar, R., de With, G., Qiao, F., Casacuberta, N., Masque, P. and Kim, Y.H. 2014b. Dispersion and fate of ^{90}Sr in the Northwestern Pacific and adjacent seas: Global fallout and the Fukushima Dai-ichi accident. *Science of the Total Environment* **494**: 261–271, https://doi.org/10.1016/j.scitotenv.2014.06.136.

Masson, O., Baeza, A., Bieringer, J., Brudecki, K., Bucci, S., Cappai, M., Carvalho, F.P., Connan, O., Cosma, C., Dalheimer, A., Didier, D., Depuydt, G., De Geer, L.E., De Vismes, A., Gini, L., Groppi, F., Gudnason, K., Gurriaran, R., Hainz, D., Halldórsson, Ó., Hammond, D., Hanley, O., Holeý, K., Homoki, Zs., Ioannidou, A., Isajenko, K., Jankovic, M., Katzlberger, C., Kettunen, M., Kierepko, R., Kontro, R., Kwakman, P.J.M., Lecomte, M., Leon Vintro, L., Leppänen, A.-P., Lind, B., Lujanienė, G., McGinnity, P., McMahon, C., Malá, H., Manenti, S., Manolopoulou, M., Mattila, A., Mauring, A., Mietelski, J.W., Møller, B., Nielsen, S.P., Nikolic, J., Overwater, R.M.W., Pálsson, S.E., Papastefanou, C., Penev, I., Pham, M.K., Povinec, P.P., Ramebäck, H., Reis, M.C., Ringer, W., Rodriguez, A., Rulík, P., Saey, P.R.J., Samsonov, V., Schlosser, C., Sgorbati, G., Silobritiene, B.V., Söderström, C., Sogni, R., Solier, L., Sonck, M., Steinhauser, G., Steinkopff, T., Steinmann, P., Stoulos, S., Sýkora, I., Todorovic, D., Tooloutalaie, N., Tositti, L., Tschiersch, J., Ugron, A., Vagena, E., Vargas, A., Wershofen, H. and Zhukova, O. 2011. Tracking of airborne radionuclides from the damaged Fukushima Dai-ichi nuclear reactors by European networks. *Environmental Science and Technology* **45**: 7670–7677, https://doi.org/10.1021/es2017158.

Masson, O., Ringer, W., Malá, H., Rulik, P., Dlugosz-Lisiecka, M., Eleftheriadis, K., Meisenberg, O., De Vismes-Ott, A. and Gensdarmes, F. 2013. Size distributions of airborne radionuclides from the Fukushima nuclear accident at several places in Europe. *Environmental Science and Technology* **47**: 10,995–11,003, https://doi.org/10.1021/es401973c.

Masumoto, Y., Miyazawa, Y., Tsumune, D., Tsubono, T., Kobayashi, T., Kawamura, H., Estournel, C., Marsaleix, P., Lanerolle, L., Mehra, A. and Garraffo, S.D. 2012. Oceanic dispersion simulations of ^{137}Cs released from the Fukushima Daiichi Nuclear Power Plant. *Elements* **8**: 207–212, https://doi.org/10.2113/gselements.8.3.207.

Masumoto, T., Maruoka, T., Shimoda, G., Obata, H., Kagi, H., Suzuki, K., Yamamoto, K., Mitsuguchi, T., Hagino, K., Tomioka, N., Sambandam, C., Brummer, D., Klaus, P.M. and Aggarwal, P. 2013. Tritium in Japanese precipitation following the March 2011 Fukushima Daiichi Nuclear Plant accident. *Science of the Total Environment* **445–446**: 365–370, https://doi.org/10.1016/j.scitotenv.2012.12.069.

Men, W., He, J., Wang, F., Yu, W., Li, Y., Huang, J. and Yu, X. 2015. Radioactive status of seawater in the northwest Pacific more than one year after the Fukushima nuclear accident. *Scientific Reports* **5**: 7757, https://doi.org/10.1038/srep07757.

Merz, S., Steinhauser, G. and Hamada, N. 2013. Anthropogenic radionuclides in Japanese food: environmental and legal implications. *Environmental Science and Technology* **47**: 1248–1256, https://doi.org/10.1021/es3037498.

MEXT (Japanese Ministry of Education, Culture, Sports, Science and Technology). 2010. Environmental Radiation Database. http://search.kankyo-hoshano.go.jp/servlet/search.top (in Japanese).

MEXT. 2011. Environmental Radiation Database. http://search.kankyo-hoshano.go.jp/servlet/search.top (in Japanese).

Mietelski, J.W., Kierepko, R., Brudecki, K., Janowski, P., Kleszcz, K. and Tomankiewicz, E. 2014. Long-range transport of gaseous ^{131}I and other radionuclides from Fukushima accident to Southern Poland. *Atmospheric Environment* **91**: 137–145, https://doi.org/10.1016/j.atmosenv.2014.03.065.

Miki, S., Fujimoto, K., Shigenobu, Y., Ambe, D., Kaeriyama, H., Takagi, K., Ono, T., Watanabe, T., Sugisaki, H. and Morita, T. 2017. Concentrations of ^{90}Sr and ^{137}Cs/^{90}Sr activity ratios in marine fishes after the Fukushima Dai-ichi Nuclear Power Plant accident. *Fisheries Oceanography* **26**: 221–233, https://doi.org/10.1111/fog.12182.

Min, B.-I., Periáñez, R., Kim, I.-G. and Suh, K.-S. 2013. Marine dispersion assessment of ^{137}Cs released from the Fukushima nuclear accident. *Marine Pollution Bulletin* **72**: 22–33, https://doi.org/10.1016/j.marpolbul.2013.05.008.

Miramand, P. and Bentley, D. 1992. Concentration and distribution of heavy metals in tissues of two cephalopods, *Eledone cirrhosa* and *Sepia officinalis*, from the French coast of the English Channel. *Marine Biology* **114**: 407–414, https://doi.org/10.1007/BF00350031.

Miyazawa, Y., Masumoto, Y., Varlomov, S.M., Miyama, T., Takigawa, M., Honda, M. and Saino, T. 2013. Inverse estimation of source parameters of oceanic radioactivity dispersion models associated with the Fukushima accident. *Biogeosciences* **10**: 2349–2363, https://doi.org/10.5194/bg-10-2349-2013.

Miyazawa, Y., Masumoto, Y., Varlamov, S.M. and Miyama, T. 2012. Transport simulation of the radionuclide from the shelf to open ocean around Fukushima. *Continental Shelf Research* **50**: 16–29, https://doi.org/10.1016/j.csr.2012.09.002.

Narimatsu, Y., Sohtome, T., Tamada, M., Shigenou, Y., Kurita, Y., Hattori, T. and Inagawa, R. 2015. Why do the radionuclide concentrations of Pacific cod depend on the body size? pp. 123–137 *in:* Impacts of the Fukushima Nuclear Accident on Fish and Fishing Grounds *edited by* K. Nakata and H. Sugisaki, Springer, Tokyo, https://doi.org/10.1007/978-4-431-55537-7_10.

Nitta, W., Sanada, T., Isogai, K. and Schlosser, C. 2014. Atmospheric ^{85}Kr and ^{133}Xe activity concentrations at locations across Japan following the Fukushima Dai-ichi Nuclear Power Plant accident. *Journal of Nuclear Science and Technology* **51**: 712–719, https://doi.org/10.1080/00223131.2014.888960.

Oikawa, S., Takata, H., Watabe, T., Misonoo, J. and Kusakabe, M. 2013a. Distribution of the Fukushima-derived radionuclides in seawater in the Pacific off the coast of Miyagi, Fukushima, and Ibaraki Prefectures, Japan. *Biogeosciences* **10**: 5031–5047, https://doi.org/10.5194/bg-10-5031-2013.

Oikawa, S., Watabe, T., Takata, H., Suzuki, M., Nakahara, M. and Misonoo, J. 2013b. Long term temporal changes of ^{90}Sr and ^{137}Cs in seawater, bottom sediment and marine organism samples. From the Chernobyl accident to immediately after the Fukushima accident. *Bunseki Kagaku* **62**: 455–474, https://doi.org/10.2116/bunsekikagaku.62.455 (in Japanese with English abstract).

Oka, E. and Qiu, B. 2012. Progress of North Pacific mode water research in the past decade. *Journal of Oceanography* **68**: 5–20, https://doi.org/10.1007/s10872-011-0032-5.

Oka, E., Qiu, B., Kouketsu, S., Uehara, K. and Suga, T. 2012. Decadal seesaw of the Central and Subtropical Mode Water formation associated with the Kuroshio Extension variability. *Journal of Oceanography* **68**: 355–360, https://doi.org/10.1007/s10872-011-0098-0.

Oka, E., Qiu, B., Takatani, Y., Enyo, K., Sasano, D., Kosugi, N., Ishii, M., Nakano, T. and Suga, T. 2015. Decadal variability of Subtropical Mode Water subduction and its impact on biogeochemistry. *Journal of Oceanography* **71**: 389–400, https://doi.org/10.1007/s10872-015-0300-x.

Okamura, H., Ikeda, S., Morita, T. and Eguchi, S. 2016. Risk assessment of radioisotope contamination for aquatic living resources in and around Japan. *Proceedings of the National Academy of Sciences* **113**: 3838–3843, https://doi.org/10.1073/pnas.1519792113.

Ono, T., Ambe, D., Kaeriyama, H., Shigenobu, Y., Fujimoto, K., Sogame, K., Nishiura, N., Fujikawa, T., Morita, T. and Watanabe, T. 2015. Concentration of ^{134}Cs and ^{137}Cs bonded to the organic fraction of sediments offshore Fukushima, Japan. *Geochemical Journal* **49**: 219–227, https://doi.org/10.2343/geochemj.2.0351.

Orr, B., Schöppner, M., Tinker, R. and Plastino, W. 2013. Detection of radioxenon in Darwin, Australia following the Fukushima Dai-ichi nuclear power plant accident. *Journal of Environmental Radioactivity* **126**: 40–44, https://doi.org/10.1016/j.jenvrad.2013.07.002.

Otosaka, S. and Kato, Y. 2014. Radiocesium derived from the Fukushima Daiichi Nuclear Power Plant accident in seabed sediments: Initial deposition and inventories. *Environmental Science: Processes and Impacts* **16**: 978–990, DOI:10.1039/c4em00016a.

Otosaka, S. and Kobayashi, T. 2013. Sedimentation and remobilization of radiocesium in the coastal area of Ibaraki, 70 km south of the Fukushima Dai-ichi Nuclear Power Plant. *Environmental Monitoring and Assessment* **185**: 5419–5433, https://doi.org/10.1007/s10661-012-2956-7.

Periáñez, R., Suh, K.S., Byung-Il, M., Casacuberta, N. and Masqué, P. 2013. Numerical modeling of the releases of ^{90}Sr from Fukushima to the ocean: an evaluation of the source term. *Environmental Science and Technology* **47**: 12,305–12,313, https://doi.org/10.1021/es4031408.

Povinec, P.P., Hirose, K. and Aoyama, M. 2012. Radiostrontium in the western North Pacific: characteristics, behavior, and the Fukushima impact. *Environmental Science and Technology* **46**: 10,356–10,363, https://doi.org/10.1021/es301997c.

Povinec, P.P., Hirose, K. and Aoyama, M. 2013a. Fukushima Accident: Radioactivity Impact on the Environment, Elsevier, 400 pp., https://doi.org/10.1016/C2012-0-06837-8.

Povinec, P.P., Gera, M., Holý, K., Hirose, K., Lujanienė, G., Nakano, M., Plastino, W., Sýkora, I., Bartok, J. and Gažák M. 2013b. Dispersion of Fukushima radionuclides in the global atmosphere and the ocean. *Applied Radiation and Isotopes* **81**: 383–392, https://doi.org/10.1016/j.apradiso.2013.03.058.

Povinec, P.P., Aoyama, M., Biddulph, D., Breier, R., Buesseler, K., Chang, C.C., Golser, R., Hou, X.L., Ješkovsky, M., Jull, A.J.T., Kaizer, J., Nakano, M., Nies, H., Palcsu, L., Papp, L., Pham, M.K., Steier, P. and Zhang, L.Y. 2013c. Cesium, iodine and tritium in NW Pacific waters – a comparison of the Fukushima impact with global fallout. *Biogeosciences* **10**: 5481–5496, https://doi.org/10.5194/bg-10-5481-2013.

Priyadarshi, A., Dominguez, G. and Thiemens, M.H. 2011. Evidence of neutron leakage at the Fukushima nuclear plant from measurements of radioactive ^{35}S in California. *Proceedings of the National Academy of Sciences* **108**: 14,422–14,425, https://doi.org/10.1073/pnas.1109449108.

Priyadarshi, A., Hill-Falkenthal, J., Thiemens, M.H., Yoshida, N., Toyoda, S., Yamada, K., Mukotaka, A., Fujii, A., Uematsu, M., Hatakeyama, S., Noguchi, I., Nojiri, Y. and Tanimoto, H. 2013. Detection of radioactive ^{35}S at Fukushima and other Japanese sites. *Journal of Geophysical Research: Atmospheres* **118**: 1020–1027, https://doi.org/10.1029/2012JD018485.

Ramzaev, V., Barkovsky, A., Goncharova, Yu, Gromov, A., Kaduka, M. and Romanovich, I. 2013. Radiocesium fallout in the grasslands on Sakhalin, Kunashir and Shikotan Islands due to Fukushima accident: the radioactive contamination of soil and plants in 2011. *Journal of Environmental Radioactivity* **118**: 128–142, https://doi.org/10.1016/j.jenvrad.2012.12.006.

Rossi, V., van Sebille, E., Sen Gupta, A., Garçon, V. and England, M. 2013. Multi-decadal projections of surface and interior pathways of the Fukushima Cesium-137 radioactive plume. *Deep-Sea Research I* **80**: 37–46, https://doi.org/10.1016/j.dsr.2013.05.015.

Rossi, V., van Sebille, E., Sen Gupta, A., Garçon, V. and England, M. 2014. Corrigendum to "Multi-decadal projections of surface and interior pathways of the Fukushima cesium-137 radioactive plume." *Deep-Sea Research I* **93**: 162–164, https://doi.org/10.1016/j.dsr.2014.08.007.

Rypina, I.I., Jayne, S.R., Yoshida, S., Macdonald, A.M., Douglass, E. and Buesseler, K. 2013. Short-term dispersal of Fukushima-derived radionuclides off Japan: modeling efforts and model-data intercomparison. *Biogeosciences* **10**: 4973–4990, https://doi.org/10.5194/bg-10-4973-2013.

Rypina, I.I., Jayne, S.R., Yoshida, S., Macdonald, A.M. and Buesseler, K. 2014. Drifter-based estimate of the 5 year dispersal of Fukushima-derived radionuclides. *Journal of Geophysical Research: Oceans* **119**: 8177–8193, https://doi.org/10.1002/2014JC010306.

Saegusa, J., Kikuta, Y. and Akino, H. 2013. Observation of gamma-rays from fallout collected at Ibaraki, Japan, during the Fukushima nuclear accident. *Applied Radiation and Isotopes* **77**: 56–60, https://doi.org/10.1016/j.apradiso.2013.02.018.

Sanial, V., Buesseler, K.O., Charette, M.A. and Nagao, S. 2017. Unexpected source of Fukushima-derived radiocesium to the coastal ocean of Japan. *Proceedings of the National Academy of Sciences* **114**: 11,092–11,096, https://doi.org/10.1073/pnas.1708659114.

Science Council of Japan. 2014. Report: A review of the model comparison of transportation and deposition of radioactive materials released to the environment as a result of the Tokyo Electric Power Company's Fukushima Daiichi nuclear power plant accident. 103 pp.

Shigenobu, Y., Fujimoto, K., Ambe, D., Kaeriyama, H., Ono, T., Morinaga, K., Nakata, K., Morita, T. and Watanabe, T. 2014. Radiocesium contamination of greenlings (*Hexagrammos otakii*) off the coast of Fukushima. *Scientific Reports* **4**: 6851, https://doi.org/10.1038/srep06851.

Shimizu, Y., Yasuda, I. and Ito, S. 2001. Distribution and circulation of the coastal Oyashio intrusion. *Journal of Physical Oceanography* **31**: 1561–1578, https://doi.org/10.1175/1520-0485(2001)031<1561:DACOTC>2.0.CO;2.

Shimizu, Y., Iwao, T., Yasuda, I., Ito, S., Watanabe, T., Uehara, K., Shikama, N. and Nalano, T. 2004. Formation process of North Pacific Intermediate Water revealed by profiling floats set to drift on 26.7 σ_θ isopycnal surface. *Journal of Oceanography* **60**: 453–462, https://doi.org/10.1023/B:JOCE.0000038061.55914.eb.

Shinonaga, T., Steier, P., Lagos, M. and Ohkura, T. 2014. Airborne plutonium and non-natural uranium from the Fukushima DNPP found at 120 km distance a few days after reactor hydrogen explosions. *Environmental Science and Technology* **48**: 3808–3814, https://doi.org/10.1021/es404961w.

Shozugawa, K., Nogawa, N. and Matsuo, M. 2012. Deposition of fission and activation products after the Fukushima Dai-ichi nuclear power plant accident. *Environmental Pollution* **163**: 243–247, https://doi.org/10.1016/j.envpol.2012.01.001.

Smith, J.T., Comans, R.N.J., Ireland, D.G., Nolan, L. and Hilton, J. 2000. Experimental and in situ study of radiocaesium transfer across the sediment–water interface and mobility in lake sediments. *Applied Geochemistry* **15**: 833–848, https://doi.org/10.1016/S0883-2927(99)00095-5.

Smith, J.N., Ellis, K.M. and Jones, E.P. 1990. ^{137}Cs transport into the Arctic Ocean through Fram Strait. *Journal of Geophysical Research: Oceans* **95**: 1693–1701, https://doi.org/10.1029/JC095iC02p01693.

Smith, J.N., Brown, R.M., Williams, W.J., Robert, M., Nelson, R. and Moran, S.B. 2015. Arrival of the Fukushima radioactivity plume in North American continental waters. *Proceedings of the National Academy of Sciences* **112**: 1310–1315, https://doi.org/10.1073/pnas.1412814112.

Sohtome, T., Wada, T., Mizuno, T., Nemoto, Y., Igarashi, S., Nishimune, A., Aono, T., Ito, Y., Kanda, J. and Ishimaru, T. 2014. Radiological impact of TEPCO's Fukushima Dai-ichi Nuclear Power Plant accident on invertebrates in the coastal benthic food web. *Journal of Environmental Radioactivity* **138**: 106–115, https://doi.org/10.1016/j.jenvrad.2014.08.008.

Steinhauser, G., Merz, S., Kübber-Heiss, A. and Katzlberger, C. 2012. Using animal thyroids as ultra-sensitive biomonitors for environmental radioiodine. *Environmental Science and Technology* **46**: 12,890–12,894, https://doi.org/10.1021/es303280g.

Steinhauser, G., Brandl, A. and Johnson, T.E. 2014. Comparison of the Chernobyl and Fukushima nuclear accidents: A review of the environmental impacts. *Science of the Total Environment* **470**: 800–817, https://doi.org/10.1016/j.scitotenv.2013.10.029.

Stohl, A., Seibert, P. and Wotawa, G. 2012a. The total release of ^{133}Xe from the Fukushima Dai-ichi nuclear power plant accident. *Journal of Environmental Radioactivity* **112**: 155–159, https://doi.org/10.1016/j.jenvrad.2012.06.001.

Stohl, A., Seibert, P., Wotawa, G., Arnold, D., Burkhart, J.F., Eckhardt, S., Tapia, C., Vargas, A. and Yasunari, T.J. 2012b. ^{133}Xe and ^{137}Cs releases into the atmosphere from the Fukushima Dai-ichi nuclear power plant: determination of the source term, atmospheric dispersion, and deposition. *Atmospheric Chemistry and Physics* **12**: 2313–2343, https://doi.org/10.5194/acp-12-2313-2012.

Suga, T. and Hanawa, K. 1990. The mixed-layer climatology in the northwestern part of the North Pacific subtropical gyre and the formation area of Subtropical Mode Water. *Journal of Marine Research* **48**: 543–566, https://doi.org/10.1357/002224090784984669.

Suga, T. and Hanawa, K. 1995. The subtropical mode water circulation in the North Pacific. *Journal of Physical Oceanography* **25**: 958–970, https://doi.org/10.1175/1520-0485(1995)025<0958:TSMWCI>2.0.CO;2.

Suzuki, Y., Nakahara, M. and Nakamura, R. 1978. Accumulation of cesium-137 by useful mollusca. *Nippon Suisan Gakk*. **44**: 325–329.

Tagami, K. and Uchida, S. 2013. Marine and freshwater concentration ratios ($CR_{wo\text{-}water}$): review of Japanese data. *Journal of Environmental Radioactivity* **126**: 420–426, https://doi.org/10.1016/j.jenvrad.2012.06.004.

Tateda, Y., Tsumune, D. and Tsubono, T. 2013. Simulation of radioactive cesium transfer in the southern Fukushima coastal biota using a dynamic food chain transfer model. *Journal of Environmental Radioactivity* **124**: 1–12, https://doi.org/10.1016/j.jenvrad.2013.03.007.

Tateda, Y., Tsumune, D., Tsubono, T., Aono, T., Kanda, J. and Ishimaru, T. 2015. Radiocesium biokinetics in olive flounder inhabiting the Fukushima accident-affected Pacific coastal waters of eastern Japan. *Journal of Environmental Radioactivity* **147**: 130–141, https://doi.org/10.1016/j.jenvrad.2015.05.025.

Tateda, Y., Tsumune, D., Misumi, K., Aono, T., Kanda, J. and Ishimaru, T. 2017. Biokinetics of radiocesium depuration in marine fish inhabiting the vicinity of the Fukushima Dai-ichi Nuclear Power Plant. *Journal of Environmental Radioactivity* **166**: 67–73, https://doi.org/10.1016/j.jenvrad.2016.02.028.

TEPCO (Tokyo Electric Power Company). 2013. Detection of radioactive materials from seawater near Fukushima Dai-ichi nuclear power station, with attachments. Press releases, http://www.tepco.co.jp/en/press/corp-com/release/.

TEPCO. 2017. Analysis results of fish and shellfish (the ocean area within 20km radius of Fukushima Daiichi NPS). http://www.tepco.co.jp/en/nu/fukushima-np/f1/smp/index-e.html (accessed on March 8, 2017).

Thakur, P., Ballard, S. and Nelson, R. 2012. Radioactive fallout in the United States due to the Fukushima nuclear plant accident. *Journal of Environmental Monitoring* **14**: 1317–1324, DOI:10.1039/c2em11011c.

Thakur, P., Ballard, S. and Nelson, R. 2013. An overview of Fukushima radionuclides measured in the northern hemisphere. *Science of the Total Environment* **458**: 577–613, https://doi.org/10.1016/j.scitotenv.2013.03.105.

Thomson, R.E. and Fine, I.V. 2009. A diagnostic model for mixed layer depth estimation with application to Ocean Station P in the Northeast Pacific. *Journal of Physical Oceanography* **39**: 1399–1415, https://doi.org/10.1175/2008JPO3984.1.

Thornton, B., Ohnishi, S., Ura, T., Odano, N., Sasaki, S., Fujita, T., Watanabe, T., Nakata, K., Ono, T. and Ambe, D. 2013. Distribution of local ^{137}Cs anomalies on the seafloor near the Fukushima Dai-ichi Nuclear Power Plant. *Marine Pollution Bulletin* **74**: 344–350, https://doi.org/10.1016/j.marpolbul.2013.06.031.

Tositti, L., Brattich, E., Cinelli, G., Prevti, A. and Mostacci, D. 2012. Comparison of radioactivity data measured in PM10 aerosol samples at two elevated stations in northern Italy during the Fukushima event. *Journal of Environmental Radioactivity* **114**: 105–112, https://doi.org/10.1016/j.jenvrad.2012.01.016.

Tsumune, D., Aoyama, M. and Hirose, K. 2003. Behavior of ^{137}Cs concentrations in the North Pacific in an ocean general circulation model. *Journal of Geophysical Research* **108**: 3262, https://doi.org/10.1029/2002JC001434.

Tsumune, D., Tsubono, T., Aoyama, M. and Hirose, K. 2012. Distribution of oceanic ^{137}Cs from the Fukushima Dai-ichi Nuclear Power Plant simulated numerically by a regional ocean model. *Journal of Environmental Radioactivity* **111**: 100–108, https://doi.org/10.1016/j.jenvrad.2011.10.007.

Tsumune, D., Tsubono, T., Aoyama, M., Uematsu, M., Misumi, K., Maeda, Y., Yoshida, Y. and Hayami, H. 2013. One-year, regional-scale simulation of ^{137}Cs radioactivity in the ocean following the Fukushima Daiichi Nuclear Power Plant accident. *Biogeosciences Discussions* **10**: 5601–5617, https://doi.org/10.5194/bg-10-5601-2013.

Tupin, E.A., Boyd, M.A., Mosser, J.E. and Wieder, J.S. 2012. US EPA response to the Fukushima Daiichi Nuclear Power Plant accident. *Health Physics* **102**: 563–569, doi:10.1097/HP.0b013e31824cc02e.

Ueno, H. and Yasuda, I. 2003. Intermediate water circulation in the North Pacific subarctic and northern subtropical regions. *Journal of Geophysical Research: Oceans* **108**: https://doi.org/10.1029/2002JC001372.

UNSCEAR (United Nations Scientific Committee on the Effects of Atomic Radiation). 2000. Sources and Effects of Ionizing Radiation. New York. https://www.unscear.org/docs/publications/2000/UNSCEAR_2000_GA-Report.pdf.

UNSCEAR. 2008. Sources and effects of ionizing radiation. New York: UNSCEAR. https://www.unscear.org/unscear/en/publications/2008_1.html.

Wada, T., Nemoto, Y., Shimamura, S., Fujita, T., Mizuno, T., Sohtome, T., Kamiyama, K., Morita, T. and Igarashi, S. 2013. Effects of the nuclear disaster on marine products in Fukushima. *Journal of Environmental Radioactivity* **124**: 246–254, https://doi.org/10.1016/j.jenvrad.2013.05.008.

Wada, T., Fujita, T., Nemoto, Y., Shimamura, S., Mizuno, T., Sohtome, T., Kamiyama, K., Narita, K., Watanabe, M., Hatta, N., Ogata, Y., Morita, T. and Igarashi, S. 2016. Effects of the nuclear disaster on marine products in Fukushima: An update after five years. *Journal of Environmental Radioactivity* **164**: 312–324, https://doi.org/10.1016/j.jenvrad.2016.06.028.

Wakeford, R. 2011. And now, Fukushima. *Journal of Radiological Protection* **31**: 167–176, doi:10.1088/0952-4746/31/2/E02.

Wallace, J.M. and Hobbs, P.V. 2006. 7 - Atmospheric dynamics, pp. 271–311 *in:* Atmospheric Science (Second Edition) *edited by* J.M. Wallace and P.V. Hobbs, Academic Press, San Diego, https://doi.org/10.1016/B978-0-12-732951-2.50012-0.

Wang, R. and Chen, X. 2005. The World Ocean Economic Squid Resources and Fisheries. China Ocean Press, Beijing.

Wang, C., Baumann, Z., Madigan, D.J. and Fisher, N.S. 2016. Contaminated marine sediments as a source of cesium radioisotopes for benthic fauna near Fukushima. *Environmental Science and Technology* **50**: 10,448–10,455, https://doi.org/10.1021/acs.est.6b02984.

Whitney, F.A., Freeland, H.J. and Robert, M. 2007. Persistently declining oxygen levels in the interior waters of the eastern subarctic Pacific. *Progress in Oceanography* **75**: 179–199, https://doi.org/10.1016/j.pocean.2007.08.007.

Xu, S., Freeman, S.P., Hou, X., Watanabe, A., Yamaguchi, K. and Zhang, L. 2013. Iodine isotopes in precipitation: temporal responses to ^{129}I emissions from the Fukushima nuclear accident. *Environmental Science and Technology* **47**: 10,851–10,859, https://doi.org/10.1021/es401527q.

Yagi, H., Sugimatsu, K., Kawamata, S., Nakayama, A. and Udagawa, T. 2015. Bottom turbidity, boundary layer dynamics, and associated transport of suspended particulate materials off the Fukushima coast, pp. 77–90 *in:* Impacts of the Fukushima Nuclear Accident on Fish and Fishing Grounds *edited by* K. Nakata and H. Sugisaki, Springer, Tokyo, https://doi.org/10.1007/978-4-431-55537-7_6.

Yankovich, T.L., Beresford, N.A., Wood, M.D., Aono, T., Andersson, P., Barnett, C.L., Bennett, P., Brown, J.E., Fesenko, S., Fesenko, J., Hosseini, A., Howard, B.J., Johansen, M.P., Phaneuf, M.M., Tagami, K., Takata, H., Twining, J.R. and Uchida, S. 2010. Whole-body to tissue concentration ratios for use in biota dose assessments for animals. *Radiation and Environmental Biophysics* **49**: 549–565, https://doi.org/10.1007/s00411-010-0323-z.

Yoshida, S., Macdonald, A.M., Jayne, S.R., Rypina, I.I., and Buesseler, K.O. 2015. Observed eastward progression of the Fukushima ^{134}Cs signal across the North Pacific. *Geophysical Research Letters* **42**: 7139–7147, https://doi.org/10.1002/2015GL065259.

Yu, W., He, J., Lin, W., Li, Y., Men, W., Wang, F. and Huang, J. 2015. Distribution and risk assessment of radionuclides released by Fukushima nuclear accident at the northwest Pacific. *Journal of Environmental Radioactivity* **142**: 54–61, https://doi.org/10.1016/j.jenvrad.2015.01.005.

Zhang, Y. and Baptista, A.M. 2008. SELFE: a semi-implicit Eulerian–Lagrangian finite-element model for cross-scale ocean circulation. *Ocean Modelling* **21**: 71–96, https://doi.org/10.1016/j.ocemod.2007.11.005.

Zhao, C., Wang, G., Qiao, F., Wang, G., Jung, K.-T. and Xia, C. 2015. A numerical investigation into the long-term behaviors of Fukushima-derived ^{137}Cs in the ocean. *Acta Oceanologica Sinica* **34**: 37–43, https://doi.org/10.1007/s13131-015-0775-8.

Zhao, C., Qiao, F., Wang, G., Xia, C. and Jung, K.T. 2016. Distribution of ^{137}Cs and ^{134}Cs from the Fukushima nuclear accident. Paper presented at the China-Korea Technical Meeting for nuclear safety held in Jinan on May 23, 2016.

Zheng, J., Tagami, K., Watanabe, Y., Uchida, S., Aono, T., Ishii, N., Yoshida, S., Kubota, Y., Fuma, S. and Ihara, S. 2012. Isotopic evidence of plutonium release into the environment from the Fukushima DNPP accident. *Scientific Reports* **2**: 304, https://doi.org/10.1038/srep00304.

Appendix 1

WG 30 Terms of Reference

WG 30 term: 2013–2016
Extended 1 year to 2017
Parent Committee: MEQ

1. Determine and compare radiological doses to North Pacific marine organisms, where data are available, from natural and anthropogenic radionuclides using existing data bases, newly acquired post-Fukushima monitoring results, and state of the art dosimetric approaches.
2. Examine the utility of applying natural and artificial (Fukushima and other sources) radionuclides as tracers of circulation, ecological transfers, biogeochemical cycling and consequences of climate change in the North Pacific, including the downstream interconnectivity, with establishing link to POC or WG 29, *etc*.
3. Determine the state of the science relative to assessment and mitigation of radiological impacts to marine organisms from natural and anthropogenic releases of radionuclides into the North Pacific marine environment, including a summary of peer reviewed literature and an overview of major sources and types of radiological releases into the marine environment.
4. Foster collaboration with other expert groups, especially physical oceanographers and climate modellers, to achieve the item 1–3 goals.
5. Identify priority research requirements for knowledge gap identified in items 1–3, the impacts on marine environment from the planned expansion of nuclear facilities, other emerging nuclear issues and other sources of radionuclides in the PICES region.
6. Promote collaboration in oceanographic studies using radio-tracer distribution and exchanging available information on environmental radioactivity, and encourage joint surveys/research among PICES member countries and international organizations.
7. Contribute to FUTURE by producing report on whether radioactive pollution is an additional stressor to marine ecosystem in North Pacific Ocean.

Appendix 2

WG 30 Membership

Canada

John N. Smith
Fisheries and Oceans Canada
Bedford Institute of Oceanography
1 Challenger Dr.
Dartmouth, NS, B2Y4A2
Canada
E-mail: John.Smith@dfo-mpo.gc.ca

Japan

Takami Morita
Fisheries Resources Institute, FRA
2-12-4 Fukuura, Kanazawa-ku
Yokohama, Kanagawa, 236-8648
Japan
E-mail: takam@affrc.go.jp

Tomowo Watanabe
Fisheries Resources Institute, FRA
2-12-4 Fukuura, Kanazawa-ku
Yokohama, Kanagawa, 236-8648
Japan
E-mail: wattom@affrc.go.jp

Tsuneo Ono (2013–2014)
National Research Institute for Fisheries Science, FRA
2-12-4 Fukuura, Kanazawa-ku
Yokohama, Kanagawa, 236-8648
Japan
E-mail: tono@fra.affrc.go.jp

People's Republic of China

Hongzhi Li
Department of Marine Measurement Sensor Technology
National Ocean Technology Center, SOA
219 Jieyuanxi Rd., Nankai District
Tianjin, 300112
People's Republic of China
E-mail: lihongzhi6535@126.com

Wu Men (2017)
Laboratory of Radiochemistry
Third Institute of Oceanography, SOA
178 Daxue Rd., Siming District
Xiamen, Fujian, 361005
People's Republic of China
E-mail: menwu@tio.org.cn

Wen Yu
Laboratory of Radiochemistry
Third Institute of Oceanography, SOA
184 Daxue Rd., Siming District
Xiamen, 361005
People's Republic of China
E-mail: yuwen@tio.org.cn

Yusheng Zhang
WG 30 Co-Chair
Department of Marine Biology and Ecology
Third Institute of Oceanography, SOA
178 Daxue Rd., Siming District
Xiamen, Fujian, 361005
People's Republic of China
E-mail: zhangyusheng@tio.org.cn

Republic of Korea

In-Seong Han (2014–2017)
Fishery and Ocean Information Division
National Institute if Fisheries Science, MOF
216 Haean-ro, Gijang-up, Gijang-gun
Busan, 619-705
Republic of Korea
E-mail: hisjamstec@korea.kr

Gi-Hoon Hong (2013)
Ocean Circulation and Climate Research Division
Korea Institute of Ocean Science and Technology
787 Haean-ro, Sangnok-gu
Ansan 426-744
Republic of Korea
E-mail: ghhong@kiost.ac

Kyung Tae Jung (2014–2017)
Marine Environmental Radioactivity Research Center
Korea Institute of Ocean Science and Technology
787 Haean-ro, Sangrok-gu
Ansan, 15627
Republic of Korea
E-mail: ktjung@kiost.ac.kr

Suk Hyun Kim
Marine Radionuclide Research Center
Korea Institute of Ocean Science and Technology
787 Haean-ro, Sangrok-gu
Ansan, Gyeonggi-do, 426-744
Republic of Korea
E-mail: shkim@kiost.ac

Young-Il Kim
East Sea Environment Research Division
Korea Institute of Ocean Science and Technology
48, Haeyangscience-gil, Jukbyeon-myeon
Uljin-gun, Gyeongsangbuk-do, 767-813
Republic of Korea
E-mail: yikim@kiost.ac

Russian Federation

Vladimir Goryachev
Laboratory of Nuclear Oceanology
V.I. Il'ichev Pacific Oceanological Institute
FEB RAS
43 Baltiyskaya St.
Vladivostok, Primorsky Kray 690041
Russia
E-mail: goryachev@poi.dvo.ru

United States of America

Kathryn A. Higley
WG 30 Co-Chair
Nuclear Engineering and Radiation Health Physics
Oregon State University
100 Radiation Center
Corvallis, OR, 97331-5902
USA
E-mail: kathryn.higley@oregonstate.edu

Appendix 3

Peer-reviewed Publications of WG 30 Members

[1] Ambe, D., Kaeriyama, H., Shigenobu, Y., Fujimoto, K., Ono, T., Sawada, H., Saito, H., Tanaka, M., Miki, S. and Setou, T. 2014. Five-minute resolved spatial distribution of radiocesium in sea sediment derived from the Fukushima Dai-ichi Nuclear Power Plant. *Journal of Environmental Radioactivity* **138**: 264–275, https://doi.org/10.1016/j.jenvrad.2014.09.007.

[2] Bezhenar, R., Jung, K.T., Maderich, V. and Kim, K.O. 2016. 3D numerical model of ecohydrodynamics for shallow waters. *Journal of Coastal Research* **75**: 820–824, https://doi.org/10.2112/SI75-165.1.

[3] Bezhenar, R., Jung, K.T., Maderich, V., Willemsen, S., de With, G. and Qiao, F. 2016. Transfer of radiocaesium from contaminated bottom sediments to marine organisms through benthic food chains in post-Fukushima and post-Chernobyl periods. *Biogeosciences* **13**: 3021–3034, https://doi.org/10.5194/bg-13-3021-2016.

[4] Buesseler, K., Dai, M., Aoyama, M., Benitez-Nelson, C., Charmasson, S., Higley, K., Maderich, V., Masqué, P., Morris, P.J., Oughton, D. and Smith, J.N. 2016. Fukushima Daiichi-derived radionuclides in the ocean: transport, fate, and impacts. *Annual Review of Marine Science* **9**: 173–203, https://doi.org/10.1146/annurev-marine-010816-060733.

[5] Fujimoto, K., Miki, S., Kaeriyama, H., Shigenobu, Y., Takagi, K., Ambe, D. and Morita, T. 2015. Use of otolith for detecting strontium-90 in fish from the harbor of Fukushima Dai-ichi Nuclear Power Plant. *Environmental Science and Technology* **49**: 7294–7301, https://doi.org/10.1021/es5051315.

[6] Kaeriyama, H., Ambe, D., Shimizu, Y., Fujimoto, K., Ono, T., Yonezaki, S. and Watanabe, T. 2013. Direct observation of ^{134}Cs and ^{137}Cs in surface seawater in the western and central North Pacific after the Fukushima Dai-ichi nuclear power plant accident. *Biogeosciences* **10**: 4287–4295, https://doi.org/10.5194/bg-10-4287-2013.

[7] Kaeriyama, H., Shimizu, Y., Ambe, D., Masujima, M., Shigenobu, Y., Fujimoto, K., Ono, T., Kou, N., Taneda, T. and Kurogi, H. 2014. Southwest intrusion of ^{134}Cs and ^{137}Cs derived from the Fukushima Dai-ichi Nuclear Power Plant accident in the western North Pacific. *Environmental Science and Technology* **48**: 3120–3127, https://doi.org/10.1021/es403686v.

[8] Kaeriyama, H., Fujimoto, K., Ambe, D., Shigenobu, Y., Ono, T., Tadokoro, K., Okazaki, Y., Kakehi, S., Ito, S., Narimatsu, Y., Nakata, K., Morita, T. and Watanabe, T. 2015. Fukushima-derived ^{134}Cs and ^{137}Cs in zooplankton and seawater samples collected off the Joban-Sanriku coast, in Sendai Bay, and the Oyashio region. *Fisheries Science* **81**: 139–153, https://doi.org/10.1007/s12562-014-0827-6.

[9] Kaeriyama, H., Shimizu, Y., Setou, T., Kumamoto, Y., Okazaki, M., Ambe, D. and Ono, T. 2016. Intrusion of Fukushima-derived radiocaesium into subsurface water due to formation of mode waters in the North Pacific. *Scientific Reports* **6**: 22010, https://doi.org/10.1038/srep22010.

[10] Kakehi, S., Kaeriyama, H., Ambe, D., Ono, T., Ito, S.I., Shimizu, Y. and Watanabe, T. 2016. Radioactive cesium dynamics derived from hydrographic observations in the Abukuma River Estuary, Japan. *Journal of Environmental Radioactivity* **153**: 1–9, https://doi.org/10.1016/j.jenvrad.2015.11.015.

[11] Kim, S.H., Hong, G.H., Lee, H.M. and Cho, B.E. 2017. ^{210}Po in the marine biota of Korean coastal waters and the effective dose from seafood consumption. *Journal of Environmental Radioactivity* **174**: 30–37, https://doi.org/10.1016/j.jenvrad.2016.11.001.

[12] Kim, S.H., Lee, H.M., Lee, S.H. and Kim, I. 2019. Distribution and accumulation of artificial radionuclides in marine products around Korean Peninsula. *Marine Pollution Bulletin* **146**: 521–531, https://doi.org/10.1016/j.marpolbul.2019.06.082.

[13] Kim, S.H., Lee, S.H., Lee, H.M. and Hong, G.H. 2020. Distribution of ^{239,240}Pu in marine products from the seas around the Korean Peninsula after the Fukushima nuclear power plant accident. *Journal of Environmental Radioactivity* **217**: 106191, https://doi.org/10.1016/j.jenvrad.2020.106191.

[14] Li, H., Wang, L., Fan, S., Zhang, J. and Li, C. 2015. Research on cosmic rays effect of X-γ dose rate measurements in water. *Nuclear Electronics and Detection Technology* **35**: 1014–1022.

[15] Lin, W., Chen, L., Yu, W., Ma, H., Zeng, Z., Lin, J. and Zeng, S. 2015. Radioactivity impacts of the Fukushima Nuclear Accident on the atmosphere. *Atmospheric Environment* **102**: 311–322, https://doi.org/10.1016/j.atmosenv.2014.11.047.

[16] Lin, W.H., Chen, L.Q., Yu, W., Ma, H., Zeng, Z. and Zeng, S. 2015. Radioactive source terms for the Fukushima nuclear accident. *Science China: Earth Sciences* **59**: 214–222, https://doi.org/10.1007/s11430-015-5112-8.

[17] Maderich, V., Bezhenar, R., Heling, R., With, G.D., Jung, K.T., Myoung, J.G., Cho, Y.K., Qiao, F. and Robertson L. 2014. Regional long-term model of radioactivity dispersion and fate in the Northwestern Pacific and adjacent seas: application to the Fukushima Dai-ichi accident. *Journal of Environmental Radioactivity* **131**: 4–18, https://doi.org/10.1016/j.jenvrad.2013.09.009.

[18] Maderich, V., Jung, K.T., Bezhenar, R., de With, G., Qiao, F., Casacuberta, N., Masque, P. and Kim, Y.H. 2014. Dispersion and fate of ^{90}Sr in the Northwestern Pacific and adjacent seas: global fallout and the Fukushima Dai-ichi accident. *Science of the Total Environment* **494**: 261–271, https://doi.org/10.1016/j.scitotenv.2014.06.136.

[19] Maderich, V., Jung, K.T., Brovchenko, I. and Kim, K.O. 2017. Migration of radioactivity in multi-fraction sediments. *Environmental Fluid Mechanics* **17**: 1207–1231, https://doi.org/10.1007/s10652-017-9545-9.

[20] Maderich, V., Bezhenar, R., Tateda, Y., Aoyama, M., Tsumune, D., Jung, K.T. and de With, G. 2018. The POSEIDON-R compartment model for the prediction of transport and fate of radionuclides in the marine environment. *MethodsX* **5**: 1251–1266, https://doi.org/10.1016/j.mex.2018.10.002.

[21] Men, W., Deng, F., He, J., Yu, W., Wang, F., Li, Y., Lin, F., Lin, J., Lin, L. and Zhang, Y. 2017. Radioactive impacts on nekton species in the Northwest Pacific and humans more than one year after the Fukushima nuclear accident. *Ecotoxicology and Environmental Safety* **144**: 601–610, https://doi.org/10.1016/j.ecoenv.2017.06.042.

[22] Miki, S., Fujimoto, K., Shigenobu, Y., Ambe, D., Kaeriyama, H., Takagi, K., Ono, T., Watanabe, T., Sugisaki, H. and Morita, T. 2016. Concentrations of ^{90}Sr and ^{137}Cs/^{90}Sr activity ratios in marine fishes after the Fukushima Dai-ichi Nuclear Power Plant accident. *Fisheries Oceanography* **26**: 221–223, https://doi.org/10.1111/fog.12182.

[23] Okamura, H., Ikeda, S., Morita, T. and Eguchi, S. 2016. Risk assessment of radioisotope contamination for aquatic living resources in and around Japan. *Proceedings of the National Academy of Sciences* **113**: 3838–3843, https://doi.org/10.1073/pnas.1519792113.

[24] Ono, T., Ambe, D., Kaeriyama, H., Shigenobu, Y., Fujimoto, K., Sogame, K. and Watanabe, T. 2015. Concentration of ^{134}Cs and ^{137}Cs bonded to the organic fraction of sediments offshore Fukushima, Japan. *Geochemical Journal* **49**: 219–227, https://doi.org/10.2343/geochemj.2.0351.

[25] Shigenobu, Y., Fujimoto, K., Ambe, D., Kaeriyama, H., Ono, T., Morinaga, K., Nakata, K., Morita, T. and Watanabe, T. 2014. Radiocesium contamination of greenlings (*Hexagrammos otakii*) off the coast of Fukushima. *Scientific Reports* **4**: 6851,https://doi.org/10.1038/srep06851.

[26] Shigenobu, Y., Ambe, D., Ono, T., Fujimoto, K., Morita, T., Ichikawa, T. and Watanabe, T. 2016. Radiocesium contamination of aquatic organisms in the estuary of the Abukuma River flowing through Fukushima. *Fisheries Oceanography* **26**: 208–220, https://doi.org/10.1111/fog.12209.

[27] Smith, J.N., Brown, R.M., Williams, W.J., Robert, M., Nelson, R. and Moran, S. 2015. Arrival of the Fukushima radioactivity plume in North American continental waters. *Proceedings of the National Academy of Sciences* **112**: 1310–1315, https://doi.org/10.1073/pnas.1412814112.

[28] Smith, J.N., Brown, R.M., Williams, W.J., Robert, M., Nelson, R., and Moran, S.B. 2015. Ocean current transport of Fukushima radioactivity to North America. CMOS Bulletin SCMO **43**(2): 51–57.

[29] Smith, J.N., Rossi, V., Buesseler, K.O., Cullen, J.T., Cornett, J., Nelson, R., Macdonald, A.M., Robert, M. and Kellogg, J. 2017. Recent transport history of Fukushima radioactivity in the Northeast Pacific Ocean. *Environmental Science and Technology* **51**: 10,494–10,502, https://doi.org/10.1021/acs.est.7b02712.

[30] Su, J., Yu, W., Zeng, Z., Ma, H., Chen, L. and Cheng, J. 2014. Monte Carlo calculation of artificial radionuclide radiation dose rates for marine species in the Western Pacific. *Radiation Protection Dosimetry* **158**: 479–486, https://doi.org/10.1093/rpd/nct264.

[31] Wada, T., Nemoto, Y., Shimamura, S., Fujita, T., Mizuno, T., Sohtome, T., Kamiyama, K., Morita, T. and Igarashi, S. 2016. Effects of the nuclear disaster on marine products in Fukushima: An update after five years. *Journal of Environmental Radioactivity* **164**: 312–324, https://doi.org/10.1016/j.jenvrad.2016.06.028.

[32] Yu, W., Johansen, M.P., He, J., Men, W. and Lin, L. (2018). Artificial radionuclides in neon flying squid from the northwestern Pacific in 2011 following the Fukushima. *Biogeosciences* **15**: 7235–7242, https://doi.org/10.5194/bg-15-7235-2018.

[33] Wada, T., Nemoto, Y., Shimamura, S., Fujita, T., Mizuno, T., Sohtome, T., Kamiyama, K., Morita, T. and Igarashi, S. 2013. Effects of the nuclear disaster on marine products in Fukushima. *Journal of Environmental Radioactivity* **124**: 246–254, https://doi.org/10.1016/j.jenvrad.2013.05.008.

[34] Zhang, J., Li, H. and Tuo, X. 2019. In-situ measurement of artificial nuclides in seabed sediments based on Monte Carlo simulations and an underwater HPGe detector. *Marine Technology Society Journal* **53**: 16–22, https://doi.org/10.4031/MTSJ.53.3.1.

[35] Zhao, C., Wang, G., Qiao, F., Wang, G., Jung, K.T. and Xia, C. 2015. A numerical investigation into the long-term behaviors of Fukushima-derived ^{137}Cs in the ocean. *Acta Oceanologica Sinica* **34**: 37–43, https://doi.org/10.1007/s13131-015-0775-8.

Appendix 4

Other Products of WG 30

North Pacific Marine Science Organization (PICES)

Working Group 30: Assessment of Marine Environmental Quality of Radiation around the North Pacific

Summary

On March 11, 2011, a large magnitude 9.1 earthquake struck off the Tohoku coast of Japan, triggering large tsunami waves which struck Japan's coast, causing loss of life and significant damage. The tsunami caused an accident at the Fukushima Dai-ichi Nuclear Power Plant (FDNPP), which released a large amount of radiation into the marine environment of the North Pacific Ocean.

In 2013, PICES formed an interdisciplinary Working Group on Assessment of Marine Environmental Quality of Radiation around the North Pacific (WG 30), to assess the impact of the 2011 Fukushima Dai-ichi Nuclear Power Plant (FDNPP) accident, by documenting and evaluating in real time the environmental changes associated with the accident. Recording impacts and consequences of a specific event as they occurred was unusual for a PICES working group, making the work of this group unique, and the WG meetings an important forum for timely exchange of new information among PICES member countries.

WG 30 focused on acquiring and sharing information from seasonal cruises undertaken by each North Pacific member country, thereby expediting the international dissemination of Fukushima monitoring data. Products of this working group include a final report, two major workshops, a PICES-SCOR invited collaborative review article and over 40 scientific publications in international peer-reviewed journals.

Primary accomplishments of WG 30 included the promotion of research through coordinated communications, exchange of sampling and analytical methodologies, laboratory visits and meetings, and publication of results. The principle thrust of the collaborative research was on radionuclide transport in the ocean, ocean-atmospheric exhange of radioactivity, radionuclide uptake in sediments and marine biota, and impacts on marine food webs and ecosystems.

Additionally, WG 30 tested and evaluated a range of modeling study types, including models for: radionuclide transport, fate, radiological dosing and risk assessment.

The evaluations were enhanced by the fact that the FDNPP accident represents the largest ever point-source discharge of radioactivity into the marine environment, which provided a strong input signal with far-field features particularly amenable to model validation for WG 30 experimental data.

As the 4-year lifetime of WG 30 approached, it was clear that its members had benefited from international cross-fertilization of ideas, data sharing, and cultural exhanges that were encouraged and supported under the auspices of PICES. The FDNPP accident is unlikely to be the Pacific Ocean's last nuclear incident with potentially deleterious impacts on marine ecosystems. Within the next decade, dozens of new nuclear power plants will begin operations in Asia. Furthermore, there are other possible sources and mechanisms for the discharge of large quantities of radioactivity into the marine environment. The research and products of WG 30 can serve to guide future monitoring and assessment programs for radioactivity.

Detailed information on WG 30 accomplishments is contained in the WG 30 final report, available at: https://meetings.pices.int/members/working-groups/disbanded/wg30.

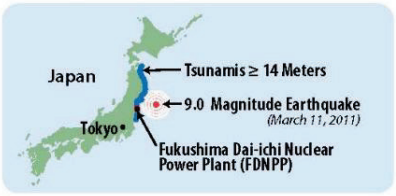

A four-page outreach brochure can be downloaded from:
https://meetings.pices.int/publications/other/members/WG-30-Brochure-2020.pdf

Appendix 5

Meeting Reports and Topic Session/Workshop Summaries from Past Annual Meetings Related to WG 30

PICES-2013
October 11–20, 2013, Nanaimo, Canada

Excerpted from:

Summary of Scientific Sessions and Workshops at PICES-2013

MEQ Paper Session

Co-Convenors: *Chuanlin Huo (China) and Darlene Smith (Canada)*

Other Co-Convenors, Elizabeth Logerwell (USA), Olga Lukyanova (Russia) and Lyman Thorsteinson (USA) were absent at PICES-2013.

Invited Speaker: *Stanley (Jeep) Rice (retired, NOAA)*

Background

The Marine Environmental Quality Committee (MEQ) has a wide range of interests spanning from traditional research areas to emerging marine environmental issues. Papers were invited on all aspects of marine environmental quality research in the North Pacific and its marginal seas, except those covered by MEQ-sponsored Topic Sessions. According to the adjusted Scientific Program and schedule, MEQ/FIS/FUTURE Topic Session (S7: Science needs for offshore oil and gas development in the North Pacific) was cancelled, and 4 submitted abstracts were moved to this MEQ Paper Session.

A total of 12 papers were approved and scheduled in this session before the Annual Meeting, in which 8 papers were about the assessment of marine radioactivity around the North Pacific (NP), 4 papers were about science needs for offshore oil and gas development in the NP. However, 2 presentations (Leslie Holland-Bartels and Lyman Thorsteinson: "*An evaluation of science needs to inform decisions on outer continental shelf energy development in the Chukchi and Beaufort seas, Alaska*"; Dee Williams: "*Monitoring effects related to offshore petroleum development in Coastal Alaska*") were cancelled, as the speakers were unable to attend the Annual Meeting due to the U.S. government partial shutdown.

Furthermore, since the Working Group on *Assessment of Marine Environmental Quality of Radiation around the North Pacific* (WG 30) was approved by the Governing Council and launched on August 1, 2013, scientists and potential WG 30 members from PICES member countries were encouraged to submit papers and to attend PICES-2013. Scientists from five PICES member countries attended this session and gave oral presentations relevant to radioactivity. The scientist from the Russia, who submitted an abstract, was not able to attend the Annual Meeting.

Summary of presentations

The MEQ Paper Session at PICES-2013 had good participation and was well attended, with a total of 8 oral presentations in a half-day. Oral presentations were given during the afternoon of October 15. Before the coffee break there was only one talk on the science needs for the oil development in the Arctic given by invited speaker (Dr. Stanley Rice, U.S., retired, NOAA). Since the other two speakers were not able to attend, Dr. Rice gave a detailed presentation followed by many questions from an appreciative audience.

The second half of the Paper Session consisted of 6 talks, all on the radioactivity, which covered a wide variety from methodology to the assessment of the radioactivity distribution in seawater, sediment and organisms. Two talks from the USA dealt with relating radiation dose to effect, and with bio-magnification of radiocesium in jellyfish. From China, one talk was on the characteristics of radionuclides in the sediment, and another talk was the combination of two papers, one on the measured distribution of seawater radioactivity, and one about the radioactivity of marine cephalopoda and fish species in the Northwest Pacific Ocean from/after the Fukushima Dai-ichi Nuclear Power Plant accident. Following these two talks was a presentation from a Japanese scientist on the estimation of river discharges and fluxes of suspended substances to the North Pacific after the Fukushima Dai-ichi nuclear power plant accident. The last presentation was from Dr. John N. Smith, Canada, on the detection of radioactivity from the 2011 Fukushima accident in the Eastern North Pacific and Arctic Oceans, which was another presentation relating Arctic Oceans. This, and Dr. Rice's presentation, stressed concern about the marine environment of the Arctic from different aspects of artificial activities, marine oil exploration and the emerging disaster.

The convenors acknowledged that the MEQ Paper Session was able to provide important opportunities for PICES scientists to present their studies not only on known areas, but on emerging marine environmental issues, and for early career scientists to participate in PICES activities. They also recognized that all the participants showed the interest and concern about the marine environmental impact of the Fukushima Dai-ichi Nuclear Power Plant accident.

List of papers

Oral presentations

Stanley D. Rice (Invited)
Oil development in the Arctic: What are the science needs?

Kathryn Higley, Elizabeth Ruedig, Emily Caffrey, Mario Gomez-Fernandez, Michelle Comolli and Delvan Neville
Relating radiation dose to effect: The importance of accurate dosimetry in assessing the impact of radioactivity on marine organisms

Jinqiu Du, Ziwei Yao, Hui Gao, Guangshui Na and Chuanlin Huo
Characteristics of radionuclides in sediment samples from coastal waters of Dalian Bay and Liaodong Bay

Delvan Neville, Kathryn Higley and Richard D. Brodeur
Radiocesium and jellyfish: Where's the biomagnification?

Wen Yu, Wu Men, Jianhua He, Yusheng Zhang and Tao Yu
Measured distribution of seawater radioactivity from Fukushima Daiichi Nuclear Power Plant in North Pacific

Jianhua He, Wen Yu, Wu Men, Tao Yu and Yusheng Zhang
Radioactivity of marine cephalopoda and fish species after 2011 Fukushima Dai-ichi Nuclear Power Plant accident in the Northwest Pacific

Shin-ichi Ito, Hiroshi Kutsukake, Kazuhiro Takeuchi, Hideki Kaeriyama, Masashi Kodama, Shigeho Kakehi, Kazuhiro Aoki, Hiroshi Kuroda, Hiroshi Yagi, Ambe Daisuke and Tsuneo Ono
Estimation of river discharges and fluxes of suspended substances to the North Pacific after the Fukushima Dai-ichi Nuclear Power Plant Accident

Vyacheslav Lobanov, Vladimir Goryachev, Aleksandr Sergeev, Dmitry Kaplunenko, Natalia Shlyk, Natalia Treshcheva, Sergei Prants and Maksim Budyansky
Fukushima 2011 derived radionuclides in the Japan and Okhotsk seas and subarctic front region of the Northwestern Pacific, one year later

John N. Smith, Robin Brown, Marie Robert, Bill Williams and Richard Nelson
Detection of radioactivity from the 2011 Fukushima accident in the Eastern North Pacific and Arctic Oceans

Annual Meeting Report (2013) of the Working Group on *Assessment of Marine Environmental Quality of Radiation around the North Pacific*

The first business meeting of Working Group (WG 30) on *Assessment of Marine Environmental Quality of Radiation around the North Pacific* (AMR) was held in Nanaimo, Canada, on October 13, 2013. Interim Chairman, Prof. Yusheng Zhang (zhangyusheng@tio.org.cn), welcomed 18 members and observers (*WG 30 Endnote 1*) and formally declared the first meeting of WG 30 was opened (at 18:00). The agenda (*WG 30 Endnote 2*) included an introduction to the establishment and objectives of WG 30 by Prof. Yusheng Zhang. Participants gave a brief overview of their activities. Discussion then moved to selecting co-chairmen and plans and schedule of future activities.

AGENDA ITEM 1
Establishment of WG 30

The Chairman noted that WG 30 was formally established on August 1, 2013, for a three-year term after being approved by Governing Council of PICES. The proposal to set up the WG was made by the People's Republic of China during the PICES-2012 in Hiroshima, Japan.

AGENDA ITEM 2
Working Group members

Prof. Yusheng Zhang noted that WG members from five member countries including Canada, China, Japan, Korea and the United States of America were present, as were observers from PICES secretariat and member countries. The Chair of WG 30's parent Committee (MEQ), Prof. Chuanlin Huo, was also in attendance.

AGENDA ITEM 3
Recommendation of Co-Chairs

The recommendation of co-chairs for the WG was discussed and Prof. Yusheng Zhang (China) and Prof. Kathryn A. Higley (USA, Kathryn.Higley@oregonstate.edu) were recommended by the WG members.

AGENDA ITEM 4
Review of Work Plan

WG members were invited to review the Work Plan through brief presentations given by each member country. After discussion, the members agreed to revise the Work Plan according to the Terms of Reference in the coming months.

AGENDA ITEM 5
Goals for the coming year

Members discussed several goals which needed to be met by WG 30 during the next year. They agreed that the next WG 30 business meeting should take place in advance of PICES-2014 in Yeosu, Korea. They also agreed that this WG meeting should be at least 1.5-day duration and occur at the location of the 2014 meeting. The purpose of the meeting will be for members to share data,

compile results, and begin preparation of draft reports required under the Work Plan. In addition, the WG members will revisit the Work Plan to assess compliance with goals of the Plan and the Terms of Reference. WG 30 members want to be given the opportunity to present data at the Annual Meeting. The Co-Chairs will remind members, several months before the meeting, of the need to submit abstracts for the 2014 meeting, most likely within the MEQ paper session. A decision whether or not to hold a workshop or topic session at PICES-2015 will be determined through correspondence between WG members prior to PICES-2014. Members agreed to establish a means to share data during the next year – through email or a web-based method. This will be determined in the next three months. Members also agreed to provide a description of their organization's research activities that relate to the Work Plan. This information will be shared between all WG members during the next year. Finally, WG 30 will discuss the Work Plan via email during the next 6 months and identify any issues or concerns that need to be addressed with the PICES Secretariat.

AGENDA ITEM 6
Actions requested of MEQ/Science Board

The Co-Chairs request support for a meeting of WG 30 at PICES-2014 of 1.5 days (total) to be scheduled right before the 2014 meeting (Friday/Saturday).

AGENDA ITEM 7
Closing remarks and announcements

The meeting was recessed at 18:30 on October 13, 2013, and reconvened at 18:00 on October 15, 2013. It was adjourned at 19:00 on October 15, 2013 by the Co-Chairs after announcements related to logistics of the next WG 30 meeting were made.

WG 30 Endnote 1

WG 30 participation list

Members

Kathryn A. Higley (USA, Co-Chairman)
Suk Hyun Kim (Korea)
John N. Smith (Canada)
Tomowo Watanabe (Japan)
Yusheng Zhang (China, Co-Chairman)

Observers

Keyseok Choe (PICES Secretariat)
Jinqiu Du (China)
In-Seong Han (Korea)
Chuanlin Huo (China, MEQ Chairman)
Dong-Woon Hwang (Korea)
Shigeru Itakura (Japan)
Peter J. Kershaw (UK)
Jung-No Kwon (Korea)
Wu Men (China)
Delvan Neville (USA)
Hiroyuki Shimada (Japan)
Atsushi Tsuda (Japan)
He Wu (China)

Participants of the first annual meeting of WG 30, at PICES-2013 in Nanaimo, Canada. Front row (left to right): Peter J. Kershaw, Tomowo Watanabe, Yusheng Zhang (Co-Chair), Kathryn A. Higley (Co-Chair), Suk Hyun Kim, John N. Smith; back row (left to right): In-Seong Han, Hiroyuki Shimada, Jinqiu Du, Wu Men, Delvan Neville.

WG 30 Endnote 2

WG 30 business meeting agenda of 2013

1. Establishment of WG 30
2. Adoption of Working Group members
3. Recommendation of Co-Chairs
4. Review of work plan
5. Goals for the coming year
6. Actions requested of MEQ/Science Board by WG 30
7. Closing remarks and announcements

PICES-2014
October 16–26, 2014, Yeosu, Korea

Excerpted from:

Summary of Scientific Sessions and Workshops at PICES-2014

BIO/MEQ Topic Session (S3)
Tipping points: defining reference points for ecological indicators of multiple stressors in coastal and marine ecosystem

Co-sponsored by the International Council for the Exploration of the Sea (ICES) and Integrated Marine Biogeochemistry and Ecosystem Research (IMBER)

Co-Convenors: *Rebecca G. Martone (USA), Ian Perry (Canada), Jameal Samhouri (USA), Motomitsu Takahashi (Japan), Maciej Tomczak (Poland / ICES), Chang Ik Zhang (Korea)*

Invited Speakers:
Phil Levin (NNOAA NW Fisheries Science Center, USA)

Tetsuo Yanagi (Research Institute for Applied Mechanics, Kyushu University, Japan)

Background

Many coastal and marine ecosystems, ranging from reefs to estuaries to pelagic systems, are exposed to multiple stressors, which can lead to rapid changes with significant, long-term consequences that are often difficult to reverse. Changes in ocean climate, the abundance of key species, nutrients, and other factors drive these shifts, which affect ocean food webs, habitats, and ecosystem functions and people's livelihoods and well-being. Determining indicators of ecological changes due to multiple stressors and defining reference points for those indicators are key steps for managers to avoid ecological degradation and loss of keys goods and services. Setting ecological reference points in ecological systems presents a challenge to resource managers because (a) reference points are often difficult to determine due to the complexity of natural systems, including the presence of thresholds, tipping points, and non-linearities; (b) the paucity of theoretical modeling and empirical understanding needed to address these complexities, identify ecological thresholds and develop early warning indicators means that managers must make decisions based on high levels of uncertainty; and, (c) many institutional and governance structures do not allow managers the necessary flexibility to take up this information and react within relevant timeframes. The aim of this session was to address these pressing challenges, and explore promising approaches to tackling them with the goal of catalyzing new research and management innovation. In particular, the convenors sought presentations that (i) define the conceptual basis for reference points and management objectives surrounding reference points; (ii) use theoretical, modeling and observational approaches to identify potential reference points for indicators of changes in marine ecosystems; (iii) incorporate risk and sources of error (measurement, model, process) in such analyses; (iv) discuss how reference points may be used in helping to manage marine ecosystems, specifically in relation to the decision-making process related to evaluating and deciding on acceptable levels of risk. Discussions were guided by the FUTURE science themes, with special attention to examining climate and anthropogenic drivers of ecological change, and identifying early warning indicators to enable forecasting to avoid crossing ecological thresholds. The outcomes are expected to contribute to the work of PICES Working Group 28 on *Development of Ecosystem Indicators to Characterize Ecosystem Responses to Multiple Stressors.*

Excerpted from:

Summary of presentations

Dr. Wen Yu presented on the effects of acute gamma radiation on the survival and physiological indices of the Chinese black sleeper. Existing studies from UNSCEAR (2008) indicate that fish are the most sensitive species based on LD50 reference points but few focus on data from marine fish and there are no data in China. By examining the Chinese black sleeper, Dr. Yu's study fills important gaps in our understanding of the response of marine species to radiation, particularly as it may be more susceptible to pollution and is economically important. Dr. Yu presented the results of a dose-response experiment that examined 5 irradiated groups and a control groups, with 60 individuals per group. Preliminary results indicate that with the 3 higher levels of irradiation, 100% mortality occurred within a few days, while the lowest level of radiation was similar to the controls. The calculated LD_{50} was 7.1 (6.3–7.9) Gy, which is lower than the 10–25 Gy summarized from UNSCEAR. Future research will include additional experiments to confirm these results, along with research on other local species and tests of the effects of chronic radiation.

Prof. Yusheng Zhang and colleagues described the fate and potential impacts from radionuclides in the NW Pacific following the Fukushima Dai-ichi Nuclear Power Plant (FDNPP) accident. Transfer of radionuclides can occur from water to fish through the food web and directly through contact with water. On a series of cruises beginning in June 2011, they collected tissue samples from 3 species, squid, saury, and dolphinfish. They used these samples to analyze radionuclide concentrations of ^{134}Cs, ^{137}Cs, and ^{110m}Ag, using the gamma spectrometry method. All radionuclides were detected in all 3 collected species of marine animals, including ^{134}Cs and ^{110m}Ag, which are important indicators of nuclear accident pollution. Squid showed higher concentrations than saury and dolphinfish, though radionuclide contents varied among tissue types. Prof. Zhang's research team also developed spatial maps of exposure, indicating where the nuclide samples were found and their magnitudes, and examined temporal patterns in radionuclide concentrations in tissues. Concentrations of most radionuclides in squid peaked in November 2011, and dropped precipitously, except for ^{90}Sr, which showed a very different temporal pattern. Radionuclide concentrations of dolphinfish also exhibited declines over time. Their results indicated that though radionuclide concentrations in marine animals increased following FDNPP accident, they were lower than the limit for seafood safety.

Dr. Hyeong-gi Kim presented work regarding thermal influence on nematodes, the most numerous metazoans worldwide and a potentially informative indicator group because of their abundance, occurrence in a wide range of habitats, habitat specificity, and a broad range of feeding types and generation times. Dr. Kim focused on the effects of thermal discharge from nuclear power plants on nematode communities in the southeastern coastal waters of Korea off Gori. The nematode community consisted of 6 dominant species, but a much larger number of species were extremely rare. Most nematodes were non-selective deposit feeders, and sediment type was a dominant factor determining nematode community composition. Interestingly, bottom temperature was not significantly correlated with the abundance of most nematodes.

Mr. Delvan Neville from Oregon State University discussed reference points in the context of radioecology. In this field, reference points are referred to as Derived Consideration Reference Level. Mr. Neville determined distribution of radionucleotides in the bodies of several Northern California Current marine species including *Thunnus aluluna* (albacore tuna). Concentrations were generally low, such that only a 10,000-fold increase in ^{137}Cs would exceed safe limits. Pink shrimp and several other species exhibited much larger responses than those seen in tuna.

List of papers

Oral presentations

Marine ecosystem regime shifts: Challenges and opportunities for Ecosystem-Based Management (Invited)
Phil Levin

Tipping points and decision-making: Why they matter, why they are hard, and practical things to do
Jake Rice

Embedding the science of tipping points into ocean management
Rebecca Martone, Carrie Kappel, Courtney Scarborough, Mary Hunsicker, Ben Halpern, Kimberly Selkoe, Phil Levin, Jameal F. Samhouri, Crow White, Ashley Erickson, Ryan Kelly, Lindley Mease, Margaret Caldwell, Larry Crowder and Rod Fujita

Ecological network indicators of ecosystem status and change in the Baltic Sea
Maciej T. Tomczak, Johanna J. Heymans, Johanna Yletyinen, Susa Niiranen, Saskia A. Otto and Thorsten Blenckner

Regional variations in ecosystem responses to anthropogenic activities and natural stressors in the Seto Inland Sea
Motomitsu Takahashi, Sachihiko Itoh, Naoki Yoshie and Kazuhiko Mochida

Potential early warning indicators of marine ecosystem changes in coastal British Columbia, Canada
R. Ian Perry

Seabird indicators and "tipping points" in North Pacific marine ecosystems
William J. Sydeman, Sarah Ann Thompson, Julie A. Thayer, Marisol Garcia-Reyes, Heather Renner, John F. Piatt, Stephanie Zador and Yutaka Watanuki

The effects of acute gamma irradiation on the survival and the physiological and biochemical indexes of Chinese black sleeper, *Bostrichthys sinensis*
Wen Yu, Tao Yu, Yusheng Zhang and Feng Lin

The combined effects of elevated CO_2 and temperature on the physiological condition of the olive flounder larvae *Paralichthys olivaceus*
Kyung-Su Kim, JeongHee Shim and Suam Kim

Eutrophication and oligotrophication processes in the Seto Inland Sea and their relationships to the Satoumi concept (Invited)
Tetsuo Yanagi

Diversity of perceptions and utility of marine ecosystem services
Kazumi Wakita, Zhonghua Shen, Taro Oishi, Nobuyuki Yagi, Hisashi Kurokura and Ken Furuya

Assessment of the magnitude and interrelationship of seasonal phytoplankton bloom occurrence at the Japanese scallop (*Mizuhopecten yessoensis*) farming area of Okhotsk Sea, Hokkaido, Japan
Christopher Mulanda Aura, Sei-Ichi Saitoh, Yang Liu and Toru Hirawake

Ordered re-assembly of marine ecosystems
Jameal F. Samhouri, Adrian C. Stier and Phil Levin

Potential reference points for mean trophic level of macrofauna in the Sea of Okhotsk
Konstantin M. Gorbatenko, Vladimir V. Kulik and Artem E. Lazshentsev

The bioconcentration of artificial radionuclides by marine animals after the Fukushima nuclear accident in the Northwest Pacific
Wu Men, Jianhua He, Wen Yu, Fenfen Wang, Wuhui Lin and Yusheng Zhang

Seasonal and spatial variations in nematode assemblages affected by thermal influence of a nuclear power plant in Korea (East Sea, Pacific Ocean)
Hyeong-gi Kim, Hyun soo Rho and Chul-woong Oh

Characterization of absorbed dose from natural and anthropogenic radionuclides for the purpose of establishing reference points within the marine environment
Delvan R. Neville and Kathryn A. Higley

MEQ Contributed Paper Session

Co-Convenors: *Chuanlin Huo (China), Darlene Smith (Canada)*

Background

Papers were invited on all aspects of marine environmental quality research in the North Pacific and its marginal seas, except those covered by Topic Sessions sponsored by the Marine Environmental Quality Committee (MEQ).

List of papers

Oral presentations

Arrival of Fukushima radioactivity in North American continental waters
John N. Smith, Robin M. Brown, Marie Robert, William J. Williams and Richard Nelson

Legacy POPs: Are they finally fading from marine food chains?
John E. Elliott, Aroha Miller, Kyle H. Elliott, Melanie F. Guigueno and Sandi Lee

POPs biotransport by Pacific salmon to the Russian coast of the Northwestern Pacific
Olga Lukyanova, Vasiliy Tsygankov, Margarita Boyarova and Nadezhda Khrisoforova

Comparison of oil exposure methods to filter feeding bivalve
Andrew Jin Yi Loh, Un Hyuk Yim, Sung Yong Ha, Joon Geon An and Won Joon Shim

Poster presentations

Assessment of marine environment quality in Peter the Great Bay (the Sea of Japan)
Tatyana A. Belan, Alexander V. Moshchenko, Boris M. Borisov, Tatiana S. Lishavskaya and Alexander V. Sevastianov

Marine environmental impacts of the Japanese nuclear power plant "Fukushima-1" accident in the Far Eastern seas
Eugene V. Karasev, Emiliya L. Chaikovskaya and Tatiana S. Lishavskaya

Toxic elements in seaweed *Undaria pinnatifida, Laminaria saccharina, Cystoseira barbata, Costaria costata* from the Peter the Great Bay (Japan Sea)
Lidia T. Kovekovdova, Denis P. Kiku and Irina S. Kasyanenko

Investigation of content of artificial radionuclides in the commercial crustacea in the North West part of the Japan Sea
Galina S. Borisenko and Yury G. Blinov

Monitoring of mercury in the Russian Far Eastern Seas
Mikhail V. Simokon and Irina S. Kasyanenko

Integrative assessment of sediment contamination by toxic organic contaminants in an enclosed bay in South Korea
Gi Myung Han, Sang Hee Hong, Won Joon Shim, Sung Yong Ha, Nam Sook Kim, Joon Geon An and Un Hyuk Yim

Effects of solvents on the photooxidation of phenanthrene and identification of its photoproducts
Ravi Shankar, Un Hyuk Yim, Song Yong Ha, Joon Geon An and Won Joon Shim

Summer variations in interleukin-1α-like substance levels in phagocytes of holothurian *Eupentacta fraudatrix* in Peter the Great Bay, Sea of Japan
Liudmila Dolmatova and Olga Ulanova

Annual Meeting Report (2014) of Working Group 30 on *Assessment of Marine Environmental Quality of Radiation around the North Pacific*

The Working Group on *Assessment of Marine Environmental Quality of Radiation around the North Pacific* (WG 30/WG-AMR) met on two days, from 9:00 to 18:00 h on October 16, 2014, and from 18:00 to 20:00 on October 17, in Yeosu, Korea. Co-Chairs Prof. Yusheng Zhang (China) and Prof. Kathryn A. Higley (USA) welcomed the members and observers and provided the opening address. Eighteen participants, including seven WG members from five member countries (except Russia) attended the meeting (*WG 30 Endnote 1*). The agenda for WG 30's second annual meeting was discussed and adopted without revision by the members (*WG 30 Endnote 2*).

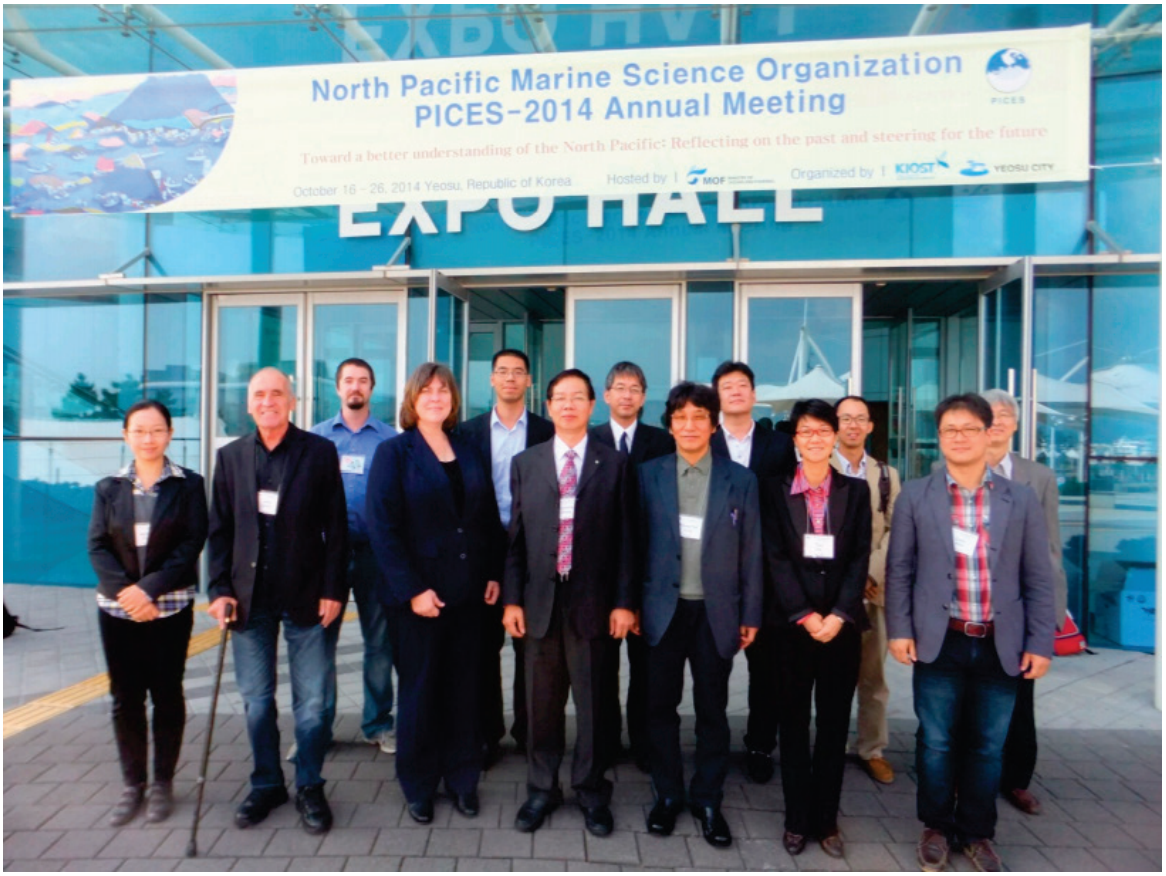

Participants of the WG 30 2014 annual meeting. First row from the left: Wen Yu, John N. Smith, Kathryn A. Higley (Co-Chair), Yusheng Zhang (Co-Chair), Kyung Tae Jung, Tao Yu, Daeji Kim; second row from the left: Delvan Neville, He Wu, Tomowo Watanabe, In-Seong Han, Jung Hyup Lee, Seokwon Choi.

AGENDA ITEM 2
Overview and update of WG 30

Professor Zhang provided an overview and update of the WG since its first meeting held during PICES-2013 (Nanaimo, Canada) and noted the changes in Korean membership, with Dr. In-Seong Han added as a new member, and Dr. Kyung Tae Jung added as a new member replacing Dr. Gi-Hoon Hong.

AGENDA ITEM 3
Country reports

Each member country of the WG 30 provided an overview of the research that they had conducted in the past year following the WG work plan.

Canada

Dr. John N. Smith gave an overview of the ongoing activities in Canada, particularly the ocean sampling efforts at Stations P26 and P4. He noted that they are seeing the arrival of the Fukushima plume along the west coast, and that this arrival is earlier than predicted by the Behrens model. He observed that the Rossi model, which overpredicted the surface concentration, has now been revised downward by a factor of 10, which now corresponds more closely with the measured data.

China

Dr. Wen Yu presented a small suggested change to the WG work plan, followed by monitored data from her institute (Third Institute of Oceanography, SOA) related to environmental concentrations of specific nuclides such as ^{134}Cs, ^{137}Cs, ^{90}Sr and ^{110m}Ag in seawater as well as in squids from the Northwest Pacific. Dr. Yu demonstrated a surprising difference in the internal organ concentrations in squid versus those in the muscle or the overall whole body concentration. Dr. Yu and colleagues have also successfully imaged a squid and have built a voxel model. She provided suggestions on the work plan of 2015 for the Working Group, including holding a workshop during PICES-2015.

Japan

Dr. Tomowo Watanabe provided an overview of the ongoing research at the National Research Institute of Fisheries Science, FRA. He discussed monitoring activities of marine environmental radioactivity; influences of FDNPP-derived radioactive nuclides on marine environment and marine products; and recent research in marine environmental radioactivity in Japan. Dr. Watanabe noted that data collected on ^{137}Cs in sediment has not shown substantial change in activity concentration since the time of the accident. He also stated that ongoing research has shown no correlation between activity in benthos and that of the marine sediment. However, he has observed that the 'excess ratio' (the ratio of detected activity >100 Bq/kg / <100 Bq/kg in fisheries samples) has been steadily decreasing post the FNNPP accident, and now represents <1% of fisheries samples.

Korea

Drs. Suk Hyun Kim and Kyung Tae Jung presented comments on the work plan – specifically items 1, 2, 5 and 7. They discussed new publications that revise the estimate of the FDNPP source term. They presented data from sampling of the edible portions of several marine fish, both those found domestically and those imported, and data from a physical model that showed a higher resolution regional dispersion of the Fukushima release, for modeled dates in April, May and June of 2011. They also showed a POSEIDON-R dynamic biota model as applied to the Pacific near China, Japan and Korea, which accurately predicted the observed biota concentrations far better than the BCF approach. They are also developing a benthic food web model.

United States

Professor Kathryn A. Higley provided an overview of the ongoing research in her laboratory at Oregon State University (OSU). OSU is continuing to develop voxel models for use in the assessment of radiation dose to biota. OSU has offered to share the models with the WG 30 members to foster collaborative research. OSU is also undertaking analysis to determine tissue densities and elemental concentrations for the models. Separate work is being done to determine the natural and anthropogenic radiation background for several marine species.

AGENDA ITEM 4
Work Plan

The components of the work plan were discussed by the members. The group reached consensus that broad goals should be maintained for the Working Group, and the plan would not be modified at this point.

The main goals of the WG in 2015 are to:
1. Write a technical paper on radionuclides in the marine environment in the North Pacific for submission to a journal (to be decided);
2. Hold a workshop on marine radioactivity at the PICES 2015 Annual Meeting;
3. Continue research by each member country in relevant sea areas following the work plan.

AGENDA ITEM 5
Data sharing

The members discussed the type of information and data that might be shared. The group requested PICES to establish a secure 'members only' section on the PICES website where WG 30 can post and share data such as papers, technical information and spreadsheets. The Secretariat has agreed to establish this site.

AGENDA ITEMS 6 AND 8
Workshop proposal for PICES-2015 and financial support

The WG 30 members discussed the content and format of a proposed ½-day workshop on "*Monitoring and assessment of environmental quality of radioactivity in the North Pacific*" [later revised to a 1-day workshop and renamed "*Monitoring and assessment of environmental radioactivity in the North Pacific*"] (*WG 30 Endnote 3*) to be held in conjunction with PICES-2015 (October 14–25, 2015, Qingdao, China). As part of this discussion, Dr. Smith provided an overview of the newly created working group associated with the Scientific Committee on Ocean Research. Working Group RiO5, led by Professors Ken Buessler and Minghan Dai, is very similar to the WG 30 mission. There was consensus that WG 30 should seek collaboration with the SCOR working group. It was suggested that one or two key members from SCOR be invited to the workshop.

a. Workshop objectives:
   i. To review the situation and to discuss the information gaps and deficiencies in monitoring and assessment of the Environmental Quality of Radioactivity and its impact on marine ecosystems in the North Pacific, especially since the FDNPP accident;
   ii. To exchange information on new techniques and methodologies for monitoring and assessment of the environmental quality of radioactivity, and to discuss development trends and research priorities.
b. The proposed workshop products:
   i. A white paper on information gaps and associated research needs;
   ii. A white paper that identifies promising new techniques and methodologies.
c. Budget for the workshop:
   The WG 30 will request $7.5 k be allocated for fund travel costs associated with three or four external participants.

AGENDA ITEM 7
Outline of WG 30 annual report

Participants compared WG 30 terms of reference and work plan with work accomplished to date and agreed this will form the basis of the Group's annual report.

WG 30 Endnote 1

WG 30 participation list

Members	Observers
In-Seong Han (Korea)	Robin Brown (Canada)
Kathryn A. Higley (USA, Co-Chair)	Seokwon Choi (Korea)
Kyung Tae Jung (Korea)	Daeji Kim (Korea)
John N. Smith (Canada)	Jung Hyup Lee (Korea)
Tomowo Watanabe (Japan)	Delvan Neville (USA)
Wen Yu (China)	He Wu (China)
Yusheng Zhang (China, Co-Chair)	Tao Yu (China)

WG 30 Endnote 2

WG 30 business meeting agenda of 2014

1. Adoption of the meeting agenda
2. Overview and update of the WG-AMR/WG 30
3. Country report representations
4. Discussion about work plan
5. Data sharing
6. Workshop proposal for the PICES 2015 Annual Meeting
7. Outline of WG 30 annual report
8. Financial support for the workshop

WG 30 Endnote 3

Proposal for a 1-day Workshop on
"*Monitoring and assessment of environmental radioactivity in the North Pacific*"
[revised and renamed from a ½-day Workshop on "*Monitoring and assessment of environmental quality of radioactivity in the North Pacific*"] at PICES-2015

Co-Convenors: Yusheng Zhang (China), Kathryn A. Higley (USA)

The Marine Environmental Quality Committee's area of responsibility is to promote and coordinate marine environmental quality and interdisciplinary research in the North Pacific. This workshop has three objectives: 1. To coordinate with external expert groups, 2. To review the situation and to discuss the information gaps and deficiencies in monitoring and assessment of the environmental quality of radioactivity and its impact on marine ecosystems in the North Pacific, especially since the FDNPP accident, and 3. To exchange information on new techniques and methodologies for monitoring and assessment of the environmental quality of radioactivity in the marine environment,

and to discuss development trends and research priorities. The main topics of the workshop include: 1. the current situation of environmental quality of radioactivity and its effects on marine ecosystems in the North Pacific, 2. new techniques for the analysis of radionuclides in the marine environment, and 3. assessment of the radiological risk to non-human species. The workshop will invite experts in relevant fields, and welcome reports on research and progress in the above topics with regard to the monitoring and assessment on the marine environmental quality of radioactivity in the North Pacific.

PICES-2015
October 15–25, 2015, Qingdao, China

Excerpted from:

Summary of Scientific Sessions and Workshops at PICES-2015

Workshop (W5)
Monitoring and assessment of environmental radioactivity in the North Pacific

Co-Sponsor: Scientific Committee on Oceanic Research (SCOR)

Co-Convenors: *Yusheng Zhang (China), Kathryn A. Higley (USA)*

Invited Speakers:
Michio Aoyama (SCOR RiO5 WG)
Minhan Dai (SCOR RiO5 WG)
Ronald Szymczak (Nuclear and Oceanographic Consultant of IAEA)

Background

The Marine Environmental Quality Committee's area of responsibility is to promote and coordinate marine environmental quality and interdisciplinary research in the North Pacific. This workshop has three objectives: 1) To coordinate with external expert groups, 2) To review the situation and to discuss the information gaps and deficiencies in monitoring and assessment of the environmental quality of radioactivity and its impact on marine ecosystems in the North Pacific, especially since the FDNPP accident, and 3) To exchange information on new techniques and methodologies for monitoring and assessment of the environmental quality of radioactivity in the marine environment, and to discuss development trends and research priorities. The main topics of the workshop include: 1) the current situation of environmental quality of radioactivity and its effects on marine ecosystems in the North Pacific, 2) new techniques for the analysis of radionuclides in the marine environment, and 3) assessment of the radiological risk to non-human species. The workshop will invite experts in relevant fields, and welcome reports on research and progress in the above topics with regard to the monitoring and assessment on the marine environmental quality of radioactivity in the North Pacific.

Summary of the workshop

The well attended 1½-day workshop, co-sponsored by SCOR, was held on October 15 and 16, 2015, in Qingdao, China, and was convened by Prof. Kathryn A. Higley (USA) and Prof. Yusheng Zhang (China). Seventeen talks were presented, including invited talks by Drs. Michio Aoyama and Minhan Dai (SCOR RiO5 WG) and Mr. Ronald Szymczak (IAEA consultant). Participant discussions centered around 1) information gaps in models and model validation with field data; 2) the technical challenges in monitoring/impact assessment, and possible solutions; 3) information gaps in seawater and biota data, and spatial and temporal change of radioactivity in the North Pacific. The outcome of the workshop was that the distribution of radionulicdes in the North Pacific was well studied, new techniques were being developed to aid in monitoring, and that little impact on the marine ecosystems is predicted, using simple models.

List of papers

Oral presentations

Asia/Pacific marine ecosystem impacts from the Fukushima Daiichi Nuclear Power Plant accident: A 2011-2015 overview (Invited)
Ronald Szymczak

^{134}Cs and ^{137}Cs in the North Pacific Ocean derived from the TEPCO Fukushima Dai-ichi Nuclear Power Plant accident, Japan in March 2011: Transport processes and estimation of ^{134}Cs and ^{137}Cs inventories (Invited)
Michio Aoyama

Sources and inventory of Cesium and Plutonium in China seas (Invited)
Junwen Wu and Minhan Dai

Development of a radionuclide transport model applicable to coastal regimes with multi-fractional cohesive and non-cohesive sediments
Kyung-Tae Jung, Igor Brovchenko, Vladimir Maderich, Kyeong Ok Kim and Fangli Qiao

Long-term transport and dispersion of ^{137}Cs released into ocean off Fukushima nuclear accident
Chang Zhao, Gang Wang, Fangli Qiao, Guansuo Wang, Changshui Xia and KyungTae Jung

Model developments to estimate movements of radioactive cesium with ocean sediment after the Fukushima Dai-ichi nuclear power plant accident
Shin-ichi Ito, Kazuhiro Aoki, Hiroshi Kuroda, Takashi Setou, Kazuhiro Takeuchi, Daisuke Hasegawa, Hideki Kaeriyama, Ambe Daisuke, Tsuneo Ono, Shigeho Kakehi, Hiroshi Yagi, Kouichi Sugimatsu and Akiyoshi Nakayama

Transport of the Fukushima radioactivity plume to the Eastern North Pacific Ocean
John N. Smith

Monitoring activity on radioactive cesium in seawater and sediment in the North Pacific by Fisheries Research Agency after the Fukushima Dai-ichi Nuclear Power Plant accident
Hideki Kaeriyama, Daisuke Ambe, Tsuneo Ono, Shigeho Kakehi and Tomowo Watanabe

Distribution and impact of radiocesium in the seawater of northwest Pacific in 2014
Wen Yu, Jianhua He, Wu Men, Tao Yu and Yusheng Zhang

The radioactive level of nekton species in the Northwest Pacific more than one year after Fukushima nuclear accident
Wu Men, Jianhua He, Fenfen Wang, Wen Yu, Yiliang Li and Yusheng Zhang

Temporal changes in the distribution of radiocesium contamination among ten dominant coastal fish species in Sendai Bay and the coastal area off Fukushima
Hiroyuki Togashi, Yukinori Nakane, Yuya Shigenobu and Yutaka Kurita

Radiocesium contamination histories of Japanese flounder *Paralichthys olivaceus* after the 2011 Fukushima Nuclear Power Plant accident
Yutaka Kurita, Hiroyuki Togashi, Yuya Shigenobu and Shin-ichi Ito

Challenges in calculating radiation dose to marine organisms
Kathryn A. Higley, Delvan Neville and Mario Gomez-Fernandez

Assessment on marine environmental impact from artificial radionuclides in the coastal waters of Liaodong Bay
Jinqiu Du, Hui Gao, Guangshui Na, Ziwei Yao and Chuanlin Huo

Use of otoliths to estimate the concentration of radioactive strontium
Ken Fujimoto, Shizuho Miki, Tomowo Watanabe and Takami Morita

A new device for precipitation and filtration of radiocesium in seawater
Jianhua He, Wu Men, Yiliang Li, Wen Yu, Tao Yu and Yusheng Zhang

Auto-system development and invention for measurement of ^{137}Cs/^{134}Cs in-situ
Zhenfang Dong, Hongqi Shi and Deyi Ma

Poster presentation

Radioactive status of seawater and assessment in the northeast South China Sea, the Luzon Strait and its adjacent area
Peng Zhou, Dongmei Li, Hongda Fang, Chuguang Huang, Haitao Li, Weixu Cai, Lingling Wu, Li Zhao, Feng Zhao, Yuanlai Zheng and Hongbiao Zhang

Monitoring of ^{134}Cs in surface sea water
Hongqi Shi, Zhenfang Dong, Jianwei Zhu and Yu Zhang

Temporal variations of ^{7}Be and ^{210}Pb activity in aerosols at Xiamen, China
Dekun Huang, Jianhua He and Tao Yu

Effects of external gamma irradiation on growth of *Phaeodactylum tricornutum*
Jianda Ji, Fulong Cai and Tao Yu

Radionuclide tracers suggest different migratory patterns in two groups of North Pacific albacore (*Thunnus alalunga*)
Jason Phillips, Owyn Snodgrass, Delvan Neville, Daniel Madigan, Lorenzo Ciannelli, Ric Brodeur, Kathryn Higley and William Pearcy

Assessment impact of radioactive contamination on the Pacific saury after the Fukushima Dai-ichi Nuclear Power Plant accident
Galina S. Borisenko, Victor N. Filatov, Yuriy G. Blinov, Yuriy V. Novikov and Nikita M. Blishchak

MEQ Contributed Paper Session

Co-Convenors: *Chuanlin Huo (China), Darlene Smith (Canada)*

Background

The Marine Environmental Quality Committee (MEQ) has a wide range of interests spanning from regular research area to emerging marine environmental issue. This session invited papers dealing with all aspects of marine environmental quality research in the North Pacific and its marginal seas, except those covered by Topic Sessions sponsored by the Marine Environmental Quality Committee (MEQ).

A total 7 papers were approved and scheduled in this session before the Annual Meeting. Three papers were about the assessment of marine radioactivity around the North Pacific, one paper was about microplastics on coastal beaches, one paper was about the hydrocarbon impact on marine ecosystems, and two papers were about the terrigenous organic carbon of Changjiang and Huanghe rivers.

Since MEQ's Working Group on *Assessment of Marine Environmental Quality of Radiation around the North Pacific* (WG 30) and Working Group on *Emerging Topics in Marine Pollution* (WG 31) had their own topic workshop and topic session, respectively, the MEQ-P Session had fewer contributed papers, which were accommodated in a ½-day session.

Summary of presentations

The MEQ Paper Session was well attended. Oral presentations were given during the morning of October 23. The first three talks were on the radioactivity which covered a wide variety from methodology to the assessment of the radioactivity distribution in seawater, sediment and organisms. The first talk (presented by Dr. Delvan Neville on behalf of Dr. Kathryn A. Higley (USA) was a summary of Workshop W5 on "*Monitoring and assessment of environmental radioactivity in the North Pacific*." Both were by early career scientists: Dr. Hongzhi Li (China) discussed radioactivity estimates in the North Pacific Ocean based on radiation dose rate; Dr. Shizuho Miki (Japan) presented on Strontium-90 in marine fishes (and received the Best Presentation award in an MEQ-sponsored session at the Closing Session); Dr. Qian Zhou (China) reported on microplastics on coastal beaches in China. Early career scientist, Dr. Sergey Kulbachnyi (Russia), reported on possible impacts on marine ecosystems in the Sea of Okhotsk due to hydrocarbon exploration on the shelf. The last two talks were from China: Dr. Yu Hao summarized the historical trends of terrigenous organic carbon transported by the Yangtze River (Changjiang), and early career scientist, Ms. Lijun Qi, described geochemical signals in the abandoned Huanghe River Delta surface sediments.

The convenors recognized that this regular session provided important opportunities for PICES scientists to present their studies not only on known areas, but also on emerging marine environmental issues, and for early career scientists to participate in PICES activities. The convenors also recognized that all the participants to the session showed the interest and concern about the marine ecosystem status of the North Pacific.

List of papers

Oral presentations

Summary of Workshop 5 on "Monitoring and assessment of environmental quality of radioactivity in the North Pacific"
Kathryn A. Higley
Presented by Delvan Neville on behalf of Kathryn A. Higley

Radioactivity estimates at North Pacific Ocean based on radiation dose rate
Hongzhi Li, He Wu, Jinzhao Zhang, Lei Wang and Chunfang Li

Strontium-90 in marine fishes
Shizuho Miki, Ken Fujimoto, Takami Morita, Yuya Shigenobu, Kaori Takagi, Tsuneo Ono, Tomowo Watanabe and Hiroya Sugisaki

Accumulation of microplastics on coastal beaches, China: Abundance, composition and sources
Qian Zhou, Haibo Zhang, Yuan Li and Yongming Luo

Hydrocarbon exploration on the Sea of Okhotsk shelf and its possible impact on marine ecosystems
Sergey E. Kulbachnyi

Historical trends of terrigenous organic carbon transported by the Yangtze River (Changjiang)
Yu Hao and Wu Ying

The geochemical signals in the abandoned Huanghe River Delta surface sediments
Lijun Qi, Ying Wu and Shenliang Chen

Poster presentations

Study of impact of moderate and heavy weathering processes on individual carbon and hydrogen isotope of n-alkanes in oils
Shijie He and Chuanyuan Wang

The role of temporary cysts in dense blooms caused by *Cochlodinium polykrikoides* Margalef
Hyeon Ho Shin, Zhun Li and Eun Song Kim

The occurrence and Distribution of HBCDs in Laizhou Bay of China
Ruijing Li, Guangshui Na, Hui Gao, Zihao Lu, Ziwei Yao and Chuanlin Huo

Responses of mesozooplankton communities to different anthropogenic activities in a subtropical eutrophic bay
Ping Du, Zhi B. Jiang, Yi B. Liao, Jiang N. Zeng, Xiao Q. Xu, Jing J. Liu, Xin Luo, Lu Shou, Quan Z. Chen and De M. Zhang

Estimation of carrying capacity by measuring coastal environmental parameters in Geoje-Hansan Bay, Korea
Dabin Lee, Jae Hyung Lee and Sang Heon Lee

Radiocesium transfer from contaminated sediment to benthic organisms and demersal fish
Yuya Shigenobu, Daisuke Ambe, Hideki Kaeriyama, Tsuneo Ono, Takami Morita, Shintaro Yamasaki Kousuke Yoshida and Seiichi Tomihara

Spatio-temporal variation of radiocesium in sea sediment on benthic marine ecosystem based on five-minute resolution mapping
Daisuke Ambe, Shigeho Kakehi, Toru Udagawa, Kazuhiro Aoki, Yuya Shigenobu, Tsuneo Ono, Takami Morita, Mikiko Tanaka, Ken Fujimoto, Hideki Kaeriyama and Shizuho Miki

Distribution of major and trace elements in surface sediments of the Gulf of Thailand
Pokin Channimitsri, Zhifei Liu and Penjai Sompongchaiyakul

Clay mineralogical records of sediment provenance change during the sea level rise of last deglaciation in the southern South China Sea
Thanakorn Jiwarungrueangkul, Zhifei Liu and Yulong Zhao

Geochemical records of provenance and East Asian monsoon evolution during the Late Quaternary in the western South China Sea
Sang Pham Nhu, Zhifei Liu and Yulong Zhao

Radioactive cesium in marine organisms around Japan
Takami Morita, Ken Fujimoto, Yuya Shigenobu, Daisuke Ambe, Hideki Kaeriyama, Shizuho Miki, Tsuneo Ono, Tomowo Watanabe and Hiroya Sugisaki

Resting cysts of potentially harmful dinoflagellates in Korean coastal area
Zhun Li, Eun Song Kim, Joo-Hwan Kim, Myung-Soo Han and Hyeon Ho Shin

Annual Meeting Report (2015) of Working Group 30 on *Assessment of Marine Environmental Quality of Radiation around the North Pacific*

The Working Group on *Assessment of Marine Environmental Quality of Radiation around the North Pacific* (WG 30/WG-AMR) gathered on October 16, 2015, from 14:00 to 18:00, in Qingdao, China. Co-Chairs Prof. Yusheng Zhang (China) and Prof. Kathryn A. Higley (USA) welcomed the members and observers and provided the opening address. Twenty-two participants, including seven WG members from five member countries (Canada, China, Japan, Korea and the USA) and three invited delegates from SCOR RiO5 WG and IAEA attended the meeting (*shown in the figure*). The work progresses related to the WG 30 work plan of each member country in the past year were presented. Next, the latest research results were discussed and summarized. And then the working focus of 2016 was discussed and drawn up. Finally, the related issues about the PICES 2016 Annual Meeting were discussed. With the joint efforts of all participants, the meeting achieved full success.

Participants of the WG 30 2015 annual meeting.

AGENDA ITEM 2
Overview and update of WG 30

Professor Zhang provided an overview and update of the WG 30 since its second meeting held during the PICES 2014 Annual Meeting (Yeosu, Korea) and noted the changes of that Dr. Tsuneo Ono as a new member of WG 30.

AGENDA ITEM 3
Country report presentations

Each member country of the WG 30 provided an overview of the research that they had conducted in the past year following the WG work plan. The following are the brief information about the country reports.

Canada

Dr. John N. Smith gave a presentation in which Fukushima inputs during 2012-2015 resulted in a factor of 5 increase in the fallout background for ^{137}Cs in seawater on Line P off the Canadian coastline. He concluded that this increase in seawater concentrations will likely result in an increment in ^{137}Cs throughout the various components of the ecosystem. Models predict that ^{137}Cs levels will continue to increase on the Canadian continental shelf for the next few years, before they level off at levels of ^{137}Cs between 5 and 10 Bq/m^3 and begin to decline in about 2017–2018. Despite the dramatic rise in ^{137}Cs concentrations, this will only return eastern North Pacific waters to fallout ^{137}Cs concentrations that prevailed in the 1980s. DFO monitoring on Line P is currently planned for missions in February and August 2016 in order to observe the continued increase and subsequent leveling off in the Fukushima signal which is expected to occur by 2017. The present results will be used to plan the frequency of future monitoring activities in 2017–2018. Currently, the DFO monitoring program for seawater is the only continuous monitoring program for Fukushima radioactivity in the Eastern North Pacific.

China

Dr. Jianhua He presented what China's WG members had done in 2015, including (1) Two marine radioactivity monitoring cruises in the Northwest Pacific; (2) Discussion on the transporting pathway of radioactive release from the Fukushima nuclear accident; (3) Radiological dose assessment for the nekton species in Northwest Pacific; (4) Effects of external gamma irradiation on growth of *Phaeodactylum tricornutum*.

Japan

Dr. Tomowo Watanabe provided an overview of the ongoing research by FRA in the past year, including monitoring activities for marine environmental radioactivity, status of the FDNPP accident to the marine environment in the area near the FDNPP and research in marine environmental radioactivity related to the FDNPP accident in Japan.

Korea

Dr. Kyung Tae Jung presented the marine radioactivity monitoring activities carried out in Korean waters. It has been found that there is a considerable amount of differences in the biological concentration factors between the values analyzed by KIOST and recommended by IAEA. Further investigation is obviously needed on this matter possibly through the cooperation, for example, between TIO (Third Institute of Oceanography), China and KIOST, Korea. Development of a marine biota model with the pelagic and benthic food webs is very much encouraging. The model might be an essential component of the decision supporting system for a future accident in the Northwestern Pacific region. Along with the biota model an advanced modeling system of predicting the marine radioactivity transport for the Yellow Sea and East China Sea are underway. It is expected that its more detailed results can be reported in 2016.

United States of America

Professor Kathryn A. Higley provided an overview of the ongoing research in her laboratory at Oregon State University (OSU). OSU continues to develop accurate 3D models for dosimetry calculations in biota. Work has also begun on the development of a 3D voxel model representing *Thunnus alalunga*, known in English as Albacore tuna. They also have conducted sampling of marine organisms along the USA West Coast, as well as water samples. In addition, they are engaged in a cell-level radiation damage simulation using Geant4 to better understand dose distribution as well as the bystander effect.

AGENDA ITEM 4
Work Plan

The components of the work plan were discussed by the WG 30 members. The group reached consensus that broad goals should be maintained for the Working Group, and the plan would not be modified at this point.

The work plan and main goals of the WG 30 in 2016 are to:
1. Write a technical paper on radionuclides in the marine environment in the North Pacific as a PICES publication. The outline of the paper should be finished by November 2015 and the first manuscript should be finished in 2016;
2. Hold a workshop on marine radioactivity at the PICES 2016 Annual Meeting during November 1–13, 2016, San Diego, USA;
3. Continue research by each member country in relevant areas following the work plan.

AGENDA ITEM 5
Workshop proposal for the PICES-2016 annual meeting and financial support

The WG 30 members discussed the content and format of a proposed ½-day workshop on "*Distribution and risk analysis of radionuclides in the North Pacific"* to be held in conjunction with the PICES 2016 Annual Meeting. It was suggested that two experts from SCOR, IAEA or ICRP would be invited to this workshop. WG 30 will request $5.0 k to be allocated for fund travel costs associated with the two external participants.

AGENDA ITEM 6
Discussion about applying for one year extension of WG 30

The members discussed the necessity of one-year extension of WG 30 and reached consensus that WG 30 should be prolonged to the end of 2017 and submit a relevant application during the PICES 2016 Annual Meeting.

AGENDA ITEM 7
Outline of WG 30 annual report

Participants compared the WG 30 terms of reference and work plan with the works accomplished to date and agreed this will form the basis of the group's annual report.

WG 30 Endnote 1

WG 30 participation list

Members	Observers
John N. Smith (Canada)	Robin Brown (PICES)
Wen Yu (China)	Jianhua He (China)
Yusheng Zhang (China, Co-Chair)	Wu Men (China)
Tomowo Watanabe (Japan)	Daeji Kim (Korea)
In-Seong Han (Korea)	Jung Hyup Lee (Korea)
Kyung Tae Jung (Korea)	Seokwon Choi (Korea)
Kathryn A. Higley (USA, Co-Chair)	Delvan Neville (USA)

WG 30 Endnote 2

WG 30 business meeting agenda of 2015

1. Revision and adoption of the draft meeting agenda
2. Overview and update of the WG-AMR/WG 30
3. Country report presentations
4. Discussion about work plan for 2016
5. Workshop proposal for the PICES 2016 Annual Meeting and financial support
6. Discussion about the application for the one-year extension of WG 30
7. Outline of WG 30 annual meeting report of 2015

PICES-2016
November 2–13, 2016, San Diego, USA

Excerpted from:

Summary of Scientific Sessions and Workshops at PICES-2016

MEQ Workshop (W10)
Distribution and risk analysis of radionuclides in the North Pacific

Co-Convenors: *Yusheng Zhang (China), Kathryn A. Higley (USA)*

Invited Speaker:
Núria Casacuberta (ETH Zürich, The Laboratory of Ion Beam Physics and Environmental Physics, Switzerland)

Background

The Fukushima Dai-ichi Nuclear Power Plant (FDNPP) accident resulted in a large pulse of radioactive contaminants being released into the North Pacific. While radiation is recognized as a potential stressor in environmental systems, this workshop considered the data collected to date to determine if the radionuclides released have had significant impacts on ecosystems within the North Pacific. Presentations included radionuclide transport and fate, and any observed impacts from the FDNPP radionuclides on the marine ecosystem in the North Pacific. Participants were also encouraged to exchange information on new techniques and methodologies for monitoring environmental radioactivity and assessing the effects of radionuclides. The workshop also discussed information gaps and research priorities in monitoring and assessment.

Summary of presentations

The session opened with a presentation by the invited speaker, Núria Casacuberta, on radionuclides distributions off the coast of Japan. Especially noteworthy was the analysis for ^{90}Sr, ^{129}I, ^{236}U and Pu isotopes, which are rarely reported due to the difficulty involved in separating and analyzing these radionuclides. At least two ^{90}Sr/^{137}Cs ratios were observed at different points in time (2011 *vs* 2013), suggesting the release pathway for ^{137}Cs detected in 2013 differed from 2011, or that they originated from separate sources. The following presentations by John N. Smith and Hideki Kaeriyama continued the theme of monitoring of seawater radionuclide levels. Smith's presentation highlighted the behavior of FDNPP-contaminated water on the eastern side of the North Pacific, including its affiliation with the so-called Warm Blob. Kaeriyama's presentation discussed both coastal areas along Japan, as well as the southward intrusion of FDNPP-contaminated water via central mode water.

The next two presentations by Takami Morita and Shizuho Miki discussed the concentrations of these radionuclides in biota. Morita's presentation discussed the ongoing monitoring of biota, showing that in recent years only a small fraction of sampled marine biota was found with substantial FDNPP contamination and the expectation that fish caught off of Fukushima prefecture are very close to being commercially viable. However, there was some uncertainty about interpreting these trends, as the number of species sampled has changed year by year and were not reported in an individual-species basis. The following presentation by Shizuho Miki specifically focused on ^{90}Sr levels in marine fish both away from Fukushima prefecture, near the prefecture as well as within the 20 km exclusion zone around FDNPP. No FDNPP influence was detectable on ^{90}Sr levels in fish collected away from the prefecture, while both fish collected near the prefecture

and those within the 20 km zone showed ^{90}Sr levels that were often above background but had no increasing trend over the last several years. One of the posters submitted for W10 also looked at concentrations in biota, specifically in *Thunnus alalonga*, and that there were significant differences in ^{134}Cs levels depending on how far north or south USA fishermen caught them.

Next came a pair of presentations on FDNPP radionuclides in marine sediment. The first, presented by Daisuke Ambe, found that the sediment inventory along the east coast of Japan was largely determined by the initial FDNPP release, over time being transported southward and downward into the sediment, with significant differences depending on particle size in the sediment. The second presentation, by early career scientist Jinqiu Du, looked at opportunistically using FDNPP ^{137}Cs (as well as signals from weapons testing and Chernobyl) as a measure of sedimentation rate. Although there were disagreeing figures on sedimentation rates from the methods, experienced members of the workshop offered to work with Du after the session to correct the estimates.

The final four presentations did not have sub-topics in common with each other. The first, by Jianhua He, demonstrated further testing of a potentially fast prototype for separation of ^{137}Cs from seawater using AMP. Early indications suggest the device and method can allow for ^{137}Cs seawater measurements in just a few hours at sea rather than hours to days spent in a land-based lab for the same separation. This was followed by a presentation by Kyung Tae Jung of a new iteration of the POSEIDON series of compartment models, titled Multi-BURN POSEIDON, which tracked separate bone, flesh and organ compartments for the fishes and sharks in the model which showed much better agreement with measurements. Finally, Wu Men presented a computer system for environmental grading of marine radioactivity, which had been used for marine radiation safety assessment in China.

List of papers

Oral presentations

Assessment of the distribution of radionuclides (^{137}Cs, ^{134}Cs, ^{90}Sr, ^{129}I, ^{236}U and Pu-isotopes) in the coast off Japan derived from the Fukushima Dai-ichi nuclear accident (Invited)
Núria Casacuberta, Pere Masqué, Maxi Castrillejo, Marcus Christl, Christof Vockenhuber, Hans-Arno Synal and Ken Buesseler

Transport of the Fukushima radioactivity plume to the Eastern North Pacific
John N. Smith

Five years monitoring activity on radioactive cesium in seawater after the Fukushima Dai-ichi Nuclear Power Plant accident
Hideki Kaeriyama, Daisuke Ambe, Yuya Shigenobu, Shizuho Miki, Tatami Morita, Hiroya Sugisaki, Manadu Shimizu and Tomoro Watanabe

Radioactive cesium in marine biota off Fukushima
Takami Morita, Ken Fujimoto, Yuya Shigenobu, Daisuke Ambe, Hideki Kaeriyama, Shizuho Miki, Tomowo Watanabe and Hiroya Sugisaki

Concentrations of strontium-90 in marine fishes after the Fukushima Dai-ichi Nuclear Power Plant accident
Shizuho Miki, Ken Fujimoto, Yuya Shigenobu, Daisuke Ambe, Hideki Kaeriyama, Kaori Takagi, Tsuneo Ono, Tomowo Watanabe, Hiroya Sugisaki and Takami Morita

Spatio-temporal variation of radiocesium in sea sediment around off Fukushima
Daisuke Ambe, Shigeho Kakehi, Toru Udagawa, Kazuhiro Aoki, Yuya Shigenobu, Tsuneo Ono, Hideki Kaeriyama, Ken Fujimoto, Shizuho Miki and Takami Morita

Distribution of radionuclides in sediment and sedimentation rates in Dalian Bay
Jinqiu Du, Ziwei Yao, Hui Gao, Daoming Guan, Guangshui Na and Chuanlin Huo

Effect of settle time on absorption of AMP to ^{137}Cs in co-precipitation method
Jianhua He, Fangfang Deng, Jing Lin, Wen Yu, Wu Men and Yusheng Zhang

Preliminary results from modeling of radionuclide transfer through marine food web using a multi-organ fish model
Kyung Tae Jung, Roman Bezhenar, Vladimir Maderich, Kyeong Ok Kim and Fangli Qiao

Marine radioactive environmental quality assessment method of China
Wu Men, Wen Yu, Jianhua He, Yusheng Zhang, Fenfen Wang and Yiliang Li

Nuclear bombs and coral: Guam coral core reveals operation-specific radiocarbon signals from the Pacific Proving Grounds
Allen H. Andrews, Ryuji Asami, Yasufumi Iryu, Don Kobayashi and Frank Camacho

Poster presentations

Effect of migratory life history on North Pacific Albacore (*Thunnus alalunga*) uptake of radiocesium
Delvan R. Neville, A. Jason Phillips and Kathryn A. Higley

Application of environmental risk assessment for strategic decision making in coastal areas: Case studies in China
Kankan Wu, Luoping Zhang, Jiwei Zhang and Jianwei Wu

Annual Meeting Report (2016) of Working Group 30 on *Assessment of Marine Environmental Quality of Radiation around the North Pacific*

The 2016 business meeting of Working Group on *Assessment of Marine Environmental Quality of Radiation around the North Pacific* (WG 30/WG-AMR) was held in San Diego, the USA, from 09:00 to 18:00 on November 4, 2016. Co-Chairs of the WG 30, Profs. Yusheng Zhang (China) and Kathryn A. Higley (USA) welcomed the members and observers and made the opening address. Eighteen participants, including seven WG members from five member countries (except Russia) attended the meeting (*WG 30 Endnote 1*). The agenda for the WG 30 2016 business meeting was discussed and adopted without revision by the WG members (*WG 30 Endnote 2*).

Participants of the WG 30 2016 annual meeting. Left photo, front row from the left: Wu Men, Suk Hyun Kim, Kathryn A. Higley (Co-Chair), Kyung Tae Jung, John N. Smith, Tomowo Watanabe, Yusheng Zhang (Co-Chair), Núria Casacuberta; back row from the left: Chuanlin Huo (MEQ Chair), Daisuke Ambe, Hideki Kaeriyama, Delvan Neville, Allen H. Andrews, Takami Morita, Shizuho Miki, Jung Hyup Lee, Jinqiu Du. Right photo, the participants at the WG 30 business meeting.

AGENDA ITEM 2
Overview and update of WG 30

After adopting the meeting agenda, Prof. Yusheng Zhang made a presentation on an overview and update of the WG since its third meeting held during the PICES 2015 Annual Meeting in Tsingdao, China to summarize the progress of the WG for the past year.

AGENDA ITEM 3
Country report presentations

Each member country of the WG 30 provided an overview of the research that they had conducted in the past year following the WG work plan. All of member country report summaries are listed in *WG 30 Endnote 3*.

AGENDA ITEM 4
Term extension of the WG 30

The members discussed about the life term of the WG 30 and agreed to prolong it one-year to the end of 2017 in order to collect more data on radioactivity to support the conclusions on the risk

assessment of the radionuclides from the FDNPP accident in the North Pacific for the final report of WG 30 and to complete the final report, one more scholar scientific paper and the brochure of WG 30.

AGENDA ITEM 5
Outline and assignment of the WG 30 final report and time schedule

A draft outline and assignment of the WG 30 Final Report provided by Co-Chair, Prof. Yusheng Zhang was discussed and revised in detail by the members. Moreover, the members discussed and formatted a time schedule to complete the outline of WG 30 final report (*WG 30 Endnote 4*).

AGENDA ITEM 6
Brochure of WG 30

The contents for the brochure of WG 30 were discussed during the meeting. The members preferred to produce a brochure introducing terms of references, on-going projects and major achievements obtained so far by the WG on monitoring and assessment of marine environmental quality of radiation around the North Pacific rather than a popular science booklet about radioactivity in (marine) environment. All of the member countries for the meeting agree to provide 2 achievement figures for the brochure before the end of November 2016.

AGENDA ITEM 7
Work Plan for 2017

The components for the work plan of WG 30 in 2017 were discussed during the meeting. The group reached consensus that the work plan and main goals of the WG in 2017 are to:

(1) Complete the WG 30 Final Report
(2) Compile a brochure of the WG 30
(3) Fulfil a new paper about lessons learned from Fukushima release as it applies to the next unplanned ocean release, etc.
(4) Collaborate with SCOR RiO5 in August 2017
(5) Hold a 2-day WG business meeting during the PICES 2017 Annual Meeting
(6) Encourage the member countries to make a proposal for further developing a new working group on radioactivity under parent committee MEQ.

WG 30 Endnote 1

WG 30 participation list

Members	Observers
Kathryn A. Higley (USA, Co-Chair)	Daisuke Ambe (Japan)
Kyung Tae Jung (Korea)	Allen H. Andrews (USA)
Suk Hyun Kim (Korea)	Núria Casacuberta (SCOR)
Takami Morita (Japan)	Jinqiu Du (China)
John N. Smith (Canada)	Jianhua He (China)
Tomowo Watanabe (Japan)	Chuanlin Huo (China, MEQ Chair)
Yusheng Zhang (China, Co-Chair)	Hideki Kaeriyama (Japan)
	Jung Hyup Lee (Korea)
	Wu Men (China)
	Shizuho Miki (Japan)
	Delvan Neville (USA)

WG 30 Endnote 2

WG 30 business meeting agenda of 2016

1. Revision and adoption of the meeting agenda
2. Overview and update of WG 30
3. Country report representations
4. Term extension of the WG 30
5. Outline and assignment of the WG 30 Final Report and time schedule
6. Brochure of the WG 30
7. Work plan for 2017

WG 30 Endnote 3

WG 30 member country report summaries

Canada

Report on Canadian Monitoring of Fukushima Radioactivity on Line P

John N. Smith
Bedford Institute of Oceanography, Fisheries and Oceans Canada, Dartmouth, N.S.,
Canada B2Y 4A2

1. Introduction

An earthquake-triggered tsunami on March 11, 2011 caused extensive damage to the nuclear power facilities in Fukushima, Japan resulting in the discharge of large quantities of ^{137}Cs and other radionuclides directly into the western North Pacific Ocean during the month following the accident (Figure 1). The radioactivity plume was immediately transported northeastward towards North America under the influence of the strong Kuroshio Current and was expected to approach the Canadian coastline within a few years. This plume of radioactivity becomes very much diluted by the time it arrives off the North American coastline, but the eventual magnitude of the signal is difficult to predict owing to uncertainties in the quantity of material initially discharged from Fukushima, the trajectory of the plume and the degree of mixing that will occur with uncontaminated water. Model projections for the eventual concentrations of radioactivity in Canadian continual shelf waters off Victoria, BC differ by as much as an order of magnitude, but the models do agree that some of the highest levels of radioactivity from Fukushima will be observed in Canadian waters.

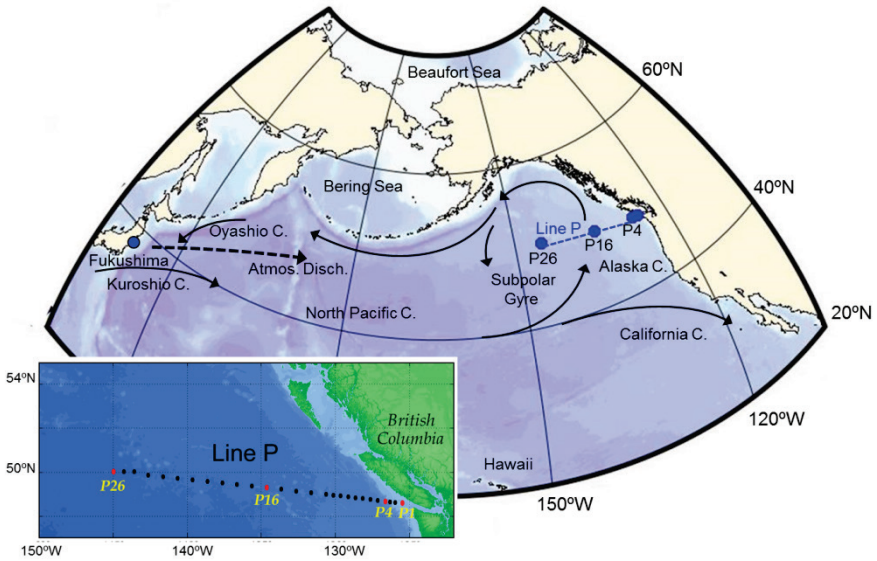

Fig. 1 Location of the site of the Fukushima Daiichi Nuclear Power Plant accident in Japan. Current (C.) systems transported direct oceanic discharges of Fukushima radioactivity eastward across the Pacific and then northward across Line P at the eastern edge of the subpolar gyre. Dashed line shows general northeastward direction for the transport of atmospheric discharges.

The Fukushima radioactivity can be identified by the presence of ^{134}Cs which has a half-life of about 2 y. Owing to its relatively short half-life (compared to that of 30 y for ^{137}Cs) virtually all of the ^{134}Cs from fallout from atmospheric nuclear weapons tests in the 1950s and 1960s has been eliminated by radioactive decay. As a result, the detection of any ^{134}Cs is a certain indicator of the presence of Fukushima radioactivity. Further, since the ratio of ^{134}Cs /^{137}Cs was about 1 for material discharged during the accident, then the contribution of Fukushima to the ^{137}Cs inventory in the ocean can be simply estimated from the measured ratios knowing the time between sample analysis and the accident, itself. This provides the fundamental rationale for a Fukushima monitoring program.

2. Monitoring program

The Fisheries and Oceans Canada (DFO) monitoring program for the sampling and analysis of seawater for the radio-isotopes, ^{134}Cs and ^{137}Cs, was initiated shortly after the accident in June, 2011. The purpose of this program was to: (1) evaluate the potential exposure of Canadian marine resources to Fukushima radioactivity and (2) determine the accuracy and future reliability of global circulation models in their predictions of radioactivity transport from Fukushima through the eastern North Pacific. Seven sampling operations were conducted in June of 2011, 2012 and 2013 and February and August of 2014, 2015 and 2016, respectively on the CCGS Tully on Line P, which extends westward from Victoria, BC (Fig. 1). Large volume water samples were collected at multiple water depths to a maximum of 1000 m at Sta. P4 on the Canadian continental shelf and at Sta. P26, approximately 1500 km offshore. Forty to sixty litres of seawater were collected at each sampling depth and the water was pumped through a cartridge containing KCFC resin which selectively adsorbs Cs ions from seawater. The resin cartridges were shipped to the radioanalytical laboratory at BIO where they were analysed on a liquid nitrogen cooled, Ge gamma ray detector for Cs isotopes.

3. Major achievements

The 2011 results reveal the presence of fallout ^{137}Cs at levels of less than 2 Bq/m^3 in seawater while levels of ^{134}Cs were below the detection limit. These data supplied an important baseline

against which subsequent measurements of Fukushima radioactivity can be evaluated. The 2012 results showed the presence of ^{134}Cs at Sta. P26, but not at Sta. P4 indicating that the Fukushima signal was approaching the Canadian continental shelf, but had not yet arrived by June, 2012. The 2013 results revealed the presence of ^{134}Cs in the upper 100 m along the entire length of Line P indicating that the Fukushima signal had fully arrived in Canadian waters. Levels of ^{137}Cs from Fukushima were estimated to be about 1 Bq/m^3 in June, 2013 which is equivalent to the previous background levels of ^{137}Cs from atmospheric fallout. These levels had increased to values of about 2-4 Bq/m^3 by February and August, 2014 and then to levels of 5-6 Bq/m^3 by February 2015 at Sta. P26 as a result of the arrival of the Fukushima plume. ^{137}Cs levels continued to increase at the inshore shelf station, Sta. P4 in 2015-16 to 4 Bq/m^3 and at Sta. 16 to 7 Bq/m^3 by February, 2016. However, the ^{137}Cs signal began to decline at the ocean interior Station, P26 and by February 2016 had returned to a value of 4 Bq/m^3. These levels of Fukushima ^{137}Cs are now equal to or higher than those in the western North Pacific with the exception of waters proximal to Fukushima itself. These results show that the main inventory of Fukushima radioactivity has shifted from the western to eastern North Pacific on a time scale of 4-5 years as predicted by ocean circulation models. The present levels of Fukushima ^{137}Cs off Canada are significant, but are still several orders of magnitude below those that would be considered to be a threat to the environment or human health.

4. Conclusions

The present monitoring results show that Fukushima inputs during 2012-2016 resulted in a factor of 5 increased in the fallout background for ^{137}Cs in seawater on Line P off the Canadian coastline. This increase in seawater concentrations would likely result in an increase in ^{137}Cs throughout the various components of the ecosystem. Models predict that ^{137}Cs levels will begin to level off on Line P in 2016 at concentrations of 5-7 Bq/m^3 and begin to decline in 2017-2018. Despite the dramatic rise in ^{137}Cs concentrations since 2013, this will only return eastern North Pacific waters to fallout ^{137}Cs concentrations that prevailed in the 1970s-1980s. DFO monitoring on Line P is currently planned for missions in February and August, 2017 in order to observe the continued increase and subsequent leveling off in the Fukushima signal. The present results will be used to plan the frequency of future monitoring activities in 2018-2019. Currently, the DFO monitoring program for seawater is the only continuous monitoring program for Fukushima radioactivity in the Eastern North Pacific.

China

Report from the People's Republic of China on Fukushima-derived Radioactivity Monitoring in the Northwest Pacific

Jianhua He, Wu Men, Wen Yu, Yusheng Zhang
Laboratory of Marine Isotopic Technology and Environmental Risk Assessment
Third Institute of Oceanography, State Oceanic Administration, 184 Daxue Road, Xiamen 361005
the People's Republic of China

1. Introduction

To better understand the distribution and impact of radionuclides released from the Fukushima nuclear accident (FNA), WG members of the People's Republic of China following the WG work plan have done the three major works since the PICES-2015 annual meeting: (1) Two cruises of marine radioactivity monitoring in the Northwest Pacific; (2) Study on the assessment method of marine radioactive environmental quality and the corresponding software development; (3) Radiological research on marine organisms in China.

2. Monitoring program

In order to understand the fate of radioactive contaminants after the Fukushima nuclear accident and to assess the relevant effect and radiological risk on the open ocean in the Northwest Pacific,

2 cruises were implemented by the Third Institute of Oceanography, State Oceanic Administration (SOA) of the People's Republic of China in September-October 2015 and May-June 2016, respectively. In these two cruises, more than 200 seawater samples were sampled at 80 stations, and squid samples were collected at some stations. The seawater and squid samples were analyzed for artificial radionuclides ^{134}Cs, ^{137}Cs, ^{90}Sr, ^{110m}Ag, *etc*.

3. Major achievements

3.1 Monitoring results of marine environment radioactivity in the Northwest Pacific

The radioactivity levels of artificial radionuclides (^{134}Cs, ^{137}Cs, ^{90}Sr, etc.) in seawater and marine biota samples were obtained.

3.2 Assessment method of marine radioactive environmental quality

Nowadays an increasing number of people has been concerned about the radioactive contamination, especially from the Fukushima nuclear accident. All countries owning nuclear power plants are making every possible effort to prevent the environment from radioactive contamination by drawing up effective management strategy. During a period of two years from 2010, Chinese marine scientists have researched an integrated approach to the scientific, managerial and societal issues surrounding the environmental effects of contaminants emitting ionizing radiation, with an emphasis on marine biota and ecosystems, which is similar to the ERICA of Europe and GRADED of the USA. ^{110m}Ag, ^{58}Co, ^{60}Co, ^{134}Cs, ^{137}Cs, ^{3}H, ^{131}I, ^{40}K, ^{54}Mn, ^{226}Ra, ^{90}Sr, ^{232}Th, ^{238}U and ^{65}Zn are chosen as assessing radionuclides. 13 types of marine organisms are selected as reference organisms. This method contains three assessment functions. The first function is the marine radioactive environmental quality grading, which includes 4 grades indicating safe to dangerous. The screening threshold between the first and the second grades is based on the corresponding radioactive background level. The screening threshold between the second and the third grades is based on the deduced safe activities of radionuclides for human beings. The screening threshold between the third and the fourth grades is based on the deduced safe activities of radionuclides for non-human organisms. The second function is radiation effect assessment of marine organism, which adopts ERICA ecosystem screening benchmark of 400 μGy/h. The third function is the risk of long-time discharge of low-level radioactive wastes. In order to simplify the related assessments, a software with the name of MREQAC has been drawn up. There are three models in the software and each of them corresponds to one function mentioned above, which are independent of each other and can be used simultaneously. The user just needs to start the software and input the corresponding parameters such as the activities of the environmental mediums, the software can output the assessment results and save them as excel documents automatically. It is powerful and easy for operation, which can meet the need of the marine radioactive environmental quality assessments.

3.3 Radiological research on marine organisms

The Laboratory of Marine Isotopic Technology and Environmental Risk Assessment, Third Institute of Oceanography, SOA, China, is also focusing on the radioecology and currently performing a study on the effects of acute external exposure on the growth of marine organisms, like marine medaka *Oryzias melastigma* and cultured shellfish abalone, *Haliotis diversicolor*, by an indoor culture system. In order to understand the half lethal dose of irradiation of marine organisms and its effect on growth and propagation, this study investigated the effects of acute radiation exposure of ^{137}Cs source of 1 Gy, 5 Gy, 10 Gy, 30 Gy, 60 Gy to the *O. melastigma* and of ^{60}Co source of 10 Gy, 30 Gy, 60 Gy, 150 Gy, 400 Gy to the economic shellfish abalone, respectively. The preliminary results showed that half lethal dose of abalone was 13.2 Gy under the ^{60}Co acute external irradiation and the feeding status of abalone in the high dose of γ irradiation was significantly reduced after a few days of incubation. For *O. melastigma*, its half lethal dose of ^{137}Cs irradiation was 26.5 Gy and the feeding status seemed to be not significantly different among diverse treatments.

4. Conclusions

In the past year, China has implemented two cruises of marine radioactivity monitoring in Northwest Pacific, set up an assessment method of marine radioactive environmental quality and the corresponding software and done some radio-ecological experiments on marine organisms. By the end of May-June 2016, ^{134}Cs still existed in the seawater of North Pacific; activities of ^{90}Sr and ^{137}Cs decreased into the range of background level. Radioactivity levels of ^{134}Cs and ^{110m}Ag were under detection limit in the marine biota samples. The software of marine radioactive environmental quality assessment developed by China has been proved to be powerful and easy for operation, which can meet the need of the marine radioactive environmental quality assessments. Radiological research on marine organisms has obtained some initial results in the past year.

Japan

Report on Japanese Research of Marine Radioactivity

Tomowo Watanabe and Takami Morita
Japan Fisheries Research and Education Agency, Yokohama, Japan

1. Introduction

After the Fukushima Dai-ichi Nuclear Power Plant (FDNPP) accident occurred in March 2011, detailed monitoring of radioactive materials is being continued in Japan. The monitoring is carried out mainly for radiocesium which is the most important nuclides in the FDNPP accident. The spatial and temporal changes of the contamination of the marine environment are described in detail by the monitoring data. We can also get lots of information about the behaviors of radiocesium in the marine environment by analysing the monitoring data. We briefly report the situation of radioactivity contamination of the marine environment in the waters of east Japan and the progress of the studies on environmental radioactivity in Japan.

2. Monitoring activities for marine environmental radioactivity

Many radioactivity monitoring projects related to the FDNPP accident are being conducted under the coordination of the Nuclear Regulation Authority (NRA) and Japan Fisheries Agency (JFA). Intensive radioactivity research activities for sea water, sea sediment and marine organisms in the waters off Fukushima Prefecture and the neighboring regions are being continued. Lots of data obtained by these research activities are published in semi-real time via the internet. Most of the data for the environmental radioactivity are available from the NRA's web site, http://radioactivity.nsr.go.jp/en/index.html. Radioactivity data for marine organisms are also published on the JFA's web site, http://www.jfa.maff.go.jp/e/inspection/index.html. The data set for the marine organisms included more than 84,200 inspection results by the end of October, 2016. Basic long-term radioactivity monitoring for environmental and dietary materials in Japan is also maintained by NRA. The data reports of the long-term radioactivity monitoring are available from the NRA operated English web site, http://www.kankyo-hoshano.go.jp/en/index.html. The database includes monitoring data in the fifteen areas around Nuclear Power Plants in Japan.

3. Status of FDNPP accident to marine environment in the area near FDNPP

The status of radioactive materials in the fisheries products off the coast of Fukushima Prefecture and the neighboring regions leaked by the FDNPP accident were summarized in the report "Report on the Monitoring of Radionuclides in Fishery Products" which was published by JFA on the web site, http://www.jfa.maff.go.jp/e/inspection/index.html. High radiocesium concentration of more than $1x10^4$ Bq/kg was detected temporarily in sea water of the surrounding waters of FDNPP in early April of 2011, then the radiocesium concentration decreased quickly after the direct leakage of highly contaminated water stopped. Although the level of radiocesium concentrations in sea water is slightly high in comparison with the level in the period before the accident, the decreasing trend is observed clearly. The level of radiocesium concentrations in sediment of the surrounding waters of

FDNPP is in the range of 10 to several thousand Bq/kg in a dry state and that are still higher than those before the accident. Although the changing trends of the radiocesium concentration of sediment are different among sites, slow decreasing trends are observed at most of the monitoring sites. The inspection results of radiocesium concentrations for the pelagic fishes show the rapid decrease in 2011 and most of the results have been included in the range below 25 Bq/kg-wet after 2012 and in the range below 10 Bq/kg-wet in 2016. As for the demersal fishes, slow but steady decreasing trends of the radiocesium concentration are observed. In the period after April of 2015, the inspection results exceeding the Japanese limit, 100 Bq/kg-wet, have not been detected in marine organisms and over 99% of inspection results for demersal fish is below 25 B/kg-wet in 2016.

4. Research in marine environmental radioactivity related to FDNPP accident in Japan

The statuses of radioactive materials leaked by FDNPP accident to marine environment have been investigated at many institutes. The modelling and simulation studies of the transport of radiocesium in the ocean have been performed at CRIEPI (Central Research Institute of Electric Power Industry), JAEA (Japan Atomic Energy Agency). Tsumune et al. (2012, 2013) and Kawamura et al. (2014) investigated the transport process of radiocesium in the North Pacific by using a general circulation model and Tsumune et al. (2013) estimated the total amount of leaked radiocesium from the results of simulation. The survey data of radiocesium concentration in the marine environment (sea water, sea sediment) have been analyzed by IER (Institute of Environmental Radioactivity, Fukushima Univ.), JAMSTEC (Japan Agency for Marine-Earth Science and Technology), JAEA, MERI (Marine Ecology Research Institute) and FRA (cf. Kaeriyama 2016). Kumamoto et al. (2014) and Kaeriyama et al. (2014, 2016) detected the southward transport of radiocesium by the North Pacific Subtropical Mode Water. Aoyama et al. (2015) showed the pathways of radiocesium in the upper layer of the North Pacific Ocean. Ambe et al. (2014) showed the detailed map of radiocesium concentration in the sea sediment off the coast of Fukushima Prefecture and adjacent area. Ono et al. (2015) investigated the radiocesium bonded to the organic fraction of sediments. Kakehi et al. (2016) described the rapid diffusion process of radiocesium contained in river water at the river mouth. The radiocesium monitoring data for marine organisms have been investigated by Fukushima Prefectural Fisheries Experimental Station (FPFES) and FRA. Wada et al. (2013), Sohtome et al. (2014) and Kaeriyama et al. (2015) showed the decreasing trends of the radiocesium concentration in fisheries products, benthic organisms and zooplankton, respectively. Wada et al. (2016) analyzed the radiocesium concentration data of marine organisms off Fukushima for the period 2011–2015 and showed the improving progress of radiocesium contamination. Shigenobu et al. (2014) performed the statistical evaluation of the extraordinarily-high value of radiocesium concentration of the fat greenling caught in the summer of 2012 and they revealed that it was an extremely rare case. Recently, the detailed statistical evaluations of monitoring data have done by Okamura et al. (2016). Fujimoto et al. (2015) analyzed the radioactivity of the otoliths of the fishes which were caught in the port of FDNPP. Tateda et al. (2013) and Tateda et al. (2015) investigated the contamination process of marine organisms off Fukushima Prefecture by using bio-kinetic models. Miki et al. (2016) summarized the results of strontium-90 measurements about marine fishes after the accident and confirmed that the strontium-90 contamination of marine fishes has remained in lower level compared to radiocesium.

5. Dissemination of accurate knowledge about radioactivity contamination

The mitigation of the damages caused by non-scientific reputation about radioactivity contamination is recognized as an important issue for society. Risk-communications concerning marine food safety related to radioactivity with the public are being conducted by JFA, Fukushima Prefectural government, etc. As one of these activities, FRA published the pamphlet explaining the basic knowledge and status of the contamination in easy words for the public (https://www.fra.affrc.go.jp/bulletin/radioactivity_pamphlet2015/cover_index.html, in Japanese). FPFES and FRA present the monitoring and research results about radioactivity contamination in

the waters off Fukushima Prefecture at the meetings of the Fukushima Prefectural Federation of Fisheries Co-operative Association every month to help fishermen's consideration about the restart of the fishery.

References

Aoyama et al. (2015), J. Oceanogr., doi:10.1007/s10872-015-0335-z
Ambe et al. (2014), J. Environ. Rad., 138, 264-275
Fujimoto et al. (2015), Environ. Sci. Technol., 49, 7294–7301
FRA (2015), Nakata K., Sugisaki H. (eds.),
http://link.springer.com/book/10.1007%2F978-4-431-55537-7, Springer Japan, Tokyo
Kaeriyama (2016), Fish. Oceanogr., doi:10.1111/fog.12177
Kaeriyama et al. (2014), Environ. Sci. Technol., 48, 3120-3127
Kaeriyama et al. (2015), Fish. Sci., 81, 139 – 153
Kaeriyama et al. (2016), Sci. Rep., doi:10.1038/srep22010
Kakehi et al. (2016), J. Environ. Rad., 153,1-9
Kawamura et al. (2014), J. Environ. Rad., 136, 64-75
Kumamoto et al. (2014), Scientific Reports, 4, Article number: 4276
Miki et al. (2016), Fish. Oceanogr. doi:10.111/fog.12182
Ono et al. (2015), Geochemical Journal, 49, 219-227
Okamura et al. (2016), PNAS, 113, 3838–3843
Shigenobu et al. (2014), Scientific Reports, 4, Article number: 6851
Sohtome et al. (2014), J. Environ. Rad. 138, 106-115.
Tateda et al. (2013), J. Environ. Rad., 124, 1-12.
Tateda et al. (2015), J. Environ. Rad., 147, 130-141.
Tsumune et al. (2012), J. Environ. Radioact., 111, 100-108.
Tsumune et al. (2013), Biogeosciences, 10, 5601-5617
Wada et al. (2013), J. Environ. Rad., 124, 246-254

Korea

Report of the Republic of Korea for 2016 marine radioactivity-related activities

Kyung Tae JUNG[1], Suk Hyun KIM[1], Kyeong Ok KIM[1] and In Seong HAN[2]
[1]Korea Institute of Ocean Science and Technology, Ansan, Gyeonggi-do, the Republic of Korea
[2]KoreaNational Institute of Fisheries Science, Busan, the Republic of Korea

1. Introduction

Marine radioactivity-related activities in the Republic of Korea include monitoring in Korean waters and modeling. Monitoring of radionuclides has continued in a regular basis since 1994. In detail, Korea Institute of Nuclear Safety (KINS) and National Institute of Fisheries Science (NIFS), formerly National Fisheries Development Research Institute (NFDRI), have carried out a Marine Environmental Radioactivity Survey (MERS) in the off coast Korea sea regions based on the Korean Atomic Safety Law 105 through their collaboration. Since the 2011 Fukushima nuclear accident, enhanced monitoring activities have been carried out. Prior to 2011 the sampling of MERS had been done biannually, but the survey frequency and area were extended after the Fukushima accident. KIOST (Korea Institute of Ocean Science and Technology) was limitedly involved in monitoring the distribution of artificial radionuclides in the seawater of the Northwestern Pacific Ocean over the period of 2012 to 2014. From 2011 KIOST has carried out researches on biological concentration factors for the major marine organisms in Korean waters.

In addition to the monitoring activities, considerable modeling works have been made in the Republic of Korea. In 2015 KIOST has focused on the development of the Northwestern Pacific marine biota model which takes into account both the pelagic and benthic food webs. Further extension of the model was made in 2016. A brief summary of modeling activities is described in this report along with monitoring activities.

2. Marine radioactivity-related research activities

2.1 Monitoring-related activities

After the Fukushima accident, regular samplings were carried out seasonally at a total of 32 stations, and monthly or bimonthly samplings were carried out at 6 stations.

KINS analyzed long-term variation in major radionuclides (^{137}Cs, ^{3}H, $^{239+240}$Pu and ^{90}Sr) in Korean waters over the period of 1994 to 2015. There are fluctuations in the concentration values but overall decreasing tendency is evidently shown (Figure. 1). It is noted that ^{3}H has values significantly higher than the other three radionuclides.

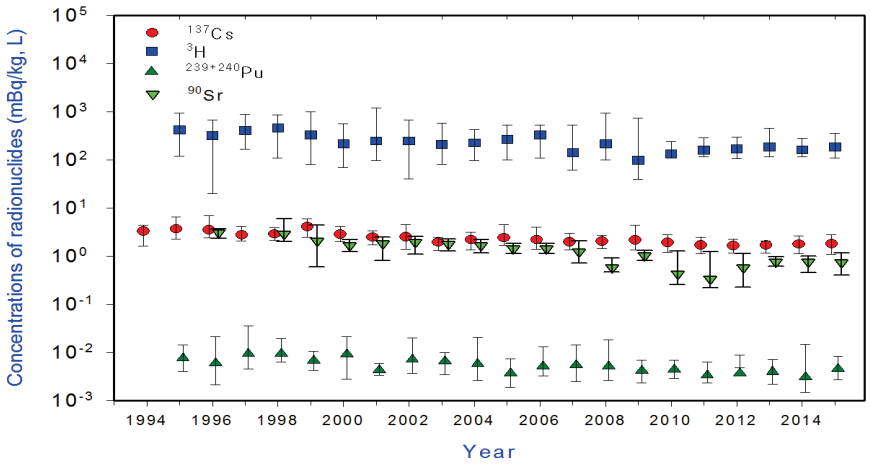

Fig. 1 Long-term variation in radionuclides (^{137}Cs, ^{3}H, $^{239+240}$Pu and ^{90}Sr) in Korean waters.

Over the period of 2015 to 2016 the Marine Radionuclide Research Group of KIOST has collected samples of major marine organisms caught from the sea regions around the Korean Peninsula shown in Fig. 2 to understand the distributions of radionuclides in biota. Lab experiments have been carried out to investigate the concentration factors for individual marine organisms. Estimated values for ^{137}Cs and $^{239+240}$Pu are shown in Fig. 3.

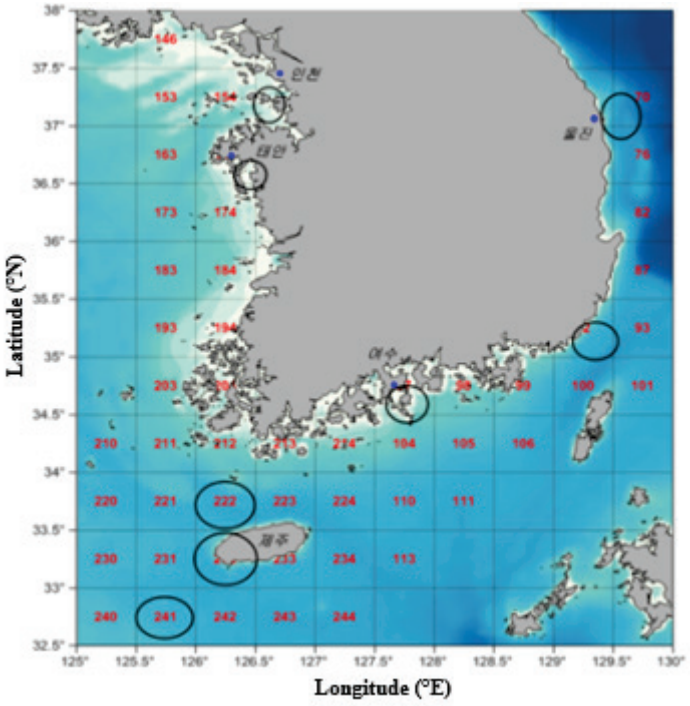

Fig. 2 Locations where samples of marine organisms were collected by KIOST over 2015 to 2016 for the estimation of biological concentration factors

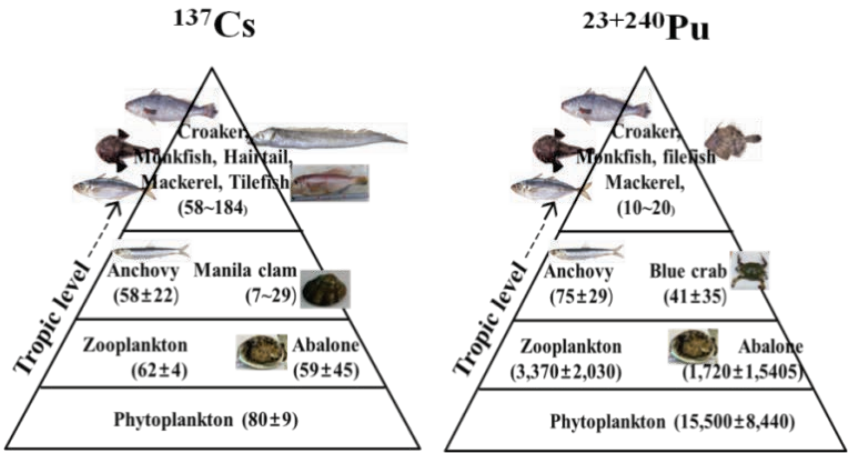

Fig. 3 Change in concentration factors of ^{137}Cs and $^{239+240}$Pu according to trophic levels estimated from laboratory experiments

2.2 Modeling-related activities

Most of marine radioactivity modeling activities in the Republic of Korea have been carried out through the cooperation among China, Korea and Ukraine. Since Dec 2011 KIOST has been carrying out a joint research with FIO (First Institute of Oceanography) of China for the development of marine radioactivity transport and fate models. The first stage cooperative research was finished at the end of 2014 and the 2nd stage cooperation started from Dec 2014. The cooperative research includes the cooperation in modeling of circulation, waves, suspended sediment and radioactivity transport. Regarding the Fukushima radioactivity problem, FIO/KIOST developed a global model to predict the long-term dispersion of radionuclides released from Fukushima Dai-ichi Nuclear Power Plant accident. In 2015 and 2016 the transport of radionuclides

^{137}Cs and ^{134}Cs was simulated with an additional consideration of Northern Pacific-scale atmospheric input along with the previously considered direct release to the ocean. Fig. 4 shows part of the simulated results in comparison with Canadian observations in sea regions of the Northeastern Pacific. Details on the Korea-China cooperative research can be found at: http://www.mrcor.org.

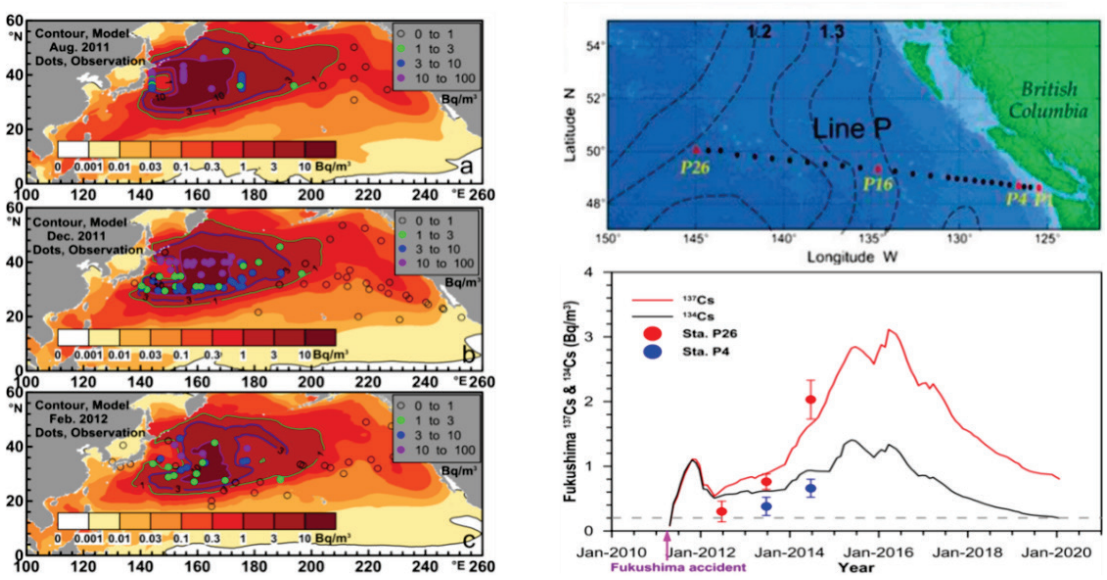

Fig. 4 Simulated results of transport of ^{134}Cs and ^{137}Cs in the Northern Pacific using a global model with atmospheric and direct release inputs. Right, below is the model validation results through the comparison with Canadian observations. (edited from Zhao *et al*., 2016)

Considerable efforts have been made to the fate modeling of artificial radionuclides. From the year 2012 researchers from IMMSP became a part of joint research teams, attending the Korea-China workshop held at Qingdao and preparing joint research papers on biota modeling. Two biota-related papers which are concerned with the influence of the global fallout and Fukushima-induced radionuclide releases of ^{137}Cs and ^{90}Sr on marine organisms through the pelagic marine food web around the Fukushima Dai-ichi Nuclear Power Plant and adjacent seas in Northwestern Pacific were jointly published in 2014. The model equipped with a pelagic marine food web is called BURN-POSEIDON. In 2015 and 2016 the benthic food web has been added to take into account the influence of radioactivity-contaminated bottom sediments on the marine organisms. Application of the model, so called Extended-BURN-POSEIDON, was made for Fukushima-derived ^{137}Cs and a related paper was jointly published in 2016. In the course of applying for ^{90}Sr, the need of model extension was raised. Close examination revealed that use of the single target tissue approach in BURN- and Extended-BURN-POSEIDON causes underestimation of ^{90}Sr concentration in fishes. The model was thereafter extended to a multi-target tissue approach. The model is called the Multi-BURN-POSEIDON model. In practice, three target tissues such as flesh, bone and organ were considered for fishes. Fig. 5 shows the marine food webs for Extended-BURN-POSEIDON and Multi-BURN-POSEIDON.

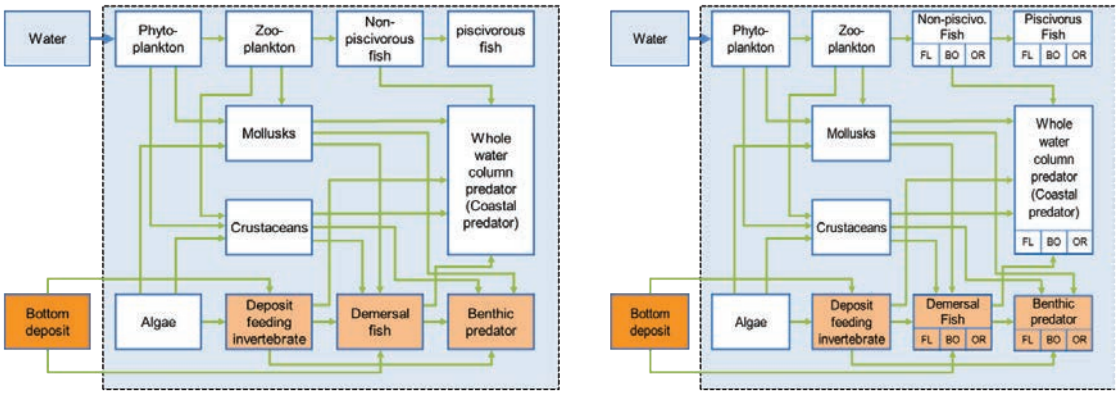

Fig. 5 Marine food webs considered in: left) Extended-BURN-POSEIDON, right) Multi-BURN-POSEIDON.

As one of the cooperative activities among China-Korea-Ukraine, the BURN-POSEIDON model has been implemented to the South China Sea. Fig. 6 shows the horizontal box configuration and a simulation example according to a hypothetical release from Changjiang Nuclear Power Plant.

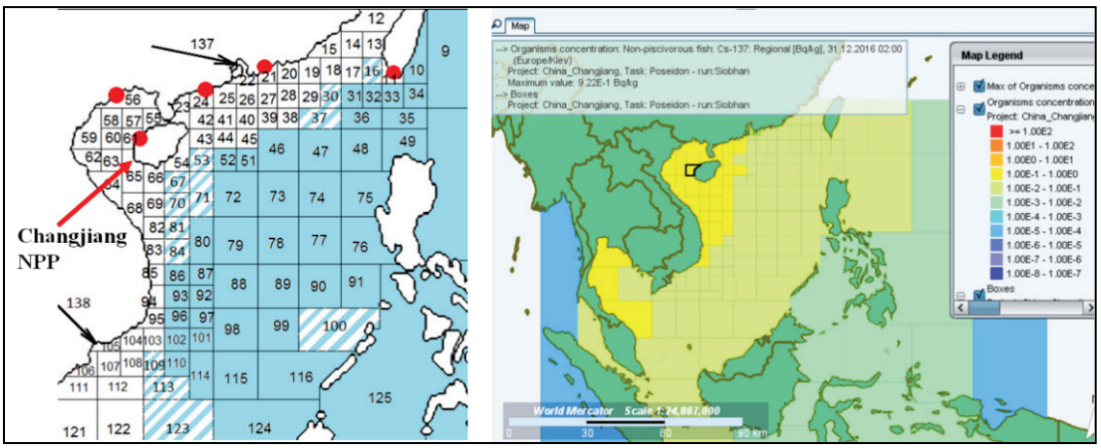

Fig. 6 BURN-POSEIDON model for the South China Sea: left) horizontal box configuration, right) simulated concentration of ^{137}Cs in non-piscivorous fish after 1 year following the hypothetical release from Changjiang Nuclear Power Plant.

3. Major achievements

Monitoring in Korean waters shows that the radioactivity concentration remains in the background level, indicating that up to now there is little impact of the Fukushima-derived radionuclides on the Korean waters. Analysis of marine organism samples in Korean waters over the period of 2012 to 2015 also indicates that levels of ^{137}Cs concentration also remain at the background level. Calculation of the biological concentration factors has revealed considerable discrepancy with recommended values in 2004 by IAEA.

International cooperation in the development of transport and biota models has been carried out. The fact that FIO/KIOST simulation of the transport of ^{134}Cs and ^{137}Cs in the Northern Pacific produced results which are in reasonable agreement with observations may be one of the achievement in modeling field. Cooperation in biota modeling may be considered as the most meaningful achievement. Long-term applications of the Extended-BURN-POSEIDON model to the Fukushima Dai-ichi Nuclear Power Plant accident were made with consideration of the global

fallout from 1945 and the Fukushima-derived atmospheric and direct oceanic releases. In 2016 a paper was published in Biogeosciences which describes how and why the concentration of ^{137}Cs in benthic fishes remains at a relatively high level, comparing pelagic fishes. Introduction of a multi-target tissue model which has solved the problem of underestimating the ^{90}Sr in the previous single target tissue model may be one of the most important achievement in radioactivity biota modeling.

4. Conclusions

Marine radioactivity monitoring activities by the Republic of Korea have been limitedly carried out in Korean waters. International cooperative researches may be required to get the more comprehensive data sets. It has been found that there is a considerable amount of difference in the biological concentration factors between the values analyzed by KIOST and recommended by IAEA. Further investigation is obviously needed on this matter possibly through the international cooperation, for example, between TIO (Third Institute of Oceanography), China and KIOST, Korea.

In addition to the development of Extended-BURN-POSEIDON equipped with the pelagic and benthic food webs, preliminary results from the further refined model Multi-BURN-POSEIDON are very much encouraging. The model might be an essential component of the decision supporting system for a future accident in the Northwestern Pacific region. Along with the biota model, an advanced modeling system for predicting the marine radioactivity transport for the Yellow Sea and the East China Sea is underway. It is expected that its more detailed results can be reported in 2017.

United States of America

Report on Marine Radioactivity Work 2016

Delvan Neville, Kathryn A. Higley
School of Nuclear Science & Engineering, Oregon State University
Corvallis, OR 97331-5903 USA

1. Introduction

Over the last year, Oregon State University has engaged in (1) Public outreach via posters, flyers and a display stand, (2) Further measurements of ^{134}Cs and ^{137}Cs in *Thunnus alalunga* (North Pacific albacore), (3) Bystander effect modelling from first-principles, (4) Laid groundwork for future work with polygonal mesh models. Measurements and public outreach have also been conducted in the US by the Our Radioactive Ocean project.

2. Public outreach

Fig. 1 Display stand at Hatfield Marine Science Center in Newport, OR

In the years since the original large-scale release at Fukushima Daiichi Nuclear Power Plant (FDNPP), the rate of inquiry and concern from members of the general public has declined significantly. Reports of ^{134}Cs detection on the USA West Coast through the Our Radioactive Ocean sparked new interest from members of the public and news organizations, but overall there does not seem to be a large outstanding concern public body at this time. The citizen-science program of Our Radioactive Ocean provided concerned members of the public the opportunity to engage in answering their own concerns first hand. In Oregon, joint work between Oregon State University, Oregon Sea Grant and NOAA allowed for the development of an easy-to-understand flyer regarding the highest observed levels of FDNPP-derived radioactivity in USA foodstuffs, including a display pictured in Figure 1.

3. Measurements

Research continues at Oregon State University to measure the concentrations of ^{134}Cs and ^{137}Cs in *Thunnus alalonga* (Pacific albacore) found along the USA West Coast. In the last few years, the albacore fishery in Southern California has not been as active as it was historically, which has drastically limited the number of samples that could be collected from the Southern California region. Nonetheless, approximately 200 albacore carcasses were collected and continue to be processed and analyzed for radiocesium concentrations. These figures inform both only human health concerns and dose calculations to the albacore themselves, both of which peaked in 2012 and never reached levels that would require intervention for human or ecological safety. Besides some water sampling done by Oregon State University in partnership with NOAA, ^{134}Cs and ^{137}Cs concentrations have been measured substantially through the Our Radioactive Ocean project (Figure 2).

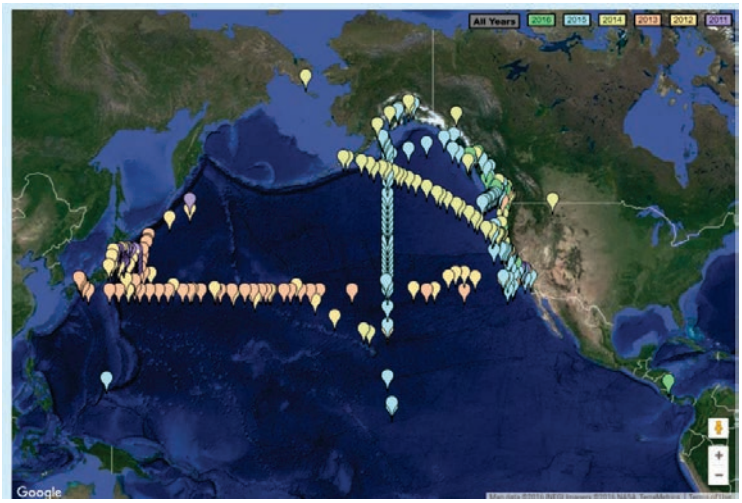

Fig. 2 http://www.ourradioactiveocean.org/results.html provides members of the public with concentrations of radiocesium both at sea and on the shoreline, largely through a crowd-funded citizen-scientist program.

Work continues at Oregon State University to measure the tissue densities and elemental compositions in select species. Both play a significant role in rates of photon and electron interactions and ultimately differences in dose conversion coefficients for both internal and external radiation sources.

4. Bystander effect via First Principles

Ongoing research at Oregon State University (Figure 3) is modelling the mechanism for radiation-induced effects in biota by coupling models operating on different time scales. This should allow for the prediction of radiation sickness as well as tumor outcomes in a manner that include the so-called bystander effect, wherein cells that did not receive a dose will die due to neighboring cells receiving a dose.

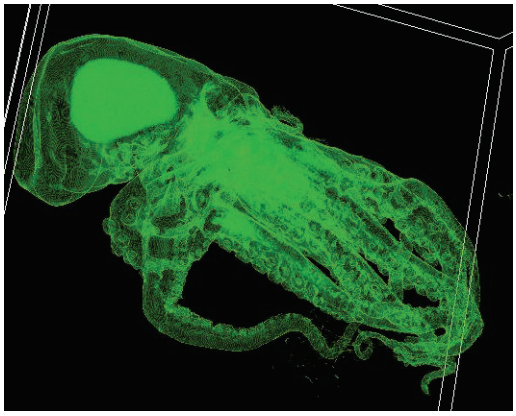

Fig. 3 Prototype surface rendering of a juvenile octopus

5. Groundwork for 2017 work

In the 2017 groundwork, a series of 26 high-resolution diffusible iodine contrast enhanced micro-CTs have been made of numerous marine life, including forage fish, mollusks, krill, and shrimp. These images will be used as part of the development of a new protocol for the creation of 3D dosimetric models of biota. By developing the new protocol using exclusively open-source software, the opportunity will be present to collaborate with scientists abroad in producing and refining these models. Further, these models will be built using polygonal surface meshes rather than voxels, allowing for more realistic curvature and fine-scale structures without forcing exceedingly high computational requirements for larger more homogenous portions of a given model.

WG 30 Endnote 4

Outline and assignment of the WG 30 Final Report and time schedule

I. Outline and assignment of the WG 30 Final Report

Final Report of Working Group 30 on *Assessment of Marine Environmental Quality of Radiation around the North Pacific*

Acknowledgements (China and USA)
Executive Summary (All member countries)
1 Background (All member countries)
2 Level and Trend of Marine Radioactivity in North Pacific
- 2.1 Coastal Waters of Japan (Japan)
  - 2.1.1 Seawater
  - 2.1.2 Biota
  - 2.1.3 Sediment
  - 2.1.4 Summary
- 2.2 Northwest Pacific (China, Japan, Korea)
  - 2.2.1 Seawater
  - 2.2.2 Biota
  - 2.2.3 Sediment
  - 2.2.4 Summary

2.3 Off-shore Waters of North America (Canada, USA)
2.3.1 Seawater
2.3.2 Biota
2.3.3 Sediment
2.3.4 Summary
2.4. Coastal Waters of China (China)
2.4.1 Seawater
2.4.2 Biota
2.4.3 Sediment
2.4.4 Summary
2.5. Coastal Waters of Korea (Korea)
2.5.1 Seawater
2.5.2 Biota
2.5.3 Sediment
2.5.4 Summary

3 Potential Radiological Impact on Marine Species (USA, China)
3.1 Assessment Method
3.2 Assessment Result
3.3 Summary

4 Technical Progress in Marine Radioactivity Monitoring, Prediction and Radiological Risk Assessment
4.1 Modeling and Prediction (Korea)
4.2 Innovation of Monitoring Devices (China)
4.3 Voxel Model etc. for Radiological Dose Assessment (USA, China)
4.4 Radiological Risk Assessment Tools (China, USA)
4.5 Summary (Korea, China, USA)

5 Inventory of Expertise and Programs Related to Marine Radioactivity in PICES Member Countries
5.1 Marine Radioactivity Expert Database (All member countries)
5.2 National Research and Monitoring Programs and Collaboration Initiatives (All member countries)

6 Collaboration between PICES WG 30 and Other Scientific Organization and between Member Countries (All member countries)

7 Summaries and Recommendations (All member countries)

Appendices

Appendix 1 WG 30 Terms of Reference (China and USA)
Appendix 2 WG 30 Membership (China and USA)
Appendix 3 Other Products of WG30 (All member countries)
Appendix 4 Meeting Reports and Workshop Summaries from the Previous PICES Annual Meetings Related to the WG 30 (USA and China)

II. Time schedule (Nov 2016-Dec 2017)

(1) Now–March 15: Finish and submit different part reports of the WG 30 Final Report by all member countries to Kathy and Yusheng.
(2) March 15–April 24: Compile the first version of manuscript (M1 of the WG 30 Final Report).
(3) April 25–May 15: Revise the manuscript (M1) and finish the 1st circulation by all member countries.
(4) May 16–June 15: Finish the second version of manuscript (M2).
(5) June 16–July 15: Revise the manuscript (M2) and finish the 2nd circulation by all member countries.

(6) July 16–August 15: Finish the 3rd version of manuscript (M3); and submit ideas, framework, texts and figures about the new paper by all member countries.
(7) August 15 – before PICES-2017: Discuss and draft the new paper.
(8) 2 days of the WG 30 business meeting during PICES-2017: All the WG 30 members review and revise the M3 and new paper manuscript.
(9) October–November: Complete the final report and new paper manuscript.
(10) December: Submit the WG30 Final Report and the new paper manuscript to PICES Secretariat.

PICES-2017
September 22–October 1, 2017, Vladivostok, Russia

Annual Meeting Report (2017) of Working Group 30 on *Assessment of Marine Environmental Quality of Radiation around the North Pacific*

The 2017 business meeting of Working Group on *Assessment of Marine Environmental Quality of Radiation around the North Pacific* (WG 30/WG-AMR) was held in Vladivostok, Russia, from 09:00 to 18:00 on September 23, 2017. Co-Chair of the WG 30, Prof. Yusheng Zhang (China) welcomed all of the members and observers to the meeting and made the opening address. Fourteen participants, including nine WG 30 members from four member countries (except Russia and USA) attended the meeting (Annex 1).

Left: Participants of the WG 30 2017 annual meeting. Right: Participants in the meeting.

AGENDA ITEM 1
Adopting the meeting agenda

First of all, the agenda for the 2017 business meeting of the WG 30 (Annex 2) was discussed and adopted without revision by the WG members.

AGENDA ITEM 2
Overview and update of WG 30

Prof. Yusheng Zhang made a presentation entitled “Overview and update of the WG 30”, giving an introduction on the progress of WG 30 since the last business meeting held during the PICES 2016 Annual Meeting in San Diego, USA.

AGENDA ITEM 3
Member country reports

Each member country of the WG 30 provided an overview of the research that they had conducted in the past year following the WG work plan.

Canada

The large discharge of radioactivity into the Pacific Ocean off Japan from the 2011 Fukushima Dai-ichi nuclear reactor accident generated considerable concern about potential impacts on marine biota in the eastern North Pacific. Time series measurements of ^{134}Cs and ^{137}Cs in seawater on Line P documented the initial arrival of the Fukushima signal by ocean current transport at a location 1500 km west of British Columbia, Canada in June, 2012, about 1.3 years after the accident. Between 2012 and 2015 the Fukushima radioactivity signal continued to increase in surface water on Line P and eventually began to level off at probable maximum values in 2016–2017 as documented by biannual monitoring surveys. Although radioactivity contamination of fish off Fukushima was initially severe, analyses of biological samples performed under the auspices of the InFORM monitoring program off British Columbia have revealed little evidence of elevated radioactivity levels in fish or other biota. These results, based on both measurements and biological modeling studies are a consequence of the low Fukushima radionuclide levels in seawater and the low biological half-lives of several months for Cs in fish. Although the ecosystem impacts off British Columbia associated with radioactivity releases from Fukushima have been minimal, the communication of these results to the public and general community acceptance of their veracity has been a challenge requiring many public lectures, scientific publications and considerable media outreach, thereby providing a cautionary note for studies of future ecosystem threats associated with grim anthropogenic drivers.

China

To improve the understanding on the transport of radioactive pollutants released from the FDNPP accident in the Northwest Pacific and their potential impact, two monitoring cruises were conducted by the Third Institute of Oceanography, SOA of China from the second half year of 2016 to the first half year of 2017. Seawater samples were collected at more than 80 stations at different depths. The biota samples were also collected in part of the stations. Radionuclides of ^{137}Cs, ^{134}Cs and ^{90}Sr were measured. By the end of June 2017, the main monitoring results were as below.

In surface water layer, ^{134}Cs signals were found in 7 stations out of 47 stations with a maximum radioactivity value of 0.76 Bq/m^3. At the depth of 100 m, ^{134}Cs signals were found in 9 stations with a maximum radioactivity value of 0.65 Bq/m^3. At the depth of 200 m, 5 stations were found containing ^{134}Cs with a maximum radioactivity value of 0.37 Bq/m^3. As for the 300-m layer, 11 stations were found with the detectable ^{134}Cs, with a maximum radioactivity value of 0.51 Bq/m^3. At the depths of 500 m and 1000 m, the numbers of stations with detectable ^{134}Cs were 5 and 7, respectively, with the maximum radioactivity level of 0.77 Bq/m^3 and 0.69 Bq/m^3. At the depths of 1500 m and 2000 m, ^{134}Cs was not detectable. As for ^{137}Cs, it was detectable at each layer above 1000-m depth. The maximum value of each depth was around 4 Bq/m^3. At the depth of 500 m, the highest ^{137}Cs value was 4.25 Bq/m^3. But at the depths of 1000 m to 2000 m, ^{137}Cs was found in some stations, with a maximum value of less than 0.5 Bq/m^3. As for the distribution of ^{90}Sr in the water column, the maximum radioactivity value of all the samples was 2 Bq/m^3. For the biota samples, activity levels of these samples were both 0.02 Bq/kg-wet, which was within the background level before FDNPP accident.

As for marine organisms, from the 10 cruises in the last few years, it was found that the radioactivity level of marine organisms in the Northwest Pacific also decreased with time.

In addition, China has also developed a marine radioactivity assessment method with the corresponding program and an equipment for in-situ pre-concentration and monitoring. Moreover, the voxel model for squids was also studied. And six papers have been published.

This year is the last year of WG 30 program. Therefore, we have also spent much time not only to summarize our survey/monitoring results these years and write the Final Report of China, but also

to compile the reports of member countries into the first version of the WG 30 Final Report for discussion, comments and revision on it during the WG business meeting of this year.

Japan

In the past year, Japan continued to carry out the marine environmental radioactivity monitoring in coastal and off-shore areas. The monitoring results showed that the seawater radioactivity level has decreased to the range of background levels before the Fukushima accident, and none of the marine organism samples exceeded the radioactivity limit of general food in Japan. Reduction of the fishery catch caused by the FDNPP accident made the marine resources off Fukushima increase.

Korea

According to the Korean Atomic Safety Law 105, Korea Institute of Nuclear Safety (KINS) and National Fisheries Institute (NIFS) have collaborated to carry out the Marine Environmental Radioactivity Survey (MERS). In 2017 regular samplings were carried out seasonally at a total of 27 stations, and monthly or bimonthly additional samplings at a total of 6 stations in the sea regions around the Korean Peninsula. Instead of reporting results from the 2017 survey, long-term monitoring results have been reported in the 2017 meeting. Time variation of ^{137}Cs, ^{3}H, $^{239+240}$Pu and ^{90}Sr sea water concentrations over past 23 years (1994~2016) have been reported. The mean concentration values of ^{137}Cs, $^{239+240}$Pu and ^{90}Sr in the sea water are found to be 1.09~2.77 mBq/kg, 1.48~14.6 μBq/kg and 0.22~1.24 mBq/kg, respectively. Long-term variation of ^{137}Cs concentration in fish, shellfish and shellfish at 7 stations and ^{137}Cs, $^{239+240}$Pu and ^{90}Sr concentration values in bottom sediments at 16 stations have been also reported.

The Marine Radionuclide Research Group of KIOST has also secured samples of major fishery products from sea regions around the Korean Peninsula. Laboratory analysis of the collected samples has been carried out to investigate the levels of radioactivity contamination. A concentration factor data base has been constructed for major radionuclides such as ^{137}Cs, $^{239+240}$Pu and ^{90}Sr.

Transport and biological fate modeling efforts of radionuclides by KIOST over the period of Dec 2011 to 2017 have been summarized with focus on the cooperation with FIO, China and IMMSP, Ukraine. In detail, recent development of two box-based fate models as well as Eulerian and Lagrangian transport models was reported. The Eulerian transport model can consider multi-fractional sediments, two-step transfer kinetics, bioturbation effects and multiple bed layers to predict depth profiles of radioactivity in water column and bottom sediments. The Lagrangian model considers single fractional sediment, one-step transfer kinetics and single bed layer. Two box-based fate models were reported. One is POSEIDON-extended BURN ver. 1 equipped with pelagic and benthic food webs and the other is Multi-target tissue fish model ver. 1 without consideration of physiological interaction between fish organs. The model results were in good agreement with measurements.

USA

In the past year, the USA has engaged in further outreach activities intended to better inform the public, especially now that there are finally reports of detectable ^{134}Cs in the coastal waters of USA. Most of the monitoring has arisen via the Our Radioactive Ocean project, although a smaller water survey conducted between NOAA and OSU is nearly ready to be published. Dosimetric modeling continues, evaluating the effects of tissue type, density and elemental composition on dose conversion coefficients. A new protocol for the creation of 3D dosimetric models using exclusively open-source software and realistic polygonal meshes is underway, which should allow for better representation of fine-scale structures and allow for better collaboration between the USA and other member countries on this front.

AGENDA ITEM 4
Discussion on the WG 30 Final Report

The Co-Chair of WG 30, Prof. Yusheng Zhang, introduced the current progress of the Final Report of WG 30 – according to the outline of Final Report agreed in the WG 30 2016 business meeting, most of the contents were submitted and integrated into the Final Report, while some contents (progress on radiological dose assessment model from USA, monitoring results at NW Pacific from Japan and Russia, simulation model comparison from Korea, *etc*.) were not submitted and integrated yet.

The WG 30 members agreed that the current section of "Expert Database" should be changed into "List of Contributing Scientists".
The WG members also agreed to the following time schedule for finalizing the report:

- WG members send revisions and comments to Dr. Wen Yu before Oct 20;
- Dr. Wen Yu integrates revisions and comments into the second draft of Final Report and send it to Dr. John N. Smith, Profs. Kathryn A. Higley and Yusheng Zhang before Nov 1;
- Dr. John N. Smith, Profs. Kathryn A. Higley and Yusheng Zhang send their revisions and comments to Dr. Wen Yu before Nov 15;
- Dr. Wen Yu sends the third draft of Final Report to WG members before Nov 22;
- WG members send their revisions and comments to Dr. Wen Yu before Nov 30;
- Submitting the Final Report to PICES secretariat before Dec 10.

AGENDA ITEM 5
Revision and finalisation of Brochure of WG 30

Based on the draft version of brochure of the WG 30, the following items were agreed on during the meeting:

- Information of workshops organized by WG 30 should be included.
- The TORs of WG 30 should be deleted, considering its overlapping with the mission statement of WG 30.
- The cartoon figure should be changed.
- More text should be added to give detail information about the figures.
- Any comments/revisions regarding the brochure should be sent to Dr. Wen Yu before Nov 15.

AGENDA ITEM 6
Proposal of establishing a new WG on radioactivity

Since the lifespan of WG 30 will finish at the end of 2017, a proposal of establishing a new WG on the Distribution and Environmental Evolution of Radionuclides in the North Pacific was brought out by Chinese delegation.

Dr. Wen Yu gave a presentation on the above proposal at the WG business meeting. After meeting discussions on the title and duty of the new WG, no consensus was reached, but the meeting agreed to put the new WG proposal into the "Recommendations" section of the WG 30 Final Report. The meeting agreed that further comments/revisions regarding the new WG should be sent to Dr. Wen Yu before Sep 25, and a revised proposal would be presented at the MEQ business meeting on Sep 27.

Annex 1

List of participants for WG 30 Business Meeting 2017

Country/ Committee	Members	Observers
Canada	John N. Smith	—
China	Yusheng Zhang (Co-Chair) Wen Yu Wu Men	Jianhua He Jinqiu Du
Japan	Tomowo Watanabe Takami Morita	Daisuke Ambe Toyomitsu Horii
Korea	Kyung Tae Jung Suk Hyun Kim In-Seong Han	Kyeongok Kim
Russia	—	—
USA	—	—
MEQ, PICES	—	Guangshui Na

Annex 2

WG 30 business meeting agenda of 2017

1. Revision and adoption of the draft meeting agenda
2. Overview and update of WG 30
3. Country report presentations of member countries
4. Discussion on the WG 30 Final Report (identification of gaps, schedule and work assignments)
5. Revision and finalisation of brochure of the WG 30
6. Discussion on the proposal for the new Working Group (title, objectives, TOR, suggested membership, *etc*.)

Appendix 6

PICES Press Article Related to WG 30

Workshop on Radionuclide Science and Environmental Quality in the North Pacific

by Yusheng Zhang, Wen Yu and Hongzhi Li

The participants of the PICES/SOA workshop on "Radionuclide science and environmental quality of radiation in the North Pacific" (March 14–15, 2013, Xiamen, China).

This was the first opportunity for the PICES Study Group on *Radionuclide Science and Environmental Quality of Radiation in the North Pacific* (SG-RS) to meet. The workshop was jointly sponsored by PICES and the State Oceanic Administration (SOA) of China and organized by the Third Institute of Oceanography (TIO/SOA) from March 14–15, 2013, in Xiamen. It was led by Prof. Yusheng Zhang (SG-RS Chairman), Prof. Chuanlin Huo (Marine Environmental Quality (MEQ) Committee Chairman), and Dr. Sinjae Yoo (Science Board Chairman). A total of 20 participants attended the workshop, including 8 SG-RS members from 5 PICES member countries: Canada, China, Japan, Korea and the United States. The International Atomic Energy Agency (IAEA) was represented by the IAEA/RCA project leading country coordinator, Mr. Ronald Szymczak (Australia).

The objectives of the workshop were:

- to review research on marine radiation in each PICES member country;
- to exchange views on how to develop a scientific focus within PICES to understand the quantities and distributions of radionuclides in the North Pacific, and
- to refine the Terms of Reference (TORs) and work plan for a new PICES Working Group on *Assessment of Marine Environmental Quality of Radiation around the North Pacific* (WG-AMR), under MEQ as Parent Committee.

The outcome from this workshop is intended to provide a sound foundation for the establishment of WG-AMR in the near future.

In his introductory remarks, Prof. Yusheng Zhang pointed out that the widespread application of nuclear science and technology as well as a recent nuclear power plant accident had led to increasing amounts of radionuclides released into the North Pacific. Radionuclides with long half-lives could potentially endanger the marine ecosystem and human health through exposures *via* the food chain. Consequently, it is important to monitor the radiation exposure level and to assess the effects of radioactive substances on marine ecosystems in the North Pacific waters. This was the rationale behind China's proposal at the 2012 PICES Annual Meeting (Hiroshima, Japan) to establish the SG-RS that would make preparations for the future establishment of the WG-AMR. The envisioned working group aims to exchange technologies and share experiences in monitoring radioactive contaminants in North Pacific waters, to assess the radiation effects and radiological risks in these waters and to promote the public understanding of radiation effects. The proposal to form the SG-RS garnered positive support from all PICES member countries and was approved by the Science Board and the Governing Council of PICES.

Dr. Sinjae Yoo and Prof. Chuanlin Huo were invited to make a presentation about the current PICES integrative science program, FUTURE (Forecasting and Understanding Trends, Uncertainty and Responses of North Pacific Marine Ecosystems) and the MEQ Action Plan. Thereafter, the participants discussed and refined the Terms of Reference for the proposed WG-AMR, including their relevance to FUTURE.

The workshop in session.

Facing from left: Prof. Chuanlin Huo (MEQ Chairman), Dr. Sinjae Yoo (Science Board Chairman), Prof. Yusheng Zhang (SG-RS Chairman), and Dr. Jian Chen (Director of Division of International Cooperation, TIO).

Following an active discussion, the TORs for the proposed WG-AMR were refined and agreed upon by all the members as follows:

1. To compare and analyze radiological doses to North Pacific marine organisms from natural and anthropogenic radionuclides in a post-Fukushima world.
2. To examine the utility of applying natural and artificial (from Fukushima and other sources) radionuclides as tracers of circulation, ecological transfers and biogeo-chemical cycling in the North Pacific (and downstream, *e.g.*, Arctic) environments undergoing modification by climate change.
3. To determine the state of the science with respect to the assessment and mitigation of radiological impacts to marine organisms from natural and anthropogenic releases of radionuclides into the marine environment.
4. To contribute to FUTURE by producing status reports for items 1–3 above, management related guidelines and/or technical manuals.
5. To foster collaboration with other expert groups to achieve the goals of items 1–3.
6. To identify priority research requirements for knowledge gaps identified in items 1–3, the planned expansion of nuclear facilities and other emerging issues in the PICES region.
7. To promote collaboration among PICES member countries and international organizations in the exchange of information on environmental radioactivity and encourage joint surveys/research among PICES member countries.

Participants discussed a 3-year work plan for the proposed working group and explored possible ways to fund the activities. A detailed work plan will be included in the 2013 Annual Report.

A list of the possible WG-AMR members developed in two weeks after the workshop includes the following scientists: John N. Smith (Canada), Hongzhi Li, Wen Yu and Yusheng Zhang (China), Takami Morita, Tsuneo Ono and Tomowo Watanabe (Japan), Gi-Hoon Hong and Suk Hyun Kim (Korea), Vladimir Goryachev (Russia) and Kathryn A. Higley (USA).

The SG-RS report and the proposal to establish WG-AMR, including the Terms of Reference, the work plan and potential members were presented and reviewed at the 2013 inter-sessional Science Board meeting held May 20–21 in St. Petersburg, Russia.

Prof. Yusheng Zhang (ys.zhang@163.com), a senior scientist from the Third Institute of Oceanography, State Oceanic Administration (SOA) of China, has been interested in radioecology and biological effects of marine pollutants on marine organisms and ecosystems. Since 2007, he has been working as a National Project Coordinator of IAEA/RCA projects. Within PICES, Prof. Zhang has been serving as the SG-RS chairman since January 2013.

Dr. Wen Yu (yuwen2001@gmail.com) is a scientific researcher at the Third Institute of Oceanography, State Oceanic Administration of China. She has a broad range of research interests related to marine biota radiation dosimetry, the destiny of radionuclides in marine species and radio-isotope application. Dr. Yu is a National Project Coordinator of the IAEA Fukushima marine impact program. She has been a member of the SG-RS since January 2013.

Mr. Hongzhi Li (lihongzhi6535@126.com) is the Director of the Department of Marine Measurement Sensor Technology at the National Oceanic Technology Center, State Oceanic Administration of China. His research focuses on marine sensor technology, model and application for monitoring of marine pollutants, as well as data processing. He has been a SG-RS member since January 2013.